HHS Public Access

Author manuscript

Chem Rev. Author manuscript; available in PMC 2019 May 01.

Published in final edited form as:

Chem Rev. 2017 October 25; 117(20): 12764–12850. doi:10.1021/acs.chemrev.7b00094.

Functional and Biomimetic Materials for Engineering of the Three-Dimensional Cell Microenvironment

Guoyou Huang[†,§,#], **Fei Li**[§,‡,#], **Xin Zhao**[§,‖], **Yufei Ma**[†,§], **Yuhui Li**[†,§], **Min Lin**[†,§], **Guorui Jin**[†,§], **Tian Jian Lu**[§,⊥], **Guy M. Genin**[†,§,▽,○], and **Feng Xu**[*,†,§]

[†]MOE Key Laboratory of Biomedical Information Engineering, School of Life Science and Technology, Xi'an Jiaotong University, Xi'an 710049, People's Republic of China

[§]Bioinspired Engineering and Biomechanics Center (BEBC), Xi'an Jiaotong University, Xi'an 710049, People's Republic of China

[‡]Department of Chemistry, School of Science, Xi'an Jiaotong University, Xi'an 710049, People's Republic of China

[‖]Interdisciplinary Division of Biomedical Engineering, The Hong Kong Polytechnic University, Hung Hom, Hong Kong, People's Republic of China

[⊥]MOE Key Laboratory for Multifunctional Materials and Structures, Xi'an Jiaotong University, Xi'an 710049, People's Republic of China

[▽]Department of Mechanical Engineering & Materials Science, Washington University in St. Louis, St. Louis 63130, MO, USA

[○]NSF Science and Technology Center for Engineering MechanoBiology, Washington University in St. Louis, St. Louis 63130, MO, USA

Abstract

The cell microenvironment has emerged as a key determinant of cell behavior and function in development, physiology, and pathophysiology. Extracellular matrix (ECM) within the cell microenvironment serves not only as a structural foundation for cells, but also as a source of three-dimensional (3D) biochemical and biophysical cues that trigger and regulate cell behaviors. Increasing evidence suggests that the 3D character of the microenvironment is required for development of many critical cell responses observed *in vivo*, fueling a surge in the development of functional and biomimetic materials for engineering the 3D cell microenvironment. Progress in the design of such materials has improved control of cell behaviors in 3D and advanced the fields of tissue regeneration, *in vitro* tissue models, large-scale cell differentiation, immunotherapy, and gene therapy. However, the field is still in its infancy, and discoveries about the nature of cell-microenvironment interactions continue to overturn much early progress in the field. Key challenges continue to be dissecting the roles of chemistry, structure, mechanics, and electrophysiology in the cell microenvironment, and understanding and harnessing the roles of

[*]Corresponding author: fengxu@mail.xjtu.edu.cn.
[#]These authors contributed equally to this work

Notes

The authors declare no competing financial interests.

periodicity and drift in these factors. This review encapsulates where recent advances appear to leave the ever-shifting state of the art, and highlights areas in which substantial potential and uncertainty remain.

Graphical Abstract

The cell microenvironment has emerged as a key determinant of cell behavior and function in development, physiology, and pathophysiology. The extracellular matrix (ECM) within the cell microenvironment serves not only as a structural foundation for cells but also as a source of three-dimensional (3D) biochemical and biophysical cues that trigger and regulate cell behaviors. Increasing evidence suggests that the 3D character of the microenvironment is required for development of many critical cell responses observed in vivo, fueling a surge in the development of functional and biomimetic materials for engineering the 3D cell microenvironment. Progress in the design of such materials has improved control of cell behaviors in 3D and advanced the fields of tissue regeneration, in vitro tissue models, large-scale cell differentiation, immunotherapy, and gene therapy. However, the field is still in its infancy, and discoveries about the nature of cell–microenvironment interactions continue to overturn much early progress in the field. Key challenges continue to be dissecting the roles of chemistry, structure, mechanics, and electrophysiology in the cell microenvironment, and understanding and harnessing the roles of periodicity and drift in these factors. This review encapsulates where recent advances appear to leave the ever-shifting state of the art, and it highlights areas in which substantial potential and uncertainty remain.

1. Introduction

Cells, studied on two-dimensional (2D) substrata for centuries, are now recognized to be controlled strongly by the highly structured and heterogeneous mix of neighboring cells, soluble factors, extracellular matrix (ECM), and biophysical fields that comprise their three-dimensional (3D) microenvironment.[1–3] This microenvironment not only serves as structural support for cells to reside within but also provides diverse biochemical and biophysical cues, such as adhesion ligands, topological features, mechanical resistance, and an adaptable and degradable scaffold for regulating such cell behaviors as spreading, proliferation, migration, differentiation, and apoptosis.[4–5] In addition, the ECM regulates the distribution, availability, and mobility of soluble factors and mediates mechanical and electrical fields. Therefore, an important focus has been the development of materials that mimic the structures, properties and functions of native ECM and enable the study of cells *in vitro* in a realistic and adaptable cell microenvironment.[6–7] Through functional and biomimetic material designs, progress in engineering the cell microenvironment has found wide applications in tissue regeneration, *in vitro* tissue models, large-scale cell differentiation, immunotherapy, and gene therapy.[8–13] New materials and fabrication technologies are emerging rapidly.[14–15]

However, many central mysteries remain. Following the development of 3D cell culture in the 1980s and 1990s,[16–18] a recognition emerged that 2D cell culture fails to produce many cell response observed *in vivo*.[19–20] A challenge in the field that persists to this day is that much of the field's view of the cell microenvironment, and indeed of cell biology, is based upon observations of cells plated on 2D substrata. Although data are limited, emerging

studies of the 3D cell microenvironment have provided a picture of cells and their microenvironments that differs substantially from the prevailing views in the literature. A key example to serve as an introduction is the role of the glycocalyx. This layer of glycoproteins is not known to develop fully in 2D cell culture, but might be critical to mechanotransduction by epithelial cells that line the vasculature.[21–22] Are endothelial cells (ECs) that maintain their 2D endothelial phenotype when cultured in 3D representative of ECs *in vivo*, or must further adjustments be made to the materials in their microenvironment? In the case of chondrocytes, 30-year-old quick-freeze/deep etch electron micrographs have shown the existence of nano-structured proteins at the cell periphery, in place of a disordered endothelial-like glycocalyx.[23] What are these structures in the cell microenvironment, and how do we regenerate them? A challenge throughout the field of cell microenvironment engineering is that idealized systems are needed not only to reproduce, but also to identify and characterize structures such as these and their roles in tissue function. Related challenges are a theme for critical re-evaluation of the field throughout this review.

Despite these challenges in understanding the details of the cell microenvironment, biomimetic materials replicating bulk ECM *macro*-environment have become widely available, and have been used effectively to foster development of engineered tissues.[13] These are typically based on 3D polymer scaffolds and hydrogels, which could afford nutrient transport, biocompatibility, structures similar to native bulk ECM, and tunable biochemical and biophysical properties.[24–27] In the following sections, we describe applications of the 3D polymer scaffolds and the three common categories of hydrogels: (1) naturally derived hydrogels based upon decellularized ECM, reconstituted proteins, and polysaccharides; (2) synthetic hydrogels including supramolecular hydrogels; and (3) hybrid hydrogels including polymer hybrid and nanocomposite hydrogels. However, we reiterate a primary limitation of the field: although the bulk properties of ECM have been well characterized, the nature of the local cell environment is largely unknown, including variations amongst cell types and developmental stages. We believe that design for cell microenvironmental properties rather than just bulk ECM properties represents a substantial opportunity in the field of tissue engineering.

Further sources of uncertainty in the field, highlighted throughout the article, are the much-debated and likely interacting roles of biochemical and biophysical factors in design of materials for the cell microenvironment.[28–30] Because even the definitions of these factors are overlapping, we list our working definitions up front and note that the field is not clear on which factors best belong in which category. In the category of biochemical design factors, we include cell adhesion ligands, soluble factor immobilization and chemical functional groups. Cell adhesion ligands can be provided inherently by the biochemistry and by the biophysical structure of naturally derived proteins that compose biomimetic materials, or by cell adhesion peptides incorporated into polymer networks via chemical modification.[31] Soluble factor immobilization involves the biochemistry and biophysics of physical (non-covalent) and chemical (covalent) interactions between soluble factors and hydrogel networks,[32] with bioactivity of the soluble factors strongly affected by different immobilization strategies, spatial distributions, and bound/released states. Chemical functional groups on the surfaces of hydrogel networks dominate properties of biomimetic

materials such as the hydrophilicity and charge, and can be modified to control protein adsorption, cell adhesion, cell function and cell fate.[33]

Under the heading of biophysical design, we include structural features, mechanical properties, degradability, and electrical conductivity.[34] Cell behavior can be impacted by the sensing of hierarchical structural features ranging from the macroscale to the micro- and nanoscales, and a range of biomimetic materials exist to exploit this, typically porous and fibrous structures.[35] Mechanical properties of the ECM, including nonlinearity, viscoelasticity,[36–37] and the ECM's fibrous nature,[38–41] significantly affect certain cell behaviors[42] and the complicated and dynamic feedback between the ECM and cell mechanics.[43–46] Spatiotemporal modulation of material mechanical properties has also been performed to mimic heterogeneous and dynamic native cell mechanical microenvironments.[47] The ECM that is degradable by technologies including enzymatic, hydrolytic, and photolytic degradation exhibits a range of biochemical and biophysical effects on cells.[48] Finally, development of electrical conductivity by pacing of cells and by use of biomimetic materials with conductive polymers or oligomers, gold nanoparticles (AuNPs), carbon nanotubes (CNTs) and graphene have found utility in cardiac and neural tissue enigneeirng.[49–50]

The aforementioned coupling of these biochemical and biophysical properties is both a challenge and an opportunity for development of materials for control of cells by manipulation of the microenvironment. As this review will expand upon, materials are needed for fundamental research to independently control their properties and identify the effects of individual biochemical and biophysical cues on cell behaviors.[14–15]

This review aims to evaluate the state of the field of functional and biomimetic materials for engineering the 3D cell microenvironment in the context of several challenges outlined below. This review is broad in scope by design, and reviews only a tiny fraction of the massive literature that was selected to describe a few important areas of progress and challenge. We apologize in advance for having to omit a very large number of excellent contributions. The review continues in Section 2 with descriptions of some key known components of the cell microenvironment, and highlights some open frontiers. Section 3 then describes the strengths, weaknesses, and uncertainties of biomimetic material systems designed to control biochemical and biophysical aspects of the 3D cell microenvironment. Section 4 reviews these materials from the perspectives of tissue regeneration, *in vitro* tissue models, cell manufacturing, immunotherapy, and gene therapy. We finally conclude with some thoughts on open challenges and future perspectives.

2. The Cell Microenvironment

Cells reside in a complex, heterotypic and dynamic set of biochemical and biophysical cues, termed the "cell microenvironment". For stem cells, a widely used alternative term is "niche,"[51–54] originally coined by Schofield[55] in 1978 to describe the hematopoietic microenvironment. While cell microenvironments are highly varied, the microenvironments of multicellular animals all share some common features of composition and function. Broadly, the four key components of the cell microenvironment include neighboring cells,

soluble factors, the surrounding ECM, and biophysical fields, which provide diverse biochemical and biophysical cues to synergistically and antagonistically regulate cell behaviors and functions such as spreading, migration, self-renewal, differentiation, and apoptosis (Figure 1).

Two central challenges in understanding the cell microenvironment *in vivo* are that it is dynamic and that feedback from the cell itself is an important factor in these dynamics. In a healthy organism, cues present themselves in a well-orchestrated manner.[56–57] Understanding the implications of these dynamics in regulating cell behaviors is essential for improving the development of biomimetic materials for both engineering the cell microenvironment and furthering many biomedical applications.[58–60] In this section, we introduce the four abovementioned key components of the cell microenvironment, and highlight how resolving uncertainties in their biochemistry, physics, and dynamics represents an important frontier that has the potential to be blazed through development of new biomaterials systems for engineering cell microenvironments.

2.1. Neighboring Cells

Cells in the human body do not live in isolation but rather interact with a range of both similar and different types of cells, and form diverse cell-cell communications and interactions that play crucial roles in cell and tissue morphogenesis and function.[61–64] However, what is not known in general is which cells are important to a specific cell type over the course of its lifecycle. This forms a key challenge in the field, and is a focus of ongoing studies using integrated organ-on-a-chip and co-culture models described below.

The pathways by which cells can interact with their neighboring cells include both direct (*i.e.*, cell-cell contact) and indirect (*e.g.*, mediated by soluble factors, as discussed in the next subsection) mechanisms. Direct cell-cell interactions include physical contact from junctions such as tight junctions, anchoring junctions, and gap junctions, and distant cell-cell interactions that take advantage of the long-distance nature of mechanical communication through fibrous ECM.[38,40,65] We discuss the former in this section, and the latter below in the section on ECM.

Tight junctions, or occluding junctions, are the closest cell-cell contacts that consist of multi-protein complexes (mainly claudins and occludins), which join together to link the membranes and cytoskeletons of adjacent cells, especially epithelial cells. Tight junctions can hold cells together, prevent the transport of water and soluble factors through the gaps between cells, and separate tissues and body cavities from their surroundings. Anchoring junctions direct the cell-cell and cell-ECM adhesions. Three types of anchoring junctions have been identified: adherens junctions, desmosomes and hemidesmosomes. The first two types can be involved in cell junctions and are usually mediated by cell adhesion proteins, such as cadherins (a family of calcium-dependent adhesion molecules) or related proteins (*e.g.*, desmogleins and desmocollins).[66] Such junctions play important roles in maintaining the shape and tension of cells and tissues, as well as in cell-cell signaling.[67] Gap junctions, or communicating junctions, are mainly composed of connexin proteins that form open pores or channels across the plasma membrane through which small molecules and ions (*e.g.*, Ca^{2+}) can pass freely. Consequently, gap junctions play a crucial role in coupling the

metabolic activities of adjacent cells and synchronizing the contractions of electrically excitable cells, such as cardiomyocytes.[68] In addition to the above cell junctions, there also exist direct cell-cell interactions mediated by the selectin and immunoglobulin (Ig) superfamilies, which are commonly found in the immune system. These are considered transient interactions because they do not involve the linking of cytoskeletons between adjacent cells.

Direct cell-cell interactions are tightly regulated by a range of microenvironmental cues and signaling pathways.[69–70] Dysregulation of direct cell-cell interactions *in vivo* can cause aberrant cell behaviors and pathologies, such as metastatic cancer.[71–74] Numerous *in vitro* cell co-culture studies have been reported and demonstrated the important roles of direct cell-cell interactions in regulating cell behaviors and tissue functions.[75–77] For instance, the co-culture of MCF-7 cancer cells with fibroblasts in alginate microparticles has been shown to induce the formation of a pro-inflammatory environment and increase both the tumor progression and angiogenic potential of MCF-7 cells.[78] The co-culture of hepatocytes and nonparenchymal fibroblasts has shown that maximizing heterotypic cell-cell contact leads to the increased synthesis of urea and albumin and enhanced hepatocyte function.[79] An increase in homotypic cell-cell contact area has also been shown to enhance both the osteogenic and adipogenic differentiation of human mesenchymal stem cells (hMSCs).[80] Another key example is the synthesis of engineered heart tissue, in which myofibroblasts are required to bring cardiomyocytes into sufficiently close proximity to one another to promote the formation of myofibrils.[81–82]

We note that the direct cell-cell interactions are relatively well understood not only owing to immunofluorescence imaging, but also owing to materials breakthroughs, including microfluidic co-culture platforms that were developed specifically to examine these interactions.[83–84] The characteristics of microfluidic technologies, such as miniaturization, automatization and integration, endow researchers with the ability to mimic complex, physiologically relevant microenvironments for culturing different cell types, such as immune cells, stem cells, cancer cells and stromal cells.[85–87] Moreover, microfluidic co-culture systems, including those based on valved microfluidics,[88] microfluidic cell trap arrays,[89] and droplet microfluidics,[90–91] have the ability to control cell-cell interactions at a single-cell resolution in a high-throughput manner by generating and manipulating cell pairs with hydrodynamic forces and/or other physical forces.[92–93] Such high-throughput, single-cell-level co-culture systems can simplify the complexity of cell-cell interactions and provide a wealth of information related to cell heterogeneity.

With this wealth of information available about how cell interact with one another through direct interactions in a steady state, the field has clearly advanced substantially. However, as alluded to above, the dynamics of these interactions and the ways that these dynamics are affected by cell-cell feedback represent important frontiers.

2.2. Soluble Factors

Although there is broad recognition throughout the field that cell-cell interactions are important, there are relatively few culture systems in which detailed knowledge of the

sources and roles of soluble factors over the cell lifecycle are known well. We summarize a few of these in this section.

In vivo, cells encounter numerous soluble factors from their aqueous microenvironment, including basic nutrients (*e.g.*, oxygen, glucose and amino acids) and soluble signaling molecules (*e.g.*, growth factors, cytokines, hormones and other small molecules). Among basic nutrients, oxygen has relatively low solubility in aqueous media and is considered the most readily depleted.[94] The inefficient supply of oxygen has been a major obstacle that has restricted the successful engineering of thick and complex tissue constructs. The need to overcome this limitation has led to the development of vascularization tissue engineering and oxygen-generating biomaterials.[95] The oxygen concentration (usually described by oxygen tension) can have significant effects on cell behaviors that vary with cell type. For instance, low oxygen tension (*i.e.*, hypoxia) has been demonstrated to benefit the maintenance of stem cell pluripotency,[96–97] promote the proliferation of cardiomyocytes for heart regeneration,[98] and enhance tumor angiogenic responses and progression.[99–102]

Among soluble signaling molecules, growth factors are the most widely investigated cues for engineering the biomimetic cell microenvironment.[2,103–104] During development, each cell has its own specific growth factor microenvironment, in which growth factors can be generated from the same cell (autocrine signaling), nearby cells (paracrine signaling), and/or the circulatory system (endocrine signaling). Many growth factor classes have been identified since the first identification of nerve growth factors (NGFs). Those studied extensively in the context of developing 3D cell culture systems include bone morphogenetic proteins (BMPs), epidermal growth factors (EGFs), fibroblast growth factors (FGFs), vascular endothelial growth factors (VEGFs), transforming growth factors (TGFs), hepatocyte growth factors (HGFs), and platelet-derived growth factors (PDGFs). These growth factors, either freely diffusing in aqueous media or immobilized within the ECM, are usually present in the form of concentration gradients and are tightly regulated in space and time. The local concentration, spatial distribution and bioactivity of growth factors can play critical roles in regulating different cell behaviors.[105] For example, VEGFs have been shown to promote the proliferation of ECs and neuronal precursors, while VEGF concentration gradients have been shown to direct the growth of vessels toward hypoxic regions.[106–107] In addition, many cell types can secrete TGF-β1, which can be immobilized and stored in the ECM in an inactive state. The increased secretion of TGF-β1 or an increased level of active TGF-β1 has been demonstrated to stimulate the differentiation of fibroblasts into myofibroblasts, which is an essential cellular event in both wound healing and fibrosis development.[108–109] Numerous similar examples can be found for other growth factors. Moreover, different growth factors may have crosstalk effects that further regulate cell behaviors.[110] Considering these and other important roles, the controlled secretion, delivery and release of growth factors in the cell microenvironment continue to be areas of intense research focus.[111]

2.3. The ECM

The niche-specific ECM is well-known to be a critical determinant of the physiology and fate of living cells. The observation that certain lineage-specific traits arise in MSCs from

the elastic stiffness of the substratum on which they are cultured helped launch mechanobiology as a modern field.[112] However, subsequent work has raised more questions than it has answered, especially about the local cell microenvironment. As we emphasize throughout this review, the local microenvironment differs in substantial ways from the bulk ECM. Amongst the most pressing needs of the entire field are understanding the biophysics, biochemistry, and cell-environmental feedback dynamics in the local microenvironment. This is largely unknown outside of the context of 2D cell culture, and is largely an open frontier in 3D cell culture.

The distinction between the bulk ECM and the ECM within a cell's local microenvironment represents one of the most important open directions both in biological characterization of tissues and in development of functional biomimetic materials for engineering the 3D cell microenvironment. The standard paradigm of tissue engineering is to provide cells a bulk ECM with properties that guide cells to develop or sustain a desired phenotype, and, implicitly, to rely upon the cells themselves to create a local 3D microenvironment that mimics the microenvironment that would exist *in vivo*. This *in vivo* microenvironment is in general poorly understood and substantially different from the bulk ECM. An example is the glycocalyx, a layer of predominantly proteoglycans that resides on the surface of a great many cells. The glycocalyx is typically not represented in 2D cell culture, but is the major component of the ventral microenvironment for ECs *in vivo* (Figure 2).[21–22] For chondrocytes that are found within articular cartilage, a highly ordered, glycocalyx-like structure dominates the cell microenvironment over a scale of tens of nanometers,[23] but, despite being observed nearly 30 years ago, this structure has not been fully characterized. Cartilage tissue engineering, especially in the context of the role of physical factors, is quite advanced,[113–116] and the important aspects of the cell microenvironment such as mechanical and structural cues are clearly established as critical to prevent the "de-differentiation" from the chondrocytic phenotype.[117–119] However, this has been achieved by providing chondrocytes with bulk ECM rather than by explicitly replicating the exquisite nanostructured microenvironment. A major opportunity exists for new materials that explicitly reconstitute a cell's local microenvironment rather than just the bulk ECM distal to the microenvironment.

In this section, we describe key factors in bulk ECM composition and design, again recognizing that a critical rethinking is required when extending from 2D to 3D, when comparing the local cell microenvironment to bulk ECM, and when considering development of cells over time. We define bulk ECM for this purpose to be a non-cellular 3D entity composed of insoluble and interlocked macromolecules secreted by cells, and, from here out, follow the convention of the rest of the field and refer to this simply as ECM. For many cell types, and for the cells of interest in this review, the ECM takes the form of a hydrogel. As a major component of the cell microenvironment, this hydrogel not only provides structural support for cells to reside within but also provides diverse biochemical (*e.g.*, cell adhesion sites and growth factor immobilization) and biophysical (*e.g.*, structural features, mechanical stiffness and degradation) cues for regulating cell behaviors (Figure 3).[104,120–123] The composition, biochemical and biophysical properties of the ECM exist in a dynamic state that is regulated by cells and their neighbors. ECM homeostasis has been widely accepted to be essential for maintaining normal cell behaviors and tissue functions,

while destruction of ECM homeostasis can be accompanied by aberrant cell behaviors and the occurrence of such diseases as fibrosis and cancer.[124–126] A major task for engineering the cell microenvironment is to mimic or recapitulate the *in vivo* forms and functions of the native ECM within biomimetic materials. Although the compositions and properties of the ECM can be highly varied in space and time, understanding their general characteristics will be beneficial to the design of biomimetic materials for engineering the cell microenvironment.

2.3.1. Compositions—Generally, the molecular components of natural, gel-like ECM can be categorized into two classes: proteins and glycosaminoglycans (GAGs).[127] ECM proteins mainly include collagen, elastin, laminin and fibronectin. Collagen is the most abundant protein in mammals. Over 28 types of collagens have been identified, of which the most common types are fibrillar type I, II, III and V collagens and non-fibrillar type IV collagens. The distribution of different collagen types varies with tissue type. For example, type I collagen is mainly present in skin, tendon, ligament, endomysium and bone, type II collagen in cartilage, and type IV collagen in basement membrane. Collagen is a main contributor that endows tissues with tensile stiffness and strength, especially at high strain levels. Elastin is distributed in skin, arteries, veins, and lungs. It is a highly elastic protein that is usually co-localized with microfibrils, such as fibrillin or fibulin, forming elastic fibers to endow tissues with stiffness at low strain levels; in addition, elastin promotes the elastic recoil of tissues.[128] Laminin and fibronectin are important nanoscale adhesion proteins that bind cells and other ECM proteins to initiate a variety of intracellular signaling pathways.[129] GAGs are negatively charged, linear polysaccharides that are swollen with water to fill the interstitial space of ECM protein fiber networks.[130] Most GAGs are attached to protein cores to form proteoglycans (PGs), including sulfated heparin, chondroitin and keratin. The main functions of GAGs are to provide compressive resistance for tissues and to sequester soluble signaling molecules for controlling cell-soluble factor interactions. In addition, non-sulfated GAGs (*e.g.*, hyaluronic acid (HA)) can also interact with cell surface receptors, such as CD44, to direct cell behaviors. Through the combination and spatiotemporal regulation of the compositions and organizations of proteins and GAGs, the ECM needs to provide the cell microenvironment with a full spectrum of biochemical and biophysical cues. These cues must guide the cell to produce its own microenvironment that reconstitutes the essential elements of what exists *in vivo*.

2.3.2. Biochemical Cues—The biochemical cues needed to guide cells to reconstitute their microenvironment, are only partially known. Substantial effort has been devoted to one specific role of the ECM, which is to provide diverse cell adhesion ligands to specifically bind cell surface receptors (typically integrins), forming focal adhesions or hemidesmosomes.[131] Such cell-ECM adhesions are essential for the cellular transduction of microenvironmental cues from or mediated by the ECM, thus playing important roles in cell survival, spreading, proliferation, migration and differentiation.[132–133] Many ECM components possess cell adhesion ligands, including proteins (*e.g.*, collagen, fibronectin, vitronectin and laminin) and GAGs (*e.g.*, HA). The absence of cell adhesion cues in *in vitro* cell culture systems may cause cell loss and other undesired cell behaviors. Various micropatterning and microfabrication techniques, including microcontact printing,[134–135]

photopatterning,[136] dip-pen lithography,[137] and microfluidics-assisted patterning,[138] have been developed to control the density and organization of cell adhesion sites on substrates *in vitro*. Moreover, a range of studies have demonstrated the important role of cell adhesion sites in spatiotemporally regulating cell such behaviors as cell morphology, migration and differentiation.[139–141] These technologies have harnessed our mature understanding of what chemicals need to be present in the cell microenvironment. As discussed at the end of this section, ongoing challenges are identifying the temporal sequence of the presentation and appearance of these substances in 3D, and producing materials that present these.[47]

Another important biochemical role of the ECM, as has been mentioned for GAGs, is to serve as a reservoir for sequestering and storing soluble signaling molecules (*e.g.*, growth factors), regulating their spatial localization, stability and bioactivity. Such sequestration is usually mediated by non-covalent interactions between ECM macromolecules and soluble signaling molecules such as electrostatic and hydrogen bond interactions. Examples include the binding of TGF-β1 and BMP-2 to collagen II, VEGFs and PDGFs to fibronectin, and VEGFs, FGFs and PDGFs to heparin/heparin sulfate.[142–144] In addition to presenting cell adhesion ligands and immobilizing growth factors, the ECM can also provide diverse chemical functional groups, such as carboxyl (–COOH), amino ($–NH_2$) and methyl ($–CH_3$) groups on the surface of macromolecular backbones that can directly interact with cells and affect cell behaviors. As described below, controlling the time variations of this sequestration, storage, and release represent important challenges in the design of materials to serve as 3D microenvironments.

2.3.3. Biophysical Cues—From the biophysical perspective, the ECM provides cells with cues including the structural presentation of macromolecules, the mechanical stiffness of the network of these molecules, and the spatiotemporal variations of these. The ECM of most tissues present hierarchically organized, anisotropic structures that can differ tremendously from tissue to tissue.[145]

Structural features of the ECM can have profound effects on cell behaviors across broad length scales and are closely related to the performances and functions of tissues. A particularly important aspect is the hierarchical structure and organization of ECM fibers such as type I collagen fibers. For instance, fiber orientation and alignment can direct the orientation/migration of many cell types[146–147] through mechanisms including contact guidance and the structure-associated organization of cell adhesion ligands.[148–149] In addition, fiber diameter and density can also affect various cell behaviors, although they are usually associated with changes in ECM mechanical properties and biochemical cues.[150–152]

A second important structural feature is the presentation of pores formed in the interstitial space of ECM networks. Pore size and density determine the available space and provide a physically confined microenvironment for cell growth. For example, human cervical carcinoma (HeLa) cells cultured in a microfluidic cell confinement device show enhanced asymmetric and multi-daughter cell division with increased levels of uniaxial confinement.[153] Well-plate mechanical confinement platforms enable culture of massive arrays of cells in custom-confined microenvironments.[154] Cancer cells of varying origin (*e.g.*, HeLa, A549, and A375 cells) displayed uniquely increased abnormal divisions in response to

confinement. Organized porous structures (*e.g.*, unidirectionally aligned pores and gradient-distributed pores) have been widely demonstrated to provide guidance cues for cell growth.[155–156] Considering the important role of structural cues in regulating cell behaviors, substrates of varying spatiotemporally controlled topographic structures have been fabricated, including pillars,[157] pits,[158–159] grooves,[160–162] tubes,[163] wrinkles,[164] and cracks.[165] Studies of cells on these 2D substrates have made remarkable progresses in understanding cell-topography interactions, and many excellent relevant reviews already exist.[166–174] Studies on structural design for engineering the 3D cell microenvironment will be reviewed in Subsection 3.3.1.

Native tissues have mechanical properties spanning orders of magnitude, from very compliant ("soft," in the terminology of biomechanics) neural tissues with effective elastic moduli of 0.1–1 kPa, to stiff ("hard") bony tissues, in which portions of mineralized fibers can reach effective elastic moduli of over 20 million times higher.[175–177] These spatially-varying mechanical properties, along with associated mechanical cues such as the stress and strain fields that are the subject of the next subsection, constitute the mechanical component of the cell microenvironment, and their effects on regulating growth, development, and sustenance of different cell types are an area of intense research focus.[178–179]

The first set of results we mention in this context are the classic works of Adam Engler and co-workers that effectively launched the modern field of mechanobiology, including the discovery that substratum stiffness could direct the lineage specification of MSCs[112] and that a substratum with a myocardium-mimicking stiffness could promote embryonic cardiomyocyte beating.[180] Since then, many studies have revealed that matrix stiffness plays a significant role in regulating almost all aspects of cell behavior, including behaviors involved in tissue and organ development, tissue repair and disease progression. For example, matrix stiffness has been shown to direct the growth and differentiation of embryonic stem cells (ESCs), leading to organ morphogenesis and maturation.[181] In addition, when subjected to a matrix stiffness gradient, fibroblasts and MSCs usually show directed migration behavior towards stiffer substrata, a behavior termed durotaxis [182–184] that is believed to contribute to tissue repair.[182] Moreover, matrix stiffening is associated with many cancers and pathological fibrosis, with abnormal dynamic changes in matrix mechanical properties promoting tumor cell invasion and myofibroblast differentiation.[185–189]

However, a challenge for engineering artificial cell mechanical microenvironments is that mechanical properties vary over time in a manner that involves feedback between the cells and the ECM. The idea that a single mechanical set point for cells exists is often termed "tensional homeostasis" and is believed by many to be essential for maintaining normal cell and tissue functions.[4,190–191] This concept is slowly giving way to a more dynamic picture of cell and tissues, with the nonlinear viscoelastic mechanical properties of the ECM and their effects on cell mechanical responses constituting an area of intense research activity.[192–195] *In vitro* studies performed to explore underlying mechanisms of mechanotransduction (*i.e.*, how cells sense and convert mechanical cues into bioelectrochemical activities) are enriching our knowledge of how to design bulk ECM for

engineering the cell microenvironment and providing potential molecular targets for mechanotherapy.[196]

Many ECM components, typically the protein components, including collagen, elastin, fibrin, fibronectin and laminin, have cleavage sites that are specifically sensitive to cell-secreted enzymes, such as matrix metalloproteinases (MMPs), plasmin and elastase, showing cell-mediated degradation properties. These can generate forces through a Brownian ratchet mechanism.[197] Such cell-mediated ECM degradation is a common process in ECM remodeling and plays a crucial role in cell migration, proliferation and differentiation. For example, EC and tumor cell invasion in collagen have been shown to require the activation of collagenases (*e.g.*, MMP-1 and MMP-8).[198–199] MSC differentiation has been found to be directed by degradation-mediated cell contraction.[200] As an important parameter for characterizing degradation, the ECM degradation rate is tightly regulated by cells through the controlled secretion of MMPs and tissue inhibitors of MMPs (TIMPs), which is particularly important for maintaining ECM hemostasis.[201] Abnormal changes in MMP and TIMP activity might be related to aberrant ECM degradation and remodeling, and pathological breakdown of connective tissues.[124]

We note that processes like those described above arise from closely coupled biochemical and biophysical ECM cues. These are in most cases closely interconnected, and the alteration of one is usually accompanied by the alteration of the other. For instance, ECM degradation is typically accompanied by structural reorganization and decreasing mechanical stiffness. Understanding this coupling and its effects on cell function is an important goal of *in vitro* studies based on biomimetic materials with independently controlled properties.

Despite the progress listed in this section, much of our understanding of the biophysical cues within the cell microenvironment is in a state of flux. Recent mechanical modeling has shown that the fibrous nature of ECM proteins provides for a mechanical environment that differs strongly from that presented by a continuous polymer.[38–39,44] The fibrous nature of tissues has long been known to dominate the properties of the bulk ECM, and this has motivated a large literature on hyperelastic, transversely isotropic constitutive models for tissues. However, what has been identified more recently is that the fibrous nature of the ECM creates the possibility of long-distance communication between cells and their neighbors, and can enable cells to remodel the mechanical properties of their local environment through cyclical loading.[38,40,65] The latter can be achieved by both plasticity of crosslinks between fibers and by physical re-arrangement of fibers. The “molecular clutch” type relationships that describe how cells interact with the materials around them through dynamically cycling focal adhesions[202–204] are fundamentally altered when cells are cultured upon a nonwoven mesh of nanofibers.[16,205] This emerging understanding of how cells respond to bulk versus fibrous materials has critical implications for the development of tissue engineered materials, and must be incorporated into the new generation of fibrous-based biomaterials for engineering the cell microenvironment in 3D.[206–207]

2.4. Physical Fields

In addition to the biochemical and biophysical cues described above, cells *in vivo* experience, sense, and respond to a range of physical stimuli including strain and stress, electrical, magnetic, acoustic and thermal fields. Here, we group these physical cues under the heading of physical fields to distinguish their effects from those that arise from the inherent biophysical properties of the ECM. These physical cues, especially the first two, usually require mediation of the ECM to act on cells. The distinction between mechanical fields and mechanical properties has been critical since the earliest days of mechanobiology, and was the focus of foundational work from the Kaplan lab wherein mechanical stress was identified as a determinant of cell differentiation.[208]

Depending on their sources and locations, cells may experience a vast range of different stress and strain fields *in vivo*. These fields are modulated by their direct mechanical microenvironment.[209] In the vasculature, blood cells experience shear stress and shear strain from blood flow. In the heart and lungs, cells mainly experience cyclical tensile stress and strain fields. In cartilage and bone, cells mainly experience compressive stress and strain during body movement, with additional shear stresses arising from fluid flow.

The study of the effects of mechanical fields on cells has been advanced substantially by progress in materials science, both by materials and devices. Pivotal advances include technologies to produce physiologically relevant stress and strain fields for *in vitro* mechanotransduction investigations and for mechanically conditioning engineered tissue constructs to promote tissue maturation and regeneration.[210–211] These mechanical fields affect cell behaviors differently depending on cell type, loading method and loading parameters (*e.g.*, amplitude, waveform, frequency, and duration). For example, microfluidic technologies have been widely employed to fabricate vascular tissue models with endothelialized microchannels mimicking the structure and function of blood vessels. Under perfusion culture, adhered cells experience shear stress, whose amplitude can be simply adjusted by regulating the flow rate and whose patterns can be well controlled by designing the configuration of the microfluidic channels. Using these technologies, shear stress has been shown to modulate EC cytoskeletal remodeling and adhesion[212] and EC-smooth muscle cell (SMC) interaction,[213–214] and furthermore to promote cancer cell migration by activating yes-associated protein 1 (YAP-1).[215] In addition to shear stress, certain regimes of tensile stressing and straining have been shown to promote the spreading, proliferation and alignment of fibroblasts[216] and ECs,[217–219] the maturation of neonatal cardiomyocytes,[220] the myotube differentiation of myoblasts,[221] and the differentiation of MSCs toward the SMC lineage.[222] Dynamic compressive stress and strain have been shown to modulate chondrocyte biosynthesis depending on the loading amplitude, waveform and frequency.[223] Many similar examples can be listed.

In the context of tissue engineering, a broad direction for the application of mechanical fields is the guidance of cell migration, often for the purpose of seeding scaffolds. Strain and mechanical restraints are critical for determining cytoskeletal dynamics and for cell polarity.[224–226] Factors such as actin stress fiber dynamics, focal contact dynamics, and filopodial dynamics determine whether cells fluidize, reinforce, migrate, or undergo apoptosis in response to a mechanical field.[202,227] Tailoring the surface energy of tissue-engineered

scaffolds has been used to direct the mechanically induced migration of cells deep into a tissue construct.[228–229] Stress and strain fields can also guide cell distribution and invasion. Provided that stress fibers within cells do not depolymerize in response to a mechanical load,[230–231] the mechanical guidance of cells via applied stretching can be used to guide the outcome of wound healing situations and optimize the disposition and function of scar tissues.[232–233] Although the principles underlying the responses to these mechanobiological cues are still under debate,[217–219,234] and the differences between contact guidance and the effects of mechanical fields remain an open area of research,[149–150] guiding cells during tissue remodeling by controlling mechanical fields in the cell microenvironment is a promising direction.

In addition to stress and strain fields, cells may also experience physical fields such as electrical, magnetic, acoustic and thermal fields. Electrical fields can regulate cell migration, organization, proliferation, and differentiation.[235–236] In cases including cardiac tissue engineering, the electrical fields and their spatiotemporal modulation constitute a desired output rather than just an input to define composition.[50,237] From the perspective of tissue engineering, electrical fields have emerged as an effective tool to facilitate cell and tissue maturation in cardiac,[238–239] skeletal muscle,[240] neural,[241–242] and bone[243] tissue engineering. For instance, in cardiac tissue engineering, externally applied, pulsed electrical stimulation has been found to enhance the electrical communication between cardiomyocytes, synchronize their beating, and promote their maturation and mechanical output.[244–245] Although electrical and mechanical conditioning protocols are both widespread for promoting the maturation of cardiac tissue constructs, much is still unknown about how best to provide such tissue constructs with the most realistic microenvironment; about how electrical, mechanical, and material factors interact; and about how cell-cell interactions modulate the effects of these physical fields.

Magnetic, acoustic and thermal fields are not widely used for engineering the cell microenvironment, but nevertheless have potential. Although magnetic fields arising in clinical scanning such as the magnetic resonance imaging (MRI) are known to be safe for humans, and adverse effects on cultured cells in 3D have not been observed, high magnetic fields are known to align the mitotic spindle during mitosis and to align collagen and fibronectin during polymerization. Magnetic fields are thus a potential tool for engineering the cell microenvironment. Acoustic fields may induce deformation of soft materials, including cells and tissues, through generating acoustic radiation force.[246–247] Xin and Lu recently developed a novel acoustomechanical field theory[248–250] to describe how soft materials respond to ultrasonic waves, enlightening the potential application of acoustic fields in engineering the cell mechanical microenvironment. Regarding thermal fields, although the human body is often considered an isothermal system, cell activity across temperature ranges is important in both physiology and pathophysiology, with temperature varying over the body and over the course of a day. The enzyme-catalyzed biochemical reactions central to metabolism are sensitive to temperature variation,[251] and temperature changes in the cell microenvironment is well known to impact cell behavior in thermal pain, in fever from viral and bacterial infections, and in autoimmune disorders and certain cancers.[252–253] Thermal interventions are widely used in cancer therapy[254] and Chinese traditional moxibustion. Despite progress in engineering the thermal cell microenvironment

through theranostic-type nanoparticles that both generate heat and sense temperature,[255–259] little is known about how to employ this to engineer the cell microenvironment.

2.5. Dimensionality: From 2D to 3D and 4D

A central theme in our discussion is the need to understand and emulate how the cell microenvironment evolves over time. This has been termed engineering of the 4D cell microenvironment (Figure 4),[260] and we note it as a critical need for development in tissue engineering. Most of what is known about engineering the cell microenvironment has come from 2D monolayer cell culture models. However, reductionist 2D models oversimplify the 3D *in vivo* cell microenvironment. For instance, cells cultured in 2D can only have cell-ECM adhesions on the substrate side and cell-cell adhesions in the horizontal plane, while in 3D, cells can generate adhesions on all sides. The extreme asymmetry of the adhesion distribution may result in unnatural apical-basal cell polarity and corresponding changes in different cell functions.[261] In addition, cells cultured in 2D can spread and migrate freely without physical constraints, whereas cells cultured in 3D are usually constrained by a surrounding matrix and must fit through matrix pores and even degrade the matrix for spreading and migrating.[262] Consequently, cell migration speed and its responses to stiffness changes in 2D and 3D can be dramatically different.[263] Moreover, soluble factors in 2D cell culture systems can undergo free diffusion and rapid convective transport in an aqueous medium, whereas in 3D matrices, the transport and distribution of soluble factors are usually affected by barrier and immobilization effects of the matrix components, leading to spatially graded cell responses.[264–268]

Cells cultured in 3D exhibit behaviors more relevant to *in vivo* conditions than do cells cultured on 2D substrata, including adhesion, spreading, mechanics, cytoskeletal organization, proliferation, migration, differentiation, apoptosis, and responses to signaling molecules and drugs.[269–273] A classical example, mentioned above, is de-differentiation of chondrocytes away from their physiological phenotype when cultured in 2D.[117] Benya and Shaffer[274] showed these de-differentiated chondrocytes could recover their physiological phenotype via 3D culture. Bissell and colleagues[275] showed that normal human breast epithelial cells exhibit a tumorigenic phenotype in 2D culture, but maintain a normal phenotype in 3D culture. Significant ongoing efforts directed toward engineering 3D tumor models and recapitulating the associated tumor microenvironment[276–279] demonstrate that 3D tumor models better represent both *in vivo* tumor cell growth and *in vivo* responses to drugs than can traditional 2D monolayer models, including Ewing sarcoma cells,[280] breast cancer cells,[281] and prostate cancer cells.[282]

On account of the above findings, numerous 3D biomimetic materials (typically hydrogels) and fabrication approaches have been developed for constructing 3D cell culture models and engineering the 3D cell microenvironment.[283–284] However, as discussed throughout this section, nearly all components of both the cell and the bulk ECM change over time, leading to dynamic variation or continuous remodeling of the 3D cell microenvironment (Figure 4). In cases of cancer cell models, understanding and modeling this 4D evolution is critical to producing realistic *in vitro* culture models. In cases of engineered tissues for surgical use,

drug screening, or basic science, controlling the 4D evolution of the cell microenvironment is of critical importance for replicating physiological tissues.

An example of engineering the 4D cell microenvironment is using biomimetic materials with time-modulated properties (*i.e.*, 4D biomimetic materials) that respond to external stimuli, such as light, temperature, and magnetic fields.[285–286] In particular, the development of photoclick chemistry has enabled the development of many types of photosensitive hydrogels that provide cells with well-controlled spatiotemporal biochemical and biophysical cues.[47] Another example involves exploiting the active remodeling of the microenvironment by cells themselves, including soluble factor secretion and matrix deposition, degradation, and reorganization. For instance, the pathological transition of cardiac fibroblasts to myofibroblasts can lead to significant collagen secretion and accumulation and ultimately result in matrix stiffening, which can in turn further promote the generation of myofibroblasts.[287–288]

A more recent direction is 4D bioprinting technologies that aim to fabricate engineered tissue constructs, taking into account 4D biomimetic materials and cell-induced matrix remodeling.[289–291] Accordingly, 4D characterization technologies that enable the real-time and *in situ* monitoring of cell microenvironment changes have also drawn much research attention.[292–293] These technologies offer much promise, and represent an important direction for future development in this area.

3. Functional and Biomimetic Material Designs

Having laid out the key challenges in understanding the cell microenvironment in Section 2, we now describe the state of the art in designing functional and biomimetic materials to engineer the cell microenvironment. A central challenge is providing both bulk ECM and local environmental properties to a cell, and because this challenge cannot usually be met, one must often choose between the two. However, this is not in vain: the technological need for such materials is not only to recapitulate *in vivo* ECM and cell-microenvironment interactions, but also to construct synthetic microenvironments that are not usually encountered by cells *in vivo* for fundamental studies.[294–296] Large numbers of studies over the past decade[297–299] have generated material systems that enabled the development of our understanding of how biochemical (*e.g.*, cell adhesion ligands, soluble factor immobilization, and chemical functional groups) and biophysical (*e.g.*, structural properties, mechanical properties, degradability, and electrical conductivity) cues affect cells (Figure 5).[300–303] However, the ways that these cues vary in space and time and can act independently or synergistically on cells to form complex microenvironmental networks are still uncertain.[285] We describe in this section the broad classes of state of the art approaches to synthesizing materials that can both guide development of the cell microenvironment and serve as tools for understanding it.

3.1. Classification of Biomimetic Materials

We begin by defining biomimetic materials as materials with structures, properties or functions mimicking those of natural or living matter.[304–308] From the materials perspective, biomimetic materials can be generally classified as metallic, ceramic, or polymeric

materials. Traditional metallic and ceramic materials have been extensively investigated and engineered into hard tissue implants for clinical applications, while polymeric materials, especially 3D polymer scaffolds and hydrogels, have attracted much more interest in soft tissue engineering.[304,309–310] Most biomimetic materials used for engineering the 3D cell microenvironment are based on hydrogels,[302] and our focus therefore lies on these.

Hydrogels are water-swollen networks of polymeric materials. The main advantages of hydrogels for engineering the cell microenvironment include their high water content, their biocompatibility, their structural similarity to native ECM, their easy handling and processing, and their tunable biochemical and biophysical properties.[311–312] The various types of hydrogels that have been developed can be classified in many ways, as follows: physically or chemically crosslinked hydrogels, according to their crosslinking strategies; neutral, anionic, or cationic hydrogels, according to their electrical properties; and magnetically responsive, electrically conductive, temperature-sensitive or photosensitive hydrogels, according to their physical performances. Here, we first briefly present 3D polymer scaffolds, and then introduce hydrogels by classifying them as naturally derived, synthetic or hybrid hydrogels, according to their origins and compositions (Figure 6).

3.1.1. 3D Polymer Scaffolds—3D polymer scaffolds discussed in this section, as a wide class of traditional biomimetic material platforms used for 3D cell culture, mainly refer to water-insoluble polymer scaffolds with porous structures that allow the ingrowth of surface-seeded cells. These have enjoyed widespread application, but are in general highly limited both because of the constraints that they impose upon cells and because they fail to recapitulate the fibrous character of native ECM proteins.

Polymers used for fabricating scaffolds are usually dissolved in organic solvents and engineered into 3D porous forms after the organic solvents are removed or substituted. The most commonly used degradable synthetic polymers are poly(α-esters), typically including poly(glycolic acid) (PGA), poly(lactic acid) (PLA), polycaprolactone (PCL) and their copolymers such as poly(lactide-co-glycolide) (PLGA, random copolymerization of PGA and PLA). Poly(α-esters) are thermoplastic polymers that contain aliphatic ester linkages in the backbone and therefore are usually hydrolytically degradable. The degradation rate and mechanical property of different types of poly(α-esters) can be significantly different. For example, PGA normally exhibits a rapid degradation rate, resulting in rapid loss of mechanical strength of the polymer scaffolds and local accumulation of glycolic acid that may induce intense inflammatory response. Compared to PGA, PLA exhibits a much slower degradation rate and is mechanically stiffer and much more stable in aqueous environment. Accordingly, as a copolymer of PGA and PLA, PLGA integrates the advantages of both PGA and PLA and shows well-controllable degradation rates and mechanical properties. The above poly(α-esters) have been approved by the US Food and Drug Administration (FDA) for biomedical applications and widely used in absorbable sutures, stents, drug delivery vehicles, wound dressings, and 3D polymer scaffolds for hard tissue engineering.[313–314] However, the 3D polymer scaffolds derived from poly(α-esters) typically present high rigidity and low ductility, which has limited their broad application in soft tissue engineering.[315] In addition, poly(α-esters) are often hydrophobic with poor wetting and cell adhesion capacity. Moreover, poly(α-esters) often undergo bulk erosion (*i.e.*, degradation

occurs both on the surface and within the interior) with non-linear degradation kinetics, which can be disadvantageous in controlled release applications. In this regard, surface eroding (*i.e.*, degradation occurs only on the surface) polymers such as polycarbonates and polyanhydrides can be preferred.[316–319]

3D polymer scaffolds normally work as temporary structures for supporting cell growth and implantation. The objective is for the scaffold materials to degrade and be gradually replaced by cell-secreted ECM. Therefore, the compatibility of the scaffold materials and their degradation byproducts should be ensured, and the degradation rate should match the generation rate of new ECM.[320] Since cells are often seeded post fabrication, the geometries and porous structures of the 3D polymer scaffolds can be well controlled by employing various microfabrication technologies, although many of these are toxic to cells.[319]

However, many important and persistent challenges exist for using such materials for engineering the cell microenvironment. The distribution and organization of cells in the scaffolds are usually poorly controlled because cells are often locked into their positions (usually on the surface) after setting of the polymer, and in 3D polymer scaffolds these positions are typically a result of random motion during mixing. In addition, as described in Section 2, the absence of a fibrous character can obstruct the development of normal cell-cell communication and disrupt normal cell-ECM mechanobiology including cycling of molecular clutches. In contrast, the hydrogels introduced below allow 3D cell encapsulation during hydrogel formation and thus hold the potential to precisely control the distribution and organization of cells in 3D. Moreover, hydrogels can be engineered to have stiffness spanning a wide range (from Pa level to GPa level) and be highly stretchable, thus showing great promises in engineering the 3D cell microenvironment for both soft and hard tissues. Finally, hydrogels can be readily functionalized in ways that enable them to vary over time, thereby serving as platforms for 4D cell culture.

3.1.2. Naturally Derived Hydrogels—Naturally derived hydrogels are extracted or reconstituted from natural sources, including both mammalian and non-mammalian sources. One type of commonly used naturally derived hydrogel from mammalian sources is based on decellularized ECM, which can be harvested by removing cells and antigens from tissues with detergents.[321–322] Many types of decellularized ECM have been developed from different organs or tissues, such as the heart,[323–324] liver,[325] lung,[326] kidney,[327] skeletal muscle,[328] tendon,[329] cartilage,[330] dermis,[331] bladder,[332] and adipose tissue,[333] as well as the central nervous system (CNS).[334] Such decellularized ECM can retain a close-to-native tissue or organ architecture (*e.g.*, vascular networks) and composition containing multiple native proteins, specific cell adhesion ligands and soluble factors such as angiogenic factors.[335–336] In one example, the Taylor group[337] decellularized a whole rat heart and repopulated it with neonatal cardiac cells and aortic ECs. These cells were found to form a native-like organization in the decellularized heart ECM. After perfusion culture under simulated cardiac physiological conditions, an artificial heart with macroscopic contraction and nascent pumping function was obtained. Similar studies have also been reported for engineering other tissues/organs such as the liver,[325] lung,[326] bone,[338] and blood vessel.[339] This progress shows promise, but, as described below, challenges remain.

Decellularized ECM can be processed into hydrogel forms with different shapes for cell culture or for injection into the body for *in situ* tissue regeneration.[327,340] For example, a decellularized myocardial ECM-based hydrogel has been shown to enhance the cardiogenesis of cardiac progenitor cells in 3D *in vitro* culture.[323] A decellularized kidney ECM-based hydrogel has been shown to effectively regulate the growth and metabolism of kidney stem cells in a manner with regional specificity.[327] An injectable hydrogel derived from decellularized skeletal muscle ECM has been found to support the proliferation and infiltration of muscle cells, promote neovascularization and recruit progenitor cells *in vivo*.[328]

The technologies described in the previous two paragraphs are, however, largely pre-clinical. Despite the long history of and the striking advancements in the preparation and biomedical applications of decellularized ECM, the composition of decellularized ECM varies across donors and remains poorly understood.[341] It is therefore difficult to identify effective components and control their relevant properties for engineering the cell microenvironment for universal applications. Important areas of future inquiry are developing an understanding of the hierarchical structure and fiber-fiber crosslinking that is typical of the ECM from different organs, and developing a toolset to re-engineer these reliably and robustly for organ replacement.

In contrast with decellularized ECM-based hydrogels, purified naturally derived hydrogels have better-defined compositions and improved controllability of their biochemical and biophysical properties. Such hydrogels can be divided into two categories: protein-based hydrogels, and polysaccharide-based hydrogels. Protein-based hydrogels can be fabricated from individual protein components, such as collagen, gelatin, elastin, fibrin, fibronectin, and silk fibroin, or from protein mixtures, such as cell-derived Matrigel. These hydrogels are usually generated through the crosslinking or self-assembly of biomacromolecules composed of natural amino acid sequences under physiological conditions. They are the most commonly used biomimetic materials in 3D cell culture and microenvironment engineering, mainly due to their inherent advantageous properties, including biocompatibility, conduciveness to cell adhesion, and susceptibility to cell-secreted enzymes and cell-mediated remodeling.[342–343] In addition, many types of protein-based hydrogels (*e.g.*, those based on type I collagen, elastin, fibrin, fibronectin, or silk fibroin) have characteristics of controlled fibrous and hierarchical structures, which provide additional topographic and mechanical cues for guiding cell behaviors.[344–346] Nevertheless, protein-based hydrogels also have shortcomings that need to be overcome.

Foremost amongst the shortcomings of protein-based hydrogels is batch−to−batch variability. One central challenge is that, possibly because physiological heterogeneity of collagen crosslinking is not well understood.[REF 671] collagenous tissue constructs synthesized under nominally identical conditions can have stiffnesses that can differ by more than a factor of two.[347] Furthermore, the stiffness of reconstituted collagen hydrogels is typically orders of magnitude lower than that of native tissues.[348] Poorly controlled degradation, unquantified impurities and undesired immunogenicity are additional challenges.[349] Moreover, the materials are inherently complicated because they are rich in bioactive cues, many of which are not understood. These numerous interactions with cells

make it challenging to independently study the effects of individual material cues on cell behaviors. In the specific context of the cell microenvironment, the specific compositions and spatial disposition of protein fibers are not known for most cell types, and one cannot be certain from behavior at the level of the tissue construct whether the local microenvironment is representative of that which might exist *in vivo*. Finally, the ability to enable true 4D control of the cell microenvironment is limited when using protein-based hydrogels.

Compared with protein-based hydrogels, polysaccharide-based hydrogels (*e.g.*, those based on chitosan, alginate, agarose, dextran, or HA) are also biocompatible and gellable under mild conditions, but they can be less immunogenic and have more widely tunable mechanical properties.[350] However, some important polysaccharide-based hydrogels, such as those based on chitosan or alginate, cannot support cell adhesion and are not biodegradable. Therefore, chemical modification is usually required to incorporate cell adhesion and/or degradable sites into such hydrogels.[351–352] While many protein- and polysaccharide-based hydrogels (*e.g.*, those based on collagen, gelatin, chitosan, alginate, or HA) can be physically crosslinked by varying the temperature, pH or ion concentrations, they may lack sufficient mechanical strength and stability for long-term cell culture and *in vivo* tissue regeneration applications. For this reason, chemical crosslinking via glutaraldehyde, genipin, or microbial transglutaminase is often applied; however, these methods may generate toxic byproducts or require long reaction times that restrict their application in 3D cell culture or the rapid prototyping-based fabrication of complex tissue constructs.[353]

To overcome these limitations, chemical approaches, typically acrylate and thiol modifications, have been developed to modify macromers of the above naturally derived hydrogels to render them rapidly crosslinkable under cytocompatible conditions.[354–355] It should be noted that the chemical modification of collagen and gelatin is usually accompanied by a decrease in bioactivity. Although these materials have already shown potential in engineering the 3D cell microenvironment and been implemented in a variety of biomedical applications, substantial work in both characterization and synthesis is needed to overcome the above many persistent challenges.[354,356]

3.1.3. Synthetic Hydrogels—Synthetic hydrogels are hydrogels fabricated using synthetic chemistry strategies, typically the crosslinking of bioinert chemical monomers or macromers. As an alternative to naturally derived hydrogels, synthetic hydrogels have their own specific advantages. For example, the composition and chemistry of synthetic hydrogels can often be custom-designed and precisely controlled, significantly improving their reproducibility and physicochemical tailorability.[357–358] Although synthetic hydrogels are usually bioinert and nondegradable, they can be readily modified to have user-desired biological functionality.[312,359–360]

Numerous synthetic hydrogels, including those based on poly(acrylamide) (PA), poly(ethylene glycol) (PEG), poly(vinyl alcohol) (PVA), poly(2-hydroxyethyl methacrylate) (PHEMA), poly(*N*-isopropylacrylamide) (PNIPAAm), and their derivatives, have been developed to engineer the cell microenvironment for biomedical applications.[317] While PA hydrogel substrates coated with such biological proteins as collagen and fibronectin have

been widely used for engineering the 2D cell microenvironment, PEG-based hydrogels are perhaps the most commonly explored synthetic hydrogels for engineering the 3D cell microenvironment. PEG-based hydrogels can be formed under cytocompatible conditions via numerous crosslinking strategies, such as chain-growth polymerization, Michael-type addition, thiol-ene addition, Diels-Alder chemistry, and strain-promoted azide-alkyne cycloaddition (SPAAC).[361] These hydrogels exhibit unique properties, such as high hydrophilicity and low protein adsorption, and they are usually considered "blank state" materials that enable the user-defined incorporation of a wealth of bioactive molecules.[360,362] Moreover, PEG-based hydrogels that are sensitive to light are particularly useful for engineering the 3D cell microenvironment in a spatiotemporally controlled manner. As described at the end of this section, these strengths are tempered by a range of limitations.

In addition to the above traditional synthetic hydrogels, hydrogels synthesized using supramolecular chemistry (*i.e.*, supramolecular hydrogels) have attracted great research interest in the past decade for applications in tissue engineering and regenerative medicine.[363–365] Supramolecular hydrogels are rationally designed hydrogels that exploit the specific, tunable, reversible and non-covalent supramolecular interactions between molecular recognition motifs, which are typically custom-designed peptides. Reversible supramolecular interactions are particularly useful in creating stimuli-responsive supramolecular hydrogels that can be remodeled by cells for dynamically engineering the cell microenvironment.[366] Moreover, such supramolecular interactions give rise to supramolecular hydrogels (especially peptide- or recombinant protein-based supramolecular hydrogels) with unique biochemical and biophysical properties that are difficult to achieve using traditional synthetic hydrogels.[367–368] For instance, by custom-designing the sequences of peptide building blocks and controlling their self-assembly process, it is possible to generate supramolecular hydrogels that can replicate hierarchically organized structural features of the native ECM from the nano- to the macroscale and replicate the cell adhesion cues, biodegradability and growth factor-binding affinity of naturally derived hydrogels.[369–372] These are highly amenable to photodegradable crosslinks that can enable changes in material properties over time and help implement 4D control of the cell microenvironment. However, despite these advantages, supramolecular hydrogels are far from perfect for engineering the cell microenvironment.

Supramolecular hydrogel chemistry has several limitations in the context of engineering the cell microenvironment. Foremost amongst these limitations is the relatively weak mechanical strength and stiffness of supramolecular hydrogels compared with those of naturally derived and traditional synthetic hydrogels.[373] In addition, the self-assembly process of peptide building blocks and thus the structural and mechanical properties of the generated hydrogels are susceptible to bioactive peptide modifications. Furthermore, it is currently not cost-effective to use peptide-based supramolecular hydrogels for large-scale biomedical applications. Important directions for future inquiry with these materials include development of peptide chemistry that can enable mass production of peptide-based supramolecular hydrogels,[374–375] and improvement in their mechanical properties.

3.1.4. Hybrid Hydrogels—The development of hybrid hydrogels is motivated by the limitations of the aforementioned technologies. The individual components of neither

naturally derived nor synthetic hydrogels are capable of meeting all of the requirements for 3D and 4D cell culture and corresponding biomedical applications. Although chemical modifications can be used to enhance the biochemical and biophysical performances of single-component hydrogels, the modification process can be harmful to cells, time consuming, expensive, and too complex to be widely adopted. In contrast, hybrid approaches enable the simple and rapid generation of hydrogels that integrate the advantages of each component and potentially exhibit novel attractive properties.[376]

Hybrid approaches that have met with success largely involve blending, copolymerization and interpenetration. Blending and copolymerization are representative physical and chemical approaches, respectively, to generate hybrid hydrogels from two or more components. Although easy to perform, they are limited, in part because one cannot in general retain the full advantages of each individual component, and in part because only certain combinations of hydrogels can be copolymerized. By comparison, interpenetration is an interesting approach to fabricate interpenetrating polymer network (IPN) hybrid hydrogels, which are characterized by partially or fully interlaced polymer networks and may exhibit surprising properties that cannot be achieved by using single network.[377–379] For instance, collagen has been combined with alginate[380–381] or PEG[382–383] to fabricate IPN hybrid hydrogels in which the bioactivity of collagen is retained and the mechanical properties of the hybrid hydrogels are tuned by adjusting the alginate (or PEG) concentration or crosslinking density. Alginate has also been combined with PEG,[384–385] PVA,[386] PNIPAAm[387] or PA[388–390] to generate IPN hybrid hydrogels with exceptional mechanical properties such as high stiffness, ductility, strength or toughness. These hybrid hydrogels have properties that are often difficult to predict using homogenization theory, and can have properties such as stiffness or toughness that are greater than the stiffness or toughness of either of the constituents. A limitation of approaches is that, because no universal framework exists for predicting the properties of a hybrid hydrogel from the properties and volume fractions of its constituents, the concentration of each component and the ratios of the different components must be carefully optimized in an *ad hoc* fashion for each practical application, and the approach is therefore somewhat limited. Mathematical homogenization theories to predict how the properties of such hydrogels emerge from the properties of their constituents represent a pressing need.

Alternatively, hybrid hydrogels can also be generated by incorporating nanoparticles into hydrogels. We term these nanocomposite hydrogels.[391] The generation of nanocomposite hydrogels was initially inspired by the compositions and structures of nano-reinforced native bone tissues, which are mainly composed of collagen, water, and hydroxylapatite nanocrystals.[304] Nanoparticles can be physically entrapped within hydrogel networks or chemically used as crosslinkers to crosslink hydrogels. Mobility of crosslinking nanoparticles is hypothesized to endow networks with enhanced toughness.[392–394] Several successful classes of hybrid hydrogels containing nanoparticles or nanostructures have been developed. These include inorganic and non-metallic nanoparticles (*e.g.*, hydroxyapatite, calcium phosphate, silica and silicate nanoparticles),[395–398] metal/metal-oxide nanoparticles (*e.g.*, gold, silver, and iron-oxide nanoparticles),[399–404] polymeric nanoparticles (*e.g.*, cyclodextrin and hyper-branched polyester nanoparticles),[405–406] and carbon-based nanostructures (*e.g.*, CNTs and graphene).[407–409] These nanocomposite hydrogels can

exhibit enhanced properties such as improved mechanical stiffness and strength and enhanced magnetic responsiveness, electrical conductivity, and optical and thermal properties.[410–411] They may provide well-controlled biophysical cues for engineering the cell microenvironment and have been implemented in a wide variety of applications in drug delivery and hyperthermia therapies, as well as proposed theranostic procedures.[412–413] However, as described below, these materials are fundamentally limited at present for tissue engineering applications.

A major issue associated with nanoparticle-containing hydrogels is biocompatibility: nanoparticles are in general questionable for use *in vivo* due to uncertainties about their long-term toxicity. Because the nanometer scale of these particles is needed for successful doping of the polymer backbone of the hydrogel, substantially more must be known about the long-term toxicity of nanoparticles before these materials can reach widespread *in vivo* application.

3.2. Biochemical Designs

The biochemical properties of biomimetic materials can exert important influences on cell behaviors including cell adhesion, spreading, migration, proliferation, alignment and differentiation.[414–415] Subtle variations in a material's biochemical properties may lead to significant changes in cell behaviors. Therefore, biomimetic materials and their chemical modifications offer broad potential for designing a bulk ECM that enables cells to reconstitute their own local microenvironment, or that mimics the biochemical aspects of the native microenvironment itself. We critique the state of this effort below.

3.2.1. Cell Adhesion Ligands—Cells in solid tissues rely on adhesion to their microenvironment and the ECM to maintain their activity and perform many of their biological functions. Therefore, cell adhesivity is a critical component that should be considered in biomimetic material design.

Naturally derived proteins (*e.g.*, collagen, gelatin, laminin, vitronectin, and fibronectin) retain many cell adhesion ligands that can be recognized by heterodimeric cell surface integrin receptors. In contrast, some polysaccharide-based natural materials (*e.g.*, alginate and agarose) and most synthetic materials (*e.g.*, PEG) are non-adhesive to cells due to a lack of adhesion ligands and therefore require surface or bulk modifications for engineering the cell adhesion microenvironment. A straightforward way to endow such materials with cell adhesive cues is to incorporate full-length ECM proteins, such as collagen, gelatin, laminin and fibronectin.[416] These full-length proteins can be physically trapped in a bulk hydrogel if their hydrodynamic radius is larger than the mesh size of the hydrogel, non-covalently absorbed onto a hydrogel surface through electrostatic interactions, or even covalently linked to a hydrogel network via chemical bonds.[417] Although this approach is effective, it is not the most widely used because of the limitations of poorly controlled spatial distribution and temporal presentation of full-length proteins.

To overcome these limitations, bioorthogonal photochemistries have recently been extended to reversibly pattern full-length proteins in hydrogels in a spatiotemporally controlled manner (Figure 7).[418] These offer controllable 4D constructs that can present cells with

spatiotemporally varying biochemical cues. Nevertheless, more work is needed to refine these approaches because multiple ligand-receptor interactions can occur in a single system due to the presence of multiple ligands in individual full-length proteins, making it difficult to independently investigate separate signaling pathways for fundamental cell biology studies. In addition, the use of native proteins is also less desirable because of the possibility of eliciting immune responses.

With the development of synthetic biology, bioactive peptide modification has emerged as an alternative and facile way to induce cell adhesion cues into inert biomaterials.[312] Peptides consisting of select amino acid building blocks can mimic the functional unit of full-length proteins. However, peptide sequences are much shorter and their structures are much simpler than those of full-length proteins, making their synthesis and purification much easier. Moreover, peptides can be custom-designed and engineered into hydrogels in a well-controlled manner. Many kinds of peptides have been identified and artificially produced, including Arg-Gly-Asp (RGD), Ile-Lys-Val-Ala-Val (IKVAV), Tyr-Ile-Gly-Ser-Arg (YIGSR), Arg-Glu-Asp-Val (REDV), and Gly-Phe-Hyp-Gly-Glu-Arg (GFOGER).[419–420] Studies have shown that the ligand type, concentration and spatial distribution (*e.g.*, ligand gradient, ligand separation, and individual pattern size) can affect cell adhesion, spreading, migration, proliferation and differentiation.[421–426] For instance, by controlling cell shape (*e.g.*, spreading area, aspect ratio, and curvature) with adhesive islands on substrates, the fate and function of stem cells (*e.g.*, hMSCs and human ESCs) can be regulated independently from other cues, such as soluble factors.[427–429] Moreover, adhesive cues that are dynamically switchable on 2D substrata under various stimuli (*e.g.*, biological signaling, voltage, light, mechanical force, and click chemistry) have been fabricated to elucidate dynamic cell responses to adhesive cue changes.[430–431] Translating these 2D successes to 3D and 4D represents an important challenge.

The successes of these 2D studies have motivated extension of these approaches to bulk modification of hydrogels with peptides for 3D cell culture. In early studies of bulk 3D hydrogel modification, peptides were usually mixed thoroughly with a hydrogel precursor solution and covalently bound to the polymer network during the gelation process, resulting in a homogeneous peptide distribution in the hydrogel.[432–433] This approach has seen widespread use, especially with cysteine-containing peptide sequences conjugated into PEG-based hydrogels via thiol-acrylate mixed-mode photopolymerization,[434] thiol-acrylate or thiol-vinyl sulfone Michael-type addition,[435–437] or thiol-norbornene step-growth photopolymerization.[438] Peptide epitopes can also be conjugated to precursor molecules before gelation, as in the case of alginate molecules modified with RGD and heparin-binding peptides via carbodiimide chemistry[439–440] for the purpose of developing macroporous scaffolds for neonatal rat cardiac tissue constructs. These modified, thoroughly mixed 3D hydrogels have been used to mimic cell-cell interactions including tumor microenvironments. Bian *et al.*[441] incorporated N-cadherin mimetic peptides into HA hydrogels to interact with encapsulated hMSCs, mimicking cell-cell adhesion mediated by N-cadherin; the conjugated peptides promoted chondrogenesis and neocartilage formation both *in vitro* and *in vivo*. An example of a successful model of cancer cell invasion consists of four-arm PEG functionalized with peptide motifs (*i.e.*, RGD, GFOGER, or IKVAV) that was obtained and then gelled with heparin via Michael-type addition to form hybrid

hydrogels in the presence of breast (MCF-7) or prostate (PC-3, LNCaP) cancer cells.[442] These systems are promising, and subsequent development of technologies to enable spatiotemporally tunable adhesive epitopes[443] might serve as a foundation to enable replication of the heterogeneous 4D cell microenvironments found *in vivo*.

A simple way to fabricate bioactive hydrogels with spatially patterned adhesive cues is by blending and gelling adhesive-modified and unmodified hydrogel precursors in a single system. In this way, bimodal alginate hydrogels with alternatingly presented RGD-modified and RGD-free microchanneled blocks were developed. Aligned microchannels can be subsequently introduced by uniaxial freeze-drying.[444] The spreading, viability, spatial organization, and differentiation of human bone marrow MSCs (hBMSCs) in microchannels with the RGD modification are significantly enhanced compared with those in microchannels without RGD modification. In another study, HA hydrogels with RGD clusters, fabricated by mixing and gelling RGD pre-functionalized and un-functionalized portions of acrylated HA showed significant changes in the spreading of and integrin expression by encapsulated mouse MSCs compared to MSCs in HA hydrogels with un-clustered (*i.e.*, homogeneously distributed) RGD.[445] Despite these promising findings, the above methods can only be used to produce simple and static adhesive patterns in hydrogels. Supramolecular systems based on hydrogen-bond or host-guest interactions have emerged to enable dynamic tuning of the presence of bioactive ligands, thereby offering improved controllability.[446] However, much work remains to be done to exploit the capacity of these systems for engineering the 3D adhesion microenvironment.

To enable the well-controlled 4D spatiotemporal generation of cell adhesion patterns in hydrogels, several groups have directed significant efforts toward developing advanced hydrogel photopatterning systems. The Shoichet group reported a photolithography method for patterning maleimide-functionalized Gly-Arg-Gly-Asp-Ser (GRGDS) into agarose hydrogels modified with 2-nitrobenzyl (2-NB)-protected cysteine (Figure 8A).[447] Dorsal root ganglia cells seeded on top of the hydrogel were guided to migrate and grow along the patterned domains. This method was later expanded to more complex 3D patterns in agarose hydrogels modified with a 6-bromo-7-hydroxycoumarin sulfide derivative using two-photon photolithography.[448] Recently, the Schlierf group developed a method for creating 3D patterns in PEG hydrogels based on the infrared (IR) light-mediated two-photon cycloaddition of maleimide groups.[449] Although these methods enable the formation of complex adhesion patterns in 3D hydrogels without changing the bulk mechanical properties of the hydrogels, the use of cytotoxic maleimides may limit their *in situ* 3D patterning applications.[450] Alternatively, the West group[451–453] developed an approach for spatiotemporally patterning cell adhesion moieties (*e.g.*, acryl-PEG-RGDS) in pre-crosslinked PEG diacrylate (PEGDA) hydrogels. In their approach, PEGDA hydrogels were first fabricated via an initial radical chain photopolymerization. Acryl-PEG-RGDS was then swollen into the network and immobilized in particular regions via selective ultraviolet (UV) light exposure in the presence of a photoinitiator and living cells. This approach enabled the creation of highly complex cell adhesion patterns in hydrogels that mimic specialized tissue features (*e.g.*, 3D vasculature of the retina, cerebral cortex, and heart, as well as essential elements of the subependymal zone neural stem cell (NSC) niche) for guiding cell

organization.[454] This work represents important progress, but, as described below, much work remains to be done.

As mentioned above, a limitation of hydrogels based upon click reactions is cytotoxicity. A photopatterning hydrogel system that overcomes this was developed by the Anseth group (Figure 8B),[455] who reported the generation of PEG-based hydrogels via a copper-free SPAAC click reaction, followed by the photopatterning of biochemical molecules through an orthogonal thiol-ene photocoupling reaction. By overcoming the cytotoxicity of traditional click reactions, their method enabled the 3D encapsulation of cells during hydrogel formation.[455] PEG-based hydrogels with various peptide ligand densities[456] and multiple well-controlled peptide gradients were fabricated[457] hMSCs in such 3D hydrogels showed a monotonic increase in cell migration speed with increasing peptide ligand density rather than a biphasic trend, as observed in 2D.[456] In addition, the Anseth group has also introduced a method to tether peptides (*e.g.*, RGDS) to a PEG backbone with a photolabile ortho-NB (o-NB) moiety, rendering the peptides photoreleasable on demand *in situ*.[458–461] Temporal removal of RGDS during cell culture did not affect hMSC viability but did induce chondrogenic differentiation[458] and local NIH 3T3 cell detachment.[461] Recently, this group introduced an allyl sulfide-functionalized PEG hydrogel system that enables the reversible exchange of biochemical ligands in the presence of living cells, further enhancing the spatiotemporal controllability of photopatterning.[462]

The above advanced hydrogel photopatterning systems have shown great promise in spatiotemporally manipulating the 3D cell biochemical microenvironment. Nevertheless, the use of small synthetic peptides can only partially mimic the structure or function of full-length proteins since such proteins can have high specificity and rather complex bioactivity. A key question is, have these major strides in cell microenvironment biochemistry come at the expense of cell microenvironment biophysics? For example, cell adhesion ligands in native proteins can be hidden under secondary protein structures and may not always be exposed to surrounding cells. Therefore, the bioactivity of these ligands is dynamically regulated by cell remodeling and external loading-induced protein deformation or conformational changes, which are difficult to fully mimic by simply incorporating small synthetic peptides into hydrogels. Additionally, by attaching these ligands to hydrogel backbones with non-physiological stiffness, it is possible that key behaviors such as those associated with molecular clutch kinetics are disrupted in such systems. Finally, these hydrogel systems present biochemical flexibility at the expense of the fibrous nature of the ECM, which, based upon earlier discussion, can be expected to interfere with long-distance cell-cell communication. Further studies are needed to engineer complete cell adhesion ligands that mimic not only the biochemistry but also the biophysics of native proteins found *in vivo*.

3.2.2. Growth Factor Immobilization—A spectrum of growth factors plays important roles in cell growth, cell fate determination, disease progression, tissue regeneration, and organ development. As discussed in Section 2, the ECM can regulate the distribution and activation of growth factors and mediate their interactions with cells via control of diffusion and sequestration.[463] While many studies have exploited the effects of freely diffusible growth factors on cell behaviors, most growth factors *in vivo* are in fact sequestered or

immobilized by ECM macromolecules, such as GAGs,[464] and function by directly interacting with cell membrane receptors or after being released in response to mechanical or enzymatic stimuli. Compared with the use of freely diffusible growth factors, immobilizing growth factors in biomimetic materials may prolong growth factor presentation, prevent enzymatic growth factor degradation, enable well-controlled growth factor delivery and release, and modulate specific growth factor bioactivity and signaling.[465–467] Therefore, the tuning of material biochemical properties for growth factor immobilization has been an important biomimetic material design consideration.[468–469] The literature on controlled release and delivery of growth factors is enormous. We limit our focus here to systems suitable for 4D design of hydrogels to mimic and guide the cell microenvironment, and refer to reader to other reviews[470–472] for coverage of release and delivery through bulk scaffolds, polymeric vesicles or particles.[473–474]

For the purpose of immobilizing growth factors in hydrogels that guide and mimic 4D evolution of the cell microenvironment, two main strategies exist: physical (non-covalent) immobilization and chemical (covalent) immobilization.[475] Physical immobilization is the use of physical affinity interactions (*e.g.*, hydrogen bonding, hydrophobic interactions, and electrostatic interactions) between the material surface and growth factors for immobilization purposes. Hydrogels made from or modified with growth factor-affinitive molecules, including biological proteins (*e.g.*, fibronectin, collagen, gelatin, elastin, and laminin), GAGs (*e.g.*, HA, heparin sulfate, and chondroitin sulfate), synthetic materials (*e.g.*, ECM molecule mimetics, and PNIPAAm), and small peptide mimics, have been applied to physically immobilize growth factors.[471,476–480] In the following, we describe successes and challenges associated with these material systems.

As an example of a success of physical immobilization of a growth factor, we describe some successes in application of hydrogels containing immobilized heparin. Heparin is a highly anionic PG that can bind various types of growth factors through electrostatic interactions and protect the growth factors from losing bioactivity.[481] The immobilization of FGF-2 and VEGFs in heparin-modified PEG hydrogels has been shown to boost angiogenesis both *in vitro* and *in vivo*.[482–483] Alternatively, the Cohen group[484] sulfated the uronic acids in alginate to mimic the affinity interactions between heparin/heparin sulfate and growth factors. The alginate-sulfate exhibited a high affinity for various heparin-binding proteins, enabled the dose-dependent and sustained release of basic FGFs from alginate/alginate-sulfate microspheres, and promoted vascularization *in vivo*. This method was later used to sequester and deliver various growth factors (*e.g.*, VEGFs, PDGF-BB, TGF-β1, HGFs, and insulin growth factor 1 (IGF)-1) for vascularization,[485–486] myocardial repair,[486–487] chondrogenesis,[488] and immunoregulation applications.[485] The Burdick group[489] applied dextran sulfate (a heparin mimetic) to modify HA hydrogels for sequestering recombinant tissue inhibitor of MMPs 3 (rTIMP-3) (Figure 9A). When injected into a myocardial infarction (MI) region in a porcine model, the hydrogels released rTIMP-3 in response to locally elevated MMP levels, which inhibited MMP activity and attenuated post-MI remodeling. One limitation of heparin is its nonspecific binding affinity to multiple types of growth factors. To overcome this problem, peptides possessing a specific physical affinity can be engineered into hydrogels to specifically immobilize target growth factors.[490] These successes show promise for the use of physical immobilization for delivering growth factors

into hydrogels, but there are limitations of these technologies because (1) the presentation and release of growth factors cannot be well controlled either spatially or temporally, and (2) large quantities of the growth factor must typically be wasted because the growth factor must be distributed throughout the entire hydrogel. Future developments that enable 4D control of this delivery constitute an important need.

Compared with physical immobilization, chemical immobilization may have some benefits since it can prolong the presentation and release of growth factors, improve their spatiotemporal controllability, and reduce the required amount.[491–492] Significant efforts have been directed toward covalently immobilizing growth factors in hydrogels under biocompatible conditions.[493–494] For example, the Anseth group modified TGF-β with a thiol group and covalently tethered the modified TGF-β to PEG hydrogels through mixed-mode photoinitiated thiol-acrylate polymerization.[495–496] The bioactivity of the immobilized TGF-β was verified using a Smad2 reporter cell line. In addition, the chondrogenic differentiation of hMSCs encapsulated in the TGF-β-tethered hydrogels was promoted.[495] Shoichet and co-workers applied a multiphoton patterning method they previously developed[447–448] to create a $VEGF_{165}$ gradient in agarose hydrogels.[497] ECs seeded on the surface of a hydrogel with a $VEGF_{165}$ gradient of 1.65 ng mL^{-1} μm^{-1} grew into the interior of the hydrogel and formed tubular-like structures. In their later work, multiple growth factors, including sonic hedgehog (SHH) and ciliary neurotrophic factor, were simultaneously incorporated into different regions of agarose hydrogels using the orthogonal chemistry of peptide binding pairs, *i.e.*, barnase–barstar and streptavidin–biotin.[498] The presence of an immobilized SHH gradient in GRGDS-agarose hydrogels was shown to promote the migration and penetration of neural precursor cells into the hydrogels. Recently, the Lutolf group reported an enzymatic hydrogel photopatterning method in which transglutaminase factor XIII (FXIIIa) was rendered photosensitive and incorporated into PEG-based hydrogels.[499] Biologically relevant signaling proteins, including $VEGF_{121}$ and PDGF-BB, as well as the recombinant fibronectin fragment $FN_{9–10}$, were subsequently patterned in hydrogels through light-activated local enzymatic crosslinking (Figure 9B). Directed MSC invasion in 3D was demonstrated *in situ* using this method. To date, such studies have shown that significantly different bioactivities can be obtained from growth factors via different immobilization strategies, bound/released states and spatial distributions.[500–501] In the context of biophysical cues for the cell microenvironment, however, these technologies must be checked carefully to ensure that the covalent bonds to the hydrogel backbone do not affect cell mechanobiology adversely.

As mentioned in the previous section, options exist beyond the use of full-length growth factor proteins. Small peptide analogs that partially mimic the bioactivity of growth factors have been developed, similar to peptides used for mimicking cell adhesion ligands. For instance, a spliced peptide analog of stromal cell-derived factor 1 alpha (SDF)-1α that mimics the bioactivity of full growth factor has been developed to promote endothelial progenitor cell migration and preserve rat ventricular function after acute MI.[502–503] In a recent study, two peptide analogs (*i.e.*, DWIVA and the knuckle epitope) of BMP-2 were fabricated and conjugated into alginate hydrogels via carbodiimide chemistry or sulfhydryl-based orthogonal coupling schemes.[504] These functionalized hydrogels were found to enhance the alkaline phosphatase activity of murine osteoblasts and the osteogenic

differentiation of murine MSCs in 3D. Compared with full-length growth factor proteins, small peptide analogs are easy to synthesize, stable, and can be incorporated into hydrogels in a well-controlled manner. Nevertheless, small peptides may not exhibit the full bioactivity of native growth factors in some instances, and may interfere with cell mechanobiology because of their reduced size and therefore altered mechanics. An ongoing challenge with the use of peptide analogs of growth factors is that the balance of potential benefits and the above-mentioned risks must currently be assessed on an *ad hoc* basis.

3.2.3. Chemical Functional Groups for Modification of Surface Chemistry—

Modification of surface chemistry is an attractive pathway for directly affecting the cell microenvironment, but special care must be taken to ensure that these alterations produce only the desired effect on encapsulated cells. Nonspecific chemical properties of biomimetic materials, including electrical charge and hydrophilicity, are known to affect protein adsorption, cell adhesion, cell function and cell fate.[505–508] Such properties are usually determined by material surface chemical groups.[17,509] Alkanethiol self-assembled monolayers have been widely used to control surface chemistry and have functioned as model biomaterial surfaces.[510–511] By employing this method, surfaces chemically functionalized with hydroxyl (–OH), carboxyl (–COOH), amino ($–NH_2$), methyl ($–CH_3$), mercapto (–SH) and sulfonic ($–SO_3H$) groups have been fabricated. The morphology, migration and differentiation of NSCs were observed to be closely regulated by surface chemical groups.[512] Specifically, NSCs cultured on $–SO_3H$- and $–CH_3$-functionalized substrates showed the most-flattened and most-rounded morphologies, respectively, at the single-cell level. The positively charged $–NH_2$ surface sustained the greatest amount of cell migration, while the neutral –OH surface exhibited the weakest cell migration. In addition, the $–NH_2$ surface showed increased neuronal differentiation compared with the negatively charged –COOH surface. For bone mineralization, most earlier studies used anionic chemical moieties inspired by the fact that negatively charged amino acids abundantly present in many glycoproteins are involved in bone mineralization *in vivo*.[32,513–514] Recently, poly(sebacoyl diglyceride) carrying free neutral hydroxyl groups was also demonstrated to promote the biomineralization of hMSCs and rat osteoblasts.[515] In addition to electrical charge, surfaces with a broad range of hydrophilicities have also been fabricated by the mixed use of different chemical groups for investigating the adhesion behavior of human umbilical vein ECs (HUVECs) and HeLa cells.[516] It was suggested that chemical group type and density can affect cell adhesion and that material hydrophilicity may play a crucial role in cell adhesion. To further spatially control the adhesion and growth of cells, patterned superhydrophobic-hydrophilic surfaces have been developed.[517–518] However, most existing studies on chemical functionalization for cell culture were performed in 2D, and few 3D studies have been reported.

The 3D studies that have been reported are limited to a handful of papers. In one study from the Anseth group,[33] PEG hydrogels were functionalized with different small-molecule chemical groups, including amino, acid, *t*-butyl, phosphate and fluoro groups (Figure 10). hMSCs encapsulated in phosphate- and t-butyl-functionalized PEG hydrogels showed osteogenic and adipogenic differentiation, respectively, in the absence of differentiation additives. In another study, ethylene glycol methacrylate phosphate (EGMP) was

incorporated into a PEG hydrogel, leading to the formation of a bone-like mineral phase.[519] The EGMP-functionalized PEG hydrogel was found to sequester cell-secreted osteopontin and thereby promote the adhesion and spreading of encapsulated hMSCs. This approach was suggested to improve cell viability from 15% to 97% when the concentration of EGMP was increased from 0 to 50 mM. These successes are each interesting and useful, but many broad-sweeping challenges remain, as described below.

Foremost amongst the limitations of these 3D applications is that the cell-chemical functional group interactions that are responsible for directing cell behaviors remain unclear. [6] One pathway observed in osteoblasts involves chemical functional groups changing the conformation of adsorbed fibronectin and altering its integrin binding specificity, which regulates osteoblast differentiation and mineralization.[520] Incorporation of phosphate functional groups into a PEG hydrogel promoted the adsorption of ECM proteins (*e.g.*, collagen I and fibronectin) from serum, which may have contributed to the enhanced osteogenic differentiation of hMSCs.[521] Chemical functional groups could also affect cell behaviors by sequestering or regulating the diffusion of soluble signaling molecules (*e.g.*, growth factors).[522] While much remains to be learned about the mechanisms underlying cell-chemical functional group interactions, the use of small-molecule chemical functional groups to control complex cell behaviors, once understood more clearly, stands to inspire the production of new therapeutic materials.[33,107]

3.3. Biophysical Designs

As mentioned in Section 2, biochemistry and biophysics overlap strongly in the cell microenvironment. We focus here on the broad category of biophysical aspects of the designs of biomimetic materials, and on techniques specifically targeting the cell microenvironment.[523–524] However, the degrees to which biophysical cues from biomimetic materials can direct cell growth, function and fate, independently or synergistically with biochemical cues, are in general poorly understood.[118,525–526] The following subsections detail successes, challenges, and opportunities, in custom-designing the structural features, mechanical properties, degradability, and electrical conductivity of hydrogels.

3.3.1. Structural Features—As discussed in Section 2, native bulk ECM is a highly hierarchical and heterogeneous complex structure, and ECM in the cell microenvironment is in general poorly characterized relative to bulk ECM. Cells can sense and respond to multiscale structural or topographic features of their microenvironment.[527–528] Therefore, structural features are important biomimetic material design considerations.[529–531] Considering the multiscale nature of the ECM and the widely varying approaches for engineering structural features of different length scales, we present this discussion in terms of three different scales: macroscale, microscale, and nanoscale (Figure 11).

3.3.1.1. Macroscale Design.: Under macroscale design we describe roles of external structure characteristics such as overall shape and size. At this level, structural features can determine how external stimuli (*e.g.*, boundary constraints and mechanical forces) are transmitted to internal cellular constructs. Cells can sense macroscale structural cues mediated by the matrix and then adjust their remodeling behaviors, leading to recursive cell

and ECM reorganization and shape evolution. Appropriate macroscale design is particularly important in tissue engineering because how well an engineered tissue construct matches the shape and size of an anatomical defect will affect its integration with adjacent tissues, defect repair and, in some cases, aesthetics. As we will describe in this section, the macroscale shape and size of an engineered tissue construct can be conveniently controlled using custom-designed molds or computer-aided additive manufacturing technologies.[532–533]

Although a great many models exist for predicting and tracking growth and development of tissues and tissue constructs,[534–538] the optimization of macroscale hydrogel design is still very much case-specific, and basic, universal principles are lacking. As an example of how the shape and size of implants can influence host recognition and foreign body responses, we note a study that observed spherical implants with a diameter of 1.5 mm or greater, regardless of material types, to be more biocompatible than other shapes or smaller counterparts in terms of foreign body reactions and fibrosis in rodents and non-human primates.[539] This provides a powerful rule-of-thumb, but further studies uncovering the mechanisms underlying foreign body responses to implant shape are needed, and a predictive framework is an important need for improved macroscale structural design of implanted biomaterials.

One notable issue for macroscale structural design is the structural evolution of tissue constructs (especially for soft tissue constructs) post-fabrication, which can be induced by environmental changes or cell traction forces.[289] This issue complicates structural design and further highlights the need for 4D design that incorporates time evolution as an additional coordinate and considers dynamic material properties and cell-material interactions. More broadly, theoretical tools and basic science studies for predicting the development of macroscale hydrogel implants represent a pressing need for the field.

3.3.1.2. Microscale Design.: Structural features at the microscale have long been known to play important roles in guiding cell behaviors and are therefore important structural design considerations.[35,540]

One widespread and simple, but ultimately limited, approach to structurally engineer the 3D cell microenvironment is to use microwells on non-adhesive hydrogels such as PEG[541–542] and agarose,[543] generated using micromolding or photopatterning methods. Such microwells provide a simple, confined 3D space for accelerating cell aggregation and directing cell spheroid formation.[544–547] Using microwell-based approaches, cell spheroids consisting of either single cell types, such as MCF-7 cells,[548] MIN6 β-cells,[546] hESCs,[545] and adipose-derived stem cells (ADSCs),[549] or multiple co-cultured cell types, such as hESCs-fibroblasts[544] and hepatocytes-fibroblasts,[550] have been generated in a high-throughput manner. These scaffold-free cell spheroids can potentially serve as building blocks for bottom-up tissue engineering and as effective 3D *in vitro* models for drug toxicity and screening applications.[551] Microwells with varied geometries and sizes can provide tunable confined spaces for regulating behaviors such as cell differentiation. For example, Werner and co-workers[552] employed microlens array photopatterning technology to locally degrade hydrogels and generate microwells and microchannels with defined architectures. The differentiation of neural precursor cells was found to be determined by the degree of spatial

confinement. Moreover, using biocompatible thermal-responsive polymers such as six-arm PEG-poly(caprolactone) (PCL), microwells with different dynamically tunable geometries have been fabricated.[553] The dynamic changes in microwell geometries resulted in alterations in the cytoskeletal organization and differentiation pathways of BMSCs cultured in these microwells. However, although these observations are physiologically relevant, they cannot overcome the limitation that microwells are only pseudo-3D systems that cannot mimic the 3D structural cues cells experience *in vivo*. We therefore feel that more advanced and integrative technologies, as discussed below, represent the future of engineering the biophysical microenvironment of cells.

One such promising technology is biomimetic materials with a microporous structure. The ECM is typically a highly porous structure with water and soluble factors filling and diffusing through the voids. The porous structure provides a large surface area for cell attachment and growth, enables efficient molecule transport, and forms localized bioreactors for biochemical reactions.[554–558] The important porous design parameters, including porosity, pore size and interconnectivity, have been found to have significant effects on cell behaviors.[229,569–573] In general, an increase in porosity, pore size or interconnectivity usually leads to improved ECM secretion, cell infiltration, tissue ingrowth, and molecular delivery, although this is very much application specific.[574–575] For cell differentiation, different pore parameters may result in different differentiation pathways. As one example, the differentiation of hMSCs in porous honeycomb polystyrene scaffolds was found to depend on pore size, with osteospecific and myospecific differentiation preferred on scaffolds with a smaller pore size (1.6 μm) and a larger pore size (3.8 μm), respectively.[576] Another important parameter in porous design is spatial distribution of pores. Anisotropic or heterogeneous pore distributions can provide structural cues for guiding cell migration, orientation, and differentiation. For instance, accordion-like honeycomb poly(glycerol sebacate) (PGS) scaffolds were fabricated with controlled anisotropic microstructures.[577] Such structures promoted heart cell alignment and induced direction-dependent electrical excitation thresholds. In addition, collagen and chitosan scaffolds with unidirectional microporous structures have been fabricated using a temperature gradient-directed freeze-drying method.[155–156,578–579] These porous structures were found to direct the migration and orientation of primary porcine trabecular meshwork cells,[155] the generation of large skeletal myotubes,[156] and the formation of functional engineered cartilage.[579] 3D microgrooved collagen scaffolds have also been fabricated using sacrificial ice templates, which have been used to create multilayered muscle tissue constructs with highly aligned muscle bundles.[580] In addition, hydrogels with gradient porosity or pore size have been generated,[581–583] which were demonstrated to enhance interfacial tissue repair.[584–585] A spectrum of approaches, including solvent casting/particle leaching,[559] freeze-drying,[560–563] gas foaming,[564–565] and solid free-form fabrication or rapid prototyping,[566] have been developed to control the porous structure of hydrogels. The first three approaches are easy to perform and are applicable to the majority of hydrogels; however, they have limited controllability on the porous structure may also suffer from poor control on cell distribution in hydrogels. In contrast, rapid prototyping may enable the creation of hydrogel constructs with any custom-designed porous structures. With the emerging of printable biomimetic

materials, rapid prototyping may hold potential for fabricating porous tissue constructs with native tissue-mimicking structures.[567–568]

One additional motivation for fabricating hydrogels with microporous structures is to enhance mass transport. Cells in native tissues are usually surrounded by abundant vascular networks, accessible within 200–300 μm, that provide transport for oxygen and nutrient delivery, as well as for waste removal. Because ischemic conditions can injure cells and promote pathology, vascularization is a major challenge for tissue engineering of large, complex tissue constructs, such as a heart, liver and kidney.[95,586–588] For this reason, hydrogels with highly interconnected porous structures are preferred, and their development is a crucial area for advancing materials for the cell microenvironment.

Key challenges are that, although helpful, mass transport mechanisms dominated by passive diffusion are often insufficient, and that the spontaneous vascularization process can be too slow. Consequently, hydrogels with microfluidic channels ("microfluidic hydrogels," Figure 12) have attracted interest in the past decade.[589–594] The creation of microfluidic channels in hydrogels greatly improves mass transport through a convection-dominated mechanism.[595] Moreover, endothelialization can enable the microfluidic channels to mimic more closely the structures and functions (*e.g.*, the barrier function) of vascular networks in native tissues. Combining these microfluidic hydrogels with pore design can further enhance the controllability of the 3D cell biochemical microenvironment.[596–597] The field is still emerging, however, and major challenges persist. Long-term stability of microchannels is limited due to clogging and collapse, and due to detachment of endothelial layers during perfusion culture or cell-induced matrix remodeling.[598] Future work is needed for developing stable, highly hierarchical biomimetic vascular networks in hydrogels, and for sealing these networks with integrity sufficient for the integration with host vascular systems upon implantation into the body.[599–602] Finally, these and all methods for introducing porosity for mass transport into hydrogels make hydrogels less stiff and thereby compounding the perennial challenge of producing hydrogel-based tissues with physiological mechanical properties.

An important feature of the microenvironment is that it often differs from the bulk ECM in and substantial ways. A strategy for achieving microenvironmental control is to use hydrogel building blocks, such as microscale hydrogel particles ("microgels.")[603] This approach is also inspired by the observation that many important tissues or organs consist of repeated functional units, including hepatic lobules in the liver, nephrons in the kidneys, and pancreas islets in the pancreas. By fabricating cell-laden microgels to mimic these functional units, one can either use them as building blocks for assembling custom-designed tissue constructs[604–606] or as *in vitro* microtissue models for pathophysiological studies and drug testing applications.[216,221,607–608] To date, microgels have been created with a wide range of shapes (*e.g.*, sphere, rectangle, cylinder, star, ring, and dumbbell), sizes, and internal microstructures.[609–611] As an example, Fan *et al.*[612] employed a two-step photopatterning method to fabricate microscale gelatin methacrylate (GelMA) hydrogel rings in a high-throughput manner. The capture and confined growth of single neurons was achieved; consequently, axonal circles formed in these hydrogel ring mimicking self-synapse diseases were achieved, demonstrating the potential application of this system in neurobiological

studies. Alternatively, microgels can be further assembled into larger 3D tissue constructs driven by such forces as magnetic force,[613–615] acoustic force,[616] electrostatic force,[617] and interface force,[618] or by using multistep photopatterning,[619] railed microfluidic channels,[620] DNA-directed self-assembly,[621–622] or bioprinting technologies.[623–625] Detailed descriptions of the development of the bottom-up assembly of microgels can be found in some recent reviews.[606,626–627] The strengths of these bottom-up approaches are the potential to construct highly complex microstructures using simple technologies including bioprinting. This includes microstructures that enable spatial control sufficient to provide cells with a microenvironment that differs from the bulk ECM. However, the technology continues to face challenges including problems with surface interconnectivity: microgel building blocks often form surfaces that do not fuse with those of neighbors sufficiently well to enable cells to penetrate and to communicate with cells in neighboring microgels.

Another class of microenvironment that is relevant physiologically is highly anisotropic and bundled microfibers such as muscle fibers and nerve networks. Hydrogel microfibers can be engineered to mimic these functional units for the bottom-up fabrication of 3D tissue constructs.[628–630] So far, hydrogel microfibers of varying compositions and microstructures, including surface-grooved microfibers,[631] ribbon-like microfibers,[632] multicompartmental or patterned microfibers,[633–636] core-shell microfibers,[637] internally aligned microfibers,[638–639] and stimuli-responsive microfibers,[640–641] have been fabricated, mostly using microfluidic technologies. For instance, Lee and co-workers[642] continuous alginate hydrogel microfibers using a microfluidic chip and a digital fluid controller. These microfibers were coded with spatiotemporally controlled topographies (*e.g.*, spindle-knots, joints, and grooves) and used to enhance the extension and alignment of rat embryonic neurons, and to create multifunctional tissue microfibers from a co-culture of rat hepatocytes and L929 fibroblasts. Takeuchi and co-workers[643] used a double-coaxial microfluidic device to fabricate meter-long, cell-laden, core-shell hydrogel microfibers, in which alginate formed the shell and cell-laden ECM proteins formed the core. After a culture period to allow cell growth and organization, the alginate shell was removed, leaving behind cell-laden ECM microfibers (termed cell fibers). Via this method, cell fibers of varying types of cells were created, with morphologies and functions mimicking those of living tissues. Moreover, the cell fibers could be assembled into different 3D higher-order macroscopic tissue constructs using a microfluidic weaving machine. The Xu group[644] developed a simple method for generating cell-laden hydrogel microfibers in a high-throughput manner, inspired by the preparation of Chinese Hele noodles (Figure 13). Fibers of this character have been used not only for tissue engineering applications but also for fundamental biophysics. Magnetic stretching of hydrogel microfibers promotes the proliferation, spreading, alignment, and differentiation of C2C12 cells. Although all of these fiber technologies provide the potential for controlled, one-dimensional tissue engineered microenvironments, the technologies for combining these into functional 3D and 4D tissues are not yet mature. The textile industry has faced these challenges for millennia, and adaptation of weaving technologies is a promising direction.[645]

3.3.1.3. Nanoscale Design.: Nanoscale structural cues within the local microenvironment of a cell are known to influence cell shape, adhesion, proliferation, migration, and

differentiation, as well as sub-cellular molecular organization.[646–650] In 3D, nanoscale structural cues are usually provided by nanofibers because many ECM proteins in native tissues are present in the form of nanofibrous structures.[413,651–652] These nanofibers not only sustain the structure in which cells reside but also provide instructive cues for guiding cell behaviors.[653–655] As mentioned in Section 2, the physiological composition and presentation of these fibers in natural 3D tissues is known in only a few special cases, and much more work is needed. The typical strategy in tissue engineering is to provide cells with a few essential nanoscale cues, and then to rely on the cells themselves to create the remainder of the nanofibers needed for their microenvironment. In the following, we describe several such approaches and their limitations.

Approaches for mimicking nanofibrous structures include phase separation,[656–659] electrospinning,[660–661] and self-assembly.[662–663] While phase separation is a simple method by which bulk nanofibrous scaffolds with nanofibers (~50–500 nm in diameter) mimicking the native ECM can be prepared, it is limited to a narrow range of polymers, such as polyesters, and lacks precise control over local nanostructures. Moreover, thermal effects and non-solvent exchange conditions may not allow 3D cell encapsulation during processing. Electrospinning enables precise control over nanofiber dimension and orientation and allows the use of a broad range of materials, including naturally derived and synthetic polymers, as well as hybrid polymers and nanocomposites.[664–666] However, cell seeding post-electrospinning is needed, thus often limiting the electrospinning process to the production of thin film constructs due to limited cell infiltration. Although thick 3D constructs can be obtained by layering or rolling cell-seeded thin films or by combining electrospinning with 3D microfabrication technologies, this method still has limited controllability in engineering the 3D cell microenvironment.[667–668] In contrast, by starting from molecular building blocks, self-assembly enables the formation of nanofibers and large fibrous tissue constructs in the presence of living cells in a more controlled manner.[669] As described at the end of this section, however, several fundamental challenges exist.

Self-assembly, mediated by non-covalent hydrogen bonding, hydrophobic, electrostatic, and van der Waals interactions, is a common strategy applied in many natural material systems for generating higher-order structures. Collagen I is the most abundant self-assembled fibrous protein in mammals. Extracted collagen can be dissolved in a weak acid and stored at a low temperature for a long time. Once neutralized and warmed to above room temperature, the collagen molecules will spontaneously self-assemble into fibrous structures and form hydrogels. By controlling the self-assembly conditions or post-processing procedures, hydrogels with collagen nanofibers of varying diameters, densities, distributions, and organizations have been fabricated and found to significantly affect cell behaviors.[670–671] For instance, many studies have reported the control of collagen fiber orientation,[146,672–675] which has been found to impact EC morphology, function, and survival,[676] increase breast cancer cell intravasation,[677] and direct neuronal alignment and growth.[672] Similar phenomena can be found with other naturally derived proteins, such as type II collagen, elastin,[678] and fibrin.[679] It is believed that by mimicking the tissue-specific orientation of nanofibrous structures (*e.g.*, parallel alignment in tendon, gradient alignment in myocardium, basket-weave meshwork in skin, orthogonal lattice in cornea, and concentric weave in bone), one can fabricate 3D tissue constructs with structures and functions more

comparable to those of native tissues.[680–681] However, as mentioned previously, a central challenge is the fact that reconstituted natural proteins cannot reconstitute the mechanical stiffnesses of native tissues, even after several days of cellular remodeling;[347,682] although structure and certain functions of native tissues can be reconstituted, mechanics typically cannot.

Synthetic strategies are therefore an area of intense activity. These strategies allow the fabrication of nanofibrous materials through the self-assembly of small molecular building blocks, such as short peptides.[662,683] One of the most commonly used molecular building blocks is peptide amphiphiles, which usually possess hydrophobic groups at one end and hydrophilic groups at the other end. In appropriate aqueous environments, peptide amphiphiles tend to isolate their hydrophobic end from contact with water and self-assemble into nanofibers (Figure 14),[684] nanotubes,[685] or other higher-order structures. In one example, a peptide amphiphile was synthesized and self-assembled into a nanofibrous scaffold when the pH was adjusted.[686] The fibers directed the mineralization of hydroxyapatite, forming a composite scaffold with bone-like anisotropic microstructures. In another example, the Stupp group[687] synthesized IKVAV (a neurite-promoting laminin epitope)-containing peptide amphiphile molecules and precipitated their self-assembly into 3D nanofibrous networks by mixing aqueous dilutions of the molecules with cell suspensions. It was found that the nanofibrous hydrogels induced the rapid and selective differentiation of the encapsulated murine neural progenitor cells into neurons. In recent work, such nanofibers were blended with collagen to form hybrid hydrogels for controlling neuronal morphogenesis, survival and maturation.[688] With the development of supramolecular chemistry, extreme controllability over nanofibrous structures can be achieved by designing the structure and controlling the self-assembly process of molecular building blocks.[363,662] However, these materials typically suffer from the challenge of achieving physiological mechanical properties.

Beyond nanofibers, nanoparticles inside scaffolds can also provide 3D nanostructural cues for cells. A typical example is hydroxyapatite nanocrystallites in bone. Many hydroxyapatite-containing nanocomposites have been developed for bone tissue engineering applications, in which the presence of hydroxyapatite enhanced osteoblast mineralizaition.[689–691] In particular, the bioactivity of hydroxyapatite nanocrystallites was found to depend on their shape and size. For example, it has been demonstrated that needle-shaped hydroxyapatite nanocrystallites could significantly upregulate osteoblast differentiation compared with rod-shaped and spherical nanocrystallites.[692] Other nanoparticles that have been employed to fabricate nanocomposites include CNTs,[693] gold nanowires,[694] and magnetic nanoparticles.[695] As most existing studies on this subject have aimed to enhance the mechanical properties or electrical conductivity of composites, the structural effects of these nanoparticles on cell behaviors need to be investigated in the future.

Finally, we reiterate that native tissue structures are hierarchically organized, and most synthetic materials for the cell microenvironment are not. Structural design at a single scale may lack instructive cues from other scales and result in insufficient structural or mechanical integrity. This has prompted the emergence and development of multiscale hierarchical structural design.[696–699] Strategies for simultaneously providing cells with appropriate

hierarchical environments at the nanoscale, microscale, and macroscale represent a pressing need for the field.

3.3.2. Mechanical Properties—As introduced in Section 2, the mechanical properties of the ECM influence cell behaviors,[700–701] as shown by numerous *in vitro* studies performed on 2D substrata of defined stiffness.[175] Several recent works argued that the coupling strength between substrates and cell surface receptors, rather than substrate stiffness, could affect cell adhesion, spreading and differentiation.[30,702–703] These studies have dramatically contributed to understanding the roles of mechanical cues in cell behaviors and mechanotransduction in 2D[704–709] and, to a more limited degree, in 3D.[179,710] The mechanical properties of the cell microenvironment are amongst the most important design considerations for engineering the 3D cell microenvironment. Most existing studies on the subject have explored the effects of 3D hydrogels with linear elasticity on cell behaviors, while other recent studies have extended the effects of hydrogel mechanical properties to include nonlinear elasticity, and more recently, viscoelasticity. Moreover, hydrogel mechanical properties have been spatially and temporally modulated to engineer the heterogeneous and dynamic cell mechanical microenvironment by mimicking spatiotemporal mechanical ECM alterations *in vivo*. However, as emphasized in Section 2, the relatively recent discovery that the fibrous nature of the native ECM is essential to cell-cell communication and cell mechanobiology requires us to critically re-evaluate what is known about the role of mechanics in the cell microenvironment.

3.3.2.1. Elasticity and Viscoelasticity.: Elasticity, described by stress-strain curves and often characterized by stiffness or Young's modulus, is the most studied mechanical property of hydrogels in engineering the 3D cell mechanical microenvironment. It represents the ability of a hydrogel to resist deformation and return to its original state when external forces are removed. Hydrogel stiffness has typically been controlled by varying the polymer concentration, crosslinking density, or molecular weight of polymer networks. For instance, reconstituted protein-based hydrogels, such as self-assembled collagen, are usually considered mechanically soft or even weak. Different covalent crosslinking strategies have been developed to improve the mechanical performance of these hydrogels; however, they are either not appropriate for cell encapsulation or limited in mechanical enhancement. To overcome this problem, Brown and co-workers[711–712] reported a plastic compression method to rapidly remove water from hyperhydrated collagen hydrogels, resulting in dramatic shrinkage (> 100-fold) and the rapid formation of dense and mechanically strong (~MPa) collagen hydrogels. This method enables the 3D encapsulation of cells, as demonstrated by the high viability of both encapsulated human dermal and limbal fibroblasts post-compression. To date, stiffnesses ranging from the order of Pa to MPa have been generated with naturally derived, synthetic or hybrid hydrogels. Cells cultured in these hydrogels respond to the magnitude of stiffness by changing their morphology, movements, mechanics, growth and functions. As a typical example, alginate hydrogels with a wide stiffness range (2.5–110 kPa) have been created.[713] Murine MSCs encapsulated in the hydrogels showed adipogenesis and osteogenesis predominantly at 2.5–5 kPa and 11–30 kPa, respectively. Similar results were also observed in RGD-modified agarose or PEG hydrogels. The formation and organization of integrin–adhesion ligand bonds were found to

mediate matrix stiffness-induced stem cell differentiation in 3D. Fibroblasts cultured in collagen will remodel the collagen, adapt their own mechanical properties to match one another, and propagate or die off to approach the steric percolation threshold.[288,714–717] In recent work, hMSCs encapsulated in 3D stiffer norbornene-functionalized HA hydrogels showed reduced cell spreading and nuclear localization of YAP/transcriptional co-activators with the PDZ-binding motif (TAZ), which was opposite to the results observed in 2D.[718] These observations clearly show differences between the effects of microenvironmental stiffness on cell behavior in 2D versus 3D, and motivate continued efforts to design material systems that help delineate the underlying mechanisms.

While many studies have investigated the effects of bulk mechanical hydrogel properties on cell behaviors, recent work indicates that cells can sense and respond to nanoscale mechanical hydrogel properties in 3D. For example, collagen hydrogels of varying local fiber stiffness have been fabricated by controlling the self-assembly temperature of collagen molecules.[719] Decreasing the self-assembly temperature resulted in increased collagen fibril bundling and increased fiber diameter, which contributed to an increase in local fiber stiffness (Figure 15A). The local rigid fibrils were found to promote the 3D adhesion turnover and maturation of human foreskin fibroblasts. In an alternative work, gold nanorods (AuNRs) were mixed with collagen to form nanocomposite hydrogels.[720] The incorporation of AuNRs resulted in an increase in the nanoscale stiffness of the hydrogels without impacting the bulk mechanical properties (Figure 15B), which was observed to promote the assembly of intercalated discs through βt-integrin-mediated signaling pathways. These results indicate the important role played by nanoscale matrix stiffness in regulating cell behaviors. Therefore, an important need for future biomaterials is hydrogels that control nanoscale mechanical properties for engineering the 3D cell microenvironment, in addition to the nanoscale structural factors associated with the fibrous presentation of ECM.

Many filamentous biopolymers, such as collagen, fibrin, actin, and vimentin, exhibit nonlinear elasticity, typically strain-stiffening or stress-stiffening (*i.e.*, the tangent stiffness increases with increasing strain or stress) behaviors.[721–723] Such nonlinear mechanical properties may play important roles in preventing large tissue deformation and maintaining tissue integrity, as well as in tissue development, mechanical homeostasis, and wound repair.[721,724–725] The fibrous nature of native ECM, including effects of plasticity, recruitment, and alignment, are central to these effects. Although important, the effects of nonlinear elastic hydrogel mechanical properties on cell behaviors have only drawn minimal attention in recent years. It has been shown that hydrogels with nonlinear elasticity can enable long-range cell-cell communication and pattern formation,[726] regulate the modes of 3D cell migration[727] and support the differentiation of stem cells.[36] For example, linear elastic cell-derived matrices from human foreskin fibroblasts (HFFs) and nonlinear elastic collagen hydrogels have been prepared. HFFs cultured in the cell-derived matrices showed lobopodia-based migration, while those cultured in the collagen hydrogels showed lamellipodia-based migration.[727–728] In a recent study, polyisocyanopeptide-based hydrogels, which have been shown to exhibit controlled stress-stiffening behavior,[729–730] were prepared with varying nonlinear behaviors, *i.e.*, with varying critical stresses (beyond which the hydrogels will show stress-stiffening behavior) (Figure 16).[36] The critical stress of the hydrogels increased with increasing polymer chain length, while the stiffness and adhesion-ligand density were

maintained. By increasing the critical stress, hMSCs cultured in these hydrogels were redirected from adipogenesis toward osteogenesis, which was found to be mediated by microtubule-associated protein DCAMKL1.[36] More broadly, the fibrous nature of ECM proteins enables the long-range transmission of mechanical forces and fields in a way that simple neo-Hookean elasticity does not,[38–41] and harnessing this type of transmission represents an important frontier in engineering the cell microenvironment.

In addition to nonlinear elasticity, most hydrogels (especially reconstituted biopolymer-based hydrogels) and soft tissues show both elastic and viscous (or dissipative, characterized by viscosity or loss modulus) properties (Figure 17A).[347,731–732] These hydrogels are viscoelastic and exhibit stress relaxation (*i.e.*, the stress decreases in response to the same applied strain) or creep (*i.e.*, the tendency toward permanent deformation in response to the same applied stress) behaviors.[194–195,682] The viscosity of a hydrogel may arise from various dissipative events, such as weak bond dissolution, polymer disentanglement, protein unfolding, and molecule slipping. The viscoelastic behaviors of hydrogels can be adjusted by controlling the hydrogel composition or concentration,[733–734] molecular weight or network chain length,[735–736] crosslink type or density,[737] and degradation.[738] Regardless, the effects of hydrogel viscoelasticity on cell behaviors have been often overlooked.[731] Recent studies revealed that hydrogel viscoelasticity could have significant effects on cell behaviors, including cell spreading, proliferation and differentiation.[37,193,739–740] For example, Mooney and co-workers[740] fabricated alginate substrates with elastic or viscoelastic properties via ionic or covalent crosslinking, respectively. The results showed that both U2OS cells and NIH 3T3 cells cultured on viscoelastic substrates at a low initial elasticity showed increased spreading and proliferation compared with those cultured on substrates with the same initial elastic modulus. Later, they developed an alternative material system in which the stress-relaxation rate of alginate hydrogels could be adjusted independent of initial stiffness, degradation, and adhesion-ligand density (Figure 17B, C).[37] This was achieved by the combinatorial use of different molecular weight alginate macromers, ionic crosslinking densities, and short PEG spacers covalently linked to the alginate backbone. It was found that the spreading and proliferation of encapsulated NIH 3T3 cells and the osteogenic differentiation of encapsulated murine MSCs were enhanced in the alginate hydrogels with faster relaxation. Such effects could be mediated through integrin adhesion, ECM ligand clustering, actomyosin contractility, and YAP nuclear translocation. Alternatively, McKinnon *et al.*[741–742] developed a hydrazone crosslinked PEG hydrogel with tunable viscoelasticity mimicking native tissues. The hydrogel maintained the integrity of the covalently crosslinked PEG network and showed viscoelasticity-dependent 3D cell spreading and growth. Given recent observations by Babaei *et al.*[45] that human dermal fibroblasts remodel the viscoelastic behavior of their microenvironment over time, the need for new materials to characterize and control the dynamic viscoelastic cell microenvironment is pressing.

The nonlinear elasticity and viscoelasticity of hydrogels may influence each other, forming complex mechanical interactions experienced by cells. Take collagen and fibrin as examples; their nonlinear mechanical responses have been found to depend on strain history.[743] Repeated large-strain loading shifted the onset of strain stiffening to higher strains, which was demonstrated to arise from the monomer slipping-induced persistent lengthening of

individual fibers. Recently, Chaudhuri and co-workers[744] found that upon increasing strain, collagen and fibrin hydrogels showed both stiffening and faster stress-relaxation behaviors. Such strain-enhanced stress-relaxation behavior is mediated by the force-dependent dissolution of weak crosslinks. Aside from elasticity and viscoelasticity, other mechanical aspects (*e.g.*, toughness, strength, and fatigue resistance) of hydrogels may also need to be considered when engineering the cell microenvironment. Take toughness as an example; toughness describes the resistance of a material to fracture under stress. As presented in Subsection 2.4, mechanical stress and strain can play important roles in controlling cell behaviors. The stress and strain applied to cells in 3D is mainly mediated by the ECM. Hydrogels are often stretched or compressed *in vitro* to reproduce the stress and strain microenvironment that cells experience *in vivo*. An appropriate toughness, or a high toughness in some cases (*e.g.*, cartilage tissue engineering), is thus required to enable hydrogel deformation without fracture. Several high-toughness hydrogel systems have been developed, most of which are based on the principles of double crosslinking[745–747] or double networks.[384,388–389,748] Future studies are needed to evaluate potential applications of these hydrogels in engineering the 3D cell microenvironment.

3.3.2.2. Spatial Modulation.: Native tissues are usually heterogeneous, with spatially-varying stiffness[749] that can have profound effects on guiding cell migration, organization, and fate, thereby playing important roles in embryonic development, disease progression, and tissue healing.[750] For instance, injured tissues usually present a stiffness gradient that enables the directional migration of cells, termed durotaxis, which is critical for recruiting cells for wound healing.[751–752] Therefore, materials are needed to reproduce the mechanical heterogeneity of cell mechanical microenvironments.

A widely used method for fabricating such heterogeneous hydrogels is photopatterning, which is often performed by crosslinking photosensitive hydrogel precursors with light through gradient-patterned or any other custom-patterned photomasks[753] (Figure 18A). This approach has been exploited to fabricate PA hydrogels with ~1 kPa/mm gradient stiffness for directing the migration and differentiation of hMSCs,[754] PA hydrogels with patterned soft and rigid domains for fibroblast mechanical sensing studies,[755] MA-modified alginate hydrogels with checkerboard, island, or strip mechanical patterns for guiding the alignment of MC3T3-E1 preosteoblasts,[756] and PEGDA hydrogels with stiffer islands mimicking myocardial fibrosis foci for engineering myocardial fibrosis models.[757] An alternative photopatterning approach for creating mechanically patterned hydrogels is using photopatterned degradation. Via this approach, PEG-based photodegradable hydrogels with random or regular mechanical patterns and different stiff-to-soft ratios have been fabricated.[758] It was found that the morphology and YAP activation of hMSCs cultured on these hydrogel surfaces were closely regulated by the mechanical pattern organization and stiff-to-soft ratio.

While photopatterning can be readily adjusted to generate varied mechanical patterns, it is limited to photosensitive hydrogels. In contrast, microfluidics, which has been widely employed for fabricating hydrogel particles, fibers, and other material forms with a heterogeneous distribution (*e.g.*, gradient distribution) of polymer compositions, soluble factors, and even cells,[759–761] enables the use of hydrogels produced by different gelling

approaches. The heterogeneous distribution of polymer compositions or concentrations often results in heterogeneous mechanical properties.[583,762] As one example, a non-planar microfluidic flow-focusing device was developed to fabricate mechanically heterogeneous ovarian microtissues, with a soft collagen core and a hard alginate shell for mimicking the medulla and cortex, respectively[763] (Figure 18B). This mechanically heterogeneous structure enhanced follicle development and ovulation. A remaining challenge for microfluidics is how to tightly and flexibly control flow conditions for generating hydrogels with complex and readily regulatable mechanical patterns.

Recently, the Discher group[764] developed a method to copolymerize collagen I with PA to form rigid-on-soft (*i.e.*, collagen-on-PA) hydrogels, mimicking mechanically heterogeneous scar tissue. An interesting finding of their work is that MSCs cultured on these mechanically patterned hydrogels exhibited less cell-to-cell variation in smooth muscle actin (SMA) expression than did those cultured on homogeneously rigid hydrogels, an effect be mediated by the transcription factor NKX2.5. Han *et al.*[765] constructed heterogeneous engineered fibrocartilaginous tissues by synthesizing non-fibrous, PG-rich microdomains (PGmDs) within a fibrous collagenous matrix: MSC micro-pellets and meniscus fibrochondrocytes (MFCs), when sandwiched between nanofibrous PCL sheets, formed PGmDs and a fibrous collagenous matrix, respectively. Other methods to fabricate mechanically heterogeneous hydrogels include soft lighography,[766–767] thermal cycling,[768–770] and microfabricated geometrically anisotropic pillar arrays.[771] Functionally graded engineered tissue constructs, which reproduce the compositional, structural, mechanical, and functional features of native fibrocartilaginous tissues, provide a promising platform for mechanobiological and therapeutic studies of fibrocartilage. More broadly, these results highlight the need for the field to develop additional material systems that present cells with spatial gradients of microenvironmental cues.

Although the existing methods provide effective tools for engineering a mechanical microenvironment with stiffness gradient features, challenges described above persist, specifically the challenge achieving a sufficient gradient range to mimic the upper range of tissue stiffness *in vivo*. A typical example is the interface between soft and hard tissues, such as tendon-to-bone attachment. The tensile modulus of tendon is ~0.4 GPa, whereas the connected bone is nearly fifty orders of magnitude stiffer than the tendon.[176] Achieving the upper range of stiffness is a challenge, as is overcoming the stress concentrations that increase the failure risk.[772] Physiologically relevant stiffnesses can be achieved in 2D, but using materials that are not themselves amenable to remodeling by cells. For example, in a recent study, a multilayered substrate composed of a stiff photopatterned KMPR resin (~4 GPa) and a soft poly(dimethyl siloxane) (PDMS) layer (~20 kPa) was successfully fabricated, allowing the study of single cell behavior under a large stiffness gradient.[767] Such methods provide promising tools for investigating cellular biophysics, but are not likely to be applicable to 3D cell culture.

Although this section provided many promising examples of 2D successes, more studies are needed to uncover the mechanisms underlying cell responses to mechanical heterogeneities in 3D and, eventually, in 4D. Future efforts should be directed toward exploring biomimetic materials with spatiotemporally modulated mechanical properties to improve the *in vivo*

therapeutic performance of engineered tissue implants. Finally, given that even graded structures in the body are fibrous in nature,[773–774] a need exists for developing materials that offer realistic, controlled, fibrous cell microenvironments.

3.3.2.3. Temporal Modulation.: The heterogeneous mechanical properties of native tissues change with time in development, wound healing, and aging. Typically, ECM stiffening can be induced by matrix overdeposition, matrix crosslinking or cell contraction[775–776] and is distinct from strain-stiffening due to fiber recruitment. ECM stiffening is a hallmark of many diseases and plays an important role in fibrosis development and tumor progression.[777–779] For example, in fibrotic cardiomyopathy, the differentiation of cardiac fibroblasts into myofibroblasts yields cells that continuously secrete and overdeposit ECM, resulting in ECM stiffening. The stiffened ECM recursively promotes cardiac myofibroblast differentiation, forming a positive feedback loop for cardiac fibrosis development.[780–782] During breast tumor progression, ECM stiffening has been found to promote integrin clustering, phosphoinositide 3-kinase (PI3K) signaling activation, and tumor invasion.[783–785] Recreating dynamic microenvironments that simulate these 4D effects represents a pressing need in materials science.[786] We describe here a few successful strategies that have been utilized to trigger hydrogel stiffening for investigating dynamic cell responses.[787–789]

As an example of a successful temporal evolution of material properties in cell culture, the Burdick group developed a sequential crosslinking approach to stiffen HA hydrogels *in situ*.[788,790–791] In their study, HA macromers were modified with MA and partially crosslinked with dithiothreitol (DTT) via Michael-type addition reactions in the presence of living cells. After a culture period, the initial hydrogels were then UV-crosslinked in the presence of a photoinitiator (Irgacure 2959), resulting in hydrogel stiffening (Figure 19B). The adhered hMSCs showed reduced secretion of key angiogenic factors and cytokines[788] and increased spreading area and traction force[790] in response to hydrogel stiffening. Long-term culture showed that hMSC differentiation was dependent on the culture period, with adipogenic and osteogenic differentiation favored with later and earlier stiffening, respectively.[790] However, such differentiation state-dependent cell responses to mechanical stiffening as observed in 2D require further investigation in 3D. In another study, the Anseth group[792] reported a PEG-based hydrogel with stiffness dynamically tunable from 0.24 kPa to 13 kPa. Valvular interstitial cells (VICs) cultured in 3D hydrogels with stiffness of 0.24 kPa for 3 days spread and 40% of them were activated into myofibroblasts, as demonstrated by α-SMA expression; subsequent stiffening of the PEG hydrogels *in situ* deactivated the myofibroblasts into quiescent VICs.[792] These are interesting findings since 2D stiffer substrates have been shown to promote the differentiation of fibroblasts into myofibroblasts (as introduced in the next paragraph), demonstrating the importance of culture dimensionality in cell responses to dynamic stiffness changes. While the above photocrosslinking-induced hydrogel stiffening typically occurs in seconds to minutes, *in vivo* matrix stiffening usually develops over days to weeks or even months.

To address this limitation, Young and Engler[787] reported a slow Michael-type addition reaction to crosslink thiolated HA with PEGDA (Figure 19A). The reaction dynamics, and thus the stiffening process, were controlled by changing the PEGDA molecular weight. To

mimic the temporal stiffening of heart muscle during mesoderm development into adult myocardium, ~3400 Da PEGDA was used to crosslink 1% thiolated HA. The stiffness of the hydrogels increased fourfold over 3 days post-polymerization, resulting in enhanced cardiomyocyte maturation compared with static PA hydrogels. These systems represent a promising foundation for 4D microenvironmental design.

ECM softening, the opposite of stiffening, is another dynamic change in ECM mechanical properties that cells may encounter *in vivo*.[793] *In vitro* studies have revealed that hydrogel softening could impact cell spreading, proliferation, mobility and differentiation. The commonly adopted approach for inducing hydrogel softening is degradation. While different degradation mechanisms exist, photolytic degradation is the most used due to its high controllability.[794–795] For example, Kloxin *et al.*[796] developed a photodegradable PEG-based hydrogel that could be softened via exposure to UV light (Figure 19C). Gradient degradation in the presence of living cells led to gradient stiffness formation *in situ*, triggering the directional spreading of hMSCs in 3D. This hydrogel system was further employed to study the softening effects on the VIC phenotype. It was found that VICs cultured on stiff hydrogels were predominantly activated into myofibroblasts, which could be deactivated into quiescent VICs after hydrogel softening.[797] The deactivated fibroblasts could then be re-activated into myofibroblasts in the presence of TGF-β1[798] or anisotropic topographies.[799] The matrix softening-induced de-activation of myofibroblasts was found to be mediated through the PI3K/Akt pathway.[800] These findings indicate that targeted matrix softening may be an effective way to suppress or reverse the progression of fibrotic diseases. In recent work, the decrosslinking of ionically crosslinked alginate was employed to soften collagen-alginate hybrid hydrogels.[801] It was found that human pluripotent stem cells (hPSCs) encapsulated in the hybrid hydrogels could maintain their stemness and self-renewal capacity. However, when the hydrogels were softened by removing the alginate component, the stem cells switched to different lineage commitment stages in a switch time-dependent manner, demonstrating that hydrogel softening may work as a mechanical switch for tuning stem cell fate.

In addition to non-reversible stiffening or softening, several hydrogel systems with reversible stiffening and softening have been developed, including Ca^{2+}-crosslinked alginate-based hydrogels,[802] temperature-sensitive PNIPAAm-based hybrid hydrogels,[803] pH-sensitive triblock hydrogels,[804] DNA-crosslinked PA hydrogels,[805–807] and supramolecular hydrogels with host-guest interactions[358,808] (Figure 20). In one example, hydrogels were fabricated by crosslinking a mixture of alginate and temperature-sensitive liposomes.[809] The liposomes were loaded with AuNRs and either calcium chloride or diethylenetriaminepentaacetic acid (DTPA). Upon near IR (NIR) laser irradiation, the AuNRs produced heat and induced the gel-to-fluid phase transition of the liposomes, releasing calcium chloride or DTPA, which further led to crosslinking (stiffening) or decrosslinking (softening) of the alginate hydrogels, respectively. This system was demonstrated to enable remote transdermal stiffness modulation, showing promise in dynamically engineering the *in vivo* cell mechanical microenvironment for promoting tissue healing. In other work, hybrid hydrogels composed of alginate and collagen were fabricated.[802] The temporal delivery of Ca^{2+} or chelating agents through a filter membrane induced the crosslinking or decrosslinking of the alginate component, thus stiffening or softening the hybrid hydrogels, respectively. Mouse

C3H/10T1/2 fibroblasts encapsulated in a Ca^{2+}-crosslinked hybrid hydrogel maintained a rounded morphology, while mechanical softening by decrosslinking the alginate led to cell spreading. Recrosslinking the alginate did not reverse the morphology of spread cells.[802] Recently, a dynamic cell-laden hydrogel system was fabricated by using the thiol-allyl ether photoclick reaction of thiolated PVA, four-arm PEG-allyl ether (PEG4AE), and mono-functional β-cyclodextrin-allyl ether (βCDAE).[808] *In situ* hydrogel stiffening and softening were achieved through controlled supramolecular host-guest interactions between supplied free adamantane-functionalized four-arm PEG (PEG4AD) and immobilized βCD. Pancreatic MIN6 β-cells encapsulated in the hydrogels showed high viability and stiffness-dependent, reversible insulin expression. These reversible crosslinked hydrogel systems provide excellent platforms for studying cell responses to dynamically changing mechanical cues in 4D.[810] In addition, related hydrogels with reversible crosslinks can be designed to self-heal, thereby potentially replicating the tendency of collagen to crosslink and self-assemble in the vicinity of a cell.[811–813] These directions are largely unexplored, but hold promise for basic studies in cell biophysics.

3.3.2.4. Cell Mechanotransduction.: A key factor that has been emphasized throughout this review is the need to develop materials that preserve the ways that cells interact with their microenvironment mechanically. An important component of this is mechanotransduction, which we define as mechanical sensing that transforms microenvironmental mechanical properties (*e.g.*, elasticity and viscoelasticity) into intracellular signals.[814] Mechanotransduction is known to be sensitive to the details of both structure and mechanics in the cell microenvironment. Given the broad uncertainties in the 3D make-up and 4D evolution of this environment in native 3D tissues, great care must be taken. We summarize in this section key components of cell mechanotransduction, and emphasize areas in which insufficient information is available (Figure 21).

Cell adhesion contributes to cellular mechanosensing through stress propagation and chemical signal activation. Cells sense the stress (strain) of the external matrix by forming a dynamic mechanical bond system (*e.g.*, slip/catch bond and sliding-rebinding/allosteric catch bond) involving hundreds of known adhesion proteins, such as integrin, talin and vinculin.[202] Cell adhesion likely enables intracellular chemical signal activation, as in the upregulation of the focal adhesion kinase (FAK) phosphorylation on Y397 (FAKpY397) within ~100 nm aggregates of integrins called focal adhesions.[815]

Mechanical cues that regulate gene expression and protein translation must be transduced from the cell-ECM interface, through the cytoplasm, and to the nucleus.[816–817] We discuss two pathways. First is a soluble factor pathway triggered by stress-activated channels. Soluble factors that arise in response to mechanical cues, including FAK, Src and Rho,[818] produce downstream signaling via the FAK-RhoA-Rho kinase cascade and likely crosstalk with the TGF-β and Hippo cascades; these may also regulate nuclear events.[819]

Second, it is possible for mechanical signals to reach the lamina that surrounds the nucleus.[820] The lamins in the nuclear lamina connect the nucleus to the cell cytoskeleton through the LINC (“linker of nucleoskeleton and cytoskeleton”) complex.[821] Contractile actomyosin units in the cytoskeleton test matrix rigidity via tension and dynamic, force-dependent

reinforcement of integrin clusters.[822] Evidence that mechanical forces may regulate the nuclear lamina itself comes from observations that nuclear lamin-A follows a power-law scaling versus matrix rigidity, with rates of phosphorylation (turnover) of lamin-A inversely related to matrix rigidity.[823] Lamin-A levels and conformations regulate the location of proteins involved in gene expression (*e.g.*, nucleocytoplasmic shuttling of etinoic acid receptor gamma (RARG) and YAP) and thus lamin-A provides a potential mechano-chemical mechanism to explain the dependence of stem cell differentiation on matrix with different rigidity. Another possibility is that nuclear membrane stretch mediates mechanotransduction.[824] Although these connections and their roles in gene expression are still hypothetical, this body of literature further highlights how changes to the cell mechanical microenvironment can perturb cell function.[825]

3.3.3. Degradability—Degradation is an essential feature of native ECM and is involved in mediating cell behaviors including spreading, migration, and differentiation, thereby playing important roles in development, tissue homeostasis and disease progression. Most ECM macromolecules and their derivatives can respond to enzymes, especially cell-secreted enzymes such as MMPs, plasmin, and elastase. This is a critical pathway for cells to modulate their environment, and for cells to dynamically sense and obtain feedback from their local microenvironment. Engineering material degradability or adaptable crosslinking (Figure 23)[891–892] in biomaterials if essential for controlling matrix presentation and distribution, soluble factor immobilization and cell mobility, and dynamic tuning of material properties.[826–827] Two ongoing challenges in this field are controlling degradation byproducts and degradation kinetics. This must be balanced as well with the challenge of presenting cells with ECM that is the right order of magnitude in stiffness, and the further challenge that degradation invariably reduces ECM stiffness even further.

A basic requirement for degradable hydrogels is that degradation byproducts should be biocompatible. In some cases, degradation byproducts can provide instructive cues for modulating cell behaviors.[828] For instance, calcium and phosphate ions, which can be generated by the degradation of mineralized materials, have been found to promote the osteogenic differentiation of hMSCs through c-Fos[829] and adenosine signals,[830] respectively. The degradation byproduct of collagen, endostatin, has been shown to regulate EC and stem cell behaviors.[6,831–832] In addition, the degradation byproduct of polyester-based hydrogels, lactic acid, has been found to impact neural cell metabolic activity and intracellular redox state.[833–834] Similar examples can be found for other degradation byproducts of natural or synthetic hydrogels. Further studies are needed to understand the interactions between cells and degradation byproducts, which will benefit the design of degradable hydrogels for engineering the cell microenvironment. The degradation rate is dependent on the hydrogel types used, the crosslinking strategy, and the microenvironmental conditions. For tissue regeneration, it is important for the degradation rate of implanted biomaterials to match the cellular regeneration rate of the ECM. To control hydrogel degradation, various degradation mechanisms and degradable molecules have been exploited.[48,130,316] A major challenge is integrating all three main degradation mechanisms in a single engineered material: enzymatic degradation, hydrolytic degradation, and photolytic degradation (Figure 22).

Synthetic systems designed to achieve this in functionalized hydrogels include enzyme-sensitive peptide-based crosslinkers and hydrogel precursors.[835–836] For example, MMP-sensitive peptides have been applied to crosslink PEG hydrogels via base-catalyzed Michael-type addition (Figure 22A),[837–839] radical polymerization,[840] or thiol-ene photopolymerization.[438,841] The degradation rate of the MMP-sensitive PEG hydrogels was found to depend strongly on the sequences of the MMP-sensitive peptides. Increased bone regeneration was observed in more rapidly MMP-degradable hydrogels in the presence of recombinant human BMP-2.[839] When combined with the incorporation of RGD and VEGFs, MMP-mediated hydrogel degradation induced the sustained release of VEGFs over two weeks and promoted vascularization *in vivo*.[842] In addition, other degradable peptides have also been used to crosslink PEG hydrogels to endow them with degradability in response to human neutrophil elastase (HNE)[843–844] or plasmin,[845–846] among other enzymes. The strength of these approaches is that they endow hydrogels with the ability to be remodeled locally by cells. However, despite advances in technologies that enable *in situ* degradation monitoring,[893–896] a weaknesses is that there is no way to be certain that this remodeling is representative of how cells adapt their microenvironment *in vivo.* The differences between a PEG hydrogel and a fibrous ECM may be alleviated or exacerbated by cell degradation.

Spatial control of hydrogel degradation has been engineered by Burdick and co-workers[847–848] via partially crosslinked multi-acrylated HA with MMP-sensitive peptides and a primary addition reaction. Sequential crosslinking of the remaining acrylates through radical polymerization inhibited the spreading of encapsulated hMSCs even in the presence of adhesive peptides. Such strategies have been applied to produce patterned MMP-degradable HA hydrogels for spatially controlling the spreading and differentiation of hMSCs[848] and for achieving *in vitro* vasculogenesis or angiogenesis in 3D.[849] To control the temporal degradation of hydrogels, multiple enzyme-degradable peptides have been used in combination. For example, MMP-7 and aggrecanase (ADAM-TS4)-sensitive peptides have been applied to crosslink streptococcal collagen-like 2 (Scl2), a recombinant bacterial collagen.[850] These two peptides were targeted toward enzymes produced by encapsulated hMSCs undergoing chondrogenesis and by newly differentiated chondrocytes, respectively. The degradation behavior of the hydrogels was tuned by varying the ratios of the two peptides to mimic the temporal expression patterns of the corresponding enzymes in hMSCs during chondrogenesis. This technique is promising for the specific microenvironment of chondrocytes, but it remains to be determined whether it can function as a replicate of stiffer tissues.

In cancer,[851–852] MI,[853] rheumatoid arthritis,[854] and other diseases, the cell microenvironment may exhibit abnormal elevations in protease activity and concentration. Hydrogels have therefore been designed to degrade in response to local protease levels, releasing drugs or cells through feedback control for therapeutic and tissue regeneration purposes.[855–857] However, the enzyme activity and therefore the degradation rate of the corresponding hydrogels can be dramatically influenced by microenvironmental conditions. In addition, the enzyme concentration may vary across different tissues and depend on specific cell types. These factors increase the complexity of optimizing enzyme-degradable hydrogels *in vitro* for use as tissue implants *in vivo*. Moreover, as for hydrolysis, which will

be discussed below, enzymolysis provides limited controllability over the spatiotemporal degradation of hydrogels.

Hydrogels containing hydrolysable linkages, such as ester, hydrazone, and acetal linkages, either within their network backbone or crosslinker, can be hydrolytically degraded. As one example, a triblock copolymer, poly(ε-caprolactone-co-lactide)-*b*-PEG-*b*-poly(ε-caprolactone-co-lactide) (PCLA-PEG-PCLA), was fabricated via ring-opening polymerization (Figure 22B).[858] The concentrated copolymer solution rapidly gelled at body temperature through the formation of percolated micelle networks, forming a hydrolytically degradable and thermoreversible PCLA-PEG-PCLA hydrogel. This hydrogel was applied to prevent post-operative intestinal adhesion. PNIPAAm-based hydrogels have been rendered hydrolytically degradable by introducing hydrolysable segments into di(meth)acrylate crosslinkers.[859–860] In a recent study, injectable and rapid-gelling PNIPAAm hydrogels were prepared by the co-extrusion of hydrazide- and aldehyde-functionalized PNIPAAm oligomers.[861] The hydrazone linkages that formed during gelling rendered the PNIPAAm hydrogels hydrolytically degradable in an acid-catalyzed manner. In some cases, hydrolytic degradation can overcome the limitations of enzymatic degradation. It can occur under quite mild conditions without involving any trigger molecules. For instance, partially oxidizing alginate polymer chains can generate acetal groups to render alginate hydrogels hydrolysable without using alginases,[862–863] where the hydrolytic degradation rate increases with increasing the oxidation degree. Such material systems have been applied for 3D cell culture and tissue regeneration with tunable material degradability and mechanical properties.[864–866] As for HA hydrogels, they can be enzyme-degradable in response to hyaluronidase; however, such degradation is slow, and the acidic pH level needs to be optimized to enhance the enzyme activity. Therefore, glycidyl methacrylate (GMA) modification has been performed to render HA hydrogels hydrolytically degradable.[867] The degradation rate can be readily regulated by adjusting the ratio of high molecular weight (220 kPa) to low molecular weight (110 kPa) HA-GMA.[867] While hydrolytic degradation is an effective way to induce the bulk degradation of hydrogels in the physiological microenvironment, it is sensitive to microenvironmental changes since the hydrolysis rate of hydrolysable linkages, including ester and hydrazone linkages, can be affected by a multitude of factors, such as pH level and water penetration.[868] This sensitivity might lead to challenges in predicting degradation kinetics. In addition, as with enzymatic degradation, controllability over the spatiotemporal degradation of hydrogels is limited.

Benefiting from the development of laser technologies and cytocompatible, photosensitive hydrogel systems, photolytic degradation has been demonstrated to enable good control over hydrogel degradation in space and time.[869–870] The Anseth group adopted a strategy that has been used for the dynamic patterning of bioactive peptides to fabricate photodegradable, PEG-based hydrogels by copolymerizing a photodegradable crosslinker with PEG monoacrylate (Figure 22C).[458–460,871] The crosslinker macromer was synthesized by conjugating a photodegradable acrylic monomer containing o-NB groups into the backbone of a PEG macromer. Hydrogel channels generated in real time through *in situ* photodegradation released encapsulated fibrosarcoma cells to migrate along the channels.[458] By combining photodegradation with RGD photopatterning, it was shown that both interstitial space and adhesion cues were required for guiding NIH 3T3 cell migration in 3D.

[460] Recently, Revzin and co-workers[872–873] developed a similar strategy for fabricating photodegradable, PEG- and heparin-based hydrogels for cell capture, culture and release. To further enhance photodegradation controllability, Griffin and Kasko[874–875] synthesized a series of o-NB linkers with varying structures and reactivities, and they linked various model therapeutic agents to the PEG backbone to form different photodegradable PEG macromers. Hydrogels made from these macromers showed o-NB linker-dependent degradation behavior. Complex, multistage release profiles of the therapeutic agents were achieved by simply changing the light wavelength, intensity, and exposure time.[874] Encapsulated hMSCs were released in a wavelength-dependent manner via combined use of two different o-NB linkers.[876] Such systems show promise for the controlled delivery and on-demand release of multiple bioactive molecules, therapeutic agents, and cells in 3D for tissue engineering and regenerative medicine applications. Nevertheless, nitrobenzene moieties were used in the above photodegradable hydrogel systems, which can absorb light strongly and thus limit the degradation depth. To overcome this limitation, a method based on oxidizing thiol-functionalized PEG macromers was reported.[877] This method enabled the degradation of up to 2 mm of the fabricated PEG hydrogels within 120 seconds upon exposure to 365 nm UV light at 10 mW/cm^2. However, long-time exposure to UV light can harm cells and tissues.

In part to overcome this challenge, photodegradable hydrogels responding to NIR light have been developed.[878–879] NIR light-mediated hydrogel degradation can be more useful for *in vivo* biomedical applications since NIR light has good tissue penetrability and causes less cellular photodamage. Nevertheless, thermal effects of NIR light must be weighed when long-time exposure to high intensity NIR light is required. Photodegradation has provided advanced controllability on hydrogel degradation in a remote manner, with varying degrees of desired degradation rates depending on light wavelength, intensity and exposure time. As with other technologies, toxic byproducts are the major challenge. Small molecules generated during hydrogel photodegradation can be toxic to surrounding cells both *in vitro* and *in vivo*. Therefore, biocompatibility is a key challenge for design and application of photodegradable hydrogels. Table 1 summarizes some important aspects of different degradation mechanisms.

Beyond those degradation mechanisms discussed above, degradation mechanisms that have been employed in tissue engineering include reduction-sensitive degradation,[880] thermal degradation,[881–882] and/or reversible click reactions.[883–884] To render hydrogels reduction-degradable, reduction-sensitive linkages, such as disulfide bonds, are routinely used. The disulfide bonds can be incorporated into hydrogels through several strategies, including the oxidation of thiol-functionalized precursors,[885] the use of disulfide-containing crosslinkers, [880] and the use of thiol-disulfide exchange reactions.[886–887] When exposed to thiol-containing reducing agents, such as glutathione (GSH) and N-acetyl-cysteine, disulfide bonds can be rapidly cleaved, resulting in hydrogel degradation. Such disulfide-crosslinked hydrogel degradation is rapid, with half-lives ranging from 8–45 min. This relatively rapid release may limit the use of this method for drug or growth factor delivery, where sustained release is usually preferred. To overcome this limitation, PEG-heparin was prepared by a reversible thiol-maleimide Michael-type reaction between thiol-functionalized PEG and maleimide-modified heparin.[888–889] The presence of GSH can trigger an exchange reaction in PEG-heparin hydrogels, leading to degradation, the rate of which can be controlled by

functionalizing PEG polymers with different arylthiol derivatives. Considering that GSH elevation has been found in the tumor microenvironment and may be associated with cancer cell activities,[890] the above reduction-sensitive degradable hydrogels have potential for various applications in targeted drug delivery for cancer therapy.[72]

3.3.4. Electrical Conductivity—Electrical communication among cells in mature tissues is achieved by direct connectivity through ion channels such as those formed by connexins. However, during development and wound healing of native tissues and development of tissue constructs, the electrical conductivity of the cell microenvironment is a critical mediator of ionic currents. The poor electrical conductivity of most biomimetic materials traditionally used in cell culture has led to the development of conductive biomaterials, which have typically been produced through the incorporation of conductive components, such as conductive polymers or oligomers,[897] AuNPs,[694] CNTs[898] and graphene[899] (Figure 24).

Conductive polymers were discovered in the mid-1970s[900] and attracted interest for biomedical applications in the 1980s.[901] Conductive polymers not only have some properties similar to those of common polymers, such as flexibility and easy processing, but also possess attractive electrical properties that can be controlled. Several conductive polymers, such as polypyrrole (PPy), polyaniline (PANi), polythiophene, poly(3,4-ethylenedioxythiophene) (PEDOT), and their derivatives, have been demonstrated to be biocompatible for *in vitro* cell culture and *in vivo* tissue regeneration.[902–905] However, due to their poor cell adhesivity, lack of biodegradability, and limited controllability over mechanical properties, conductive polymers have typically been blended or copolymerized with routinely used degradable polymers to generate conductive biomaterials. These conductive biomaterials have been engineered into the forms of particles and nanofibers with anisotropic conductive properties for synchronizing cardiomyocyte beating,[906] promoting neurite extension,[907] and enhancing myoblast differentiation,[908–910] among other purposes. Moreover, conductive hydrogels, including aniline pentamer[911] or PANi-grafted[912] gelatin, PANi-GelMA hybrid hydrogels,[913] PEDOT-coated agarose nerve conduits,[914] PPy-coated cellulose,[915] PANi nanofiber- or PEDOT nanofiber-loaded collagen,[916] and PPy-grafted chitosan,[897] have been fabricated and applied for cell culture and tissue regeneration applications.[917] Although promising, few of these conductive hydrogels have been developed for engineering the 3D cell microenvironment, in part due to the use of undesirable chemicals or incompatible conditions during the fabrication process of such conductive hydrogels.

AuNPs, as one of the most versatile noble metal nanoparticles, have found widespread biomedical applications. The excellent optical properties of AuNPs render them especially useful for surface plasmon resonance-based sensing, imaging, and thermal therapy.[918–919] In addition, due to their high electrical conductivity and biocompatibility, AuNPs have been recently employed to fabricate conductive nanocomposite hydrogels for tissue engineering applications. Several approaches have been developed to incorporate AuNPs into hydrogels. One approach is to synthesize AuNPs in hydrogels *in situ*, *i.e.*, the hydrogels were first fabricated and then used as templates for assisting the formation, morphology control and distribution of AuNPs.[920–921] Via this approach, porous conductive thiol-hydroxyethyl

methacrylate (thiol-HEMA)/HEMA hybrid hydrogels with homogeneously distributed AuNPs were fabricated.[920] The electrical conductivity and the mechanical properties of the hybrid hydrogels were controlled by adjusting the thiol-HEMA content. Neonatal rat cardiomyocytes cultured on these hydrogels showed upregulated connexin 43 (a gap junction protein) expression even in the absence of electrical stimulation. Similar approaches have been used to fabricate conductive and pH-sensitive poly(N,N-dimethylaminoethyl methacrylate) (DMAEMA)/HEMA hybrid hydrogels.[922] The conductivity of these hydrogels was demonstrated to be reversibly alterable through pH-induced volumetric swelling/deswelling. Another approach is to incorporate prefabricated AuNPs into hydrogels either during or after hydrogel formation. In a typical example, gold nanowires were incorporated into alginate scaffolds during ionic crosslinking.[694] It was shown that the embedded gold nanowires significantly improved the electrical conductivity of the alginate scaffolds and the electrical communication between adjacent neonatal rat cardiomyocytes, as well as cell organization and contraction. Recently, a similar approach was utilized to deposit AuNPs on decellularized omental matrices[923] and embed AuNRs in GelMA hydrogels[924–925] to engineer bioactive and conductive cardiac tissue constructs, which showed promise for cardiac tissue engineering applications. However, issues of uncertain long-term toxicity make these materials, like other nano-particle based materials, unlikely candidates for FDA approval.

Another type of conductive nanomaterial that has been broadly used in biomedical applications is carbon-based nanomaterials, such as CNTs and graphene. CNTs have been widely used to mechanically reinforce tissue engineered scaffolds[926] and have recently been combined with various types of hydrogels to generate conductive hydrogels for engineering cardiac and nervous tissues.[927–930] For instance, Khademhosseini and co-workers[898,931] combined multiwalled CNTs and photocrosslinkable GelMA to fabricate CNT-GelMA hybrid hydrogels. NIH 3T3 cells and hMSCs encapsulated in the hybrid hydrogels maintained high cell viability and readily spread in 3D.[931] The incorporation of CNTs into GelMA hydrogels drastically increased the spontaneous synchronous beating rates (3-fold higher) of adhered cardiomyocytes and reduced the excitation thresholds (85% lower) of the engineered myocardial tissues. Moreover, the CNT-GelMA hybrid hydrogels showed strong protective effects against cardiac inhibitors (*e.g.*, heptanol) and cardiac toxicants (*e.g.*, doxorubicin).[898] In a later study, dielectrophoresis was applied to align CNTs in GelMA, resulting in the formation of anisotropic conductive hybrid hydrogels.[932] Compared with hydrogels with randomly distributed or horizontally aligned CNTs, these hydrogels with vertically aligned CNTs enhanced the differentiation of C2C12 myoblasts and the formation of functional myofibers under electrical stimulation. An alternative method for generating vertically aligned CNT forest microelectrode arrays in GelMA hydrogels was recently developed to engineer muscle-based biohybrid actuators.[933] The beating frequency and excitation thresholds of the biohybrid actuators were found to depend on the direction of the applied electrical signal relative to the vertically aligned CNTs. In addition to CNTs, carbon nanofibers[934], graphene and their derivatives[899,935–937] have also been combined with hydrogels to create electrically conductive hybrid hydrogels. Graphene, usually in the form of reduced graphene oxide (rGO), is particularly interesting due to its flexibility, good electrical conductivity, and ease of dispersion in aqueous solutions. Despite remarkable

advances in the synthesis and functionalization of these carbon-based conductive hydrogels, the potential toxicity of CNTs and rGO currently preclude their clinical application.[938–939]

Recently, nanoelectronics that enable simultaneously generation and sensing of electrical signals have been integrated with biomaterials to generate 3D nanoelectronic scaffolds for culturing neurons, cardiomyocytes, and SMCs.[940–942] Such nanoelectronic scaffolds enable not only the delivery of electrical signals to active cells and engineered tissues but also the electrical sensing of 3D cell responses and engineered tissue performances (Figure 25).[940] These engineered nanoelectronic tissue constructs hold great potential for use in tissue engineering and biosensors, if issues of potential toxicity can be resolved. Even in the absence of FDA approval, these technologies may also be promising for high-throughput drug screening applications via combination with organ-on-chip technologies.[943]

Conductive additives to hydrogels exhibit several common strengths and weaknesses in the context of engineering the cell microenvironment. Conductive polymers are easily incorporated into biomaterials, and often display antibacterial properties due to their surface energy. However, they are poor conductors compared to nanoscale conductive additives (*e.g.*, CNTs, rGO, and AuNPs). These additives provide excellent conductivity at low concentrations, but their size and surface energy–and hence the difficulty of dispersing them in a hydrogel–make them poorly suited to large scale synthesis. Table 2 summarizes the various conductive additives used for fabricating conductive biomimetic materials and their biomedical applications and performances. The conductivities of conductive biomaterials as a function of concentrations are summarized in Figure 26. In summary, the challenge of creating a non-toxic and facile conductive microenvironment for cells encapsulated in hydrogels is still open. Although many technologies are available, each has drawbacks preventing its widespread and effective use.

3.4. Decoupling Material Properties

As discussed both in this section and in Section 2, material cues such as stiffness, porosity, and adhesion-ligand density can control a range of cell behaviors. However, these material cues are usually coupled to each other, which confounds identification of the effects of individual cues on cell behaviors.[713,976] We summarize a small portion of the very large literature on this topic in this subsection. Although we have attempted to construct a coherent narrative, the result is a dizzying array of behaviors that are difficult to interpret. The most important challenge, in our opinion, is that a fundamental understanding of the basic biophysical principles that cells follow when interacting with their microenvironments are lacking. A secondary consideration is, as mentioned previously, that the nature of these microenvironments in native tissues is often uncertain, confounding efforts to ascertain whether responses observed are relevant physiologically. Coupled materials and model development represents an important need in this area.

For example, material stiffness is usually tuned by changing the polymer concentration or crosslinking density, which might simultaneously result in variations in adhesion-ligand density and porosity. Different strategies, including microfabrication, chemical modification, composition changes, and crosslinking regulation, have therefore been developed to independently control various aspects of material properties.

Microfabrication has been used to decouple material properties by controlling topological structures, for example, to modulate substrate stiffness independent of chemical properties,[977] hydrogel permeability independent of stiffness,[978] and structural topography independent of both stiffness and chemical properties.[979–980] In an archetypal example, Chen and co-workers[977] microfabricated PDMS micropost arrays. By varying the height of the microposts but keeping the diameter the same, the effective stiffness (or spring constant) of the microposts was tuned independent of the adhesion-ligand density and surface chemical properties (Figure 27A). The same principle has also been used to create Matrigel substrates with gradient stiffness, which was achieved by continuously changing the local Matrigel thickness while keeping the concentration and other parameters the same.[981] Cell migration velocity on such substrates is driven by the stiffness gradient rather than the stiffness itself. In another example, the Long group[982] used soft lithography to fabricate PA hydrogel substrates with independently varied stiffness and topography. These factors were found to affect rat BMSC spreading, proliferation, differentiation, and cytoskeletal reorganization in an isolated manner. Recently, Kim *et al.*[980] reported that ECM protein-functionalized magnetic nanoparticles, mixed with a hydrogel precursor solution, self-assembled into different topographies under a controlled magnetic field, and then fixed in 3D by gelling the hydrogel precursors. This enabled the decoupling of topography from hydrogel stiffness and composition. It was observed that anisotropic topographies could guide 3D protrusions of NIH 3T3 cells and PC12 cells in the absence of other guiding cues. However, lacking in all of these technologies is a well-defined fibrous character of the ECM and appropriate nonlinearity. Unified models of cell mechanics and ECM remodeling are needed to translate these observations into principles that can be used for design of tissue constructs.

Chemical modification is an effective approach to decouple biophysical (*e.g.*, stiffness) and biochemical (*e.g.*, adhesion-ligand density) hydrogel properties. Toward this end, RGD-modified PEG-based hydrogels are often used. PEG provides an inert and “blank” network with a tunable stiffness, while RGD can be readily incorporated into PEG in a well-controlled manner without changing biophysical hydrogel properties, thereby allowing independent control over hydrogel stiffness and adhesion-ligand density (Figure 27B).[457] By using such hydrogel systems, it has been found that hydrogel stiffness and adhesion-ligand density (*i.e.*, nanospacing) could independently affect SMC[983] and MSC[984] behaviors. For example, increasing hydrogel stiffness independently enhanced SMC spreading and proliferation, reduced the size of focal adhesions and the degree of SMC differentiation; while increasing adhesion-ligand density independently enhanced SMC spreading with a greater degree of heterogeneity and increased the size of focal adhesions.[983] Moreover, using photopatterning methods, especially two-photon laser-scanning lithography, PEG-based hydrogels with varying complex adhesion-ligand patterns have been created independent of hydrogel stiffness and porosity for guiding cell migration in 3D.[457,460,985] In addition to PEG hydrogels, alginate and HA hydrogels have also been modified with cell adhesion ligands, such as RGD, for independently controlling biophysical and biochemical hydrogel properties.[986] Furthermore, chemical modification can also be performed on molecular crosslinkers. For example, partially oxidized methacrylic alginate (OMA) has been used to crosslink both PEG methacrylate (PEGMA) and poly(N-hydroxymethyl acrylamide) (PHMAA) to form hydrolytically degradable hydrogels.[987] By increasing the

oxidation degree of the alginate crosslinker, the degradation rate of both PEGMA and PHMAA hydrogels was increased without altering their initial stiffness. Such OMA-crosslinked hydrogels were demonstrated to enable the controlled release of proteins and enhanced angiogenesis *in vivo*. Careful controls are still needed to determine whether these effects are truly due to physical stimuli, or are in fact related to the presence of byproducts of hydrogel breakdown.

Another approach to decouple hydrogel properties is to change their chemical composition. This approach has been applied to independently control hydrogel stiffness, permeability, adhesion-ligand density, or pore size. For instance, Kong and co-workers[988] reported that by crosslinking of PEGDA with methacrylic alginate and varying the alginate concentration and methacrylic group substitution, the hydrogel stiffness could be tuned by more than one order of magnitude without significantly changing the hydrogel permeability (represented by the swelling ratio). They developed another hydrogel system with PEG monoacrylate incorporated into the PEGDA hydrogel network as hydrophilic pendant chains,[989] and found that by increasing the mass percentage of PEG monoacrylate without changing the total polymer concentration, the stiffness of the hydrogel decreased, while the swelling ratio showed only a minimal increase. The proliferation rate of encapsulated NIH 3T3 cells decreased with increasing hydrogel stiffness, while the cell viability and endogenous VEGF expression showed biphasic dependency on hydrogel stiffness. To decouple the effects of hydrogel stiffness and adhesion-ligand density on cell behaviors, Scott *et al.*[990] fabricated PEG-based modular hydrogels by crosslinking PEG-Glycine microgels with PEG-four-arm-amine. At concentrations ranging from 0 to 100 μg mL^{-1}, collagen was incorporated into the modular hydrogels during crosslinking, with no significant changes in hydrogel stiffness. In another study, the stiffness of copolymerized PEG-based hydrogels was independently tuned by changing the MMP-sensitive PEG concentration and maintaining the PEG-RGDS concentration.[991] Similarly, in an alginate-based hydrogel, the stiffness was tuned from 1.87 kPa to 5.56 kPa in the presence of a constant RGD density, which was achieved by increasing the concentration of unmodified alginate from 0.5% (w/v) to 2% (w/v) while maintaining the RGD-modified alginate concentration.[381] However, these stiffnesses are orders of magnitude lower than typical tissue moduli.

The state of the art in this area is the work of Engler and co-workers,[30] who developed a collagen-coated PA hydrogel system in which the acrylamide/bis-acrylamide ratios were adjusted to independently control hydrogel stiffness and pore size (or porosity) (Figure 27C). They demonstrated that the differentiation of hADSCs and hBMSCs cultured on the PA hydrogel substrates was regulated by substrate stiffness independent of porosity and protein tethering. Recently, by adopting this collagen-coated PA hydrogel system, Huang and co-workers[992] found that increasing substrate stiffness rather than pore size induced the differentiation of cardiac fibroblasts into myofibroblasts. Such stiffness-induced cardiac myofibroblast differentiation was mediated through angiotensin II type 1 receptor (AT_1R) and could be inhibited by hADSC-secreted HGFs via AT_1R downregulation and Smad7 upregulation. As discussed at the end of this section, these approaches have provided much insight into cellular biophysics, but are limited by several ongoing challenges.

In addition to the above approaches, some studies have explored the use of crosslinking regulation (*e.g.*, crosslinking type and density) to independently control hydrogel properties. For example, glutaraldehyde has been used to covalently crosslink self-assembled collagen hydrogels to increase the stiffness without changing the hydrogel protein concentration or pore size.[993] Breast carcinoma cells (MDA-MB 231) cultured on stiffer collagen hydrogels showed an enhanced 3D invasion depth when the hydrogel pore size was large enough to prevent excessive steric hindrance. In another study, collagen molecules were non-enzymatically glycated with ribose prior to polymerization.[994] Increasing the concentration of ribose from 0 to 250 mM led to a three-fold increase in collagen hydrogel stiffness with no changes in collagen density and minimal changes in collagen fiber structure. ECs encapsulated in the hydrogels exhibited increased cell spreading, angiogenic sprouting and spheroid outgrowth with increasing hydrogel stiffness. However, for ionically crosslinked hydrogels, it may be effective to modulate the crosslinking density and thus the hydrogel stiffness independent of its biochemical properties, and even other biophysical properties, by simply changing the concentration of small ion crosslinking agents.[377,380] For instance, the stiffness of IPN hydrogels made from a reconstituted basement membrane matrix and alginate has been tuned from 90 Pa to 945 Pa independent of pore structure and adhesion-ligand density simply by increasing the calcium concentration used for alginate crosslinking from 0 mM to 20 mM (Figure 27D).[377] It was found that increasing matrix stiffness alone could lead non-malignant MCF10A cells to exhibit a malignant phenotype in 3D, depending on the ECM composition. This effect was demonstrated to be mediated through signaling pathways involving β4 integrin, PI3K, and Rac1.[377] However, even with these crosslinking technologies, the stiffness range studied is many orders of magnitude below the stiffness of even the mammary tissue that represents the niche of MCF10A cells.

Microfluidic technologies have also been exploited to independently control the physical confinement of the microenvironment through the configurations and dimensions of microfluidic channels. Microfluidic confinement affects cancer cell division.[153–154] In microfluidic devices engineered with dimensions mimicking human capillary constrictions, [995] circulating tumor cell (CTC) clusters dynamically reorganize into single-file chains to pass through such capillary constrictions. Weakening cell-cell interactions with drugs disrupted the CTC clusters in the constrictions, suggesting a potential means of suppressing CTC cluster-mediated metastasis.[995] By measuring the times required for cells to enter and pass through microfluidic constrictions, cell deformability and corresponding cell mechanical properties can be characterized in a high-throughput manner.[996–997] Moreover, microfluidic channel design and hydrodynamic stress field control can enable not only cell separation based on deformability[998–1000] but also large-population mechanical phenotyping based on high-throughput single-cell hydrodynamic stretching.[1001–1002] Although microfluidic systems are far from the 3D microenvironment of a solid tissue, they are representative of a clinically important 3D system and enable decoupling of the effects of shape and mechanics in interpretation of circulating cell responses.

Despite the above advances, many fundamental relationships among microenvironmental cues and cell behaviors remain elusive. More efforts must be directed toward developing not only new decoupling biomimetic materials and strategies, but also associated mathematical models that enable identification of fundamental principles underlying cell-

microenvironment interactions. Biomimetic materials can provide many instructive cues that may work independently or cooperatively to form complex microenvironmental networks for regulating cell behaviors.[1003–1005] In the absence of specially designed systems and predictive models, it is often not possible to fully decouple material cues from each other. Development of mathematical models in conjunction with material systems that enable their testing is an important need in the field.

4. Biomedical Applications

Although a great number of uncertainties and challenges remain, many of the biomimetic materials described in the previous section can be produced in sufficient quantity and with sufficient reliability to enable manipulation of cells in 4D microenvironments. Although actual 4D control is still amongst the remaining challenges, the resulting tissue constructs do remodel and often reach a steady state that is useful technologically or clinically. Biomedical applications for which these have found utility include (1) promotion of tissue regeneration; (2) construction of functional *in vitro* tissue models for pathophysiological studies and drug testing; (3) enhancement of large scale cell differentiation; (4) implementation of immunotherapy; and (5) enablement of gene therapy. In this section, we briefly summarize the state of the art and open challenges in each of these biomedical application areas through the lens of engineered cell microenvironments.

4.1. Tissue Regeneration

Although the dream of tissue engineered replacement organs and tissues is still far away, biomimetic hydrogels have utility for assisting with tissue regeneration through their role in delivering therapeutic agents and bioactive factors.[1006–1008] Numerous hydrogels and corresponding fabrication technologies have been developed to afford high degrees of spatial and temporal control over therapeutic agents to enhance their therapeutic efficacies.[1009] A key challenge is engineering the cell microenvironment for the regeneration of tissues, and we review here how hydrogels may contribute to this goal.

4.1.1. Skin Tissue—Skin is essential for pathogen protection, sensation, thermoregulation, and water retention but can be damaged by physical and chemical factors such as burns, surgery, or trauma. The healing of skin requires synergistic function of numerous cell types and ECM. Dysfunctional wound healing may result in excessive scarring or even malignant transformation.[1010] Numerous biomimetic materials have been exploited to construct wound dressings or potential tissue-engineered substitutes for skin replacement.[1011–1013] A great deal of recent research have reported the use of hydrogels (mostly collagen, gelatin, chitosan and HA) in engineering the biophysical and biochemical microenvironment of cells to aid skin regeneration.[1010,1014–1015]

Hydrogels for skin regeneration require biocompatibility, bioactivity, and appropriate mechanical and degradation properties,[1016] with the goals of directing the growth and differentiation of keratinocytes and stem cells, and minimizing scarring. Hydrogel strength should be sufficient to support surgery and its mechanics should support natural skin movement. Hydrogel degradation rates should meet wound healing requirements. The commonly used naturally derived hydrogels (*e.g.*, collagen and gelatin) are biocompatible

and biologically active, however, they suffer from inadequate mechanical properties and uncontrollable degradation kinetics.

Various strategies have been therefore developed to overcome these problems, including physical treatment (*e.g.*, plastic compression of collagen) and chemical modification (*e.g.*, methacrylamide modification of gelatin).[1014] Synthetic and hybrid hydrogels have been used to improve function of tissue-engineered skin healing grafts. In addition, growth factors such as EGFs, FGFs, TGF-β, and PDGFs have been incorporated into hydrogels and tuned to optimize the biochemical microenvironment for vascularization and prevention of scarring.[1016] Moreover, gene augmentation is a promising way for functionalizing the tissue-engineered skin substitutes for further improving their clinical outcomes.[1017]

Structural features are also important. Electrospun nanofibers have been proven to be effective promoters of appropriate MSC proliferation and differentiation in skin wound healing.[1018] Bottom-up bioprinting has currently untapped potential for precise patterning of diverse cells and hydrogels, and drop-on-demand and layer-by-layer printing processes are promising for multi-layered skin tissue constructs.[1015,1019] A particularly attractive direction is the *in situ* bioprinting of skin, in which the shape and depth of the printed skin tissue constructs can be customized to closely match wound contour.[1017]

To conclude, with the development innovative bioengineering technologies and regeneration strategies, skin equivalents incorporating various appendages and appropriate culture microenvironments have been reported in a number of studies.[1020–1021] With several products already on the market and potential advanced technologies in the pipeline, transitioning from skin repair to skin regeneration as a standard of care is an exciting possibility.[1022] However, holding these advances back is the challenge of understanding how fibroblasts are controlled by their microenvironments, and cures for scars in adults as well as other desirable aesthetic outcomes remain elusive.[1016,1023]

4.1.2. Cardiac Tissue—Cardiac tissue engineering requires the use of both cells (*e.g.,* cardiomyocytes, fibroblasts, and stem cells) and supporting matrices. Biomimetic materials (especially hydrogels) are potentially useful in engineering the cardiac cell microenvironment for maintaining transplanted cells in infarction sites, restoring myocardial wall stress, and enhancing cell functions for cardiac tissue regeneration.[1024–1026]

A major challenge for cardiac tissue engineering is obtaining cardiomyocytes, which have a limited proliferation capability. Therefore, stem cells (*e.g.*, iPSCs) are often used, with the aim of deriving cardiomyocytes by engineering the stem cell microenvironment. Since many cells are required for cardiac regeneration, microenvironmental cues that can trigger stem cell proliferation, cardiac lineage-specific differentiation and maturation are needed. For this purpose, biomimetic materials containing bioactive cues have been developed to promote the differentiation of stem cells into cardiomyocytes.[1027–1029] For instance, PEG-based hydrogels have been developed to contain RGD peptides that can interact with integrins for enhancing early-stage cardiogenesis.[1030] Using embryonic carcinoma cells as a model and a cell suspension as a control, it has been shown that this 3D hydrogel matrix could result in the elevated expression of cardiac markers, *i.e.*, Nkx2.5 and myosin heavy chain. ESCs

encapsulated in alginate hydrogel shells, where they proliferated to form morula-like cell aggregates and pre-differentiated into early cardiac lineage cells under biomimetic 3D culture,[1031] have been re-encapsulated into injectable alginate-chitosan microgels for cardiac tissue regeneration (Figure 28). Attempts have also been made to explore the feasibility of using biomimetic materials that can locally and sustainably release drugs and growth factors to facilitate stem cell proliferation and differentiation for cardiac tissue engineering.[1032–1034] Moreover, electrical stimulation has been applied to direct stem cell differentiation.[1035–1036] For instance, it has been demonstrated that the homogeneity of stem cell-derived cardiomyocytes can be improved by providing exogenous electrical signals,[1036] and such findings are important for the preclinical use of cells. However, debate still exists about the degree to which iPSC derived cardiomyocytes can be induced to express a mature phenotype.

The performances of engineered cardiac tissues can be greatly affected by their microenvironmental nanostructural features.[1037–1039] By engineering the cardiac nanostructural microenvironment,[1040–1041] it has been demonstrated that the cardiomyocyte alignment, cytoskeletal organization and gap junction formation can all be controlled.[650] Extensive studies have been performed to examine the feasibility of using electrospun fibers as bioactive scaffolds,[1042] with certain mechanical and chemical properties for regulating various cardiac cell behaviors.[1043] Alternatively, rotary extrusion has been used to produce PLA fibers for culturing neonatal rat ventricular myocytes, in which a high degree of sarcomere alignment was observed.[1044] Moreover, self-assembled, biotinylated peptide nanofibers have been constructed for delivering IGF-1 and have shown promise in cell therapies for MI.[1045] In an *in vivo* study using mouse models, nanoscale filaments of peptides that were functionally analogous to VEGF were incorporated into injectable materials, which exhibited significant elevations in blood circulation and angiogenesis in damaged myocardial tissue.[1046] Cardiac cell orientation can also be controlled by aligned nanofibers made of amphiphilic peptides.

Although these accomplishments are impressive, the field of cardiac tissue engineering is just in its beginning. Optimal combinations of mechanical, electrical, biological, and structural cues are needed, but the interactions of these are poorly understood. 4D control of tissue constructs is needed to enable cells, especially iPSC-derived cardiomyocytes, to reach a mature state suitable for drug discovery and tissue engineering.

4.1.3. Neural Tissue—Neural tissue engineering aims in part to create a cell microenvironment for guiding neural cell growth and differentiation to treat diseases and/or injuries of the nervous system.[1047–1049] The complex repair processes of the nervous system and limited regenerative ability of the adult human nervous system present substantial challenges to tissue engineers. When an injury gap in the peripheral nervous is too large and direct end-to-end surgical reconnection is not possible, nerve grafts (especially autografts) are often used, but they all suffer from various drawbacks, such as potential functional loss at the donor site (autografts) and disease transmission (allografts and xenografts).[1050–1051] CNS regeneration is even more difficult because a glial reaction microenvironment is created and leads to glial scar formation after injury, inhibiting axonal regeneration and remyelination.[1052]

Early attempts used biomimetic materials containing desired biochemical cues for enhancing the regenerative growth of axons and facilitating nerve regeneration, both in terms of structure and function. In one study, peptide-derived agarose hydrogels were demonstrated to allow 3D neurite extension through interactions between peptides and cell receptors.[1053] In another study, RGD peptides were covalently immobilized onto a crosslinked poly(N-2-(hydroxypropyl) methacrylamide) (PHPMA) hydrogel, which showed regenerative axonal growth after implantation into cerebral cortex and optic tract lesions in rats[1054] and into mature and developmental spinal cord lesion models.[1055] In addition, by controlling the spatial distribution of cell adhesion cues in biomimetic materials, well-defined cell arrangement and orientation can be achieved, which have significant influence on NSC differentiation and nerve regeneration.

Numerous studies have shown that the biophysical properties of biomimetic materials should also be considered when engineering the neural cell microenvironment for nerve regeneration. For instance, stem cell fate and lineage differentiation can be greatly affected by the ECM stiffness where the cells reside.[1056] Soft substrates in the range of 100–500 Pa facilitate neuronal differentiation of adult NSCs, whereas stiff substrates in the range of 1–10 kPa facilitate glial differentiation.[1057] In addition, the microstructural alignment of biomimetic materials is another important parameter for nerve tissue engineering. Unlike most other tissues, nerve tissue structures are highly oriented in a hierarchical manner, from a single neural axon to nerve fibers, which is important for nerve impulse transmission. Studies have revealed that highly aligned nanostructures can enhance directed neuronal elongation, neuronal NSC differentiation, and nerve regeneration.[1058–1061] For instance, collagen hydrogels with 3D, aligned fibrous structures have been prepared via the mechanical conditioning-directed fibrillogenesis of collagen molecules during self-assembly.[1062] Such hydrogels were demonstrated to enhance the parallel extension of neuronal axons as well as functional connectivity. In addition, alginate hydrogel microtubes have been fabricated to create a tubular 3D microenvironment for mouse NSCs.[1063] It was found that the tubular microenvironment could sustain NSC viability and enable the formation of microfiber-shaped neural tissue in which the dendrites and axons were parallel to the direction of the microtubes. Recently, the Wang group[1064] simultaneously used electrospinning and molecular self-assembly to produce a fibrillar fibrin-based hydrogel with a stiffness and hierarchical alignment mimicking those of native nerve tissues. It was demonstrated that these two features synergistically facilitated the neurogenic differentiation of human umbilical cord MSCs as well as rapid, long neurite outgrowth, without using neurotrophic growth factors. An *in vivo* assessment based on a rat T9 dorsal hemi-section spinal cord injury model found that the fibrin hydrogel could trigger the rapid migration and axonal invasion of endogenous neural cells along the fiber direction, forming aligned tissue.

However, the field is still without a clinically useful strategy for enabling neural tissue regeneration in the spinal cord, and the inability to re-engineer the cell microenvironment is to blame.[1065] The key is that injured cells of the central nervous system form a microenvironment around themselves that prohibits regrowth and reconnection of neurons following spinal injury. Decoding and re-engineering the cell microenvironment in spinal cord tissues represents a grand challenge for materials science and biomedical engineering.

4.1.4. Cartilage Tissue—Cartilage is an avascular, alymphatic and aneural connective tissue. In diarthrodial joints, articular cartilage provides a smooth, low-friction and wear-resistant surface that can disperse mechanical loads by synergistically working with synovial fluid. Articular cartilage can be frequently damaged due to trauma and osteoarthritis. Unfortunately, it has limited capacity to repair itself spontaneously in the absence of blood and lymphatic vessels. Although a large number of studies and various strategies have been reported for promoting articular cartilage regeneration, the field is still far from fulfilling clinical requirements.[1066–1068] Recent efforts have focused on biomimetic material-based cartilage tissue engineering strategies.[1069] This is based on the observation that the cartilage ECM, which is mainly composed of fibrous type II collagen and aggregating hydrophilic proteoglycans (*e.g.*, aggrecan), provides a 3D microenvironment with numerous biochemical, structural, and mechanical cues in maintaining differentiated phenotype and proper functions of chondrocytes and MSCs.

A large number of natural, synthetic, and hybrid biomimetic materials have been developed to engineer the microenvironment of chondrocytes and MSCs for generating functional cartilage substitutes and promoting cartilage regeneration.[570,1070–1071] These biomimetic materials have been fabricated into various forms such as membranes, sponges, and hydrogels, of which hydrogels are the most widely explored.[1072–1074] Naturally derived hydrogels (typically collagen, HA and agarose) are abundant and contain many intrinsic adhesion and bioactive cues for chondrogenesis. However, they may have immunogenicity problems and are usually not mechanically stable to withstand high compressive, shear and tensile loadings in articulation. Synthetic hydrogels (typically PEG) can be designed to have well-controlled microstructures and adequate mechanical properties. However, they need bioactive modification and their degradation byproducts can be harmful to cells and cause inflammation.[1075] A trend in cartilage tissue engineering has been to develop hybrid hydrogels exploiting the advantages of both naturally derived and synthetic biomimetic materials.[1075–1076] Hydrogels can now be designed to have mechanical properties matching those of native cartilage, to enhance the chondrogenic phenotype of cells, and to be non-invasively injected to fill cartilage defects of any shape and size.[1077]

Various biomimetic material formulations are commercially available for clinical use in cartilage regeneration and have shown enhanced cartilage repair when implanted.[1069,1078]

However, full restoration of native cartilage structure and function has yet not been achieved.[1079] In the context of the cell microenvironment, construction of clinically relevant thick cartilage tissue constructs requires 4D materials that enable spatially and temporally controlled evolution of cells into a metabolically inactive chondron-like microenvironment. Hierarchical and zonally organized cartilage structure requires such advances, as does rebuilding of both bulk mechanical load-bearing and surface lubrication functions of native cartilage. Finally, the integration of engineered cartilage with surrounding tissue remains challenge due to the need to keep chondrocytes in a relatively inactive state metabolically.[579,1076,1080–1081]

4.1.5. Bone Tissue—Bone formation entails a series of sequential cellular events, from osteoprogenitor cell recruitment from the surroundings, osteoprogenitor proliferation,

osteoblast differentiation, matrix deposition, and bone mineralization.[1082] From the tissue regeneration perspective, the creation of a suitable 3D cell microenvironment is of the utmost importance for triggering osteoblastic differentiation *in vitro* as well as the bone formation process *in vivo*.[1083–1085] Bone has a very strong ability to heal itself, but only for defects below a critical size of a few centimeters. For defects larger than this, a permanent cavity is left. A pressing need exists for developing tissue engineered scaffolds that guide regeneration of these defects.

A crucial aspect lies in constructing an adequate 3D matrix in which biochemical cues, such as cell adhesion ligands and growth factors, are provided.[1086] For this reason, biomimetic hydrogels that have covalent linkages with RGD peptides have been synthesized with macromolecules that contain bioactive moieties and been shown to play roles in the adhesion of marrow stromal osteoblasts.[1087] Other than RGD peptides, peptide sequences that can interact with polysaccharide molecules on the cell surface have been used to develop biomimetic materials for bone tissue engineering due to their adhesive properties. For example, it has been demonstrated that RGD modification by itself cannot facilitate focal adhesion, while the presence of the heparin-binding domain could lead to substantial cytoskeletal clustering.[1088] Furthermore, the RGD sequence and heparin-binding domain have been shown to function in synergy by triggering osteoblastic differentiation and bone mineralization.[1089] Recently, Zhao *et al.*[1082] used microfluidic technology to encapsulate BMSCs and growth factors within injectable, photocrosslinkable GelMA microspheres (Figure 29). High cell viability, cell migration within microspheres and toward microsphere surfaces, and improved cell proliferation were observed. Both *in vitro* and *in vivo* evaluations concluded that the fabricated microspheres resulted in increased bone mineralization and enhanced osteogenesis.[1082]

Another crucial aspect lies in designing the porous characteristics of scaffold materials, such as porosity, pore size, interconnectivity, and orientation, which play important roles in osteoblast proliferation and osteogenesis.[1090] Increasing porosity has been shown to enhance permeability and bone ingrowth. However, this is often sacrificed for improved mechanical properties.[1091] Because sufficient mechanical support is needed to prevent the premature collapse of engineered bone tissue constructs, an upper limit for porosity exists, and a balance between porosity and mechanical properties should be reached to accelerate bone regeneration. In addition, bone tissue has a radial porous structure gradient, as the outer cortical bone region is more compact (porosity 5%−30%), and the inner cancellous bone region is more porous (porosity 30%−90%). Mimicking such a porous structure gradient might enhance the mechanical performance of engineered bone tissue constructs, the ingrowth of cells and new bone tissue, and the integration of implants with surrounding host tissues.[1092–1094] Efforts directed toward fabricating hierarchical porous structures for bone tissue engineering and have particularly benefited from the development of computer-aided additive manufacturing technologies.[1095–1097] Future efforts are still needed to engineer 3D bone tissues with controlled porous structure, while simultaneously being able to withstand high mechanical loads and maintain a stable structure for sufficient amount of time.

4.1.6. Concerns, Caveats, and Immunogenicity—In addition to skin, cardiac, neural, cartilage and bone tissues, engineering the cell microenvironment with biomimetic

materials is also of particular interest for the regeneration of other tissues, such as dental[1098–1099] and musculoskeletal tissues.[1100–1102] Since each targeted tissue has its own specific microenvironment, the biochemical and biophysical properties of biomimetic materials should be carefully evaluated and optimized to maximize the regenerative or therapeutic efficacy according to tissue-specific requirements. An important frontier is systems in which a spatial gradient of cell microenvironments exists. This occurs throughout interfaces in the body, such as at the attachment of tendon to bone.[1103] Here, spatial gradients emerge during development, and tissue engineered systems are needed to replicate these following healing and surgical repair.[1104–1106] Technologies now exist for controlling cell concentration gradients,[1107] but providing these in conjunction with the needed gradients in microenvironmental mechanical fields and ECM proteins represents an ongoing challenge.[176,1108]

FDA clinical trials for biomimetic materials and related products have had mixed clinical trial results that include several successes (Table 3).[319,1109] However, a major clinical concern is immunogenicity of these biomimetic materials, and associated inflammation, tissue damage, and implant rejection.[1110] Naturally derived biomimetic materials are biocompatible but all potentially immunogenic due to the presence of specific and/or nonspecific antigens such as residual oligosaccharide α–Gal epitopes, DNA molecules, and damage-associated molecular patterns.[320,1110–1111] For example, collagen-based biomaterials have been demonstrated to promote mild immunogenicity and risk of collagen-induced autoimmunity.[1112] Decellularized ECM and alginate may promote immunogenicity due to incomplete decellularization and insufficient purification, respectively.[1113–1114] The severity of the host response to naturally derived biomimetic materials is dependent on the material's origin, composition, and processing, and upon the genetics and implantation site of the patient.[1115] On the other hand, synthetic biomimetic materials can have user-defined compositions and structures without specific immunogenic components. However, they may also suffer from nonspecific immune responses due to being foreign bodies and/or due to the acidity or toxicity of their degradation byproducts.

Immune responses typically start from the adsorption of host proteins (*e.g.*, fibrinogen, albumin, and fibronectin) to the surface of material implants. The adsorbed proteins can promote the adhesion of neutrophils/macrophages and the formation of collections of fused macrophages called "foreign-body giant cells." Because reducing protein adsorption by modulating surface hydrophilicity, structural features, and degradation characteristics can alleviate immune responses,[1110,1116] implants usually require such surfaces. Common strategies for this include surface modification with hydrophilic polymers, surface grafting or coating with non-fouling polymers or proteins (*e.g.*, PEG, heparin, and osteopontin), structural adjustment such as decreasing pore size or increasing fiber organization, and controlled delivery and release of anti-inflammatory agents.[496,1110,1117–1119] While some naturally derived biomimetic materials (*e.g.*, chitosan, heparin, and high molecular weight HA) intrinsically possess anti-inflammatory cues, the majority of biomimetic materials (*e.g.*, decellularized ECM, collagen, gelatin, alginate, silk, PGA, and PCL) are pro-inflammatory and require the use of anti-inflammatory agents.[1110,1120–1121]

To control the delivery and release of anti-inflammatory agents, a range of stimuli-responsive biomimetic materials have been explored, with bioresponsive materials emerging as a promising direction.[1122–1124] Bioresponsive materials can change their properties (*e.g.*, the swelling/deswelling ratio) in response to the changes of specific biomolecules such as glucose, enzymes and antigens.[1125] Compared to traditional stimuli-responsive materials thatrespond to physicochemical changes in pH or temperature, bioresponsive materials can have several advantages. For example, by using antigen-antibody binding, antigen-responsive materials can recognize and respond to select biomolecules with high affinity and specificity.[1126–1127] In addition, multiple complementary anti-inflammatory cues can be used combinatorially in antigen-responsive materials to make the materials respond to specific immune conditions.[1128] With the development of novel anti-inflammatory strategies and in-depth understanding of the immunological mechanisms relative to material-induced recruitment, adhesion and activation of neutrophils, monocytes, macrophages, fibroblasts and foreign-body giant cells, it is reasonable to believe that increasing numbers of immunologically safe biomimetic materials and devices will be available in the near future.[1129–1130]

4.2. *In Vitro* Tissue Models for Pathophysiological Studies and Drug Screening

Conventional *in vitro* tissue models mainly focus on 2D culture platforms, which fail to capture the 3D *in vivo* microenvironment. The shortcomings of conventional tissue culture models can be resolved with biomimetic platforms that can offer improved, realistic tissue models for understanding fundamental cellular/molecular biology.[13,1131–1132] Various biomimetic *in vitro* tissue models, especially organ-on-a-chip platforms,[1133–1136] have been established to simulate the responses of the *in vivo* microenvironment for pathophysiological studies and drug testing, including heart,[1137] lung,[1138] liver,[1139] kidney,[1140] blood vessel,[1141] gut,[1142] and tumors.[1143]

4.2.1. Cardiac Tissue Model—Cardiac failure is the leading cause of death in the developed world,[287,1144] and *in vitro* testing systems are required for identification and screening of cardiovascular drugs.[1145] Conventional approaches developed for engineering cardiac tissue models mainly include 2D cardiac cell sheets[1146–1147] or cardiac tissue slices.[1148] Although simple and effective, they are still limited in mimicking physiological cell-cell and cell-ECM connections. To address such challenges, 3D cardiac tissue models based on hydrogels encapsulating cardiac cells have been established.[1149–1152] The characterization of cell contraction force has also been achieved in 3D systems including cardiac tissue models.[1153–1154] Recently, hydrogels have been combined with paper to fabricate cardiac tissue models.[1155–1156] As one example, the Whitesides group[1157] developed an MI model by co-culturing cardiac fibroblasts and cardiomyocytes in multilayer hydrogel-paper stacks. The number of upper fibroblast-cultured layers was adjusted to control the transport of oxygen and nutrients to cardiomyocytes cultured in the lower layers, mimicking the cell microenvironment of low, medium, and high ischemia.

While there are ongoing challenges in simulating heart physiology, especially with ensuring that cardiac cells represent a mature cardiomyocyte phenotype, recent reports on heart-on-a-chip studies have shown great promise for *in vitro* drug testing through physiologically

relevant models.[1158–1159] In one study, PDMS microfluidic channels were coated with hydrogels (GelMA and methacrylated tropoelastin (MeTro)) to facilitate cell attachment for culturing cardiomyocytes.[1158] It was found that the hydrogel type determined cell attachment and alignment, while matrix stiffness determined beating. In another recent study, a multimaterial 3D printing technique was used for the high-throughput generation of intelligent cardiac microtissue models on a single chip (Figure 30).[943] The tissue contractile stresses in the microtissue models could be continuously read in real time using embedded soft strain gauge sensors. The potential of these cardiac microtissue models for facilitating drug studies was demonstrated.

However, the key problem once again is ensuring a realistic 4D cell microenvironment. Cell-cell contacts as well as cardiomyocyte maturation require an evolution over time of a tissue construct and its cell microenvironments. Understanding the roles of multiple mechanical, metabolic, and electrophysiological stimuli and reconstituting these roles in a time-varying material model represent critical needs for these *in vitro* tissue models.

4.2.2. Lung Tissue Model—The lungs extract oxygen from the atmosphere and transfer it into the bloodstream via functional units called alveoli. These provide a thin mucosal barrier with a large surface area and ready, non-invasive access to the bloodstream for gas exchange. Microfluidic systems have been developed to mimic the structure and mechanical microenvironment of alveoli for engineering lung tissue models.[1160] For instance, a “breathing lung-on-a-chip” model was made by seeding human alveolar epithelial cells and microvascular ECs onto opposite sides of an ECM-coated porous PDMS membrane to recreate the alveolar-capillary barrier *in vitro*.[1138] The cells in the model experienced cyclic mechanical strain in addition to air and fluid flow to simulate normal breathing motion. It was found that the cyclic mechanical strain could enhance nanoparticle uptake and nanoparticle translocation across the alveolar-capillary interface, as well as nanoparticle cytotoxicity and alveolar epithelial cell inflammatory responses in the model (Figure 31). Therefore, such models can reconstitute the 3D microarchitecture and the mechanical movement and cohesive physiological function of the alveolar-capillary barrier.

Continuing efforts in this research area have been made toward developing on-chip human disease models, such as a drug toxicity-induced pulmonary edema model.[1161] By using the pulmonary edema model, it was demonstrated that mechanical force can promote vascular leakage and induce pulmonary edema, while circulating immune cells are not required for pulmonary edema development. Moreover, the application of such disease models in identifying potential new therapeutics was verified. These results demonstrate that on-chip lung tissue models hold great promise as alternatives to animal and clinical models for pathophysiological and drug studies. However, reaching this promise requires further identification of the specific mechanics and compositions of the cell microenvironment. Although bulk ECM properties and overall homogenized tissue response and function is recapitulated in these systems, the identification of small therapeutic molecules requires the development of a refined and improved understanding of the nanoscale features with which these molecules interact.

4.2.3. Liver Tissue Model—The study of drug hepatotoxicity is primary motivation for development of hepatic drug delivery platforms.[1162] To evaluate hepatotoxicity, a number of *in vitro* models simulating either normal or diseased liver cell microenvironments and functionalities have been developed, including 2D monolayer cultures, hepatic tissue slices, 3D hepatic spheroids, engineered models using hydrogels, and organ-on-a-chip platforms.[1139,1163] In one study, hepatocytes and fibroblasts were co-cultured in a micropatterned collagen substrate in a 24-well plate format.[1164] This model was demonstrated to promote the lasting preservation of liver-specific functions and allow the corresponding analysis of drug hepatotoxicity. In another study, the uptake of 5 nm AuNPs coated with polyvinylpyrrolidone (PVP) and associated toxicity to hepatocytes, ECs, and Kupffer cells sourced from precisely cut slices of rat liver were studied by Dragoni *et al.*[1165] However, tissue slices and biopsies are not viable for high-throughput or long-term studies due to a rapid decline in functionality observed within days of beginning *in vitro* culture. While long-term drug studies usually utilize primary human hepatocytes, 3D hepatic spheroids are promising models for the rapid and clinically pertinent assessment of new drugs.[1166–1169] For studies based on multi-organ-on-a-chip models, it is important to include a liver module since the liver is the primary site for drug metabolism.[1170] In these models, drug action occurs after the prodrug is initially metabolized by the liver module and then reaches the target organ. As one example, Wagner *et al.*[1171] combined engineered liver microtissues with skin biopsies to produce a multi-organ-on-a-chip model suitable for long-term culture. Crosstalk between the liver and skin modules was demonstrated. Such models show great potential for the systemic evaluation of drugs and other substances.[1164,1172] As before, further delineation of the physiological cell microenvironment will be of tremendous help in refining these systems and increasing their physiological relevance.

4.2.4. Tumor Tissue Models—Effective drug delivery to tumor sites is confronted by the complexity of the *in vivo* tumor microenvironment.[1147,1173] The development of drug-loaded nanoparticles targeting tumor sites for cancer treatment with minimal consequence to healthy tissues has been the focus of researchers and pharmaceutical companies alike.[1174] While numerous biological barriers have prevented the successful *in vivo* testing of nanoparticle surface targeting moieties, promising *in vitro* results have been demonstrated. Consequently, understanding nanoparticle transportation by the bloodstream, dispersion in target tissues, and subsequent cellular uptake is significant. The importance of preclinical models capable of simulating the *in vivo* tumor microenvironment, such as dynamic flow, is also evident in the study of factors affecting drug delivery and toxicology evaluations.[1175–1176]

Various 3D *in vitro* tumor tissue models have been developed and have usually leveraged various microengineering technologies, typically lab-on-a-chip technology.[1177–1179] Microfluidic networks present in 3D tissue engineered cultures enable the controlled investigation of nanoparticle transport barriers. As one example, a tumor-on-a-chip model has been developed by loading human melanoma cell spheroids with ECM (Matrigel) into a microfluidic device with precisely controlled flow conditions.[1180] The transport behavior of PEG-functionalized AuNPs with various diameters through such a tumor-mimicking tissue model was studied. It was shown that only AuNPs with a diameter less than 110 nm could

diffuse into the ECM and interact with tumor cells. Moreover, *in vivo* conditions were simulated through a laminin coating on the spheroids that functioned against AuNP transport. AuNPs functionalized with targeting groups were unable to infiltrate deep into the core and were observed to gather at the outside edge. Such studies offer important insights into the creation of nanoparticles for improved *in vivo* targeting.

Numerous tumor-on-a-chip platforms have been developed and evaluated for drug studies and treatment strategy development.[1181–1185] The Varghese group[1186] reported a tumor-on-a-chip platform (fabricated by slightly modifying a device they described previously[1187]) in which cancer spheroids (MCF-7) and HUVECs were simultaneously photoencapsulated within a GelMA hydrogel integrated in a microfluidic device. Under perfusion culture, HUVECs migrated to the hydrogel periphery to form an endothelial barrier by responding to flow-induced chemotactic gradients, while MCF-7 spheroids showed limited motility and were confined within the hydrogel interior. The potential application of this tumor-on-a-chip platform in drug screening was validated with the anti-cancer drug doxorubicin.[1186] By combining the use of chip and other advanced technologies (*e.g.*, bioprinting), tumor-on-a-chip models with well-controlled tumor microenvironments can be generated in a high-throughput manner.[1188] Such tumor-on-a-chip models are promising for future applications in the optimization of personalized chemotherapy programs.

In addition to the *in vitro* tissue models outlined above, engineering the cell microenvironment with biomimetic materials has also shown promise in promoting the development of brain,[1189–1190] blood vessel,[1191] skeletal muscle,[1192] kidney,[1193–1194] gut,[1195–1196] and other tissue and cancerous models of interest for pathophysiological studies and drug testing.[1197] Future efforts should be directed toward carefully evaluating the effectiveness of these *in vitro* tissue models in relation to their recapitulation of the cell microenvironment. Moreover, integrating various organ modules at a physiologically appropriate scale to obtain human-on-a-chip systems for systemic studies represents a critical need.[1198–1199]

4.3. Cell Manufacturing

“Cell manufacturing” refers to the use of bioprocessing technologies for the expansion of stem cells (*e.g.*, hESCs, iPSCs, and hMSCs) that have the remarkable features of self-renewal and multipotency. Stem cells are thus promising cell sources for therapeutics for tissue damage,[1200] cardiomyopathies,[1201] and neurodegenerative diseases,[1202] in which large numbers of high quality cells are required.[1203] For instance, around 1×10^9 cardiomyocytes and 1×10^6 hMSCs are needed to treat a patient with MI[1204] and bone defects,[1205] respectively. Additionally, only a few percent of transplanted stem cells survive to integrate into damaged tissues.[1206–1207] Hence the numbers needed for a successful cell therapy are even higher and expansion of stem cells without losing their self-renewal and multipotency is critical.

2D tissue culture flasks (T-flasks) are the mainstay for the expansion of stem cells in preclinical studies.[1208] However, 2D T-flasks can only produce monolayers of stem cells, limiting their scalability and reproducibility, and more broadly their suitability for therapeutic applications.[1209] To overcome these obstacles, 3D suspension systems such as

cell aggregates,[1210] cells on microcarriers,[1211] and cells in microencapsulates[1212] are attractive possibilities.[1213] However, significant challenges exist with 3D suspension cell culture systems.[1207] For example, cells in aggregated form can re-establish specific microenvironments that allow them to express a tissue-like structure, ultimately enhancing cell differentiation,[1214] leading to potency loss. Another major limitation of cell aggregate systems is the need to control the aggregate size to prevent the formation of necrotic centers. Microcarrier approaches can expose cells to harmful shear stress and[1215] cause microcarrier aggregation,[1216] and are furthermore subject to additional processing for cell–bead separation. Cell microencapsulation is an advanced cell expansion approach that shields cells from shear stress and avoids aggregation of microcarriers in culture.[1217] In addition, microencapsulated cells can have microenvironments that mimic stem cell niches for cell expansion with high quality.[1218]

Cell detachment is a critical step during large-scale cell expansion. To avoid potential damage caused by enzyme for cell detachment, thermally responsive microcarriers and encapsulation hydrogels have been developed to allow for enzyme-free cell detachment under reduced temperature.[1207–1208,1219]

As compared to 3D suspension systems, bioreactor systems have the merits of efficient stem cell seeding and nutrition supplement, as well as supporting the scalable expansion of stem cells. Moreover, with operations such as agitation and perfusion, bioreactors can achieve enhanced mass transport, which is critical for 3D cell culture at high density.[1220] Furthermore, by using microcarriers in bioreactors, the size of cellular aggregations can be well controlled, preventing the formation of necrotic centers.[1221] For example, alginate beads have been applied as microcarriers in a bioreactor for the expansion of hESCs and maintained hESC pluripotency up to 260 days, suggesting that microcarrier-based cell culture in bioreactors is favorable for large-scale expansion of stem cells.[1222] It is important to bear in mind that stem cells are highly responsive to biophysical cues such as matrix stiffness. Therefore, the mechanical properties of the developed microcarriers or encapsulation matrices should be carefully characterized and optimized to maintain stem cell phenotype during expansion.

4.4. Immunotherapy

Immunotherapy is the treatment or prevention of diseases by inducing, enhancing, or suppressing host immune response. Many pathologies, including autoimmune disorders, cancers, infections, and allergies, can be associated with dysregulation of the host immune response. As a typical example, cancer cells often express surface antigens that are poorly immunogenic and experience an immunosuppressive microenvironment due to the presence of immune-inhibitory cytokines (*e.g.*, IL-10 and TGF-β),[1223–1224] which result in reduced T-cell recognition and activation. Cancer immunotherapy aims to treat cancers by efficiently inducing and enhancing systemic antitumor immune response. Such treatment provides improved immune system-associated specificity and immunological memory-associated long-term protection effects. They offer promise in some cancers in which chemotherapy and radiotherapy offer little.[1225–1226]

Our focus here is biomimetic material-based immunotherapy. In contrast to traditional design of biomimetic materials that aims to minimize immune response, biomimetic material-based immunotherapy seeks to initiate specific therapeutic immune responses by harnessing the immunomodulatory capacity of biomimetic materials.[1115,1227] Attractive features of biomimetic material-based immunotherapy include delivery of multiple immunomodulatory agents with a single material carrier, promotion of local and durable release of immunomodulatory agents, targeting of specific cell populations and subcellular compartments, reduction of high dosage-associated systemic toxicity, and supply of diverse biophysical cues for controlling cell function.[276,1228–1229]

Immunomodulatory biomimetic materials can manipulate immune cells (typically dendritic cells (DCs) and T cells) and modulate immune system for immunotherapy through two primary mechanisms: *ex vivo* priming and delivery of activated immune cells,[1230–1231] and *in situ* recruitment and programing of host immune cells.[1232–1235] For each mechanism, a range of microenvironmental factors, including material biochemical properties such as cell adhesivity, biophysical properties such as structural features and mechanical properties, the 4D delivery and release of immunomodulatory agents, and the subjection of mechanical forces, may need to be taken into account to improve immunotherapy outcomes.[1236–1241] This is because these factors (particularly mechanical cues) have been shown to play vital roles in immune cell migration and activation, lymphoid tissue development and function, and immune-related disease progression such as malignant transformation.[1111,1242–1244]

For practical applications, the form of immunomodulatory biomimetic materials is also an important aspect that should be carefully evaluated. Generally speaking, immunomodulatory biomimetic materials can take the forms of implantable macroscale 3D scaffolds and hydrogels, or injectable micro-/nanoparticles and *in situ* crosslinking hydrogels.[1227] Several important factors should be considered when choosing material forms, mainly including the material fabrication conditions, the tissue being targeted, the immunomodulatory agents being delivered and their delivery kinetics. Macroscale 3D scaffolds and hydrogels can be produced *in vitro* by using various biofabrication technologies in well-controlled conditions, thus enabling the generation of custom-engineered microenvironment for programming immune cells. They can be used to deliver immunomodulatory agents including proteins, genes, and drugs, as well as programed immune cells. The delivery kinetics can be tightly regulated by engineering material porosity, degradation, and affinity to carried agents.

However, these systems require surgical implantation, which may result in traumatogenic wounds that slow therapeutic progress. In contrast, micro-/nanoparticles or *in situ* gelling hydrogels can be injected in a minimally invasive manner, avoiding the use of open surgery.[1235,1245] They are most suitable for delivering immunomodulatory proteins, genes, and drugs, but have limited potential to control engineering biophysical cues for programing of immune cells. In addition, burst release of immunomodulatory agents may make it challenging to control the delivery kinetics for persistent immunomodulation. Nevertheless, recent studies recommended that injectable nanoscale hydrogels (*i.e.*, nanogels) could be a novel attractive form of immunomodulatory biomimetic materials that holds promise in immunotherapy (Table 4).[1246–12481128,1223]

The promise of biomimetic material-based immunotherapy is illustrated by recent studies on preclinical and clinical trials of vaccine scaffolds.[1227] However, it is still far from a true clinical success. Further efforts are needed to engineer biomimetic materials for producing clinically required immune cells and functional tissues, reducing the cost and improving the efficiency of immune cell activation and delivery, and promoting the development of effective personalized immunotherapy.[1128] In this context, the rapidly developed stem cell and gene technologies may provide great benefits.[1223] Recently, biomimetic material-based 3D immune organoids have attracted particular interests as they could provide powerful platforms for studying biomimetic material-immune cell interactions in a native-like immune microenvironment.[1111,1249–1252] Such studies may improve the mechanistic understanding and predication of molecular and cellular events in immune system, and accelerate the design of 4D biomimetic materials and cell microenvironments for immunotherapy.

4.5. Gene Therapy

Gene therapy seeks to express therapeutic genes in target cells, or to replace absent or disease-associated genes.[1266] MicroRNAs (miRNAs) and small interfering RNA (siRNAs) are generally negatively charged, and cannot cross the cell membrane.[1267–1268] In addition, they undergo degradation *in vivo*.[1269] Hence, vectors that can effectively deliver therapeutic genes into cells and protect them from degradation are required for gene therapy. Various vectors such as inorganic nanoparticles,[1270] liposomes,[1271] and micelles,[1272] and polymeric nanoparticles[1273] have been explored for gene delivery. However, their therapeutic outcomes are usually poor, due to the unmet challenges in terms of gene dissociation from the vector, poor stability and toxicity of the vector, and inefficient targeting.[1274] Moreover, after systemic administration, these vectors are likely to induce nonspecific transfection or systemic immune responses.[1275–1276]

In this context, a local delivery carrier that can intensively transmit therapeutic genes to a target site for a sufficient period can overcome the above mentioned drawbacks.[1276] For instance, hydrogels with appropriate microenvironments have been used as local delivery carriers for siRNA transfection and realized effective gene knockdown in different cell lines (*e.g.*, kidney, epithelial, ovarian, and hepatoma).[1277] Due to the tunable biochemical and biophysical properties of hydrogels, they are capable of delivering genes to a wide range of tissues *in vivo*.[1278] Other commonly applied scaffolds fabricated from cationic polymers such as chitosan, poly(ethyleneimine) (PEI), poly-L-(lysine) (PLL) and poly(2-(N,N-dimethylamino)ethyl methacrylate) (PDMAEMA) have also been used for local gene delivery.[1279] However, cationic polymeric scaffolds usually suffer from toxicity if high transfection efficiency is required. In addition, therapeutic genes that are physically loaded within hydrogels or cationic polymeric scaffolds may have a short half-life *in vivo* and low gene silencing efficiency, because of the uncontrollability in holding and delivering the genes.[1276,1280]

Responsive polymeric nanoparticle-embedded scaffolds are emerging as advanced local delivery carriers to solve the above-mentioned issues. Responsive nanoparticles with pH, GSH or intracellular enzyme-regulated endosomal escape behavior have been found to

efficiently enhance intracellular gene delivery.[1272,1281–1283] To further enhance this delivery approach, siRNA loaded pH-responsive nanoparticles have been incorporated into porous polyester urethane scaffolds.[1284] Effective gene silencing *in vivo* and angiogenesis promotion within tissue defects have been achieved using this platform. Therefore, encapsulating responsive gene delivery vectors inside scaffolds such as hydrogels is a versatile approach for manipulating the cell microenvironment and directing cell functions while minimizing gene loss due to nonspecific delivery.[1285]

5. Conclusions and Outlook

Functional and biomimetic materials for engineering the 3D cell microenvironment form the foundation for a number of technological innovations. However, much work remains to be done. We conclude with some thoughts on five sets of challenges and opportunities in the field as it currently stands: dynamic 4D cell microenvironments; single-cell analysis; high-throughput assays; identification of fundamental and universal principles; and translation of these principles into predictive computational models and useful products.

The dynamic character of the cell microenvironment complicates the design of material systems. Throughout the development, cells exist in lineage-specific microenvironments that change with the age of the cell and/or organism. For tissue engineering applications, the key challenges are determining which aspects of these changing microenvironments are important for the development of an adult tissue and which are needed to maintain the adult tissue. For drug screening, the key challenges are identifying which aspects of the dynamically changing environments affect the cellular responses to small molecules, and more broadly, determining whether developmental stage matters when assessing drug efficacy and safety. For example, the ongoing effort to determine the safety of drugs during pregnancy needs to be informed by determining the ways that the cell microenvironment evolves with age. More broadly, studying the aging cell microenvironment and enabling 4D temporal control of the cell microenvironment are important to the long-term goal of identifying universal criteria for designing biomimetic materials across cell type and developmental stage.

The vast majority of what we know about cell microenvironments and their control is the result of observations of how populations of cells respond to biomimetic materials. These ensemble averages capture dominant cell-biomimetic material interactions but mask how local details of the microenvironment promote cell fate and function. Increasing evidence from single-cell analysis indicates broad cellular heterogeneity, which may arise from the cell cycle, cell lineage, cell aging, microenvironmental heterogeneity, gene mutations, or intrinsic noise in gene expression.[1286–1288] Cellular heterogeneity can be essential in carcinogenesis and stem cell fate determination.[1289–1292] Identifying and understanding the biological function of cellular heterogeneity will benefit the design of biomimetic materials for controlling heterogeneous cell-biomimetic material interactions. To this end, significant recent efforts have been directed toward developing microengineering technologies that enable single-cell analysis at the genetic, proteomic, or phenotypic level.[1293–1294] While most existing approaches are limited by high cost and low throughput, rapidly developing

microfluidic technologies for single-cell separation and analysis show promise for scalability and automation.[1295–1297]

More broadly, an enabling technology that has not yet been fully harnessed is high-throughput screening. Advances in synthetic chemistry and biology have provided powerful tools for producing vast amounts of biomimetic materials.[1298–1300] Efficient identification of key factors among the abundant material cues for engineering specific cell microenvironments is critical, and high-throughput assays that enable the performance of multiple experiments in parallel are vital.[1301–1303] High-throughput assays are often based on the production of material gradients, microarrays or combinatorial libraries.[1304–1310] Although effective, material systems generated in current assays are often too simple, and future studies should be performed to develop well-defined high-throughput biomaterial systems with more biologically relevant cell-microenvironment interactions in 3D.[1311–1313] Accordingly, methods that enable the high-throughput, real-time *in situ* characterization of the 3D cell microenvironment, including chemical, physical and biological aspects of cells, biomaterials and cell-biomaterial interactions, need to be further explored. This exploration can benefit from progress in advanced bioimaging and biosensing technologies.[997,1314–1318]

As high-throughput systems come online, the possibility of identifying universal principles governing the design of cell microenvironments will emerge. Developing a better understanding of the fundamental principles of life processes, such as organ development, tissue homeostasis and disease progression, is one of the primary motivations in engineering the cell microenvironment with biomimetic materials.[1319] Although current research has dramatically broadened our knowledge of how cells respond to material cues, many aspects, especially how biophysical cues interact with cells in 4D, are still on debate. The interplay and crosstalk among microenvironmental cues and signaling pathways increases the difficulty of deducing and dissecting the underlying mechanisms. Future efforts should be directed toward combining studies at different levels, including the tissue, cellular, molecular, and gene levels, to establish extracellular and intracellular signaling networks that can facilitate a comprehensive understanding of cell-microenvironment interactions.

Another main motivation in engineering the cell microenvironment with biomimetic materials is the regeneration of injured tissues *in vivo*. While *in vitro* engineering of the cell microenvironment has promoted the formation of functional engineered tissue constructs for implantation purposes, these engineered tissue constructs may fail or show limited regeneration capacity when implanted into the body. Therefore, *in vivo* engineering of the cell microenvironment is emerging with the aim of improving the performances of biomaterials and engineered tissue constructs *in vivo*.[1128,1320–1321] Moreover, the rapid development of stem cell biology, injectable biomaterials and corresponding injection therapies have further motivated studies on *in vivo* engineering of the cell microenvironment.[1322–1327]

Finally, a frontier that is only now being reached is the translation of what we know of governing principles into predictive computational models. With the development of computer technologies, computational material science and computational biology have made considerable advancements.[1328–1329] However, efforts to combine the two for

engineering the 3D cell microenvironment are still emerging. As in other areas, we anticipate that computational tools will not only accelerate the design of biomimetic materials but also facilitate investigations into how these biomimetic materials interact with cells.[202,1330] Moreover, computational tools may enable complex research that would not be feasible using experimental tools. As such, it is important to establish detailed databases for cells, biomaterials, and cell-biomaterial interactions from available knowledge. With the development of multiscale and multifield theoretical and mathematical models for cell-biomaterial interactions, computational modeling will provide increasingly predictable and reliable results in the future.[1331–1333] Altogether, we believe that functional and biomimetic materials to dissect and engineer the 3D cell microenvironment will enable a new generation of breakthroughs in biophysics, drug discovery, personalized medicine, and regenerative medicine.

Acknowledgements

This work was supported financially by the National Natural Science Foundation of China (Nos. 11532009, 11522219, 11602191 and 11372243), the NIH (Nos. U01EB016422 and R01HL109505), and the US NSF through the NSF Science and Technology Center for Engineering MechanoBiology (CMMI 1548571).

Biography

Guoyou Huang received a B.S. in Physics in 2008 and Ph.D. in Biomechanics in 2013 from Xi'an Jiaotong University, China. Afterward, he worked as a post-doctoral fellow at Washington University in St. Louis then joined the faculty of Life Sciences and Technology at Xi'an Jiaotong University. He has extensive expertise with biomaterials (hydrogels), biomechanics, mechanobiology, and tissue engineering. His current research focuses on advanced biomaterials and technologies to engineer the cell microenvironment and to construct *in vitro* tissue models for mechanotransduction, tissue engineering, and drug screening applications.

Fei Li received a B.S. in Chemistry at Northwestern University (China) in 2001 and M.S. in Analytical Chemistry at Changchun Institute of Applied Chemistry of Chinese Academy of Sciences (China) under the supervision of Prof. Yuanhua Shao in 2004. She received a "Dorothy Hodgkin Postgraduate Award" from the British government to pursue a Ph.D. in the United Kingdom, which she did in the field of electrochemistry under the supervision of Prof. Patrick R. Unwin at the University of Warwick. After postdoctoral study with Prof. Hubert H. Girault's group at Ecole Polytechnique Federale de Lausanne (Switzerland) and Prof. Eric Borguet's group at Temple University (U.S.A.), she joined the faculty of the School of Science of Xi'an Jiaotong University (China) as an associate professor. Fei Li has research experience in electroanalytical fields, and her interests include interfacial reactions including heterogeneous spectro-electrochemical processes, nano-materials catalysis, biological system electrochemistry, and electrochemical scanning probe microscopy techniques. Her current research is focused on chemical and electrophysiologic behaviors of cells in three-dimensional microenvironments using spectroelectrochemical and scanning probe microscopy techniques.

Xin Zhao is an assistant professor at the Interdisciplinary Division of Biomedical Engineering, the Hong Kong Polytechnic University, China. She received a Ph.D. in Biomaterials and Tissue Engineering from University College London, UK (2010). Prior to her current position, she worked as a postdoctoral research fellow at Harvard University, Harvard-MIT Health Science & Technology and School of Engineering of Applied Sciences and as associate professor at Xi'an Jiaotong University. Her research focuses on the development of multi-disciplinary approaches including nanotechnology, pharmacology, material science and cell biology to generate tissue-engineered organs and controlling cell behaviors for addressing clinical problems.

Yufei Ma studied biofunctional materials in the School of Materials Science and Engineering at Beijing University of Chemical Technology (China) from 2005 to 2009, where she obtained a B.S. Afterward, she earned a Ph.D. in the School of Materials Science and Engineering at Tsinghua University (China), where she specialized in biomineralization and biomimetic materials. She is now on the faculty of the School of Life Science and Technology at Xi'an Jiaotong University (China), where her research focuses on the stem cell mechanical microenvironment and 3D bioprinting. She is currently on leave at the Harvard Medical School.

Yuhui Li received a B.S. in Materials Science from Shaanxi University of Science & Technology, China, an M.S. in Biomedical Engineering from Northwestern Polytechnical University, China, and a Ph.D. in Biomedical Engineering in 2016 from Xi'an Jiaotong University, China. His current research aims to engineering cell microenvironments *in vitro* and focuses on how cells sense and respond to their extracellular matrix in both 2D and 3D. He has developed magnetically assisted methods to control cell-laden hydrogels at microscale, enabling the study of strain- and stiffness-induced cell responses in 3D hydrogels. These platforms have been successfully utilized for engineering functional tissue constructs *in vitro*, suggesting potential for tissue engineering and regenerative medicine.

Min Lin achieved B.S. degree in Material Science and Engineering from Hefei University of Technology, China and M.S. degree in Material Science and Engineering from Xi'an Jiaotong University, China. After completing his Ph.D. degree at the Bioinspired Engineering and Biomechanics Center in Xi'an Jiaotong University, he joined the faculty of Xi'an Jiaotong University and was subsequently promoted to associate professor. During 2014–2015, he worked as a research fellow at Harvard Medical School and Massachusetts General Hospital. His current research is focused on biomechanics and mechanobiology of tissues and cells, and on and bio- and nano-material synthesis for biomedical applications including photo-responsive cell microenvironments, gene/drug delivery, and point-of-care diagnosis. He is recipient of the Chinese Government's "Natural Science Award", and of the Shaanxi Provincial Government Education Department's "Excellent Doctoral Dissertation Award."

Guorui Jin received his Ph.D. in Engineering from National University of Singapore (NUS) in 2013. During 2013–2015, he worked as a research scientist at Institute of Materials Research and Engineering (IMRE), A*Star, Singapore. Currently, he is an associate professor at the School of Life Science and Technology, Xi'an Jiaotong University. His

current research aims at development of multifunctional fluorescent nanoprobes for bioimaging, biosensor and drug delivery applications.

Tian Jian Lu received his Ph.D. in Engineering Sciences from Harvard University in 1995. Before taking up his current post at Xi'an Jiaotong University, he was Lecturer, Reader and Professor of Materials Engineering at Cambridge University Engineering Department from 1996 to 2006. During this period, he was also Fellow and Director of Studies of Queens' College. He is the Founding Director of MOE Key Laboratory for Multifunctional Materials and Structures (LMMS). He uses theoretical, experimental, and numerical approaches to investigate various research frontiers in engineering sciences, addressing challenges in mechanics of materials, noise and vibration, heat transfer, and biomechanics. Between 2005–2016, he was the Chief Scientist for the National Basic Research Program (973 Project) of China. He is the recipient of many prestigious awards, including the National Natural Science Award of China and the Young Chinese Scientist Award. He is the Editor-in-Chief of Acta Mechanica Sinica (AMS), the Founding Editor of International Journal of Applied Mechanics, and serves as the Associate Editor or member of the Editorial Board for more than 10 professional journals. From 2010 to 2014, he served as the Vice President of the Chinese Society of Theoretical and Applied Mechanics (CSTAM). At present, representing China, he holds important positions in the International Union of Theoretical and Applied Mechanics (IUTAM).

Guy M. Genin studies the mechanobiology of interfaces and adhesion in nature and physiology. He is a professor at Washington University in St. Louis (WUSTL), serving on the faculties of Mechanical Engineering & Materials Science, Biomedical Engineering, and Neurological Surgery; he is Changjiang Professor at Xi'an Jiaotong University in Xi'an, China; and he is co-director of the Center for Engineering Mechanobiology, a NSF Science and Technology Center operated jointly by Washington University and the University of Pennsylvania. He serves as chief engineer for WUSTL's Center for Innovation in Neuroscience and Technology and is active in several start-ups. He currently serves as co-lead of the NIH/Interagency Modeling and Analysis Group's working group on integrated multiscale biomechanics experiment and modeling, and has served as an editor, guest editor, or associate editor of a number of leading journals. Guy M. Genin's training includes B.S.C.E. and M.S. degrees from Case Western Reserve University, S.M. and Ph.D. degrees in solid mechanics from Harvard, and post-doctoral training at Cambridge and Brown. He is the recipient of a number of awards for engineering design, teaching, and research, including a Research Career Award from the NIH, the Skalak Medal from the ASME, the Northcutt-Coil Professor of the Year and Advisor of the Year from Washington University, Professor of the Year Awards from the WUSTL Student Union, and the Yangtze River Scholar Award from the Chinese Ministry of Education. He is a fellow of ASME and AIMBE.

Feng Xu received his Ph.D. in Engineering from Cambridge University in 2008. During 2008–2011, he worked as a research fellow at Harvard Medical School and Harvard-MIT Health Science & Technology (HST). He found the first interdisciplinary biomedical engineering center of Xi'an Jiaotong University (Bioinspired Engineering & Biomechanics Center) with Prof. Tian Jian Lu in 2007. Currently, he is a full professor and Associate Dean at the School of Life Science and Technology, Xi'an Jiaotong University. His current

research aims at advancing human health through academic excellence in education and research that integrates engineering, science, biology and medicine with focus on Bio-thermo-mechanics, Engineering of the Cell Microenvironment, and Point-of-Care Technologies.

References

(1). Scadden DT The stem-cell niche as an entity of action. Nature 2006, 441, 1075–1079. [PubMed: 16810242]

(2). Discher DE; Mooney DJ; Zandstra PW Growth factors, matrices, and forces combine and control stem cells. Science 2009, 324, 1673–1677. [PubMed: 19556500]

(3). Scadden David T. Nice neighborhood: Emerging concepts of the stem cell niche. Cell 2014, 157, 41–50. [PubMed: 24679525]

(4). Humphrey JD; Dufresne ER; Schwartz MA Mechanotransduction and extracellular matrix homeostasis. Nat. Rev. Mol. Cell Bio 2014, 15, 802–812. [PubMed: 25355505]

(5). Lu P; Weaver VM; Werb Z The extracellular matrix: A dynamic niche in cancer progression. J. Cell Biol 2012, 196, 395–406. [PubMed: 22351925]

(6). Murphy WL; McDevitt TC; Engler AJ Materials as stem cell regulators. Nat. Mater. 2014, 13, 547–557. [PubMed: 24845994]

(7). Lutolf MP; Gilbert PM; Blau HM Designing materials to direct stem-cell fate. Nature 2009, 462, 433–441. [PubMed: 19940913]

(8). Lane SW; Williams DA; Watt FM Modulating the stem cell niche for tissue regeneration. Nat. Biotechnol 2014, 32, 795–803. [PubMed: 25093887]

(9). Little L; Healy KE; Schaffer D Engineering biomaterials for synthetic neural stem cell microenvironments. Chem. Rev 2008, 108, 1787–1796. [PubMed: 18476674]

(10). Kong HJ; Mooney DJ Microenvironmental regulation of biomacromolecular therapies. Nat. Rev. Drug Discov 2007, 6, 455–463. [PubMed: 17541418]

(11). Khademhosseini A; Langer R A decade of progress in tissue engineering. Nat. Protoc 2016, 11, 1775–1781. [PubMed: 27583639]

(12). Perez RA; Choi S-J; Han C-M; Kim J-J; Shim H; Leong KW; Kim H-W Biomaterials control of pluripotent stem cell fate for regenerative therapy. Prog. Mater. Sci 2016, 82, 234–293.

(13). Elson EL; Genin GM Tissue constructs: Platforms for basic research and drug discovery. Interface Focus 2016, 6, 20150095. [PubMed: 26855763]

(14). Tibbitt MW; Rodell CB; Burdick JA; Anseth KS Progress in material design for biomedical applications. Proc. Natl. Acad. Sci. U.S.A 2015, 112, 14444–14451. [PubMed: 26598696]

(15). Shao Y; Fu J Integrated micro/nanoengineered functional biomaterials for cell mechanics and mechanobiology: a materials perspective. Adv. Mater. 2014, 26, 1494–1533. [PubMed: 24339188]

(16). Baker BM; Chen CS Deconstructing the third dimension – how 3D culture microenvironments alter cellular cues. J. Cell Sci 2012, 125, 3015–3024. [PubMed: 22797912]

(17). Guillame-Gentil O; Semenov O; Roca AS; Groth T; Zahn R; Voros J; Zenobi-Wong M Engineering theextracellular environment: strategies for building 2D and 3D cellular structures. Adv. Mater. 2010, 22, 5443–5462. [PubMed: 20842659]

(18). Griffith LG; Swartz MA Capturing complex 3D tissue physiology in vitro. Nat. Rev. Mol. Cell Bio 2006, 7, 211–224. [PubMed: 16496023]

(19). Dubiel EA; Martin Y; Vermette P Bridging the gap between physicochemistry and interpretation prevalent in cell–surface interactions. Chem. Rev 2011, 111, 2900–2936. [PubMed: 21319750]

(20). Tay CY; Muthu MS; Chia SL; Nguyen KT; Feng S-S; Leong DT Realitycheck for nanomaterial-mediated therapy with 3D biomimetic culture systems. Adv. Func. Mater. 2016, 26, 4046–4065.

(21). van den Berg BM; Vink H; Spaan JAE The endothelial glycocalyx protects against myocardial edema. Circ. Res 2003, 92, 592–594. [PubMed: 12637366]

(22). Discher D; Dong C; Fredberg JJ; Guilak F; Ingber D; Janmey P; Kamm RD; Schmid-Schönbein GW; Weinbaum S Biomechanics: Cell research and applications for the next decade. Ann. Biomed. Eng 2009, 37, 847–859. [PubMed: 19259817]

(23). Mecham RP; Heuser J Three-dimensional organization of extracellular matrix in elastic cartilage as viewed by quick freeze, deep etch electron microscopy. Connect. Tissue. Res 1990, 24, 83–93. [PubMed: 2354636]

(24). Tibbitt MW; Anseth KS Hydrogels as extracellular matrix mimics for 3D cell culture. Biotechnol. Bioeng 2009, 103, 655–663. [PubMed: 19472329]

(25). Higuchi A; Ling Q-D; Hsu S-T; Umezawa A Biomimetic cell culture proteins as extracellular matrices for stem cell differentiation. Chem. Rev 2012, 112, 4507–4540. [PubMed: 22621236]

(26). Annabi N; Tamayol A; Uquillas JA; Akbari M; Bertassoni LE; Cha C; Camci-Unal G; Dokmeci MR; Peppas NA; Khademhosseini A 25th anniversary article: Rational design and applications of hydrogels in regenerative medicine. Adv. Mater. 2013, 26, 85–123.

(27). Green JJ; Elisseeff JH Mimicking biological functionality with polymers for biomedical applications. Nature 2016, 540, 386–394. [PubMed: 27974772]

(28). Seliktar D Designing cell-compatible hydrogels for biomedical applications. Science 2012, 336, 1124–1128. [PubMed: 22654050]

(29). Kinney MA; McDevitt TC Emerging strategies for spatiotemporal control of stem cell fate and morphogenesis. Trends Biotechnol 2013, 31, 78–84. [PubMed: 23219200]

(30). Wen JH; Vincent LG; Fuhrmann A; Choi YS; Hribar KC; Taylor-Weiner H; Chen S; Engler AJ Interplay of matrix stiffness and protein tethering in stem cell differentiation. Nat. Mater. 2014, 13, 979–987. [PubMed: 25108614]

(31). Ahadian S; Sadeghian RB; Salehi S; Ostrovidov S; Bae H; Ramalingam M; Khademhosseini A Bioconjugated hydrogels for tissue engineering and regenerative medicine. Bioconjugate Chem 2015, 26, 1984–2001.

(32). Place ES; Evans ND; Stevens MM Complexity in biomaterials for tissue engineering. Nat. Mater. 2009, 8, 457–470. [PubMed: 19458646]

(33). Benoit DSW; Schwartz MP; Durney AR; Anseth KS Small functional groups for controlled differentiation of hydrogel-encapsulated human mesenchymal stem cells. Nat. Mater. 2008, 7, 816–823. [PubMed: 18724374]

(34). Higuchi A; Ling Q-D; Chang Y; Hsu S-T; Umezawa A Physical cues of biomaterials guide stem cell differentiation fate. Chem. Rev 2013, 113, 3297–3328. [PubMed: 23391258]

(35). Zorlutuna P; Annabi N; Camci-Unal G; Nikkhah M; Cha JM; Nichol JW; Manbachi A; Bae H; Chen S; Khademhosseini A Microfabricated biomaterials for engineering 3D tissues. Adv. Mater. 2012, 24, 1782–1804. [PubMed: 22410857]

(36). Das RK; Gocheva V; Hammink R; Zouani OF; Rowan AE Stress-stiffening-mediated stem-cell commitment switch in soft responsive hydrogels. Nat. Mater. 2016, 15, 318–325. [PubMed: 26618883]

(37). Chaudhuri O; Gu L; Klumpers D; Darnell M; Bencherif SA; Weaver JC; Huebsch N; Lee H.-p.; Lippens E; Duda GN; Mooney DJ Hydrogels with tunable stress relaxation regulate stem cell fate and activity. Nat. Mater. 2016, 15, 326–334. [PubMed: 26618884]

(38). Wang H; Abhilash AS; Chen Christopher S.; Wells Rebecca G.; Shenoy Vivek B. Long-range force transmission in fibrous matrices enabled by tension-driven alignment of fibers. Biophys. J. 2014, 107, 2592–2603. [PubMed: 25468338]

(39). Abhilash AS; Baker Brendon M.; Trappmann B; Chen Christopher S.; Shenoy Vivek B. Remodeling of fibrous extracellular matrices by contractile cells: Predictions from discrete fiber network simulations. Biophys. J. 2014, 107, 1829–1840. [PubMed: 25418164]

(40). Aghvami M; Barocas VH; Sander EA Multiscale mechanical simulations of cell compacted collagen gels. J. Biomech. Eng 2013, 135, 071004.

(41). Ma X; Schickel ME; Stevenson Mark D.; Sarang-Sieminski Alisha L.; Gooch Keith J.; Ghadiali Samir N.; Hart Richard T. Fibers in the extracellular matrix enable long-range stress transmission between cells. Biophys. J. 2013, 104, 1410–1418. [PubMed: 23561517]

(42). Janmey PA; Miller RT Mechanisms of mechanical signaling in development and disease. J. Cell Sci 2010, 124, 9.

(43). Baker BM; Trappmann B; Wang WY; Sakar MS; Kim IL; Shenoy VB; Burdick JA; Chen CS Cell-mediated fibre recruitment drives extracellular matrix mechanosensing in engineered fibrillar microenvironments. Nat. Mater. 2015, 14, 1262–1268. [PubMed: 26461445]

(44). Rowe Roger A.; Pryse Kenneth M.; Asnes Clara F.; Elson Elliot L.; Genin Guy M. Collective matrix remodeling by isolated cells: Unionizing home improvement do-it-yourselfers. Biophys. J. 2015, 108, 2611–2612. [PubMed: 26039161]

(45). Babaei B; Davarian A; Lee S-L; Pryse KM; McConnaughey WB; Elson EL; Genin GM Remodeling by fibroblasts alters the rate-dependent mechanical properties of collagen. Acta Biomater 2016, 37, 28–37. [PubMed: 27015891]

(46). Nematbakhsh Y; Lim CT Cell biomechanics and its applications in human disease diagnosis. Acta Mechanica Sinica 2015, 31, 268–273.

(47). Burdick JA; Murphy WL Moving from static to dynamic complexity in hydrogel design. Nat. Commun 2012, 3, 1269. [PubMed: 23232399]

(48). Kharkar PM; Kiick KL; Kloxin AM Designing degradable hydrogels for orthogonal control of cell microenvironments. Chem. Soc. Rev 2013, 42, 7335–7372. [PubMed: 23609001]

(49). Shi Z; Phillips GO; Yang G Nanocellulose electroconductive composites. Nanoscale 2013, 5, 3194–3201. [PubMed: 23512106]

(50). Radisic M; Park H; Shing H; Consi T; Schoen FJ; Langer R; Freed LE; Vunjak-Novakovic G Functional assembly of engineered myocardium by electrical stimulation of cardiac myocytes cultured on scaffolds. Proc. Natl. Acad. Sci. U.S.A 2004, 101, 18129–18134. [PubMed: 15604141]

(51). Spradling A; Drummond-Barbosa D; Kai T Stem cells find their niche. Nature 2001, 414, 98–104. [PubMed: 11689954]

(52). Wilson A; Trumpp A Bone-marrow haematopoietic-stem-cell niches. Nat. Rev. Immunol 2006, 6, 93–106. [PubMed: 16491134]

(53). Li L; Xie T Stem cell niche: Structure and function. Annu. Rev. Cell Dev. Bi 2005, 21, 605–631.

(54). Morrison SJ; Spradling AC Stem cells and niches: Mechanisms that promote stem cell maintenance throughout life. Cell 2008, 132, 598–611. [PubMed: 18295578]

(55). Schofield R Relationship between spleen colony-forming cell and hematopoietic stem-cell - hypothesis. Blood Cells 1978, 4, 7–25. [PubMed: 747780]

(56). Lane SW; Williams DA; Watt FM Modulating the stem cell niche for tissue regeneration. Nat Biotechnol 2014, 32, 795–803. [PubMed: 25093887]

(57). Dellatore SM; Garcia AS; Miller WM Mimicking stem cell niches to increase stem cell expansion. Curr. Opin. Biotech 2008, 19, 534–540. [PubMed: 18725291]

(58). Bissell MJ; LaBarge MA Context, tissue plasticity, and cancer: Are tumor stem cells also regulated by the microenvironment? Cancer Cell 2005, 7, 17–23. [PubMed: 15652746]

(59). Kise K; Kinugasa-Katayama Y; Takakura N Tumor microenvironment for cancer stem cells. Adv. Drug Deliver. Rev 2016, 99, 197–205.

(60). Wang H; Leinwand LA; Anseth KS Cardiac valve cells and their microenvironment—insights from in vitro studies. Nat. Rev. Cardiol 2014, 11, 715–727. [PubMed: 25311230]

(61). Weaver VM; Lelièvre S; Lakins JN; Chrenek MA; Jones JCR; Giancotti F; Werb Z; Bissell MJ β4 integrin-dependent formation of polarized three-dimensional architecture confers resistance to apoptosis in normal and malignant mammary epithelium. Cancer Cell 2002, 2, 205–216. [PubMed: 12242153]

(62). Xin T; Greco V; Myung P Hardwiring stem cell communication through tissue structure. Cell 2016, 164, 1212–1225. [PubMed: 26967287]

(63). Nitsan I; Drori S; Lewis YE; Cohen S; Tzlil S Mechanical communication in cardiac cell synchronized beating. Nat. Phys 2016, DOI:10.1038/nphys3619.

(64). Mao AS; Shin J-W; Mooney DJ Effects of substrate stiffness and cell-cell contact on mesenchymal stem cell differentiation. Biomaterials 2016, 98, 184–191. [PubMed: 27203745]

(65). Sarvestani AS; Picu CR Network model for the viscoelastic behavior of polymer nanocomposites. Polymer 2004, 45, 7779–7790.

(66). Ebnet K Organization of multiprotein complexes at cell–cell junctions. Histochem. Cell Biol 2008, 130, 1–20. [PubMed: 18365233]

(67). Thompson SA; Copeland CR; Reich DH; Tung L Mechanical coupling between myofibroblasts and cardiomyocytes slows electric conduction in fibrotic cell monolayers. Circulation 2011, 123, 2083–U2071. [PubMed: 21537003]

(68). Potter GD; Byrd TA; Mugler A; Sun B Communication shapes sensory response in multicellular networks. Proc. Natl. Acad. Sci. U.S.A 2016, 113, 10334–10339. [PubMed: 27573834]

(69). Dejana E Endothelial cell-cell junctions: Happy together. Nat. Rev. Mol. Cell Bio 2004, 5, 261–270. [PubMed: 15071551]

(70). Li N; Lü S; Zhang Y; Long M Mechanokinetics of receptor–ligand interactions in cell adhesion. Acta Mechanica Sinica 2015, 31, 248–258.

(71). Gomez GA; McLachlan RW; Yap AS Productive tension: force-sensing and homeostasis of cell–cell junctions. Trends Cell Biol 2011, 21, 499–505. [PubMed: 21763139]

(72). Yankeelov TE; An G; Saut O; Luebeck EG; Popel AS; Ribba B; Vicini P; Zhou X; Weis JA; Ye K; Genin GM Multi-scale modeling in clinical oncology: Opportunities and barriers to success. Ann. Biomed. Eng 2016, 44, 2626–2641. [PubMed: 27384942]

(73). Cox BN; Smith DW On strain and stress in living cells. J. Mech. Phys. Solids 2014, 71, 239–252.

(74). Cox BN; Snead ML Cells as strain-cued automata. J. Mech. Phys. Solids 2016, 87, 177–226.

(75). Berg EL, ; Hsu Y-C; Lee JA Consideration of the cellular microenvironment: Physiologically relevant co-culture systems in drug discovery. Adv. Drug Deliver. Rev 2014, 69–70, 190–204.

(76). Goers L; Freemont P; Polizzi KM Co-culture systems and technologies: Taking synthetic biology to the next level. J. R. Soc. Interface 2014, 11, 1058–1069.

(77). Battiston KG; Cheung JWC; Jain D; Santerre JP Biomaterials in co-culture systems: Towards optimizing tissue integration and cell signaling within scaffolds. Biomaterials 2014, 35, 4465–4476. [PubMed: 24602569]

(78). Estrada MF; Rebelo SP; Davies EJ; Pinto MT; Pereira H; Santo VE; Smalley MJ; Barry ST; Gualda EJ; Alves PM; Anderson E; Brito C Modelling the tumour microenvironment in long-term microencapsulated 3D co-cultures recapitulates phenotypic features of disease progression. Biomaterials 2016, 78, 50–61. [PubMed: 26650685]

(79). Bhatia SN; Balis UJ; Yarmush ML; Toner M Effect of cell-cell interactions in preservation of cellular phenotype: cocultivation of hepatocytes and nonparenchymal cells. Faseb J. 1999, 13, 1883–1900. [PubMed: 10544172]

(80). Tang J; Peng R; Ding JD The regulation of stem cell differentiation by cell-cell contact on micropatterned material surfaces. Biomaterials 2010, 31, 2470–2476. [PubMed: 20022630]

(81). Eschenhagen T; Fink C; Remmers U; Scholz H; Wattchow J; Weil J; Zimmermann W; Dohmen HH; Schäfer H; Bishopric N; Wakatsuki T; Elson EL Three-dimensional reconstitution of embryonic cardiomyocytes in a collagen matrix: a new heart muscle model system. Faseb J. 1997, 11, 683–694. [PubMed: 9240969]

(82). Vunjak Novakovic G; Eschenhagen T; Mummery C Myocardial tissue engineering: In vitro models. CSH Perspect. MED. 2014, 4, pii: a014076.

(83). Guo F; French JB; Li P; Zhao H; Chan CY; Fick JR; Benkovic SJ; Huang TJ Probing cell-cell communication with microfluidic devices. Lab Chip 2013, 13, 3152–3162. [PubMed: 23843092]

(84). van Duinen V; Trietsch SJ; Joore J; Vulto P; Hankemeier T Microfluidic 3D cell culture: From tools to tissue models. Curr. Opin. Biotech 2015, 35, 118–126. [PubMed: 26094109]

(85). Businaro L; De Ninno A; Schiavoni G; Lucarini V; Ciasca G; Gerardino A; Belardelli F; Gabriele L; Mattei F Cross talk between cancer and immune cells: Exploring complex dynamics in a microfluidic environment. Lab Chip 2013, 13, 229–239. [PubMed: 23108434]

(86). Chen Y-C; Zhang Z; Fouladdel S; Deol Y; Ingram PN; McDermott SP; Azizi E; Wicha MS; Yoon E Single cell dual adherent-suspension co-culture micro-environment for studying tumor-stromal interactions with functionally selected cancer stem-like cells. Lab Chip 2016, 16, 2935–2945. [PubMed: 27381658]

(87). Menon NV; Chuah YJ; Cao B; Lim M; Kang Y A microfluidic co-culture system to monitor tumor-stromal interactions on a chip. Biomicrofluidics 2014, 8, 064118. [PubMed: 25553194]

(88). Ma C; Fan R; Ahmad H; Shi Q; Comin-Anduix B; Chodon T; Koya RC; Liu C-C; Kwong GA; Radu CG; Ribas A; Heath JR A clinical microchip for evaluation of single immune cells reveals high functional heterogeneity in phenotypically similar T cells. Nat. Med 2011, 17, 738–743. [PubMed: 21602800]

(89). Dura B; Dougan SK; Barisa M; Hoehl MM; Lo CT; Ploegh HL; Voldman J Profiling lymphocyte interactions at the single-cell level by microfluidic cell pairing. Nat. Commun 2015, 6, 5940. [PubMed: 25585172]

(90). Tumarkin E; Tzadu L; Csaszar E; Seo M; Zhang H; Lee A; Peerani R; Purpura K; Zandstra PW; Kumacheva E High-throughput combinatorial cell co-culture using microfluidics. Integr. Biol 2011, 3, 653–662.

(91). Konry T; Golberg A; Yarmush M Live single cell functional phenotyping in droplet nano-liter reactors. Sci. Rep 2013, 3, 3179. [PubMed: 24212247]

(92). Dura B; Voldman J Spatially and temporally controlled immune cell interactions using microscale tools. Curr. Opin. Immunol 2015, 35, 23–29. [PubMed: 26050635]

(93). Hong S; Pan Q; Lee LP Single-cell level co-culture platform for intercellular communication. Integr. Biol 2012, 4, 374–380.

(94). Simon KA; Mosadegh B; Minn KT; Lockett MR; Mohammady MR; Boucher DM; Hall AB; Hillier SM; Udagawa T; Eustace BK; Whitesides GM Metabolic response of lung cancer cells to radiation in a paper-based 3D cell culture system. Biomaterials 2016, 95, 47–59. [PubMed: 27116031]

(95). Gholipourmalekabadi M; Zhao S; Harrison BS; Mozafari M; Seifalian AM Oxygen-generating biomaterials: A new, viable paradigm for tissue engineering? Trends Biotechnol 2016, 34, 1010–1021. [PubMed: 27325423]

(96). Ezashi T; Das P; Roberts RM Low O2 tensions and the prevention of differentiation of hES cells. Proc. Natl. Acad. Sci. U.S.A 2005, 102, 4783–4788. [PubMed: 15772165]

(97). Forristal CE; Wright KL; Hanley NA; Oreffo ROC; Houghton FD Hypoxia inducible factors regulate pluripotency and proliferation in human embryonic stem cells cultured at reduced oxygen tensions. Reproduction 2010, 139, 85–97. [PubMed: 19755485]

(98). Nakada Y; Canseco DC; Thet S; Abdisalaam S; Asaithamby A; Santos CX; Shah A; Zhang H; Faber JE; Kinter MT; Szweda LI; Xing C; Deberardinis R; Oz O; Lu Z; Zhang CC; Kimura W; Sadek HA Hypoxia induces heart regeneration in adult mice. Nature 2017, 541, 222–227. [PubMed: 27798600]

(99). Dewhirst MW; Cao Y; Moeller B Cycling hypoxia and free radicals regulate angiogenesis and radiotherapy response. Nat. Rev. Cancer 2008, 8, 425–437. [PubMed: 18500244]

(100). Martinive P; Defresne F; Bouzin C; Saliez J; Lair F; Gregoire V; Michiels C; Dessy C; Feron O Preconditioning of the tumor vasculature and tumor cells by intermittent hypoxia: implications for anticancer therapies. Cancer Res 2006, 66, 11736–11744. [PubMed: 17178869]

(101). Rofstad EK; Gaustad JV; Egeland TAM; Mathiesen B; Galappathi K Tumors exposed to acute cyclic hypoxic stress show enhanced angiogenesis, perfusion and metastatic dissemination. Int. J. Cancer 2010, 127, 1535–1546. [PubMed: 20091868]

(102). Sara R; Iwona TD; Eugene YK; Marrison ST; Van Thuc V Hypoxia and radiation therapy: Past history, ongoing research, and future promise. Curr. Mol. Med 2009, 9, 442–458. [PubMed: 19519402]

(103). Martino MM; Tortelli F; Mochizuki M; Traub S; Ben-David D; Kuhn GA; Müller R; Livne E; Eming SA; Hubbell JA Engineering the growth factor microenvironment with fibronectin domains to promote wound and bone tissue healing. Sci. Transl. Med 2011, 3, 100ra189.

(104). Brizzi MF; Tarone G; Defilippi P Extracellular matrix, integrins, and growth factors as tailors of the stem cell niche. Curr. Opin. Cell Biol 2012, 24, 645–651. [PubMed: 22898530]

(105). Cezar CA; Mooney DJ Biomaterial-based delivery for skeletal muscle repair. Adv. Drug Deliver. Rev 2015, 84, 188–197.

(106). Jin K; Zhu Y; Sun Y; Mao XO; Xie L; Greenberg DA Vascular endothelial growth factor (VEGF) stimulates neurogenesis in vitro and in vivo. Proc. Natl. Acad. Sci. U.S.A 2002, 99, 11946–11950. [PubMed: 12181492]

(107). Briquez PS; Clegg LE; Martino MM; Gabhann FM; Hubbell JA Design principles for therapeutic angiogenic materials. Nat. Rev. Mater. 2016, 1, 15006.

(108). Scharenberg MA; Pippenger BE; Sack R; Zingg D; Ferralli J; Schenk S; Martin I; Chiquet-Ehrismann R TGF-β-induced differentiation into myofibroblasts involves specific regulation of two MKL1 isoforms. J. Cell Sci 2014, 127, 1079–1091. [PubMed: 24424023]

(109). Lafyatis R Transforming growth factor β—at the centre of systemic sclerosis. Nat. Rev. Rheumatol 2014, 10, 706–719. [PubMed: 25136781]

(110). Iekushi K; Taniyama Y; Kusunoki H; Azuma J; Sanada F; Okayama K; Koibuchi N; Iwabayashi M; Rakugi H; Morishita R Hepatocyte growth factor attenuates transforming growth factor-beta-angiotensin II crosstalk through inhibition of the PTEN/Akt pathway. Hypertension 2011, 58, 190–196. [PubMed: 21670418]

(111). Dingal PCDP; Discher DE Combining insoluble and soluble factors to steer stem cell fate. Nat. Mater 2014, 13, 532–537. [PubMed: 24845982]

(112). Engler AJ; Sen S; Sweeney HL; Discher DE Matrix elasticity directs stem cell lineage specification. Cell 2006, 126, 677–689. [PubMed: 16923388]

(113). Kim YJ; Sah RLY; Grodzinsky AJ; Plaas AHK; Sandy JD Mechanical regulation of cartilage biosynthetic behavior: Physical stimuli. Arch. Biochem. Biophys 1994, 311, 1–12. [PubMed: 8185305]

(114). Mauck RL; Soltz MA; Wang CCB; Wong DD; Chao P-HG; Valhmu WB; Hung CT; Ateshian GA Functional tissue engineering of articular cartilage through dynamic loading of chondrocyte-seeded agarose gels. J. Biomech. Eng 2000, 122, 252–260. [PubMed: 10923293]

(115). Mauck RL; Nicoll SB; Seyhan SL; Ateshian GA; Hung CT Synergistic action of growth factors and dynamic loading for articular cartilage tissue engineering. Tissue Eng 2003, 9, 597–611. [PubMed: 13678439]

(116). Mauck RL; Seyhan SL; Ateshian GA; Hung CT Influence of seeding density and dynamic deformational loading on the developing structure/function relationships of chondrocyte-seeded agarose hydrogels. Ann. Biomed. Eng 2002, 30, 1046–1056. [PubMed: 12449765]

(117). Abbott J; Holtzer H The loss of phenotypic traits by differentiated cells. III. The reversible behavior of chondrocytes in primary cultures. J. Cell Biol 1966, 28, 473–487. [PubMed: 4163861]

(118). Guilak F; Cohen DM; Estes BT; Gimble JM; Liedtke W; Chen CS Control of stem cell fate by physical interactions with the extracellular matrix. Cell Stem Cell 2009, 5, 17–26. [PubMed: 19570510]

(119). Guilak F; Hung CT In Basic Orthopaedic Biomechanics and Mechano-Biology, 2005; Vol. 3.

(120). Huang N; Li S Regulation of the matrix microenvironment for stem cell engineering and regenerative medicine. Ann. Biomed. Eng 2011, 39, 1201–1214. [PubMed: 21424849]

(121). Liu WF; Chen CS Engineering biomaterials to control cell function. Mater. Today 2005, 8, 28–35.

(122). Watt FM; Huck WTS Role of the extracellular matrix in regulating stem cell fate. Nat. Rev. Mol. Cell Bio 2013, 14, 467–473. [PubMed: 23839578]

(123). Khalil AS; Xie AW; Murphy WL Context clues: The importance of stem cell–material interactions. ACS Chem. Biol 2014, 9, 45–56. [PubMed: 24369691]

(124). Bonnans C; Chou J; Werb Z Remodelling the extracellular matrix in development and disease. Nat. Rev. Mol. Cell Bio 2014, 15, 786–801. [PubMed: 25415508]

(125). Malanchi I; Santamaria-Martinez A; Susanto E; Peng H; Lehr H-A; Delaloye J-F; Huelsken J Interactions between cancer stem cells and their niche govern metastatic colonization. Nature 2012, 481, 85–89.

(126). Frantz C; Stewart KM; Weaver VM The extracellular matrix at a glance. J. Cell Sci 2010, 123, 4195–4200. [PubMed: 21123617]

(127). Theocharis AD; Skandalis SS; Gialeli C; Karamanos NK Extracellular matrix structure. Adv. Drug Deliver. Rev 2015, 97, 4–27.

(128). Wagenseil JE; Mecham RP Elastin in large artery stiffness and hypertension. J. Cardiovasc. Transl 2012, 5, 264–273.

(129). Rico P; Mnatsakanyan H; Dalby MJ; Salmerón-Sánchez M Material-driven fibronectin assembly promotes maintenance of mesenchymal stem cell phenotypes. Adv. Func. Mater. 2016, 26, 6563–6573.

(130). Freudenberg U; Liang Y; Kiick KL; Werner C Glycosaminoglycan-based biohybrid hydrogels: A sweet and smart choice for multifunctional biomaterials. Adv. Mater. 2016, 28, 8861–8891. [PubMed: 27461855]

(131). Geiger B; Spatz JP; Bershadsky AD Environmental sensing through focal adhesions. Nat. Rev. Mol. Cell Bio 2009, 10, 21–33. [PubMed: 19197329]

(132). Kanzaki Y; Terasaki F; Okabe M; Fujita S; Katashima T; Otsuka K; Ishizaka N Three-dimensional architecture of cardiomyocytes and connective tissue in human heart revealed by scanning electron microscopy. Circulation 2010, 122, 1973–1974. [PubMed: 21060087]

(133). Gumbiner BM Cell adhesion: The molecular basis of tissue architecture and morphogenesis. Cell 1996, 84, 345–357. [PubMed: 8608588]

(134). Qin D; Xia Y; Whitesides GM Soft lithography for micro- and nanoscale patterning. Nat. Protoc 2010, 5, 491–502. [PubMed: 20203666]

(135). Desai RA; Khan MK; Gopal SB; Chen CS Subcellular spatial segregation of integrin subtypes by patterned multicomponent surfaces. Integr. Biol 2011, 3, 560–567.

(136). Théry M Micropatterning as a tool to decipher cell morphogenesis and functions. J. Cell Sci 2010, 123, 4201–4213. [PubMed: 21123618]

(137). Zheng Z; Daniel WL; Giam LR; Huo F; Senesi AJ; Zheng G; Mirkin CA Multiplexed protein arrays enabled by polymer pen lithography: Addressing the inking challenge. Angew. Chem. Int. Edit 2009, 48, 7626–7629.

(138). Chiu DT; Jeon NL; Huang S; Kane RS; Wargo CJ; Choi IS; Ingber DE; Whitesides GM Patterned deposition of cells and proteins onto surfaces by using three-dimensional microfluidic systems. Proc. Natl. Acad. Sci. U.S.A 2000, 97, 2408–2413. [PubMed: 10681460]

(139). van Dongen SFM; Maiuri P; Marie E; Tribet C; Piel M Triggering cell adhesion, migration or shape change with a dynamic surface coating. Adv. Mater. 2013, 25, 1687–1691. [PubMed: 23355329]

(140). Vignaud T; Galland R; Tseng Q; Blanchoin L; Colombelli J; Théry M Reprogramming cell shape with laser nano-patterning. J. Cell Sci 2012, 125, 2134. [PubMed: 22357956]

(141). Hui EE; Bhatia SN Micromechanical control of cell–cell interactions. Proc. Natl. Acad. Sci. U.S.A 2007, 104, 5722–5726. [PubMed: 17389399]

(142). Wijelath ES; Rahman S; Namekata M; Murray J; Nishimura T; Mostafavi-Pour Z; Patel Y; Suda Y; Humphries MJ; Sobel M Heparin-II domain of fibronectin is a vascular endothelial growth factor-binding domain. Circ. Res 2006, 99, 853. [PubMed: 17008606]

(143). Zhu J; Clark RAF Fibronectin at select sites binds multiple growth factors and enhances their activity: Expansion of the collaborative ECM-GF paradigm. J. Invest. Dermatol 2014, 134, 895–901. [PubMed: 24335899]

(144). Hynes RO The extracellular matrix: Not just pretty fibrils. Science 2009, 326, 1216–1219. [PubMed: 19965464]

(145). Mouw JK; Ou G; Weaver VM Extracellular matrix assembly: A multiscale deconstruction. Nat. Rev. Mol. Cell Bio 2014, 15, 771–785. [PubMed: 25370693]

(146). Riching Kristin M.; Cox BL; Salick Max R.; Pehlke C; Riching Andrew S.; Ponik SM; Bass Benjamin R.; Crone Wendy C.; Jiang Y; Weaver AM; Eliceiri Kevin W.; Keely Patricia J. 3D collagen alignment limits protrusions to enhance breast cancer cell persistence. Biophys. J. 2014, 107, 2546–2558. [PubMed: 25468334]

(147). Chaubaroux C; Perrin-Schmitt F; Senger B; Vidal L; Voegel J-C; Schaaf P; Haikel Y; Boulmedais F; Lavalle P; Hemmerlé J Cell alignment driven by mechanically induced collagen fiber alignment in collagen/alginate coatings. Tissue Eng. Part C Meth 2015, 21, 881–888.

(148). Teixeira AI; Abrams GA; Bertics PJ; Murphy CJ; Nealey PF Epithelial contact guidance on well-defined micro- and nanostructured substrates. J. Cell Sci 2003, 116, 1881. [PubMed: 12692189]

(149). Provenzano PP; Inman DR; Eliceiri KW; Trier SM; Keely PJ Contact guidance mediated three-dimensional cell migration is regulated by Rho/ROCK-dependent matrix reorganization. Biophys. J. 2008, 95, 5374–5384. [PubMed: 18775961]

(150). Meehan S; Nain Amrinder S. Role of suspended fiber structural stiffness and curvature on single-cell migration, nucleus shape, and focal-adhesion-cluster length. Biophys. J. 2014, 107, 2604–2611. [PubMed: 25468339]

(151). Sheets K; Sharma P; Koons B; Nain A In Handbook of Imaging in Biological Mechanics; CRC Press, 2014.

(152). Sheets K; Wunsch S; Ng C; Nain AS Shape-dependent cell migration and focal adhesion organization on suspended and aligned nanofiber scaffolds. Acta Biomater 2013, 9, 7169–7177. [PubMed: 23567946]

(153). Tse HTK; Weaver WM; Di Carlo D Increased asymmetric and multi-daughter cell division in mechanically confined microenvironments. PLOS ONE 2012, 7, e38986. [PubMed: 22761717]

(154). Kittur H; Weaver W; Di Carlo D Well-plate mechanical confinement platform for studies of mechanical mutagenesis. Biomed. Microdevices 2014, 16, 439–447. [PubMed: 24619125]

(155). Osmond M; Bernier SM; Pantcheva MB; Krebs MD Collagen and collagen-chondroitin sulfate scaffolds with uniaxially aligned pores for the biomimetic, three dimensional culture of trabecular meshwork cells. Biotechnol. Bioeng 2016, DOI: 10.1002/bit.26206.

(156). Jana S; Cooper A; Zhang M Chitosan scaffolds with unidirectional microtubular pores for large skeletal myotube generation. Adv. Healthc. Mater. 2013, 2, 557–561. [PubMed: 23184507]

(157). Viela F; Granados D; Ayuso-Sacido A; Rodríguez I Biomechanical cell regulation by high aspect ratio nanoimprinted pillars. Adv. Func. Mater. 2016, 26, 5599–5609.

(158). Dalby MJ; Gadegaard N; Tare R; Andar A; Riehle MO; Herzyk P; Wilkinson CD; Oreffo RO The control of human mesenchymal cell differentiation using nanoscale symmetry and disorder. Nat. Mater. 2007, 6, 997–1003. [PubMed: 17891143]

(159). McMurray RJ; Gadegaard N; Tsimbouri PM; Burgess KV; McNamara LE; Tare R; Murawski K; Kingham E; Oreffo ROC; Dalby MJ Nanoscale surfaces for the long-term maintenance of mesenchymal stem cell phenotype and multipotency. Nat. Mater. 2011, 10, 637–644. [PubMed: 21765399]

(160). Bae W-G; Kim J; Choung Y-H; Chung Y; Suh KY; Pang C; Chung JH; Jeong HE Bio-inspired configurable multiscale extracellular matrix-like structures for functional alignment and guided orientation of cells. Biomaterials 2015, 69, 158–164. [PubMed: 26285083]

(161). Sia J; Yu P; Srivastava D; Li S Effect of biophysical cues on reprogramming to cardiomyocytes. Biomaterials 2016, 103, 1–11. [PubMed: 27376554]

(162). Bettadapur A; Suh GC; Geisse NA; Wang ER; Hua C; Huber HA; Viscio AA; Kim JY; Strickland JB; McCain ML Prolonged culture of aligned skeletal myotubes on micromolded gelatin hydrogels. Sci. Rep 2016, 6, 28855. [PubMed: 27350122]

(163). Oh S; Brammer KS; Li YSJ; Teng D; Engler AJ; Chien S; Jin S Stem cell fate dictated solely by altered nanotube dimension. Proc. Natl. Acad. Sci. U.S.A 2009, 106, 2130–2135. [PubMed: 19179282]

(164). Guvendiren M; Burdick JA The control of stem cell morphology and differentiation by hydrogel surface wrinkles. Biomaterials 2010, 31, 6511–6518. [PubMed: 20541257]

(165). Zhu X; Mills KL; Peters PR; Bahng JH; Liu EH; Shim J; Naruse K; Csete ME; Thouless MD; Takayama S Fabrication of reconfigurable protein matrices by cracking. Nat. Mater. 2005, 4, 403–406. [PubMed: 15834415]

(166). Flemming RG; Murphy CJ; Abrams GA; Goodman SL; Nealey PF Effects of synthetic micro- and nano-structured surfaces on cell behavior. Biomaterials 1999, 20, 573–588. [PubMed: 10213360]

(167). Bettinger CJ; Langer R; Borenstein JT Engineering substrate topography at the micro- and nanoscale to control cell function. Angew. Chem. Int. Edit 2009, 48, 5406–5415.

(168). Tawfick S; De Volder M; Copic D; Park SJ; Oliver CR; Polsen ES; Roberts MJ; Hart AJ Engineering of micro- and nanostructured surfaces with anisotropic geometries and properties. Adv. Mater. 2012, 24, 1628–1674. [PubMed: 22396318]

(169). Nikkhah M; Edalat F; Manoucheri S; Khademhosseini A Engineering microscale topographies to control the cell–substrate interface. Biomaterials 2012, 33, 5230–5246. [PubMed: 22521491]

(170). Kim D-H; Provenzano PP; Smith CL; Levchenko A Matrix nanotopography as a regulator of cell function. J. Cell Biol 2012, 197, 351–360. [PubMed: 22547406]

(171). Liu X; Wang S Three-dimensional nano-biointerface as a new platform for guiding cell fate. Chem. Soc. Rev 2014, 43, 2385–2401. [PubMed: 24504119]

(172). Dobbenga S; Fratila-Apachitei LE; Zadpoor AA Nanopattern-induced osteogenic differentiation of stem cells – A systematic review. Acta Biomater 2016, 46, 3–14. [PubMed: 27667018]

(173). Li Y; Huang G; Zhang X; Wang L; Du Y; Lu TJ; Xu F Engineering cell alignment in vitro. Biotechnol. Adv 2014, 32, 347–365. [PubMed: 24269848]

(174). Wang P-Y; Thissen H; Kingshott P Modulation of human multipotent and pluripotent stem cells using surface nanotopographies and surface-immobilised bioactive signals: A review. Acta Biomater 2016, 45, 31–59. [PubMed: 27596488]

(175). Nemir S; West JL Synthetic materials in the study of cell response to substrate rigidity. Ann. Biomed. Eng 2010, 38, 2–20. [PubMed: 19816774]

(176). Genin GM; Kent A; Birman V; Wopenka B; Pasteris JD; Marquez PJ; Thomopoulos S Functional grading of mineral and collagen in the attachment of tendon to bone. Biophys. J. 2009, 97, 976–985. [PubMed: 19686644]

(177). Liu Y; Thomopoulos S; Chen C; Birman V; Buehler MJ; Genin GM Modelling the mechanics of partially mineralized collagen fibrils, fibres and tissue. J. R. Soc. Interface 2013, 11, 20130835. [PubMed: 24352669]

(178). Rehfeldt F; Engler AJ; Eckhardt A; Ahmed F; Discher DE Cell responses to the mechanochemical microenvironment—Implications for regenerative medicine and drug delivery. Adv. Drug Deliver. Rev 2007, 59, 1329–1339.

(179). Huang G; Wang L; Wang S; Han Y; Wu J; Zhang Q; Xu F; Lu TJ Engineering three-dimensional cell mechanical microenvironment with hydrogels. Biofabrication 2012, 4, 042001. [PubMed: 23164720]

(180). Engler AJ; Carag-Krieger C; Johnson CP; Raab M; Tang H-Y; Speicher DW; Sanger JW; Sanger JM; Discher DE Embryonic cardiomyocytes beat best on a matrix with heart-like elasticity: scar-like rigidity inhibits beating. J. Cell Sci 2008, 121, 3794–3802. [PubMed: 18957515]

(181). Mammoto T; Ingber DE Mechanical control of tissue and organ development. Development 2010, 137, 1407. [PubMed: 20388652]

(182). Lo C-M; Wang H-B; Dembo M; Wang Y.-l. Cell movement is guided by the rigidity of the substrate. Biophys. J. 2000, 79, 144–152. [PubMed: 10866943]

(183). Isenberg BC; DiMilla PA; Walker M; Kim S; Wong JY Vascular smooth muscle cell durotaxis depends on substrate stiffness gradient strength. Biophys. J. 2009, 97, 1313–1322. [PubMed: 19720019]

(184). Harland B; Walcott S; Sun SX Adhesion dynamics and durotaxis in migrating cells. Biophys. J. 2011, 8, 015011.

(185). Paszek MJ; Zahir N; Johnson KR; Lakins JN; Rozenberg GI; Gefen A; Reinhart-King CA; Margulies SS; Dembo M; Boettiger D; Hammer DA; Weaver VM Tensional homeostasis and the malignant phenotype. Cancer Cell 2005, 8, 241–254. [PubMed: 16169468]

(186). Dupont S; Morsut L; Aragona M; Enzo E; Giulitti S; Cordenonsi M; Zanconato F; Le Digabel J; Forcato M; Bicciato S; Elvassore N; Piccolo S Role of YAP/TAZ in mechanotransduction. Nature 2011, 474, 179–183. [PubMed: 21654799]

(187). Erler JT Remodeling and homeostasis of the extracellular matrix: implications for fibrotic diseases and cancer. Radiother. Oncol 2012, 102, S33.

(188). Urciuolo A; Quarta M; Morbidoni V; Gattazzo F; Molon S; Grumati P; Montemurro F; Tedesco FS; Blaauw B; Cossu G; Vozzi G; Rando TA; Bonaldo P Collagen VI regulates satellite cell self-renewal and muscle regeneration. Nat. Commun 2013, 4, 1964. [PubMed: 23743995]

(189). Kai F; Laklai H; Weaver VM Force matters: Biomechanical regulation of cell invasion and migration in disease. Trends Cell Biol 2016, 26, 486–497. [PubMed: 27056543]

(190). DuFort CC; Paszek MJ; Weaver VM Balancing forces: architectural control of mechanotransduction. Nat. Rev. Mol. Cell Bio 2011, 12, 308–319. [PubMed: 21508987]

(191). Yu H; Mouw JK; Weaver VM Forcing form and function: Biomechanical regulation of tumor evolution. Trends Cell Biol 2011, 21, 47–56. [PubMed: 20870407]

(192). Nam S; Lee J; Brownfield Doug G.; Chaudhuri O Viscoplasticity enables mechanical remodeling of matrix by cells. Biophys. J. 2016, 111, 2296–2308. [PubMed: 27851951]

(193). Cameron AR; Frith JE; Cooper-White JJ The influence of substrate creep on mesenchymal stem cell behaviour and phenotype. Biomaterials 2011, 32, 5979–5993. [PubMed: 21621838]

(194). Chandran PL; Barocas VH Microstructural mechanics of collagen gels in confined compression: Poroelasticity, viscoelasticity, and collapse. J. Biomech. Eng 2004, 126, 152–166. [PubMed: 15179845]

(195). Babaei B; Abramowitch SD; Elson EL; Thomopoulos S; Genin GM A discrete spectral analysis for determining quasi-linear viscoelastic properties of biological materials. J. R. Soc. Interface 2015, 12, 21050707.

(196). Huang C; Holfeld J; Schaden W; Orgill D; Ogawa R Mechanotherapy: Revisiting physical therapy and recruiting mechanobiology for a new era in medicine. Trends. Mol. Med 2013, 19, 555–564. [PubMed: 23790684]

(197). Saffarian S; Qian H; Collier I; Elson E; Goldberg G Powering a burnt bridges Brownian ratchet: A model for an extracellular motor driven by proteolysis of collagen. Physical Review E 2006, 73, 041909.

(198). Ellis V; Murphy G Cellular strategies for proteolytic targeting during migration and invasion. FEBS Lett 2001, 506, 1–5. [PubMed: 11591360]

(199). Murphy G; Gavrilovic J Proteolysis and cell migration: Creating a path? Curr. Opin. Cell Biol 1999, 11, 614–621. [PubMed: 10508651]

(200). Khetan S; Guvendiren M; Legant WR; Cohen DM; Chen CS; Burdick JA Degradation-mediated cellular traction directs stem cell fate in covalently crosslinked three-dimensional hydrogels. Nat. Mater. 2013, 12, 458–465. [PubMed: 23524375]

(201). Hynes RO Stretching the boundaries of extracellular matrix research. Nat. Rev. Mol. Cell Bio 2014, 15, 761–763. [PubMed: 25574535]

(202). Cheng B; Lin M; Li Y; Huang G; Yang H; Genin GM; Deshpande VS; Lu TJ; Xu F An Integrated Stochastic Model of Matrix-Stiffness-Dependent Filopodial Dynamics. Biophysical journal 2016, 111, 2051–2061. [PubMed: 27806285]

(203). Mitchison T; Kirschner M Cytoskeletal dynamics and nerve growth. Neuron 1988, 1, 761–772. [PubMed: 3078414]

(204). Chan CE; Odde DJ Traction dynamics of filopodia on compliant substrates. Science 2008, 322, 1687–1691. [PubMed: 19074349]

(205). Cao X; Ban E; Baker BM; Lin Y; Burdick JA; Chen CS; Shenoy VB Multiscale model predicts increasing focal adhesion size with decreasing stiffness in fibrous matrices. Proc. Natl. Acad. Sci. U.S.A 2017, Doi: 10.1073/pnas.1620486114.

(206). Gronau G; Krishnaji ST; Kinahan ME; Giesa T; Wong JY; Kaplan DL; Buehler MJ A review of combined experimental and computational procedures for assessing biopolymer structure–process–property relationships. Biomaterials 2012, 33, 8240–8255. [PubMed: 22938765]

(207). Shakiba D; Babaei B; Saadat F; Thomopoulos S; Genin GM The fibrous cellular microenvironment, and how cells make sense of a tangled web. Proc. Natl. Acad. Sci. U.S.A 2017.

(208). Altman GH; Horan RL; Martin I; Farhadi J; Stark PRH; Volloch V; Richmond JC; Vunjak-Novakovic G; Kaplan DL Cell differentiation by mechanical stress. Faseb J. 2001, 16, 270–272. [PubMed: 11772952]

(209). Pablo Marquez J; Genin GM; Elson EL On the application of strain factors for approximation of the contribution of anisotropic cells to the mechanics of a tissue construct. J. Biomech 2006, 39, 2145–2151. [PubMed: 16055135]

(210). Zeng Y; Feng S; Liu W; Fu Q; Li Y; Li X; Chen C; Huang C; Ge Z; Du Y Preconditioning of mesenchymal stromal cells toward nucleus pulposus-like cells by microcryogels-based 3D cell

culture and syringe-based pressure loading system. J. Biomed. Mater. Res. B 2015, DOI: 10.1002/jbm.b.33509.

(211). Cezar CA; Roche ET; Vandenburgh HH; Duda GN; Walsh CJ; Mooney DJ Biologic-free mechanically induced muscle regeneration. Proc. Natl. Acad. Sci. U.S.A 2016, 113, 1534–1539. [PubMed: 26811474]

(212). Hur SS; Del Alamo JC; Park JS; Li YS; Nguyen HA; Teng D; Wang KC; Flores L; Alonso-Latorre B; Lasheras JC; Chien S Roles of cell confluency and fluid shear in 3-dimensional intracellular forces in endothelial cells. Proc. Natl. Acad. Sci. U.S.A 2012, 109, 11110–11115. [PubMed: 22665785]

(213). Qi Y-X; Jiang J; Jiang X-H; Wang X-D; Ji S-Y; Han Y; Long D-K; Shen B-R; Yan Z-Q; Chien S; Jiang Z-L PDGF-BB and TGF-β1 on cross-talk between endothelial and smooth muscle cells in vascular remodeling induced by low shear stress. Proc. Natl. Acad. Sci. U.S.A 2011, 108, 1908–1913. [PubMed: 21245329]

(214). Wang L; Han Y; Shen Y; Yan Z-Q; Zhang P; Yao Q-P; Shen B-R; Gao L-Z; Qi Y-X; Jiang Z-L Endothelial insulin-like growth factor-1 modulates proliferation and phenotype of smooth muscle cells induced by low shear stress. Ann. Biomed. Eng 2014, 42, 776–786. [PubMed: 24322591]

(215). Lee HJ; Diaz MF; Price KM; Ozuna JA; Zhang S; Sevick-Muraca EM; Hagan JP; Wenzel PL Fluid shear stress activates YAP1 to promote cancer cell motility. Nat. Commun 2017, 8, 14122. [PubMed: 28098159]

(216). Li Y; Huang G; Li M; Wang L; Elson EL; Lu TJ; Genin GM; Xu F An approach to quantifying 3D responses of cells to extreme strain. Sci. Rep 2016, 6, 19550. [PubMed: 26887698]

(217). Elson EL; Genin GM The role of mechanics in actin stress fiber kinetics. Exp. Cell Res 2013, 319, 2490–2500. [PubMed: 23906923]

(218). McGarry JP; Fu J; Yang MT; Chen CS; McMeeking RM; Evans AG; Deshpande VS Simulation of the contractile response of cells on an array of micro-posts. Philosophical Transactions of the Royal Society A: Mathematical, Physical and Engineering Sciences 2009, 367, 3477–3497.

(219). Tondon A; Kaunas R The direction of stretch-induced cell and stress fiber orientation depends on collagen matrix stress. PLOS ONE 2014, 9, e89592. [PubMed: 24586898]

(220). Zimmermann WH; Melnychenko I; Wasmeier G; Didie M; Naito H; Nixdorff U; Hess A; Budinsky L; Brune K; Michaelis B; Dhein S; Schwoerer A; Ehmke H; Eschenhagen T Engineered heart tissue grafts improve systolic and diastolic function in infarcted rat hearts. Nat. Med 2006, 12, 452–458. [PubMed: 16582915]

(221). Li Y; Huang G; Gao B; Li M; Genin GM; Lu TJ; Xu F Magnetically actuated cell-laden microscale hydrogels for probing strain-induced cell responses in three dimensions. NPG Asia Mater. 2016, 8, e238.

(222). Rothdiener M; Hegemann M; Uynuk-Ool T; Walters B; Papugy P; Nguyen P; Claus V; Seeger T; Stoeckle U; Boehme KA; Aicher WK; Stegemann JP; Hart ML; Kurz B; Klein G; Rolauffs B Stretching human mesenchymal stromal cells on stiffness-customized collagen type I generates a smooth muscle marker profile without growth factor addition. Sci. Rep 2016, 6, 35840. [PubMed: 27775041]

(223). Sah RLY; Kim Y-J; Doong J-YH; Grodzinsky AJ; Plass AHK; Sandy JD Biosynthetic response of cartilage explants to dynamic compression. J. Orthor. Res 1989, 7, 619–636.

(224). De R; Zemel A; Safran SA Do cells sense stress or strain? Measurement of cellular orientation can provide a clue. Biophys. J. 2008, 94, L29–L31. [PubMed: 18192355]

(225). Friedrich Benjamin M.; Buxboim A; Discher Dennis E.; Safran Samuel A. Striated acto-myosin fibers can reorganize and register in response to elastic interactions with the matrix. Biophys. J. 2011, 100, 2706–2715. [PubMed: 21641316]

(226). Hsu H-J; Lee C-F; Kaunas R A Dynamic stochastic model of frequency-dependent stress fiber alignment induced by cyclic stretch. PLOS ONE 2009, 4, e4853. [PubMed: 19319193]

(227). Krishnan R; Park CY; Lin Y-C; Mead J; Jaspers RT; Trepat X; Lenormand G; Tambe D; Smolensky AV; Knoll AH; Butler JP; Fredberg JJ Reinforcement versus fluidization in cytoskeletal mechanoresponsiveness. PLOS ONE 2009, 4, e5486. [PubMed: 19424501]

(228). Rustom LE; Boudou T; Nemke BW; Lu Y; Hoelzle DJ; Markel MD; Picart C; Johnson AJW Multiscale porosity directs bone regeneration in biphasic calcium phosphate scaffolds. ACS Biomater. Sci. Eng 2016, DOI: 10.1021/acsbiomaterials.1026b00632.

(229). Polak SJ; Rustom LE; Genin GM; Talcott M; Wagoner Johnson AJ A mechanism for effective cell-seeding in rigid, microporous substrates. Acta Biomater 2013, 9, 7977–7986. [PubMed: 23665116]

(230). Lee S-L; Nekouzadeh A; Butler B; Pryse KM; McConnaughey WB; Nathan AC; Legant WR; Schaefer PM; Pless RB; Elson EL; Genin GM Physically-induced cytoskeleton remodeling of cells in three-dimensional culture. PLOS ONE 2012, 7, e45512. [PubMed: 23300512]

(231). Nekouzadeh A; Pryse KM; Elson EL; Genin GM Stretch-activated force shedding, force recovery, and cytoskeletal remodeling in contractile fibroblasts. J. Biomech 2008, 41, 2964–2971. [PubMed: 18805531]

(232). Rouillard Andrew D.; Holmes Jeffrey W. Mechanical boundary conditions bias fibroblast invasion in a collagen-fibrin wound model. Biophys. J. 2014, 106, 932–943. [PubMed: 24559996]

(233). Genin Guy M.; Elson Elliot L. Mechanically guided cell migration: Less of a stretch than ever. Biophys. J. 2014, 106, 776–777. [PubMed: 24559979]

(234). Shenoy VB; Wang H; Wang X A chemo-mechanical free-energy-based approach to model durotaxis and extracellular stiffness-dependent contraction and polarization of cells. Interface Focus 2016, 6, 20150067. [PubMed: 26855753]

(235). Song B; Zhao M; Forrester JV; McCaig CD Electrical cues regulate the orientation and frequency of cell division and the rate of wound healing in vivo. Proc. Natl. Acad. Sci. U.S.A 2002, 99, 13577–13582. [PubMed: 12368473]

(236). Shi Z; Gao X; Ullah MW; Li S; Wang Q; Yang G Electroconductive natural polymer-based hydrogels. Biomaterials 2016, 111, 40–54. [PubMed: 27721086]

(237). Spencer TM; Blumenstein RF; Pryse KM; Lee SL; Glaubke DA; Carlson BE; Elson EL; Genin GM Fibroblasts slow conduction velocity in a reconstituted tissue model of fibrotic cardiomyopathy. ACS Biomater. Sci. Eng 2016, DOI: 10.1021/acsbiomaterials.1026b00576.

(238). Ghafar-Zadeh E; Waldeisen JR; Lee LP Engineered approaches to the stem cell microenvironment for cardiac tissue regeneration. Lab Chip 2011, 11, 3031–3048. [PubMed: 21785806]

(239). Wang L; Jiang J; Hua W; Darabi A; Song X; Song C; Zhong W; Xing MMQ; Qiu X Mussel-Inspired conductive cryogel as cardiac tissue patch to repair myocardial infarction by migration of conductive nanoparticles. Adv. Func. Mater. 2016, 26, 4293–4305.

(240). Jana S; Levengood SKL; Zhang M Anisotropicmaterials for skeletal-muscle-tissue engineering. Adv. Mater. 2016, 28, 10588–10612. [PubMed: 27865007]

(241). Green RA; Lovell NH; Wallace GG; Poole-Warren LA Conducting polymers for neural interfaces: Challenges in developing an effective long-term implant. Biomaterials 2008, 29, 3393–3399.

(242). Fattahi P; Yang G; Kim G; Abidian MR A review of organic and inorganic biomaterials for neural interfaces. Adv. Mater. 2014, 26, 1846–1885. [PubMed: 24677434]

(243). Cui H; Liu Y; Deng M; Pang X; Zhang P; Wang X; Chen X; Wei Y Synthesis of biodegradable and electroactive tetraaniline grafted poly(ester amide) copolymers for bone tissue engineering. Biomacromolecules 2012, 13, 2881–2889. [PubMed: 22909313]

(244). Tandon N; Cannizzaro C; Chao P-HG; Maidhof R; Marsano A; Au HTH; Radisic M; Vunjak-Novakovic G Electrical stimulation systems for cardiac tissue engineering. Nat. Protoc 2009, 4, 155–173. [PubMed: 19180087]

(245). Richards DJ; Tan Y; Coyle R; Li Y; Xu R; Yeung N; Parker A; Menick DR; Tian B; Mei Y Nanowires andelectrical stimulation synergistically improve functions of hiPSC cardiac spheroids. Nano lett 2016, 16, 4670–4678. [PubMed: 27328393]

(246). Xin FX; Lu TJ Acoustomechanical giant deformation of soft elastomers with interpenetrating networks. Smart Mater. Struct 2016, 25, 07LT02.

(247). Xin F; Lu T Tensional acoustomechanical soft metamaterials. Sci. Rep 2016, 6, 27432. [PubMed: 27264106]

(248). Xin F; Lu TJ A nonlinear acoustomechanical field theory of polymeric gels. International Journal of Solids and Structures 2017, 112, 133–142.

(249). Xin FX; Lu TJ Acoustomechanical constitutive theory for soft materials. Acta Mechanica Sinica 2016, 32, 828–840.

(250). Xin F; Lu TJ Nonlinear large deformation of acoustomechanical soft materials. Mechanics of Materials 2017, 107, 71–80.

(251). Kucsko G; Maurer PC; Yao NY; Kubo M; Noh HJ; Lo PK; Park H; Lukin MD Nanometre-scale thermometry in a living cell. Nature 2013, 500, 54–58. [PubMed: 23903748]

(252). Lepock JR How do cells respond to their thermal environment? Int. J. Hyperther 2005, 21, 681–687.

(253). Lin M; Liu F; Liu S; Ji C; Li A; Lu TJ; Xu F The race to the nociceptor: mechanical versus temperature effects in thermal pain of dental neurons. Acta Mechanica Sinica 2017, 33, 260–266.

(254). Sanz B; Calatayud MP; Torres TE; Fanarraga ML; Ibarra MR; Goya GF Magnetic hyperthermia enhances cell toxicity with respect to exogenous heating. Biomaterials 2017, 114, 62–70. [PubMed: 27846403]

(255). Ji T; Zhao Y; Ding Y; Nie G Using functional nanomaterials to target and regulate the tumor microenvironment: Diagnostic and therapeutic applications. Adv. Mater. 2013, 25, 3508–3525. [PubMed: 23703805]

(256). Shapiro MG; Homma K; Villarreal S; Richter C-P; Bezanilla F Infrared light excites cells by changing their electrical capacitance. Nat. Commun 2012, 3, 736. [PubMed: 22415827]

(257). Eom K; Kim J; Choi JM; Kang T; Chang JW; Byun KM; Jun SB; Kim SJ Enhanced infrared neural stimulation using localized surface plasmon resonance of gold nanorods. Small 2014, 10, 3853–3857. [PubMed: 24975778]

(258). Chen R; Romero G; Christiansen MG; Mohr A; Anikeeva P Wireless magnetothermal deep brain stimulation. Science 2015, 347, 1477. [PubMed: 25765068]

(259). Cheng X; Sun R; Yin L; Chai Z; Shi H; Gao M Light-triggered assembly of gold nanoparticles for photothermal therapy and photoacoustic imaging of tumors in vivo. Adv. Mater. 2017, 29, DOI: 10.1002/adma.201604894.

(260). Tibbitt MW; Anseth KS Dynamic microenvironments: The fourth dimension. Sci. Transl. Med 2012, 4, 160ps124–160ps124.

(261). Cukierman E; Pankov R; Stevens DR; Yamada KM Taking cell-matrix adhesions to the third dimension. Science 2001, 294, 1708–1712. [PubMed: 11721053]

(262). Wolf K; Friedl P Extracellular matrix determinants of proteolytic and non-proteolytic cell migration. Trends Cell Biol 2011, 21, 736–744. [PubMed: 22036198]

(263). Even-Ram S; Yamada KM Cell migration in 3D matrix. Curr. Opin. Cell Biol 2005, 17, 524–532. [PubMed: 16112853]

(264). Bell SE; Mavila A; Salazar R; Bayless KJ; Kanagala S; Maxwell SA; Davis GE Differential gene expression during capillary morphogenesis in 3D collagen matrices. J. Cell Sci 2001, 114, 2755. [PubMed: 11683410]

(265). Wang F; Weaver VM; Petersen OW; Larabell CA; Dedhar S; Briand P; Lupu R; Bissell MJ Reciprocal interactions between β1-integrin and epidermal growth factor receptor in three-dimensional basement membrane breast cultures: A different perspective in epithelial biology. Proc. Natl. Acad. Sci. U.S.A 1998, 95, 14821–14826. [PubMed: 9843973]

(266). Weber LM; Lopez CG; Anseth KS Effects of PEG hydrogel crosslinking density on protein diffusion and encapsulated islet survival and function. J. Biomed. Mater. Res. A 2009, 90A, 720–729.

(267). Cruise GM; Scharp DS; Hubbell JA Characterization of permeability and network structure of interfacially photopolymerized poly(ethylene glycol) diacrylate hydrogels. Biomaterials 1998, 19, 1287–1294. [PubMed: 9720892]

(268). Xu J; Heys JJ; Barocas VH; Randolph TW Permeability and diffusion in vitreous humor: Implications for drug delivery. Pharm. Res 2000, 17, 664–669. [PubMed: 10955838]

(269). Zahir N; Weaver VM Death in the third dimension: apoptosis regulation and tissue architecture. Curr. Opin. Genet. Dev 2004, 14, 71–80. [PubMed: 15108808]

(270). Geckil H; Xu F; Zhang XH; Moon S; Utkan Demirci U Engineering hydrogels as extracellular matrix mimics. Nanomedicine 2010, 5, 469–484. [PubMed: 20394538]

(271). Schwartz MA; Chen CS Deconstructing dimensionality. Science 2013, 339, 402–404. [PubMed: 23349278]

(272). Rubashkin MG; Ou G; Weaver VM Deconstructing signaling in three dimensions. Biochemistry 2014, 53, 2078–2090. [PubMed: 24649923]

(273). Tokuda EY; Jones CE; Anseth KS PEG-peptide hydrogels reveal differential effects of matrix microenvironmental cues on melanoma drug sensitivity. Integr. Biol 2017, 9, 76–87.

(274). Benya PD; Shaffer JD Dedifferentiated chondrocytes reexpress the differentiated collagen phenotype when cultured in agarose gels. Cell 1982, 30, 215–224. [PubMed: 7127471]

(275). Petersen OW; Rønnov-Jessen L; Howlett AR; Bissell MJ Interaction with basement membrane serves to rapidly distinguish growth and differentiation pattern of normal and malignant human breast epithelial cells. Proc. Natl. Acad. Sci. U.S.A 1992, 89, 9064–9068. [PubMed: 1384042]

(276). Gu L; Mooney DJ Biomaterials and emerging anticancer therapeutics: engineering the microenvironment. Nat. Rev. Cancer 2016, 16, 56–66. [PubMed: 26694936]

(277). Vinci M; Gowan S; Boxall F; Patterson L; Zimmermann M; Court W; Lomas C; Mendiola M; Hardisson D; Eccles SA Advances in establishment and analysis of three-dimensional tumor spheroid-based functional assays for target validation and drug evaluation. BMC Biol 2012, 10, 29. [PubMed: 22439642]

(278). Mehta G; Hsiao AY; Ingram M; Luker GD; Takayama S Opportunities and challenges for use of tumor spheroids as models to test drug delivery and efficacy. J. Control. Release 2012, 164, 192–204. [PubMed: 22613880]

(279). Song H-HG; Park KM; Gerecht S Hydrogels to model 3D in vitro microenvironment of tumor vascularization. Adv. Drug Deliver. Rev 2014, 79–80, 19–29.

(280). Fong ELS; Lamhamedi-Cherradi S-E; Burdett E; Ramamoorthy V; Lazar AJ; Kasper FK; Farach-Carson MC; Vishwamitra D; Demicco EG; Menegaz BA; Amin HM; Mikos AG; Ludwig JA Modeling Ewing sarcoma tumors in vitro with 3D scaffolds. Proc. Natl. Acad. Sci. U.S.A 2013, 110, 6500–6505. [PubMed: 23576741]

(281). Hongisto V; Jernström S; Fey V; Mpindi J-P; Kleivi Sahlberg K; Kallioniemi O; Perälä M High-throughput 3D screening reveals differences in drug sensitivities between culture models of JIMT1 breast cancer cells. PLOS ONE 2013, 8, e77232. [PubMed: 24194875]

(282). Chambers KF; Mosaad EMO; Russell PJ; Clements JA; Doran MR 3D cultures of prostate cancer cells cultured in a novel high-throughput culture platform are more resistant to chemotherapeutics compared to cells cultured in monolayer. PLOS ONE 2014, 9, e111029. [PubMed: 25380249]

(283). Chelsea MM; Daniel LA; Kristi SA Bio-inspired 3D microenvironments: a new dimension in tissue engineering. Biomed. Mater. 2016, 11, 022001. [PubMed: 26942469]

(284). Caiazzo M; Okawa Y; Ranga A; Piersigilli A; Tabata Y; Lutolf MP Defined three-dimensional microenvironments boost induction of pluripotency. Nat. Mater. 2016, 15, 344–352. [PubMed: 26752655]

(285). Kim J; Hayward RC Mimicking dynamic in vivo environments with stimuli-responsive materials for cell culture. Trends Biotechnol 2012, 30, 426–439. [PubMed: 22658474]

(286). Higuchi A; Ling Q-D; Kumar SS; Chang Y; Kao T-C; Munusamy MA; Alarfaj AA; Hsu S-T; Umezawa A External stimulus-responsive biomaterials designed for the culture and differentiation of ES, iPS, and adult stem cells. Prog. Polym. Sci 2014, 39, 1585–1613.

(287). Yong KW; Li Y; Huang G; Lu TJ; Safwani WKZW; Pingguan-Murphy B; Xu F Mechano-regulation of cardiac myofibroblast differentiation: Implications for cardiac fibrosis and therapy. Am. J. Physiol. Heart. Circ. Physiol 2015, 309, H532–H542. [PubMed: 26092987]

(288). Genin GM; Abney TM; Wakatsuki T; Elson EL In Mechanobiology of Cell-Cell and Cell-Matrix Interactions; Wagoner Johnson A, Harley BAC, Eds.; Springer US: Boston, MA, 2011.

(289). Gao B; Yang Q; Zhao X; Jin G; Ma Y; Xu F 4D bioprinting for biomedical applications. Trends Biotechnol 2016, 34, 746–756. [PubMed: 27056447]

(290). Sydney Gladman A; Matsumoto EA; Nuzzo RG; Mahadevan L; Lewis JA Biomimetic 4D printing. Nat. Mater 2016, 15, 413–418. [PubMed: 26808461]

(291). Ge Q; Qi HJ; Dunn ML Active materials by four-dimension printing. Appl. Phys. Lett 2013, 103, 131901.

(292). Serwane F; Mongera A; Rowghanian P; Kealhofer DA; Lucio AA; Hockenbery ZM; Campas O In vivo quantification of spatially varying mechanical properties in developing tissues. Nat. Meth 2017, 14, 181–186.

(293). Qiu L; Zhang T; Jiang J; Wu C; Zhu G; You M; Chen X; Zhang L; Cui C; Yu R; Tan W Cell membrane-anchored biosensors for real-time monitoring of the cellular microenvironment. J. Am. Chem. Soc 2014, 136, 13090–13093. [PubMed: 25188419]

(294). Kuo CK; Smith ML Biomaterial design motivated by characterization of natural extracellular matrices. MRS Bull. 2014, 39, 18–24.

(295). Gattazzo F; Urciuolo A; Bonaldo P Extracellular matrix: A dynamic microenvironment for stem cell niche. BBA 2014, 1840, 2506–2519. [PubMed: 24418517]

(296). Huebsch N; Mooney DJ Inspiration and application in the evolution of biomaterials. Nature 2009, 462, 426–432. [PubMed: 19940912]

(297). Sanchez C; Arribart H; Giraud Guille MM Biomimetism and bioinspiration as tools for the design of innovative materials and systems. Nat. Mater. 2005, 4, 277–288. [PubMed: 15875305]

(298). Wade RJ; Burdick JA Engineering ECM signals into biomaterials. Mater. Today 2012, 15, 454–459.

(299). Choi CK; Breckenridge MT; Chen CS Engineered materials and the cellular microenvironment: a strengthening interface between cell biology and bioengineering. Trends Cell Biol 2010, 20, 705–714. [PubMed: 20965727]

(300). Kyburz K; Anseth K Synthetic mimics of the extracellular matrix: How simple is complex enough? Ann. Biomed. Eng 2015, 43, 489–500. [PubMed: 25753017]

(301). Gjorevski N; Ranga A; Lutolf MP Bioengineering approaches to guide stem cell-based organogenesis. Development 2014, 141, 1794–1804. [PubMed: 24757002]

(302). Edalat F; Sheu I; Manoucheri S; Khademhosseini A Material strategies for creating artificial cell-instructive niches. Curr. Opin. Biotech 2012, 23, 820–825. [PubMed: 22705446]

(303). Yao X; Peng R; Ding J Cell–material interactions revealed via material techniques of surface patterning. Adv. Mater. 2013, 25, 5257–5286. [PubMed: 24038153]

(304). Ma PX Biomimetic materials for tissue engineering. Adv. Drug Deliver. Rev 2008, 60, 184–198.

(305). Aizenberg J; Fratzl P Biological and biomimetic materials. Adv. Mater. 2009, 21, 387–388.

(306). Fisher OZ; Khademhosseini A; Langer R; Peppas NA Bioinspired materials for controlling stem cell fate. Acc. Chem. Res 2010, 43, 419–428. [PubMed: 20043634]

(307). Kushner AM; Guan Z Modular design in natural and biomimetic soft materials. Angew. Chem. Int. Edit 2011, 50, 9026–9057.

(308). Holzapfel BM; Reichert JC; Schantz J-T; Gbureck U; Rackwitz L; Nöth U; Jakob F; Rudert M; Groll J; Hutmacher DW How smart do biomaterials need to be? A translational science and clinical point of view. Adv. Drug Deliver. Rev 2013, 65, 581–603.

(309). Balakrishnan B; Banerjee R Biopolymer-based hydrogels for cartilage tissue engineering. Chem. Rev 2011, 111, 4453–4474. [PubMed: 21417222]

(310). Sands RW; Mooney DJ Polymers to direct cell fate by controlling the microenvironment. Curr. Opin. Biotech 2007, 18, 448–453. [PubMed: 18024105]

(311). Caliari SR; Burdick JA A practical guide to hydrogels for cell culture. Nat. Meth 2016, 13, 405–414.

(312). Deforest CA; Anseth KS Advances in bioactive hydrogels to probe and direct cell fate. Annu. Rev. Chem. Biomol 2012, 3, 421–424.

(313). Serrano MC; Chung EJ; Ameer GA Advances and applications of biodegradable elastomers in regenerative medicine. Adv. Func. Mater. 2010, 20, 192–208.

(314). Ulery BD; Nair LS; Laurencin CT Biomedical applications of biodegradable polymers. J. Polym. Sci. Polym. Phys 2011, 49, 832–864.

(315). Frydrych M; Román S; MacNeil S; Chen B Biomimetic poly(glycerol sebacate)/poly(l-lactic acid) blend scaffolds for adipose tissue engineering. Acta Biomater 2015, 18, 40–49. [PubMed: 25769230]

(316). Hsu S.-h.; Hung K-C; Chen C-W Biodegradable polymer scaffolds. J. Mater. Chem. B 2016, 4, 7493–7505.

(317). Place ES; George JH; Williams CK; Stevens MM Synthetic polymer scaffolds for tissue engineering. Chem. Soc. Rev 2009, 38, 1139–1151. [PubMed: 19421585]

(318). Lluch AV; Cruz DMG; Luis J; Ivirico E; Ramos CM; Pradas MM Polymers as materials for tissue engineering scaffolds. Polymers in Regenerative Medicine: Biomedical Applications from Nano-to Macro-Structures 2015, 1–47.

(319). Damodaran VB; Bhatnagar D; Murthy NS Biomedical polymers : Synthesis and processing; Springer: Switzerland, 2016.

(320). Nair LS; Laurencin CT Biodegradable polymers as biomaterials. Prog. Polym. Sci 2007, 32, 762–798.

(321). Faulk DM; Johnson SA; Zhang L; Badylak SF Role of the extracellular matrix in whole organ engineering. J. Cell Physiol 2014, 229, 984–989. [PubMed: 24347365]

(322). Aamodt JM; Grainger DW Extracellular matrix-based biomaterial scaffolds and the host response. Biomaterials 2016, 86, 68–82. [PubMed: 26890039]

(323). Gaetani R; Yin C; Srikumar N; Braden R; Doevendans PA; Sluijter JPG; Christman KL Cardiac-derived extracellular matrix enhances cardiogenic properties of human cardiac progenitor cells. Cell Transplant 2016, 25, 1653–1663. [PubMed: 26572770]

(324). Wolf MT; Daly KA; Brennan-Pierce EP; Johnson SA; Carruthers CA; D'Amore A; Nagarkar SP; Velankar SS; Badylak SF A hydrogel derived from decellularized dermal extracellular matrix. Biomaterials 2012, 33, 7028–7038. [PubMed: 22789723]

(325). Uygun BE; Soto-Gutierrez A; Yagi H; Izamis M-L; Guzzardi MA; Shulman C; Milwid J; Kobayashi N; Tilles A; Berthiaume F; Hertl M; Nahmias Y; Yarmush ML; Uygun K Organ reengineering through development of a transplantable recellularized liver graft using decellularized liver matrix. Nat. Meth 2010, 16, 814–820.

(326). Petersen TH; Calle EA; Zhao L; Lee EJ; Gui L; Raredon MB; Gavrilov K; Yi T; Zhuang ZW; Breuer C; Herzog E; Niklason LE Tissue-engineered lungs for in vivo implantation. Science 2010, 329, 538–541. [PubMed: 20576850]

(327). O'Neill JD; Freytes DO; Anandappa AJ; Oliver JA; Vunjak-Novakovic GV The regulation of growth and metabolism of kidney stem cells with regional specificity using extracellular matrix derived from kidney. Biomaterials 2013, 34, 9830–9841. [PubMed: 24074840]

(328). DeQuach JA; Lin JE; Cam C; Hu D; Salvatore MA; Sheikh F; Christman KL In Eur. Cells Mater., 2012; Vol. 23.

(329). Yin Z; Chen X; Zhu T; Hu J.-j.; Song H.-x.; Shen W.-l.; Jiang L.-y.; Heng BC; Ji J.-f.; Ouyang H-W The effect of decellularized matrices on human tendon stem/progenitor cell differentiation and tendon repair. Acta Biomater 2013, 9, 9317–9329. [PubMed: 23896565]

(330). Yang Q; Peng J; Guo Q; Huang J; Zhang L; Yao J; Yang F; Wang S; Xu W; Wang A A cartilage ECM-derived 3-D porous acellular matrix scaffold for in vivo cartilage tissue engineering with PKH26-labeled chondrogenic bone marrow-derived mesenchymal stem cells. Biomaterials 2008, 29, 2378–2387. [PubMed: 18313139]

(331). Hoganson DM; O'Doherty EM; Owens GE; Harilal DO; Goldman SM; Bowley CM; Neville CM; Kronengold RT; Vacanti JP The retention of extracellular matrix proteins and angiogenic and mitogenic cytokines in a decellularized porcine dermis. Biomaterials 2010, 31, 6730–6737. [PubMed: 20576289]

(332). Freytes DO; Martin J; Velankar SS; Lee AS; Badylak SF Preparation and rheological characterization of a gel form of the porcine urinary bladder matrix. Biomaterials 2008, 29, 1630–1637. [PubMed: 18201760]

(333). Cheung HK; Han TTY; Marecak DM; Watkins JF; Amsden BG; Flynn LE Composite hydrogel scaffolds incorporating decellularized adipose tissue for soft tissue engineering with adipose-derived stem cells. Biomaterials 2014, 35, 1914–1923. [PubMed: 24331712]

(334). Crapo PM; Medberry CJ; Reing JE; Tottey S; van der Merwe Y; Jones KE; Badylak SF Biologic scaffolds composed of central nervous system extracellular matrix. Biomaterials 2012, 33, 3539–3547. [PubMed: 22341938]

(335). Chen F-M; Liu X Advancing biomaterials of human origin for tissue engineering. Prog. Polym. Sci 2016, 53, 83–168.

(336). Perez-Castillejos R Replication of the 3D architecture of tissues. Mater. Today 2010, 13, 32–41.

(337). Ott HC; Matthiesen TS; Goh SK; Black LD; Kren SM; Netoff TI; Taylor DA Perfusion-decellularized matrix: Using nature's platform to engineer a bioartificial heart. Nat. Med 2008, 14, 213–221. [PubMed: 18193059]

(338). Grayson WL; Fröhlich M; Yeager K; Bhumiratana S; Chan ME; Cannizzaro C; Wan LQ; Liu XS; Guo XE; Vunjak-Novakovic G Engineering anatomically shaped human bone grafts. Proc. Natl. Acad. Sci. U.S.A 2010, 107, 3299–3304. [PubMed: 19820164]

(339). Quint C; Kondo Y; Manson RJ; Lawson JH; Dardik A; Niklason LE Decellularized tissue-engineered blood vessel as an arterial conduit. Proc. Natl. Acad. Sci. U.S.A 2011, 108, 9214–9219. [PubMed: 21571635]

(340). Saldin LT; Cramer MC; Velankar SS; White LJ; Badylak SF Extracellular matrix hydrogels from decellularized tissues: Structure and function. Acta Biomater 2017, 49, 1–15. [PubMed: 27915024]

(341). Jhala D; Vasita R A review on extracellular matrix mimicking strategies for an artificial stem cell niche. Polym. Rev 2015, 55, 561–595.

(342). Wolf MT; Dearth CL; Sonnenberg SB; Loboa EG; Badylak SF Naturally derived and synthetic scaffolds for skeletal muscle reconstruction. Adv. Drug Deliver. Rev 2015, 84, 208–221.

(343). Caliari SR; Burdick JA A practical guide to hydrogels for cell culture. Nat. Meth 2016, 13, 405–414.

(344). Buehler MJ; Yung YC Deformation and failure of protein materials in physiologically extreme conditions and disease. Nat. Mater. 2009, 8, 175–188. [PubMed: 19229265]

(345). Kim U-J; Park J; Li C; Jin H-J; Valluzzi R; Kaplan DL Structure and properties of silk hydrogels. Biomacromolecules 2004, 5, 786–792. [PubMed: 15132662]

(346). Huang G; Tian L; Liu K-K; Hu B; Xu F; Lu TJ; Naik RR; Singamaneni S Elastoplastic deformation of silk micro- and nanostructures. ACS Biomater. Sci. Eng 2016, 2, 893–899.

(347). Pryse KM; Nekouzadeh A; Genin GM; Elson EL; Zahalak GI Incremental mechanics of collagen gels: New experiments and a new viscoelastic model. Ann. Biomed. Eng 2003, 31, 1287–1296. [PubMed: 14649502]

(348). Genin G; Elson E In Cell and Matrix Mechanics; CRC Press, 2014.

(349). Shafiq M; Jung Y; Kim SH Insight on stem cell preconditioning and instructive biomaterials to enhance cell adhesion, retention, and engraftment for tissue repair. Biomaterials 2016, 90, 85–115. [PubMed: 27016619]

(350). Diekjürgen D; Grainger DW Polysaccharide matrices used in 3D in vitro cell culture systems. Biomaterials 2017, 141, 96–115. [PubMed: 28672214]

(351). Rowley JA; Madlambayan G; Mooney DJ Alginate hydrogels as synthetic extracellular matrix materials. Biomaterials 1999, 20, 45–53. [PubMed: 9916770]

(352). Pawar SN; Edgar KJ Alginate derivatization: A review of chemistry, properties and applications. Biomaterials 2012, 33, 3279–3305. [PubMed: 22281421]

(353). Zhang Y-N; Avery RK; Vallmajo-Martin Q; Assmann A; Vegh A; Memic A; Olsen BD; Annabi N; Khademhosseini A A highly elastic and rapidly crosslinkable elastin-like polypeptide-based hydrogel for biomedical applications. Adv. Func. Mater. 2015, 25, 4814–4826.

(354). Klotz BJ; Gawlitta D; Rosenberg AJWP; Malda J; Melchels FPW Gelatin-methacryloyl hydrogels: Towards biofabrication-based tissue repair. Trends Biotechnol 2016, 34, 394–407. [PubMed: 26867787]

(355). Liu ZQ; Wei Z; Zhu XL; Huang GY; Xu F; Yang JH; Osada Y; Zrínyi M; Li JH; Chen YM Dextran-based hydrogel formed by thiol-Michael addition reaction for 3D cell encapsulation. Colloids and Surfaces B: Biointerfaces 2015, 128, 140–148. [PubMed: 25744162]

(356). Yue K; Trujillo-de Santiago G; Alvarez MM; Tamayol A; Annabi N; Khademhosseini A Synthesis, properties, and biomedical applications of gelatin methacryloyl (GelMA) hydrogels. Biomaterials 2015, 73, 254–271. [PubMed: 26414409]

(357). Lutolf MP; Hubbell JA Synthetic biomaterials as instructive extracellular microenvironments for morphogenesis in tissue engineering. Nat. Biotechnol 2005, 23, 47–55. [PubMed: 15637621]

(358). Feng Q; Wei K; Lin S; Xu Z; Sun Y; Shi P; Li G; Bian L Mechanically resilient, injectable, and bioadhesive supramolecular gelatin hydrogels crosslinked by weak host-guest interactions assist cell infiltration and in situ tissue regeneration. Biomaterials 2016, 101, 217–228. [PubMed: 27294539]

(359). Rice JJ; Martino MM; De Laporte L; Tortelli F; Briquez PS; Hubbell JA Engineering the regenerative microenvironment with biomaterials. Adv. Healthc. Mater. 2013, 2, 57–71. [PubMed: 23184739]

(360). Zhu JM Bioactive modification of poly(ethylene glycol) hydrogels for tissue engineering. Biomaterials 2010, 31, 4639–4656. [PubMed: 20303169]

(361). Liu SQ; Tay R; Khan M; Rachel Ee PL; Hedrick JL; Yang YY Synthetic hydrogels for controlled stem cell differentiation. Soft Matter 2010, 6, 67–81.

(362). Gjorevski N; Sachs N; Manfrin A; Giger S; Bragina ME; Ordóñez-Morán P; Clevers H; Lutolf MP Designer matrices for intestinal stem cell and organoid culture. Nature 2016, 539, 560–564. [PubMed: 27851739]

(363). Du X; Zhou J; Shi J; Xu B Supramolecular hydrogelators and hydrogels: From soft matter to molecular biomaterials. Chem. Rev 2015, 115, 13165–13307. [PubMed: 26646318]

(364). Highley CB; Rodell CB; Burdick JA Direct 3D printing of shear-thinning hydrogels into self-healing hydrogels. Adv. Mater. 2015, 27, 5075–5079. [PubMed: 26177925]

(365). Dou X-Q; Feng C-L Amino acids and peptide-based supramolecular hydrogels for three-dimensional cell culture. Adv. Mater. 2017, DOI: 10.1002/adma.201604062.

(366). De Leon-Rodriguez LM; Hemar Y; Mo G; Mitra AK; Cornish J; Brimble MA Multifunctional thermoresponsive designer peptide hydrogels. Acta Biomater 2017, 47, 40–49. [PubMed: 27744067]

(367). Smith KH; Tejeda-Montes E; Poch M; Mata A Integrating top-down and self-assembly in the fabrication of peptide and protein-based biomedical materials. Chem. Soc. Rev 2011, 40, 4563–4577. [PubMed: 21629920]

(368). Collier JH; Rudra JS; Gasiorowski JZ; Jung JP Multi-component extracellular matrices based on peptide self-assembly. Chem. Soc. Rev 2010, 39, 3413–3424. [PubMed: 20603663]

(369). Capito RM; Azevedo HS; Velichko YS; Mata A; Stupp SI Self-assembly of large and small molecules into hierarchically ordered sacs and membranes. Science 2008, 319, 1812–1816. [PubMed: 18369143]

(370). Hauser CAE; Zhang S Designer self-assembling peptide nanofiber biological materials. Chem. Soc. Rev 2010, 39, 2780–2790. [PubMed: 20520907]

(371). O'Leary LER; Fallas JA; Bakota EL; Kang MK; Hartgerink JD Multi-hierarchical self-assembly of a collagen mimetic peptide from triple helix to nanofibre and hydrogel. Nat. Chem 2011, 3, 821–828. [PubMed: 21941256]

(372). Pugliese R; Gelain F Peptidic biomaterials: From self-assembling to regenerative medicine. Trends Biotechnol 2017, 35, 145–158. [PubMed: 27717599]

(373). Castillo Diaz LA; Saiani A; Gough JE; Miller AF Human osteoblasts within soft peptide hydrogels promote mineralisation in vitro. J. Tissue Eng 2014, 5, 2041731414539344. [PubMed: 25383164]

(374). Webber MJ; Appel EA; Meijer EW; Langer R Supramolecular biomaterials. Nat. Mater. 2016, 15, 13–26. [PubMed: 26681596]

(375). Voorhaar L; Hoogenboom R Supramolecular polymer networks: hydrogels and bulk materials. Chem. Soc. Rev 2016, 45, 4013–4031. [PubMed: 27206244]

(376). Visser J; Melchels FPW; Jeon JE; van Bussel EM; Kimpton LS; Byrne HM; Dhert WJA; Dalton PD; Hutmacher DW; Malda J Reinforcement of hydrogels using three-dimensionally printed microfibres. Nat. Commun 2015, 6, 6933. [PubMed: 25917746]

(377). Chaudhuri O; Koshy ST; Branco da Cunha C; Shin J-W; Verbeke CS; Allison KH; Mooney DJ Extracellular matrix stiffness and composition jointly regulate the induction of malignant phenotypes in mammary epithelium. Nat. Mater. 2014, 13, 970–978. [PubMed: 24930031]

(378). Sun W; Xue B; Li Y; Qin M; Wu J; Lu K; Wu J; Cao Y; Jiang Q; Wang W Polymer-supramolecular polymer double-network hydrogel. Adv. Func. Mater. 2016, 26, 9044–9052.

(379). Daniele MA; Adams AA; Naciri J; North SH; Ligler FS Interpenetrating networks based on gelatin methacrylamide and PEG formed using concurrent thiol click chemistries for hydrogel tissue engineering scaffolds. Biomaterials 2014, 35, 1845–1856. [PubMed: 24314597]

(380). Branco da Cunha C; Klumpers DD; Li WA; Koshy ST; Weaver JC; Chaudhuri O; Granja PL; Mooney DJ Influence of the stiffness of three-dimensional alginate/collagen-I interpenetrating networks on fibroblast biology. Biomaterials 2014, 35, 8927–8936. [PubMed: 25047628]

(381). Khavari A; Nydén M; Weitz DA; Ehrlicher AJ Composite alginate gels for tunable cellular microenvironment mechanics. Sci. Rep 2016, 6, 30854. [PubMed: 27484403]

(382). Munoz-Pinto DJ; Jimenez-Vergara AC; Gharat TP; Hahn MS Characterization of sequential collagen-poly(ethylene glycol) diacrylate interpenetrating networks and initial assessment of their potential for vascular tissue engineering. Biomaterials 2015, 40, 32–42. [PubMed: 25433604]

(383). Chan BK; Wippich CC; Wu CJ; Sivasankar PM; Schmidt G Robust and Semi-Interpenetrating Hydrogels from Poly(ethylene glycol) and Collagen for Elastomeric Tissue Scaffolds. Macromol Biosci 2012, 12, 1490–1501. [PubMed: 23070957]

(384). Hong S; Sycks D; Chan HF; Lin S; Lopez GP; Guilak F; Leong KW; Zhao X 3D printing of highly stretchable and tough hydrogels into complex, cellularized structures. Adv. Mater. 2015, 27, 4035–4040. [PubMed: 26033288]

(385). Zeng Y; Chen C; Liu W; Fu Q; Han Z; Li Y; Feng S; Li X; Qi C; Wu J; Wang D; Corbett C; Chan BP; Ruan D; Du Y Injectable microcryogels reinforced alginate encapsulation of mesenchymal stromal cells for leak-proof delivery and alleviation of canine disc degeneration. Biomaterials 2015, 59, 53–65. [PubMed: 25956851]

(386). Hu C; Wang MX; Sun L; Yang JH; Zrínyi M; Chen YM Dual-physical cross-linked tough and photoluminescent hydrogels with good biocompatibility and antibacterial activity. Macromol. Rapid Comm 2017, 38, 1600788.

(387). Zheng WJ; An N; Yang JH; Zhou J; Chen YM Tough Al-alginate/poly(N-isopropylacrylamide) hydrogel with tunable LCST for soft robotics. ACS Appl. Mater. Inter 2015, 7, 1758–1764.

(388). Sun JY; Zhao X; Illeperuma WRK; Chaudhuri O; Oh KH; Mooney DJ; Vlassak JJ; Suo Z Highly stretchable and tough hydrogels. Nature 2012, 489, 133–136. [PubMed: 22955625]

(389). Li J; Illeperuma WRK; Suo Z; Vlassak JJ Hybrid hydrogels with extremely high stiffness and toughness. ACS Macro Lett 2014, 3, 520–523.

(390). Yang CH; Wang MX; Haider H; Yang JH; Sun J-Y; Chen YM; Zhou J; Suo Z Strengthening alginate/polyacrylamide hydrogels using various multivalent cations. ACS Appl. Mater. Inter 2013, 5, 10418–10422.

(391). Mehrali M; Thakur A; Pennisi CP; Talebian S; Arpanaei A; Nikkhah M; Dolatshahi-Pirouz A Nanoreinforced hydrogels for tissue engineering: Biomaterials that are compatible with load-bearing and electroactive tissues. Adv. Mater. 2017, 29, DOI: 10.1002/adma.201603612.

(392). Lipner J; Boyle JJ; Xia Y; Birman V; Genin GM; Thomopoulos S Toughening of fibrous scaffolds by mobile mineral deposits. Acta Biomater 2017, 58, 492–501. [PubMed: 28532898]

(393). Katsamenis OL; Jenkins T; Thurner PJ Toughness and damage susceptibility in human cortical bone is proportional to mechanical inhomogeneity at the osteonal-level. Bone 2015, 76, 158–168. [PubMed: 25863123]

(394). Markus JB Molecular nanomechanics of nascent bone: Fibrillar toughening by mineralization. Nanotechnology 2007, 18, 295102.

(395). Aminzare M; Eskandari A; Baroonian M; Berenov A; Hesabi ZR; Taheri M; Sadrnezhaad S Hydroxyapatite nanocomposites: Synthesis, sintering and mechanical properties. Ceram. Int 2013, 39, 2197–2206.

(396). Heinemann S; Heinemann C; Wenisch S; Alt V; Worch H; Hanke T Calcium phosphate phases integrated in silica/collagen nanocomposite xerogels enhance the bioactivity and ultimately manipulate the osteoblast/osteoclast ratio in a human co-culture model. Acta Biomater 2013, 9, 4878–4888. [PubMed: 23072829]

(397). Mishra AK; Bose S; Kuila T; Kim NH; Lee JH Silicate-based polymer-nanocomposite membranes for polymer electrolyte membrane fuel cells. Prog. Polym. Sci 2012, 37, 842–869.

(398). Thakur A; Jaiswal MK; Peak CW; Carrow JK; Gentry J; Dolatshahi-Pirouz A; Gaharwar AK Injectable shear-thinning nanoengineered hydrogels for stem cell delivery. Nanoscale 2016, 8, 12362–12372. [PubMed: 27270567]

(399). Shi J; Yu X; Wang L; Liu Y; Gao J; Zhang J; Ma R; Liu R; Zhang Z PEGylated fullerene/iron oxide nanocomposites for photodynamic therapy, targeted drug delivery and MR imaging. Biomaterials 2013, 34, 9666–9677. [PubMed: 24034498]

(400). Skardal A; Zhang J; McCoard L; Oottamasathien S; Prestwich GD Dynamically crosslinked gold nanoparticle – hyaluronan hydrogels. Adv. Mater. 2010, 22, 4736–4740. [PubMed: 20730818]

(401). Baranes K; Shevach M; Shefi O; Dvir T Gold nanoparticle-decorated scaffolds promote neuronal differentiation and maturation. Nano lett 2016, 16, 2916–2920. [PubMed: 26674672]

(402). Jaiswal MK; Xavier JR; Carrow JK; Desai P; Alge D; Gaharwar AK Mechanically stiff nanocomposite hydrogels at ultralow nanoparticle content. ACS Nano 2016, 10, 246–256. [PubMed: 26670176]

(403). Song J; Zhang P; Cheng L; Liao Y; Xu B; Bao R; Wang W; Liu W Nano-silver in situ hybridized collagen scaffolds for regeneration of infected full-thickness burn skin. J. Mater. Chem. B 2015, 3, 4231–4241.

(404). Qu Y; Chu BY; Peng JR; Liao JF; Qi TT; Shi K; Zhang XN; Wei YQ; Qian ZY A biodegradable thermo-responsive hybrid hydrogel: therapeutic applications in preventing the post-operative recurrence of breast cancer. NPG Asia Mater. 2015, 7, e207.

(405). Zhao H; Ji X; Wang B; Wang N; Li X; Ni R; Ren J An ultra-sensitive acetylcholinesterase biosensor based on reduced graphene oxide-Au nanoparticles-β-cyclodextrin/Prussian blue-chitosan nanocomposites for organophosphorus pesticides detection. Biosens. Bioelectron 2015, 65, 23–30. [PubMed: 25461134]

(406). Benhadjala W; Gravoueille M; Bord-Majek I; Bechou L; Suhir E; Buet M; Louarn M; Weiss M; Rougé F; Gaud V Inorganic/organic nanocomposites: Reaching a high filler content without increasing viscosity using core-shell structured nanoparticles. Appl. Phys. Lett 2015, 107, 211903.

(407). Tjong SC Recent progress in the development and properties of novel metal matrix nanocomposites reinforced with carbon nanotubes and graphene nanosheets. Mater. Sci. Eng. R Rep 2013, 74, 281–350.

(408). Zhu J; Chen M; He Q; Shao L; Wei S; Guo Z An overview of the engineered graphene nanostructures and nanocomposites. RSC Adv 2013, 3, 22790–22824.

(409). Sun H; Tang J; Mou Y; Zhou J; Qu L; Duval K; Huang Z; Lin N; Dai R; Liang C; Chen Z; Tang L; Tian F Carbon nanotube-composite hydrogels promote intercalated disc assembly in engineered cardiac tissues through β1-integrin mediated FAK and RhoA pathway. Acta Biomater 2017, 48, 88–99. [PubMed: 27769942]

(410). Thoniyot P; Tan MJ; Karim AA; Young DJ; Loh XJ Nanoparticle–hydrogel composites: Concept, design, and applications of these promising, multi-functional materials. Adv. Sci 2015, 2, DOI: 10.1002/advs.201400010.

(411). Haider H; Yang CH; Zheng WJ; Yang JH; Wang MX; Yang S; Zrinyi M; Osada Y; Suo Z; Zhang Q; Zhou J; Chen YM Exceptionally tough and notch-insensitive magnetic hydrogels. Soft Matter 2015, 11, 8253–8261. [PubMed: 26350404]

(412). Campbell SB; Hoare T Externally addressable hydrogel nanocomposites for biomedical applications. Curr. Opin. Chem. Eng 2014, 4, 1–10.

(413). Dvir T; Timko BP; Kohane DS; Langer R Nanotechnological strategies for engineering complex tissues. Nat. Nanotechnol 2011, 6, 13–22. [PubMed: 21151110]

(414). Custódio CA; Reis RL; Mano JF Engineering biomolecular microenvironments for cell instructive biomaterials. Adv. Healthc. Mater. 2014, 3, 797–810. [PubMed: 24464880]

(415). Moon JJ; Saik JE; Poché RA; Leslie-Barbick JE; Lee S-H; Smith AA; Dickinson ME; West JL Biomimetic hydrogels with pro-angiogenic properties. Biomaterials 2010, 31, 3840–3847. [PubMed: 20185173]

(416). Li H; Wen F; Chen H; Pal M; Lai Y; Zhao AZ; Tan LP Micropatterning extracellular matrix proteins on electrospun fibrous substrate promote human mesenchymal stem cell differentiation toward neurogenic lineage. ACS Appl. Mater. Inter 2016, 8, 563–573.

(417). Vega L JCM; Lee MK; Qin EC; Rich M; Lee KY; Kim DH; Chung HJ; Leckband DE; Kong H Three dimensional conjugation of recombinant N-cadherin to a hydrogel for in vitro anisotropic neural growth. J. Mater. Chem. B 2016, 4, 6803–6811. [PubMed: 28503305]

(418). DeForest CA; Tirrell DA A photoreversible protein-patterning approach for guiding stem cell fate in three-dimensional gels. Nat. Mater. 2015, 14, 523–531. [PubMed: 25707020]

(419). Lai Y; Xie C; Zhang Z; Lu W; Ding J Design and synthesis of a potent peptide containing both specific and non-specific cell-adhesion motifs. Biomaterials 2010, 31, 4809–4817. [PubMed: 20346502]

(420). Ruoslahti E RGD and other recognition sequences for integrins. Annu. Rev. Cell Dev. Bi 1996, 12, 697–715.

(421). Chen CS; Mrksich M; Huang S; Whitesides GM; Ingber DE Geometric control of cell life and death. Science 1997, 276, 1425–1428. [PubMed: 9162012]

(422). Lee KY; Alsberg E; Hsiong S; Comisar W; Linderman J; Ziff R; Mooney D Nanoscale adhesion ligand organization regulates osteoblast proliferation and differentiation. Nano lett 2004, 4, 1501–1506. [PubMed: 25067913]

(423). Xia N; Thodeti CK; Hunt TP; Xu Q; Ho M; Whitesides GM; Westervelt R; Ingber DE Directional control of cell motility through focal adhesion positioning and spatial control of Rac activation. Faseb J. 2008, 22, 1649–1659. [PubMed: 18180334]

(424). Kilian KA; Mrksich M Directing stem cell fate by controlling the affinity and density of ligand–receptor interactions at the biomaterials interface. Angew. Chem. Int. Edit 2012, 51, 4891–4895.

(425). Lee J; Abdeen AA; Zhang D; Kilian KA Directing stem cell fate on hydrogel substrates by controlling cell geometry, matrix mechanics and adhesion ligand composition. Biomaterials 2013, 34, 8140–8148. [PubMed: 23932245]

(426). Wang X; Yan C; Ye K; He Y; Li Z; Ding J Effect of RGD nanospacing on differentiation of stem cells. Biomaterials 2013, 34, 2865–2874. [PubMed: 23357372]

(427). McBeath R; Pirone DM; Nelson CM; Bhadriraju K; Chen CS Cell shape, cytoskeletal tension, and rhoa regulate stem cell lineage commitment. Dev. Cell 2004, 6, 483–495. [PubMed: 15068789]

(428). Kilian KA; Bugarija B; Lahn BT; Mrksich M Geometric cues for directing the differentiation of mesenchymal stem cells. Proc. Natl. Acad. Sci. U.S.A 2010, 107, 4872–4877. [PubMed: 20194780]

(429). Peng R; Yao X; Ding J Effect of cell anisotropy on differentiation of stem cells on micropatterned surfaces through the controlled single cell adhesion. Biomaterials 2011, 32, 8048–8057. [PubMed: 21810538]

(430). Li W; Wang J; Ren J; Qu X Endogenous signalling control of cell adhesion by using aptamer functionalized biocompatible hydrogel. Chem. Sci 2015, 6, 6762–6768. [PubMed: 28757967]

(431). Weis S; Lee TT; del Campo A; García AJ Dynamic cell-adhesive microenvironments and their effect on myogenic differentiation. Acta Biomater 2013, 9, 8059–8066. [PubMed: 23791677]

(432). Hern DL; Hubbell JA Incorporation of adhesion peptides into nonadhesive hydrogels useful for tissue resurfacing. J. Biomed. Mater. Res 1998, 39, 266–276. [PubMed: 9457557]

(433). Burdick JA; Anseth KS Photoencapsulation of osteoblasts in injectable RGD-modified PEG hydrogels for bone tissue engineering. Biomaterials 2002, 23, 4315–4323. [PubMed: 12219821]

(434). Salinas CN; Anseth KS Mixed mode thiol–acrylate photopolymerizations for the synthesis of PEG–peptide hydrogels. Macromolecules 2008, 41, 6019–6026.

(435). Lutolf MP; Tirelli N; Cerritelli S; Cavalli L; Hubbell JA Systematic modulation of michael-type reactivity of thiols through the use of charged amino acids. Bioconjugate Chem 2001, 12, 1051–1056.

(436). Miller JS; Shen CJ; Legant WR; Baranski JD; Blakely BL; Chen CS Bioactive hydrogels made from step-growth derived PEG–peptide macromers. Biomaterials 2010, 31, 3736–3743. [PubMed: 20138664]

(437). Lutolf MP; Hubbell JA Synthesis and physicochemical characterization of end-linked poly(ethylene glycol)-co-peptide hydrogels formed by michael-type addition. Biomacromolecules 2003, 4, 713–722. [PubMed: 12741789]

(438). Fairbanks BD; Schwartz MP; Halevi AE; Nuttelman CR; Bowman CN; Anseth KS A Versatile synthetic extracellular matrix mimic via thiol-norbornene photopolymerization. Adv. Mater. 2009, 21, 5005–5010. [PubMed: 25377720]

(439). Sapir Y; Kryukov O; Cohen S Integration of multiple cell-matrix interactions into alginate scaffolds for promoting cardiac tissue regeneration. Biomaterials 2011, 32, 1838–1847. [PubMed: 21112626]

(440). Shachar M; Tsur-Gang O; Dvir T; Leor J; Cohen S The effect of immobilized RGD peptide in alginate scaffolds on cardiac tissue engineering. Acta Biomater 2011, 7, 152–162. [PubMed: 20688198]

(441). Bian L; Guvendiren M; Mauck RL; Burdick JA Hydrogels that mimic developmentally relevant matrix and N-cadherin interactions enhance MSC chondrogenesis. Proc. Natl. Acad. Sci. U.S.A 2013, 110, 10117–10122. [PubMed: 23733927]

(442). Taubenberger AV; Bray LJ; Haller B; Shaposhnykov A; Binner M; Freudenberg U; Guck J; Werner C 3D extracellular matrix interactions modulate tumour cell growth, invasion and angiogenesis in engineered tumour microenvironments. Acta Biomater 2016, 36, 73–85. [PubMed: 26971667]

(443). Kirschner CM; Anseth KS Hydrogels in healthcare: From static to dynamic material microenvironments. Acta Mater. 2013, 61, 931–944. [PubMed: 23929381]

(444). Lee MK; Rich MH; Lee J; Kong H A bio-inspired, microchanneled hydrogel with controlled spacing of cell adhesion ligands regulates 3D spatial organization of cells and tissue. Biomaterials 2015, 58, 26–34. [PubMed: 25941779]

(445). Lam J; Segura T The modulation of MSC integrin expression by RGD presentation. Biomaterials 2013, 34, 3938–3947. [PubMed: 23465825]

(446). Brinkmann J; Cavatorta E; Sankaran S; Schmidt B; van Weerd J; Jonkheijm P About supramolecular systems for dynamically probing cells. Chem. Soc. Rev 2014, 43, 4449–4469. [PubMed: 24681633]

(447). Luo Y; Shoichet MS A photolabile hydrogel for guided three-dimensional cell growth and migration. Nat. Mater. 2004, 3, 249–253. [PubMed: 15034559]

(448). Wosnick JH; Shoichet MS Three-dimensional chemical patterning of transparent hydrogels. Chem. Mater. 2008, 20, 55–60.

(449). Jungnickel C; Tsurkan MV; Wogan K; Werner C; Schlierf M Bottom-up structuring and site-selective modification of hydrogels using a two-photon [2+2] cycloaddition of maleimide. Adv. Mater. 2016, 29, DOI: 10.1002/adma.201603327.

(450). Torgersen J; Qin X-H; Li Z; Ovsianikov A; Liska R; Stampfl J Hydrogels for two-photon polymerization: A toolbox for mimicking the extracellular matrix. Adv. Func. Mater. 2013, 23, 4542–4554.

(451). Hahn MS; Miller JS; West JL Three-dimensional biochemical and biomechanical patterning of hydrogels for guiding cell behavior. Adv. Mater. 2006, 18, 2679–2684.

(452). Lee S-H; Moon JJ; West JL Three-dimensional micropatterning of bioactive hydrogels via two-photon laser scanning photolithography for guided 3D cell migration. Biomaterials 2008, 29, 2962–2968. [PubMed: 18433863]

(453). Hoffmann JC; West JL Three-dimensional photolithographic patterning of multiple bioactive ligands in poly(ethylene glycol) hydrogels. Soft Matter 2010, 6, 5056–5063.

(454). Culver JC; Hoffmann JC; Poché RA; Slater JH; West JL; Dickinson ME Three-dimensional biomimetic patterning in hydrogels to guide cellular organization. Adv. Mater. 2012, 24, 2344–2348. [PubMed: 22467256]

(455). DeForest CA; Polizzotti BD; Anseth KS Sequential click reactions for synthesizing and patterning three-dimensional cell microenvironments. Nat. Mater. 2009, 8, 659–664. [PubMed: 19543279]

(456). Kyburz KA; Anseth KS Three-dimensional hMSC motility within peptide-functionalized PEG-based hydrogels of varying adhesivity and crosslinking density. Acta Biomater 2013, 9, 6381–6392. [PubMed: 23376239]

(457). DeForest CA; Sims EA; Anseth KS Peptide-functionalized click hydrogels with independently tunable mechanics and chemical functionality for 3D cell culture. Chem. Mater. 2010, 22, 4783–4790. [PubMed: 20842213]

(458). Kloxin AM; Kasko AM; Salinas CN; Anseth KS Photodegradable hydrogels for dynamic tuning of physical and chemical properties. Science 2009, 324, 59–63. [PubMed: 19342581]

(459). Kloxin AM; Tibbitt MW; Anseth KS Synthesis of photodegradable hydrogels as dynamically tunable cell culture platforms. Nat. Protoc 2010, 5, 1867–1887. [PubMed: 21127482]

(460). DeForest CA; Anseth KS Cytocompatible click-based hydrogels with dynamically tunable properties through orthogonal photoconjugation and photocleavage reactions. Nat. Chem 2011, 3, 925–931. [PubMed: 22109271]

(461). DeForest CA; Anseth KS Photoreversible patterning of biomolecules within click-based hydrogels. Angew. Chem. Int. Edit 2012, 51, 1816–1819.

(462). Gandavarapu NR; Azagarsamy MA; Anseth KS Photo-click living strategy for controlled, reversible exchange of biochemical ligands. Adv. Mater. 2014, 26, 2521–2526. [PubMed: 24523204]

(463). Wipff PJ; Rifkin DB; Meister JJ; Hinz B Myofibroblast contraction activates latent TGF-beta1 from the extracellular matrix. J. Cell Biol 2007, 179, 1311–1323. [PubMed: 18086923]

(464). Gama CI; Tully SE; Sotogaku N; Clark PM; Rawat M; Vaidehi N; Goddard WA; Nishi A; Hsieh-Wilson LC Sulfation patterns of glycosaminoglycans encode molecular recognition and activity. Nat. Chem. Biol 2006, 2, 467–473. [PubMed: 16878128]

(465). Mann BK; Schmedlen RH; West JL Tethered-TGF-β increases extracellular matrix production of vascular smooth muscle cells. Biomaterials 2001, 22, 439–444. [PubMed: 11214754]

(466). Nur-E-Kamal A; Ahmed I; Kamal J; Babu AN; Schindler M; Meiners S Covalently attached FGF-2 to three-dimensional polyamide nanofibrillar surfaces demonstrates enhanced biological stability and activity. Mol. Cell Biochem 2008, 309, 157–166. [PubMed: 18008136]

(467). Hudalla GA; Koepsel JT; Murphy WL Surfaces that sequester serum-borne heparin amplify growth factor activity. Adv. Mater. 2011, 23, 5415–5418. [PubMed: 22028244]

(468). Hettiaratchi MH; Guldberg RE; McDevitt TC Biomaterial strategies for controlling stem cell fate via morphogen sequestration. J. Mater. Chem. B 2016, 4, 3464–3481.

(469). Lienemann PS; Lutolf MP; Ehrbar M Biomimetic hydrogels for controlled biomolecule delivery to augment bone regeneration. Adv. Drug Deliver. Rev 2012, 64, 1078–1089.

(470). Silva AKA; Richard C; Bessodes M; Scherman D; Merten O-W Growth factor delivery approaches in hydrogels. Biomacromolecules 2009, 10, 9–18. [PubMed: 19032110]

(471). Lee K; Silva EA; Mooney DJ Growth factor delivery-based tissue engineering: general approaches and a review of recent developments. J. R. Soc. Interface 2010, 8, 153. [PubMed: 20719768]

(472). Gabriel D; Dvir T; Kohane DS Delivering bioactive molecules as instructive cues to engineered tissues. Expert Opin. Drug Del 2012, 9, 473–492.

(473). Richardson TP; Peters MC; Ennett AB; Mooney DJ Polymeric system for dual growth factor delivery. Nat. Biotechnol 2001, 19, 1029–1034. [PubMed: 11689847]

(474). Hill E; Boontheekul T; Mooney DJ Regulating activation of transplanted cells controls tissue regeneration. Proc. Natl. Acad. Sci. U.S.A 2006, 103, 2494–2499. [PubMed: 16477029]

(475). Nguyen MK; Alsberg E Bioactive factor delivery strategies from engineered polymer hydrogels for therapeutic medicine. Prog. Polym. Sci 2014, 39, 1235–1265.

(476). Hosseinkhani H; Hosseinkhani M; Khademhosseini A; Kobayashi H; Tabata Y Enhanced angiogenesis through controlled release of basic fibroblast growth factor from peptide amphiphile for tissue regeneration. Biomaterials 2006, 27, 5836–5844. [PubMed: 16930687]

(477). Martino MM; Briquez PS; Ranga A; Lutolf MP; Hubbell JA Heparin-binding domain of fibrin(ogen) binds growth factors and promotes tissue repair when incorporated within a synthetic matrix. Proc. Natl. Acad. Sci. U.S.A 2013, 110, 4563–4568. [PubMed: 23487783]

(478). Hudalla GA; Murphy WL Biomaterials that regulate growth factor activity via bioinspired interactions. Adv. Func. Mater. 2011, 21, 1754–1768.

(479). Nie T; Baldwin A; Yamaguchi N; Kiick KL Production of heparin-functionalized hydrogels for the development of responsive and controlled growth factor delivery systems. J. Control. Release 2007, 122, 287–296. [PubMed: 17582636]

(480). Lee AC; Yu VM; Lowe Iii JB; Brenner MJ; Hunter DA; Mackinnon SE; Sakiyama-Elbert SE Controlled release of nerve growth factor enhances sciatic nerve regeneration. Exp. Neurol 2003, 184, 295–303. [PubMed: 14637100]

(481). Liang Y; Kiick KL Heparin-functionalized polymeric biomaterials in tissue engineering and drug delivery applications. Acta Biomater 2014, 10, 1588–1600. [PubMed: 23911941]

(482). Zieris A; Prokoph S; Levental KR; Welzel PB; Grimmer M; Freudenberg U; Werner C FGF-2 and VEGF functionalization of starPEG–heparin hydrogels to modulate biomolecular and physical cues of angiogenesis. Biomaterials 2010, 31, 7985–7994. [PubMed: 20674970]

(483). Zieris A; Chwalek K; Prokoph S; Levental KR; Welzel PB; Freudenberg U; Werner C Dual independent delivery of pro-angiogenic growth factors from starPEG-heparin hydrogels. J. Control. Release 2011, 156, 28–36. [PubMed: 21763368]

(484). Freeman I; Kedem A; Cohen S The effect of sulfation of alginate hydrogels on the specific binding and controlled release of heparin-binding proteins. Biomaterials 2008, 29, 3260–3268. [PubMed: 18462788]

(485). Freeman I; Cohen S The influence of the sequential delivery of angiogenic factors from affinity-binding alginate scaffolds on vascularization. Biomaterials 2009, 30, 2122–2131. [PubMed: 19152972]

(486). Ruvinov E; Leor J; Cohen S The effects of controlled HGF delivery from an affinity-binding alginate biomaterial on angiogenesis and blood perfusion in a hindlimb ischemia model. Biomaterials 2010, 31, 4573–4582. [PubMed: 20206988]

(487). Ruvinov E; Leor J; Cohen S The promotion of myocardial repair by the sequential delivery of IGF-1 and HGF from an injectable alginate biomaterial in a model of acute myocardial infarction. Biomaterials 2011, 32, 565–578. [PubMed: 20889201]

(488). Re'em T; Kaminer-Israeli Y; Ruvinov E; Cohen S Chondrogenesis of hMSC in affinity-bound TGF-beta scaffolds. Biomaterials 2012, 33, 751–761. [PubMed: 22019120]

(489). Purcell BP; Lobb D; Charati MB; Dorsey SM; Wade RJ; Zellers KN; Doviak H; Pettaway S; Logdon CB; Shuman J; Freels PD; Gorman JH; Gorman RC; Spinale FG; Burdick JA Injectable and bioresponsive hydrogels for on-demand matrix metalloproteinase inhibition. Nat. Mater. 2014, 13, 653–661. [PubMed: 24681647]

(490). Impellitteri NA; Toepke MW; Lan Levengood SK; Murphy WL Specific VEGF sequestering and release using peptide-functionalized hydrogel microspheres. Biomaterials 2012, 33, 3475–3484. [PubMed: 22322198]

(491). Zisch AH; Schenk U; Schense JC; Sakiyama-Elbert SE; Hubbell JA Covalently conjugated VEGF–fibrin matrices for endothelialization. J. Control. Release 2001, 72, 101–113. [PubMed: 11389989]

(492). Alge DL; Anseth KS Bioactive hydrogels: Lighting the way. Nat. Mater. 2013, 12, 950–952.

(493). Saik JE; Gould DJ; Watkins EM; Dickinson ME; West JL Covalently immobilized platelet-derived growth factor-BB promotes angiogenesis in biomimetic poly(ethylene glycol) hydrogels. Acta Biomater 2011, 7, 133–143. [PubMed: 20801242]

(494). DeLong SA; Moon JJ; West JL Covalently immobilized gradients of bFGF on hydrogel scaffolds for directed cell migration. Biomaterials 2005, 26, 3227–3234. [PubMed: 15603817]

(495). McCall JD; Luoma JE; Anseth KS Covalently tethered transforming growth factor beta in PEG hydrogels promotes chondrogenic differentiation of encapsulated human mesenchymal stem cells. Drug Deliv. Transl. Re 2012, 2, 305–312.

(496). Hume PS; He J; Haskins K; Anseth KS Strategies to reduce dendritic cell activation through functional biomaterial design. Biomaterials 2012, 33, 3615–3625. [PubMed: 22361099]

(497). Aizawa Y; Wylie R; Shoichet M Endothelial cell guidance in 3D patterned scaffolds. Adv. Mater. 2010, 22, 4831–4835. [PubMed: 20683863]

(498). Wylie RG; Ahsan S; Aizawa Y; Maxwell KL; Morshead CM; Shoichet MS Spatially controlled simultaneous patterning of multiple growth factors in three-dimensional hydrogels. Nat. Mater. 2011, 10, 799–806. [PubMed: 21874004]

(499). Mosiewicz KA; Kolb L; van der Vlies AJ; Martino MM; Lienemann PS; Hubbell JA; Ehrbar M; Lutolf MP In situ cell manipulation through enzymatic hydrogel photopatterning. Nat. Mater. 2013, 12, 1072–1078. [PubMed: 24121990]

(500). Kopesky PW; Vanderploeg EJ; Kisiday JD; Frisbie DD; Sandy JD; Grodzinsky AJ Controlled delivery of transforming growth factor β1 by self-assembling peptide hydrogels induces chondrogenesis of bone marrow stromal cells and modulates Smad2/3 signalingn. Tissue Eng. Part A 2010, 17, 83–92. [PubMed: 20672992]

(501). Cosson S; Allazetta S; Lutolf MP Patterning of cell-instructive hydrogels by hydrodynamic flow focusing. Lab Chip 2013, 13, 2099–2105. [PubMed: 23598796]

(502). Hiesinger W; Frederick JR; Atluri P; McCormick RC; Marotta N; Muenzer JR; Woo YJ Spliced stromal cell-derived factor-1α analog stimulates endothelial progenitor cell migration and improves cardiac function in a dose-dependent manner after myocardial infarction. J. Thorac. Cardiov. Sur 2010, 140, 1174–1180.

(503). MacArthur JW; Purcell BP; Shudo Y; Cohen JE; Fairman A; Trubelja A; Patel J; Hsiao P; Yang E; Lloyd K; Hiesinger W; Atluri P; Burdick JA; Woo YJ Sustained release of engineered stromal cell–derived factor 1-α from injectable hydrogels effectively recruits endothelial progenitor cells and preserves ventricular function after myocardial infarction. Circulation 2013, 128, 79–86. [PubMed: 23817483]

(504). Madl CM; Mehta M; Duda GN; Heilshorn SC; Mooney DJ Presentation of BMP-2 mimicking peptides in 3D hydrogels directs cell fate commitment in osteoblasts and mesenchymal stem cells. Biomacromolecules 2014, 15, 445–455. [PubMed: 24400664]

(505). Bacakova L; Filova E; Parizek M; Ruml T; Svorcik V Modulation of cell adhesion, proliferation and differentiation on materials designed for body implants. Biotechnol. Adv 2011, 29, 739–767. [PubMed: 21821113]

(506). Liu L; Chen S; Giachelli CM; Ratner BD; Jiang S Controlling osteopontin orientation on surfaces to modulate endothelial cell adhesion. J. Biomed. Mater. Res. A 2005, 74A, 23–31.

(507). Curran JM; Chen R; Hunt JA Controlling the phenotype and function of mesenchymal stem cells in vitro by adhesion to silane-modified clean glass surfaces. Biomaterials 2005, 26, 7057–7067. [PubMed: 16023712]

(508). Higuchi A; Ling Q-D; Kumar SS; Munusamy M; Alarfajj AA; Umezawa A; Wu G-J Design of polymeric materials for culturing human pluripotent stem cells: Progress toward feeder-free and xeno-free culturing. Prog. Polym. Sci 2014, 39, 1348–1374.

(509). Dhowre HS; Rajput S; Russell NA; Zelzer M Responsive cell–material interfaces. Nanomedicine 2015, 10, 849–871. [PubMed: 25816884]

(510). Chen Z; Kang L; Wang Z; Xu F; Gu G; Cui F; Guo Z Recent progress in the research of biomaterials regulating cell behavior. RSC Adv 2014, 4, 63807–63816.

(511). Jiang X; Bruzewicz DA; Wong AP; Piel M; Whitesides GM Directing cell migration with asymmetric micropatterns. Proc. Natl. Acad. Sci. U.S.A 2005, 102, 975–978. [PubMed: 15653772]

(512). Ren Y-J; Zhang H; Huang H; Wang X-M; Zhou Z-Y; Cui F-Z; An Y-H In vitro behavior of neural stem cells in response to different chemical functional groups. Biomaterials 2009, 30, 1036–1044. [PubMed: 19026444]

(513). Song J; Malathong V; Bertozzi CR Mineralization of synthetic polymer scaffolds: A bottom-up approach for the development of artificial bone. J. Am. Chem. Soc 2005, 127, 3366–3372. [PubMed: 15755154]

(514). Keselowsky BG; Collard DM; García AJ Surface chemistry modulates focal adhesion composition and signaling through changes in integrin binding. Biomaterials 2004, 25, 5947–5954. [PubMed: 15183609]

(515). Bi X; You Z; Gao J; Fan X; Wang Y A functional polyester carrying free hydroxyl groups promotes the mineralization of osteoblast and human mesenchymal stem cell extracellular matrix. Acta Biomater 2014, 10, 2814–2823. [PubMed: 24560799]

(516). Arima Y; Iwata H Effect of wettability and surface functional groups on protein adsorption and cell adhesion using well-defined mixed self-assembled monolayers. Biomaterials 2007, 28, 3074–3082. [PubMed: 17428532]

(517). Falde EJ; Yohe ST; Colson YL; Grinstaff MW Superhydrophobic materials for biomedical applications. Biomaterials 2016, 104, 87–103. [PubMed: 27449946]

(518). Ishizaki T; Saito N; Takai O Correlation of cell adhesive behaviors on superhydrophobic, superhydrophilic, and micropatterned superhydrophobic/superhydrophilic surfaces to their surface chemistry. Langmuir the ACS Journal of Surfaces & Colloids 2010, 26, 8147–8154. [PubMed: 20131757]

(519). Nuttelman CR; Benoit DSW; Tripodi MC; Anseth KS The effect of ethylene glycol methacrylate phosphate in PEG hydrogels on mineralization and viability of encapsulated hMSCs. Biomaterials 2006, 27, 1377–1386. [PubMed: 16139351]

(520). Keselowsky BG; Collard DM; García AJ Integrin binding specificity regulates biomaterial surface chemistry effects on cell differentiation. Proc. Natl. Acad. Sci. U.S.A 2005, 102, 5953–5957. [PubMed: 15827122]

(521). Gandavarapu NR; Mariner PD; Schwartz MP; Anseth KS Extracellular matrix protein adsorption to phosphate-functionalized gels from serum promotes osteogenic differentiation of human mesenchymal stem cells. Acta Biomater 2013, 9, 4525–4534. [PubMed: 22982322]

(522). Yao X; Chen L; Ju J; Li C; Tian Y; Jiang L; Liu M Superhydrophobic diffusion barriers for hydrogels via confined interfacial modification. Adv. Mater. 2016, 28, 7383–7389. [PubMed: 27309131]

(523). Han YL; Wang S; Zhang X; Li Y; Huang G; Qi H; Pingguan-Murphy B; Li Y; Lu TJ; Xu F Engineering physical microenvironment for stem cell based regenerative medicine. Drug Discov. Today 2014, 19, 763–773. [PubMed: 24508818]

(524). Sun Y; Chen CS; Fu J Forcing stem cells to behave: A biophysical perspective of the cellular microenvironment. Annu. Rev. Biophys 2012, 41, 519–542. [PubMed: 22404680]

(525). Kshitiz Park, J.; Kim P; Helen W; Engler AJ; Levchenko A; Kim D-H Control of stem cell fate and function by engineering physical microenvironments. Integr. Biol 2012, 4, 1008–1018.

(526). Charras G; Sahai E Physical influences of the extracellular environment on cell migration. Nat. Rev. Mol. Cell Bio 2014, 15, 813–824. [PubMed: 25355506]

(527). Lee J; Cuddihy MJ; Kotov NA Three-dimensional cell culture matrices: State of the art. Tissue Eng. Part B Rev 2008, 14, 61–86. [PubMed: 18454635]

(528). Hoffman-Kim D; Mitchel JA; Bellamkonda RV Topography, cell response, and nerve regeneration. Annu. Rev. Biomed. Eng 2010, 12, 203–231. [PubMed: 20438370]

(529). Naleway SE; Porter MM; McKittrick J; Meyers MA Structural design elements in biological materials: Application to bioinspiration. Adv. Mater. 2015, 27, 5455–5476. [PubMed: 26305858]

(530). Zhang Q; Yang X; Li P; Huang G; Feng S; Shen C; Han B; Zhang X; Jin F; Xu F; Lu TJ Bioinspired engineering of honeycomb structure – Using nature to inspire human innovation. Prog. Mater. Sci 2015, 74, 332–400.

(531). Wegst UGK; Bai H; Saiz E; Tomsia AP; Ritchie RO Bioinspired structural materials. Nat. Mater. 2015, 14, 23–36. [PubMed: 25344782]

(532). Anowarul I; Katherine C; Mousa Y; Ozan A Computer aided biomanufacturing of mechanically robust pure collagen meshes with controlled macroporosity. Biofabrication 2015, 7, 035005. [PubMed: 26200002]

(533). Melchels FPW; Domingos MAN; Klein TJ; Malda J; Bartolo PJ; Hutmacher DW Additive manufacturing of tissues and organs. Prog. Polym. Sci 2012, 37, 1079–1104.

(534). Meng H; Tutino VM; Xiang J; Siddiqui A High WSS or low WSS? Complex interactions of hemodynamics with intracranial aneurysm initiation, growth, and rupture: Toward a unifying hypothesis. Am. J. Neuroradiol 2014, 35, 1254–1262. [PubMed: 23598838]

(535). Hung CT; Mauck RL; Wang CCB; Lima EG; Ateshian GA A paradigm for functional tissue engineering of articular cartilage via applied physiologic deformational loading. Ann. Biomed. Eng 2004, 32, 35–49. [PubMed: 14964720]

(536). Shi Y; Yao J; Xu G; Taber LA Bending of the looping heart: Differential growth revisited. J. Biomech. Eng 2014, 136, 081002.

(537). Sherratt JA; Chaplain MAJ A new mathematical model for avascular tumour growth. J. Math. Biol 2001, 43, 291–312. [PubMed: 12120870]

(538). Boyle JJ; Kume M; Wyczalkowski MA; Taber LA; Pless RB; Xia Y; Genin GM; Thomopoulos S Simple and accurate methods for quantifying deformation, disruption, and development in biological tissues. J. R. Soc. Interface 2014, 11, 20140685. [PubMed: 25165601]

(539). Veiseh O; Doloff JC; Ma M; Vegas AJ; Tam HH; Bader AR; Li J; Langan E; Wyckoff J; Loo WS; Jhunjhunwala S; Chiu A; Siebert S; Tang K; Hollister-Lock J; Aresta-Dasilva S; Bochenek M; Mendoza-Elias J; Wang Y; Qi M; Lavin DM; Chen M; Dholakia N; Thakrar R; Lacik I; Weir GC; Oberholzer J; Greiner DL; Langer R; Anderson DG Size- and shape-dependent foreign body immune response to materials implanted in rodents and non-human primates. Nat. Mater. 2015, 14, 643–651. [PubMed: 25985456]

(540). Stevens KR; Ungrin MD; Schwartz RE; Ng S; Carvalho B; Christine KS; Chaturvedi RR; Li CY; Zandstra PW; Chen CS; Bhatia SN InVERT molding for scalable control of tissue microarchitecture. Nat. Commun 2013, 4, 1847. [PubMed: 23673632]

(541). Kloxin AM; Lewis KJR; DeForest CA; Seedorf G; Tibbitt MW; Balasubramaniam V; Anseth KS Responsive culture platform to examine the influence of microenvironmental geometry on cell function in 3D. Integr. Biol 2012, 4, 1540–1549.

(542). El Assal R; Gurkan UA; Chen P; Juillard F; Tocchio A; Chinnasamy T; Beauchemin C; Unluisler S; Canikyan S; Holman A; Srivatsa S; Kaye KM; Demirci U 3-D microwell array system for culturing virus infected tumor cells. Sci. Rep 2016, 6, 39144. [PubMed: 28004818]

(543). Gong X; Lin C; Cheng J; Su J; Zhao H; Liu T; Wen X; Zhao P Generation of multicellular tumor spheroids with microwell-based agarose scaffolds for drug testing. PLOS ONE 2015, 10, e0130348. [PubMed: 26090664]

(544). Khademhosseini A; Ferreira L; Blumling Iii J; Yeh J; Karp JM; Fukuda J; Langer R Co-culture of human embryonic stem cells with murine embryonic fibroblasts on microwell-patterned substrates. Biomaterials 2006, 27, 5968–5977. [PubMed: 16901537]

(545). Hwang Y-S; Chung BG; Ortmann D; Hattori N; Moeller H-C; Khademhosseini A Microwell-mediated control of embryoid body size regulates embryonic stem cell fate via differential expression of WNT5a and WNT11. Proc. Natl. Acad. Sci. U.S.A 2009, 106, 16978–16983. [PubMed: 19805103]

(546). Bernard AB; Lin C-C; Anseth KS A Microwell cell culture platform for the aggregation of pancreatic β-cells. Tissue Eng. Part C Meth 2012, 18, 583–592.

(547). Qi H; Huang G; Han YL; Lin W; Li X; Wang S; Lu TJ; Xu F In vitro spatially organizing the differentiation in individual multicellular stem cell aggregates. Crit. Rev. Biotechnol 2016, 36, 20–31. [PubMed: 25025275]

(548). Ling K; Huang G; Liu J; Zhang X; Ma Y; Lu T; Xu F Bioprinting-based high-throughput fabrication of three-dimensional MCF-7 human breast cancer cellular spheroids. Engineering 2015, 1, 269–274.

(549). Kim B-C; Kim JH; An HJ; Byun W; Park J-H; Kwon IK; Kim JS; Hwang Y-S Microwell-mediated micro cartilage-like tissue formation of adipose-derived stem cell. Macromol. Res 2014, 22, 287–296.

(550). Fukuda J; Khademhosseini A; Yeo Y; Yang X; Yeh J; Eng G; Blumling J; Wang C-F; Kohane DS; Langer R Micromolding of photocrosslinkable chitosan hydrogel for spheroid microarray and co-cultures. Biomaterials 2006, 27, 5259–5267. [PubMed: 16814859]

(551). Laschke MW; Menger MD Life is 3D: Boosting spheroid function for tissue engineering. Trends Biotechnol 2017, 35, 133–144. [PubMed: 27634310]

(552). Tsurkan MV; Wetzel R; Pérez-Hernández HR; Chwalek K; Kozlova A; Freudenberg U; Kempermann G; Zhang Y; Lasagni AF; Werner C Photopatterning of multifunctional hydrogels to direct adult neural precursor cells. Adv. Healthc. Mater. 2015, 4, 516–521. [PubMed: 25323149]

(553). Gong T; Lu L; Liu D; Liu X; Zhao K; Chen Y; Zhou S Dynamically tunable polymer microwells for directing mesenchymal stem cell differentiation into osteogenesis. J. Mater. Chem. B 2015, 3, 9011–9022.

(554). O'Brien FJ; Harley BA; Yannas IV; Gibson LJ The effect of pore size on cell adhesion in collagen-GAG scaffolds. Biomaterials 2005, 26, 433–441. [PubMed: 15275817]

(555). Loh QL; Choong C Three-dimensional scaffolds for tissue engineering applications: Role of porosity and pore size. Tissue Eng. Part B Rev 2013, 19, 485–502. [PubMed: 23672709]

(556). Thomas AM; Kubilius MB; Holland SJ; Seidlits SK; Boehler RM; Anderson AJ; Cummings BJ; Shea LD Channel density and porosity of degradable bridging scaffolds on axon growth after spinal injury. Biomaterials 2013, 34, 2213–2220. [PubMed: 23290832]

(557). Zhao X; Kim J; Cezar CA; Huebsch N; Lee K; Bouhadir K; Mooney DJ Active scaffolds for on-demand drug and cell delivery. Proc. Natl. Acad. Sci. U.S.A 2011, 108, 67–72. [PubMed: 21149682]

(558). O'Brien FJ; Harley BA; Waller MA; Yannas IV; Gibson LJ; Prendergast PJ The effect of pore size on permeability and cell attachment in collagen scaffolds for tissue engineering. Technol. Health Care 2007, 15, 3–17. [PubMed: 17264409]

(559). Ford MC; Bertram JP; Hynes SR; Michaud M; Li Q; Young M; Segal SS; Madri JA; Lavik EB A macroporous hydrogel for the coculture of neural progenitor and endothelial cells to form functional vascular networks invivo. Proc. Natl. Acad. Sci. U.S.A 2006, 103, 2512–2517. [PubMed: 16473951]

(560). Madihally SV; Matthew HWT Porous chitosan scaffolds for tissue engineering. Biomaterials 1999, 20, 1133–1142. [PubMed: 10382829]

(561). Kang H-W; Tabata Y; Ikada Y Fabrication of porous gelatin scaffolds for tissue engineering. Biomaterials 1999, 20, 1339–1344. [PubMed: 10403052]

(562). Ho M-H; Kuo P-Y; Hsieh H-J; Hsien T-Y; Hou L-T; Lai J-Y; Wang D-M Preparation of porous scaffolds by using freeze-extraction and freeze-gelation methods. Biomaterials 2004, 25, 129–138. [PubMed: 14580916]

(563). Donius AE; Liu A; Berglund LA; Wegst UGK Superior mechanical performance of highly porous, anisotropic nanocellulose–montmorillonite aerogels prepared by freeze casting. J. Mech. Behav. Biomed 2014, 37, 88–99.

(564). Ji C; Annabi N; Hosseinkhani M; Sivaloganathan S; Dehghani F Fabrication of poly-DL-lactide/polyethylene glycol scaffolds using the gas foaming technique. Acta Biomater 2012, 8, 570–578. [PubMed: 21996623]

(565). Ali ZM; Gibson LJ The structure and mechanics of nanofibrillar cellulose foams. Soft Matter 2013, 9, 1580–1588.

(566). Hollister SJ Porous scaffold design for tissue engineering. Nat. Mater. 2005, 4, 518–524. [PubMed: 16003400]

(567). Billiet T; Vandenhaute M; Schelfhout J; Van Vlierberghe S; Dubruel P A review of trends and limitations in hydrogel-rapid prototyping for tissue engineering. Biomaterials 2012, 33, 6020–6041. [PubMed: 22681979]

(568). Lee VK; Dai G Printing of three-dimensional tissue analogs for regenerative medicine. Ann. Biomed. Eng 2017, 45, 115–131. [PubMed: 27066784]

(569). Somo SI; Akar B; Bayrak ES; Larson JC; Appel AA; Mehdizadeh H; Cinar A; Brey EM Pore interconnectivity influences growth factor-mediated vascularization in sphere-templated hydrogels. Tissue Eng. Part C Meth 2015, 21, 773–785.

(570). Zhang Q; Lu H; Kawazoe N; Chen G Pore size effect of collagen scaffolds on cartilage regeneration. Acta Biomater 2014, 10, 2005–2013. [PubMed: 24384122]

(571). Viswanathan P; Ondeck MG; Chirasatitsin S; Ngamkham K; Reilly GC; Engler AJ; Battaglia G 3D surface topology guides stem cell adhesion and differentiation. Biomaterials 2015, 52, 140–147. [PubMed: 25818420]

(572). Woodard JR; Hilldore AJ; Lan SK; Park CJ; Morgan AW; Eurell JAC; Clark SG; Wheeler MB; Jamison RD; Wagoner Johnson AJ The mechanical properties and osteoconductivity of hydroxyapatite bone scaffolds with multi-scale porosity. Biomaterials 2007, 28, 45–54. [PubMed: 16963118]

(573). Cordell JM; Vogl ML; Wagoner Johnson AJ The influence of micropore size on the mechanical properties of bulk hydroxyapatite and hydroxyapatite scaffolds. J. Mech. Behav. Biomed 2009, 2, 560–570.

(574). Miron-Mendoza M; Seemann J; Grinnell F The differential regulation of cell motile activity through matrix stiffness and porosity in three dimensional collagen matrices. Biomaterials 2010, 31, 6425–6435. [PubMed: 20537378]

(575). Wolf K; te Lindert M; Krause M; Alexander S; te Riet J; Willis AL; Hoffman RM; Figdor CG; Weiss SJ; Friedl P Physical limits of cell migration: Control by ECM space and nuclear deformation and tuning by proteolysis and traction force. J. Cell Biol 2013, 201, 1069. [PubMed: 23798731]

(576). Kawano T; Sato M; Yabu H; Shimomura M Honeycomb-shaped surface topography induces differentiation of human mesenchymal stem cells (hMSCs): uniform porous polymer scaffolds prepared by the breath figure technique. Biomater. Sci 2014, 2, 52–56.

(577). Engelmayr GC; Cheng MY; Bettinger CJ; Borenstein JT; Langer R; Freed LE Accordion-like honeycombs for tissue engineering of cardiac anisotropy. Nat. Mater 2008, 7, 1003–1010. [PubMed: 18978786]

(578). Pot MW; Faraj KA; Adawy A; van Enckevort WJP; van Moerkerk HTB; Vlieg E; Daamen WF; van Kuppevelt TH Versatile wedge-based system for the construction of unidirectional collagen scaffolds by directional freezing: Practical and theoretical considerations. ACS Appl. Mater. Inter 2015, 7, 8495–8505.

(579). Zhang Y; Yang F; Liu K; Shen H; Zhu Y; Zhang W; Liu W; Wang S; Cao Y; Zhou G The impact of PLGA scaffold orientation on in vitro cartilage regeneration. Biomaterials 2012, 33, 2926–2935. [PubMed: 22257722]

(580). Chen S; Nakamoto T; Kawazoe N; Chen G Engineering multi-layered skeletal muscle tissue by using 3D microgrooved collagen scaffolds. Biomaterials 2015, 73, 23–31. [PubMed: 26398306]

(581). Duncombe TA; Kang C-C; Maity S; Ward TM; Pegram MD; Murthy N; Herr AE Hydrogel pore-size modulation for enhanced single-cell western blotting. Adv. Mater. 2016, 28, 327–334. [PubMed: 26567472]

(582). Luo R; Wu J; Dinh N-D; Chen C-H Gradient porous elastic hydrogels with shape-memory property and anisotropic responses for programmable locomotion. Adv. Func. Mater. 2015, 25, 7272–7279.

(583). He JK; Du YA; Villa-Uribe JL; Hwang CM; Li DC; Khademhosseini A Rapid generation of biologically relevant hydrogels containing long-range chemical gradients. Adv. Func. Mater. 2010, 20, 131–137.

(584). Han F; Yang X; Zhao J; Zhao Y; Yuan X Photocrosslinked layered gelatin-chitosan hydrogel with graded compositions for osteochondral defect repair. J. Mater. Sci. Mater. Med 2015, 26, 160. [PubMed: 25786398]

(585). Caliari SR; Weisgerber DW; Grier WK; Mahmassani Z; Boppart MD; Harley BAC Collagen scaffolds incorporating coincident gradations of instructive structural and biochemical cues for osteotendinous junction engineering. Adv. Healthc. Mater. 2015, 4, 831–837. [PubMed: 25597299]

(586). Rouwkema J; Rivron NC; van Blitterswijk CA Vascularization in tissue engineering. Trends Biotechnol 2008, 26, 434–441. [PubMed: 18585808]

(587). Novosel EC; Kleinhans C; Kluger PJ Vascularization is the key challenge in tissue engineering. Adv. Drug Deliver. Rev 2011, 63, 300–311.

(588). Atala A; Kasper FK; Mikos AG Engineering complex tissues. Sci. Transl. Med 2012, 4, 160rv112.

(589). Huang GY; Zhou LH; Zhang QC; Chen YM; Sun W; Xu F; Lu TJ Microfluidic hydrogels for tissue engineering. Biofabrication 2011, 3, 012001. [PubMed: 21372342]

(590). Bersini S; Yazdi IK; Talò G; Shin SR; Moretti M; Khademhosseini A Cell-microenvironment interactions and architectures in microvascular systems. Biotechnol. Adv 2016, 34, 1113–1130. [PubMed: 27417066]

(591). Miller JS; Stevens KR; Yang MT; Baker BM; Nguyen D-HT; Cohen DM; Toro E; Chen AA; Galie PA; Yu X; Chaturvedi R; Bhatia SN; Chen CS Rapid casting of patterned vascular networks for perfusable engineered three-dimensional tissues. Nat. Mater. 2012, 11, 768–774. [PubMed: 22751181]

(592). He J; Mao M; Liu Y; Shao J; Jin Z; Li D Fabrication of nature-inspired microfluidic network for perfusable tissue constructs. Adv. Healthc. Mater. 2013, 2, 1108–1113. [PubMed: 23554383]

(593). Kolesky DB; Homan KA; Skylar-Scott MA; Lewis JA Three-dimensional bioprinting of thick vascularized tissues. Proc. Natl. Acad. Sci. U.S.A 2016, 113, 3179–3184. [PubMed: 26951646]

(594). Kolesky DB; Truby RL; Gladman AS; Busbee TA; Homan KA; Lewis JA 3D bioprinting of vascularized, heterogeneous cell-laden tissue constructs. Adv. Mater. 2014, 26, 3124–3130. [PubMed: 24550124]

(595). Choi NW; Cabodi M; Held B; Gleghorn JP; Bonassar LJ; Stroock AD Microfluidic scaffolds for tissue engineering. Nat. Mater. 2007, 6, 908–915. [PubMed: 17906630]

(596). Park JH; Chung BG; Lee WG; Kim J; Brigham MD; Shim J; Lee S; Hwang CM; Durmus NG; Demirci U; Khademhosseini A Microporous cell-laden hydrogels for engineered tissue constructs. Biotechnol. Bioeng 2010, 106, 138–148. [PubMed: 20091766]

(597). Zhang B; Montgomery M; Chamberlain MD; Ogawa S; Korolj A; Pahnke A; Wells LA; Masse S; Kim J; Reis L; Momen A; Nunes SS; Wheeler AR; Nanthakumar K; Keller G; Sefton MV; Radisic M Biodegradable scaffold with built-in vasculature for organ-on-a-chip engineering and direct surgical anastomosis. Nat. Mater. 2016, 15, 669–678. [PubMed: 26950595]

(598). Huang G; Zhang X; Xiao Z; Zhang Q; Zhou J; Xu F; Lu TJ Cell-encapsulating microfluidic hydrogels with enhanced mechanical stability. Soft Matter 2012, 8, 10687–10694.

(599). Whisler JA; Chen MB; Kamm RD Control of perfusable microvascular network morphology using a multiculture microfluidic system. Tissue Eng. Part C Meth 2013, 20, 543–552.

(600). Chen X; Aledia AS; Ghajar CM; Griffith CK; Putnam AJ; Hughes CCW; George SC Prevascularization of a fibrin-based tissue construct accelerates the formation of functional anastomosis with host vasculature. Tissue Eng. Part A 2008, 15, 1363–1371.

(601). Morin KT; Tranquillo RT In vitro models of angiogenesis and vasculogenesis in fibrin gel. Exp. Cell Res 2013, 319, 2409–2417. [PubMed: 23800466]

(602). Moya ML; Hsu Y-H; Lee AP; Hughes CCW; George SC In vitro perfused human capillary networks. Tissue Eng. Part C Meth 2013, 19, 730–737.

(603). Eydelnant IA; Betty Li B; Wheeler AR Microgels on-demand. Nat. Commun 2014, 5, 3355. [PubMed: 24566526]

(604). Nichol JW; Khademhosseini A Modular tissue engineering: Engineering biological tissues from the bottom up. Soft Matter 2009, 5, 1312–1319. [PubMed: 20179781]

(605). McGuigan AP; Sefton MV Vascularized organoid engineered by modular assembly enables blood perfusion. Proc. Natl. Acad. Sci. U.S.A 2006, 103, 11461–11466. [PubMed: 16864785]

(606). Guven S; Chen P; Inci F; Tasoglu S; Erkmen B; Demirci U Multiscale assembly for tissue engineering and regenerative medicine. Trends Biotechnol 2015, 33, 269–279. [PubMed: 25796488]

(607). Yufei M; Yuan J; Guoyou H; Kai L; Xiaohui Z; Feng X Bioprinting 3D cell-laden hydrogel microarray for screening human periodontal ligament stem cell response to extracellular matrix. Biofabrication 2015, 7, 044105. [PubMed: 26696269]

(608). Wang L; Huang G; Sha B; Wang S; Han YL; Wu J; Li Y; Du Y; Lu TJ; Xu F Engineering three-dimensional cardiac microtissues for potential drug screening applications. Curr. Med. Chem 2014, 21, 2497–2509. [PubMed: 24358973]

(609). Zhang X; Meng Z; Ma J; Shi Y; Xu H; Lykkemark S; Qin J Flexible fabrication of shape-controlled collagen building blocks for self-assembly of 3D microtissues. Small 2015, 11, 3666–3675. [PubMed: 25920010]

(610). Wang L; Qiu M; Yang Q; Li Y; Huang G; Lin M; Lu TJ; Xu F Fabrication of microscale hydrogels with tailored microstructures based on liquid bridge phenomenon. ACS Appl. Mater. Inter 2015, 7, 11134–11140.

(611). Mao AS; Shin J-W; Utech S; Wang H; Uzun O; Li W; Cooper M; Hu Y; Zhang L; Weitz DA; Mooney DJ Deterministic encapsulation of single cells in thin tunable microgels for niche modelling and therapeutic delivery. Nat. Mater. 2016, 16, 236–243. [PubMed: 27798621]

(612). Fan Y; Xu F; Huang G; Lu TJ; Xing W Single neuron capture and axonal development in three-dimensional microscale hydrogels. Lab Chip 2012, 12, 4724–4731. [PubMed: 22858829]

(613). Xu F; Wu CAM; Rengarajan V; Finley TD; Keles HO; Sung YR; Li BQ; Gurkan UA; Demirci U Three-dimensional magnetic assembly of microscale hydrogels. Adv. Mater. 2011, 23, 4254–4260. [PubMed: 21830240]

(614). Tasoglu S; Diller E; Guven S; Sitti M; Demirci U Untethered micro-robotic coding of three-dimensional material composition. Nat. Commun 2014, 5, 3124. [PubMed: 24469115]

(615). Huang G; Li M; Yang Q; Li Y; Liu H; Yang H; Xu F Magnetically actuated droplet manipulation and its potential biomedical applications. ACS Appl. Mater. Inter 2016, 9, 1155–1166.

(616). Xu F; Finley TD; Turkaydin M; Sung YR; Gurkan UA; Yavuz AS; Guldiken RO; Demirci U The assembly of cell-encapsulating microscale hydrogels using acoustic waves. Biomaterials 2011, 32, 7847–7855. [PubMed: 21820734]

(617). Han YL; Yang Y; Liu S; Wu J; Chen Y; Lu TJ; Xu F Directed self-assembly of microscale hydrogels by electrostatic interaction. Biofabrication 2013, 5, 035004. [PubMed: 23715009]

(618). Du Y; Lo E; Ali S; Khademhosseini A Directed assembly of cell-laden microgels for fabrication of 3D tissue constructs. Proc. Natl. Acad. Sci. U.S.A 2008, 105, 9522–9527. [PubMed: 18599452]

(619). Gurkan UA; Fan Y; Xu F; Erkmen B; Urkac ES; Parlakgul G; Bernstein J; Xing W; Boyden ES; Demirci U Simple precision creation of digitally specified, spatially heterogeneous, engineered tissue architectures. Adv. Mater. 2013, 25, 1192–1198. [PubMed: 23192949]

(620). Chung SE; Park W; Shin S; Lee SA; Kwon S Guided and fluidic self-assembly of microstructures using railed microfluidic channels. Nat. Mater. 2008, 7, 581–587. [PubMed: 18552850]

(621). Qi H; Ghodousi M; Du Y; Grun C; Bae H; Yin P; Khademhosseini A DNA-directed self-assembly of shape-controlled hydrogels. Nat. Commun 2013, 4, 2275. [PubMed: 24013352]

(622). Qi H; Huang G; Han Y; Li Y; Zhang X; Pingguan-Murphy B; Lu TJ; Xu F; Wang L Engineering artificial machines from designable DNA materials for biomedical applications. Tissue Eng. Part B Rev 2014, 21, 288–297.

(623). Murphy SV; Atala A 3D bioprinting of tissues and organs. Nat. Biotechnol 2014, 32, 773–785. [PubMed: 25093879]

(624). Kang H-W; Lee SJ; Ko IK; Kengla C; Yoo JJ; Atala A A 3D bioprinting system to produce human-scale tissue constructs with structural integrity. Nat. Biotechnol 2016, 34, 312–319. [PubMed: 26878319]

(625). Jungst T; Smolan W; Schacht K; Scheibel T; Groll J Strategies and molecular design criteria for 3D printable hydrogels. Chem. Rev 2016, 116, 1496–1539. [PubMed: 26492834]

(626). Gurkan UA; Tasoglu S; Kavaz D; Demirel MC; Demirci U Emerging technologies for assembly of microscale hydrogels. Adv. Healthc. Mater. 2012, 1, 149–158. [PubMed: 23184717]

(627). Liu H; Huang G; Li Y; Zhang X; Lu TJ; Xu F Advances in hydrogel-based bottom-up tissue engineering. Scientia Sinica Vitae 2015, 45, 256–270.

(628). Tamayol A; Akbari M; Annabi N; Paul A; Khademhosseini A; Juncker D Fiber-based tissue engineering: Progress, challenges, and opportunities. Biotechnol. Adv 2013, 31, 669–687. [PubMed: 23195284]

(629). Jun Y; Kang E; Chae S; Lee SH Microfluidic spinning of micro- and nano-scale fibers for tissue engineering. Lab Chip 2014, 14, 2145–2160. [PubMed: 24647678]

(630). Onoe H; Takeuchi S Cell-laden microfibers for bottom-up tissue engineering. Drug Discov. Today 2015, 20, 236–246. [PubMed: 25448757]

(631). Shi XT; Ostrovidov S; Zhao YH; Liang XB; Kasuya M; Kurihara K; Nakajima K; Bae H; Wu HK; Khademhosseini A Microfluidicspinning of cell-responsive grooved microfibers. Adv. Func. Mater. 2015, 25, 2250–2259.

(632). Han L-H; Yu S; Wang T; Behn AW; Yang F Microribbon-like elastomers for fabricating macroporous and highly flexible scaffolds that support cell proliferation in 3D. Adv. Func. Mater. 2013, 23, 346–358.

(633). Leng L; McAllister A; Zhang B; Radisic M; Günther A Mosaic hydrogels: One-step formation of multiscale soft materials. Adv. Mater. 2012, 24, 3650–3658. [PubMed: 22714644]

(634). Yoichi K; Yoji N; Yuya Y; Masumi Y; Minoru S Patterned hydrogel microfibers prepared using multilayered microfluidic devices for guiding network formation of neural cells. Biofabrication 2014, 6, 035011. [PubMed: 24876343]

(635). Cheng Y; Zheng F; Lu J; Shang L; Xie Z; Zhao Y; Chen Y; Gu Z Bioinspired multicompartmental microfibers from microfluidics. Adv. Mater. 2014, 26, 5184–5190. [PubMed: 24934291]

(636). Lata JP; Guo F; Guo J; Huang P-H; Yang J; Huang TJ Surface acoustic waves grant superior spatial control of cells embedded in hydrogel fibers. Adv. Mater 2016, 28, 8632–8638. [PubMed: 27571239]

(637). Grolman JM; Zhang D; Smith AM; Moore JS; Kilian KA Rapid 3D extrusion of synthetic tumor microenvironments. Adv. Mater. 2015, 27, 5512–5517. [PubMed: 26283579]

(638). Zhang S; Greenfield MA; Mata A; Palmer LC; Bitton R; Mantei JR; Aparicio C; de la Cruz MO; Stupp SI A self-assembly pathway to aligned monodomain gels. Nat. Mater. 2010, 9, 594–601. [PubMed: 20543836]

(639). Zhang S; Liu X; Barreto-Ortiz SF; Yu Y; Ginn BP; DeSantis NA; Hutton DL; Grayson WL; Cui F-Z; Korgel BA; Gerecht S; Mao H-Q Creating polymer hydrogel microfibres with internal alignment via electrical and mechanical stretching. Biomaterials 2014, 35, 3243–3251. [PubMed: 24439410]

(640). Lim D; Lee E; Kim H; Park S; Baek S; Yoon J Multi stimuli-responsive hydrogel microfibers containing magnetite nanoparticles prepared using microcapillary devices. Soft Matter 2015, 11, 1606–1613. [PubMed: 25594916]

(641). Shang S; Liu Z; Zhang Q; Wang H; Li Y Facile fabrication of a magnetically induced structurally colored fiber and its strain-responsive properties. J. Mater. Chem. A 2015, 3, 11093–11097.

(642). Kang E; Jeong GS; Choi YY; Lee KH; Khademhosseini A; Lee S-H Digitally tunable physicochemical coding of material composition and topography in continuous microfibres. Nat. Mater. 2011, 10, 877–883. [PubMed: 21892177]

(643). Onoe H; Okitsu T; Itou A; Kato-Negishi M; Gojo R; Kiriya D; Sato K; Miura S; Iwanaga S; Kuribayashi-Shigetomi K; Matsunaga YT; Shimoyama Y; Takeuchi S Metre-long cell-laden microfibres exhibit tissue morphologies and functions. Nat. Mater. 2013, 12, 584–590. [PubMed: 23542870]

(644). Li Y; Poon CT; Li M; Lu TJ; Pingguan-Murphy B; Xu F Chinese-noodle-inspired muscle myofiber fabrication. Adv. Func. Mater. 2015, 25, 5999–6008.

(645). Akbari M; Tamayol A; Laforte V; Annabi N; Najafabadi AH; Khademhosseini A; Juncker D Composite living fibers for creating tissue constructs using textile techniques. Adv. Func. Mater. 2014, 24, 4060–4067.

(646). Stevens MM; George JH Exploring and engineering the cell surface interface. Science 2005, 310, 1135–1138. [PubMed: 16293749]

(647). Saracino GAA; Cigognini D; Silva D; Caprini A; Gelain F Nanomaterials design and tests for neural tissue engineering. Chem. Soc. Rev 2013, 42, 225–262. [PubMed: 22990473]

(648). Dalby MJ; Gadegaard N; Oreffo ROC Harnessing nanotopography and integrin-matrix interactions to influence stem cell fate. Nat. Mater. 2014, 13, 558–569. [PubMed: 24845995]

(649). Mendes PM Cellular nanotechnology: Making biological interfaces smarter. Chem. Soc. Rev 2013, 42, 9207–9218. [PubMed: 24097313]

(650). Kim D-H; Lipke EA; Kim P; Cheong R; Thompson S; Delannoy M; Suh K-Y; Tung L; Levchenko A Nanoscale cues regulate the structure and function of macroscopic cardiac tissue constructs. Proc. Natl. Acad. Sci. U.S.A 2010, 107, 565–570. [PubMed: 20018748]

(651). Beachley V; Wen X Polymer nanofibrous structures: Fabrication, biofunctionalization, and cell interactions. Prog. Polym. Sci 2010, 35, 868–892. [PubMed: 20582161]

(652). Fleischer S; Dvir T Tissue engineering on the nanoscale: Lessons from the heart. Curr. Opin. Biotech 2013, 24, 664–671. [PubMed: 23142543]

(653). Sapudom J; Rubner S; Martin S; Kurth T; Riedel S; Mierke CT; Pompe T The phenotype of cancer cell invasion controlled by fibril diameter and pore size of 3D collagen networks. Biomaterials 2015, 52, 367–375. [PubMed: 25818443]

(654). Lee NM; Erisken C; Iskratsch T; Sheetz M; Levine WN; Lu HH Polymer fiber-based models of connective tissue repair and healing. Biomaterials 2017, 112, 303–312. [PubMed: 27770633]

(655). Condeelis J; Segall JE Intravital imaging of cell movement in tumours. Nat. Rev. Cancer 2003, 3, 921–930. [PubMed: 14737122]

(656). Ma PX; Zhang R Synthetic nano-scale fibrous extracellular matrix. J. Biomed. Mater. Res 1999, 46, 60–72. [PubMed: 10357136]

(657). Yang F; Murugan R; Ramakrishna S; Wang X; Ma YX; Wang S Fabrication of nano-structured porous PLLA scaffold intended for nerve tissue engineering. Biomaterials 2004, 25, 1891–1900. [PubMed: 14738853]

(658). Liu X; Ma PX Phase separation, pore structure, and properties of nanofibrous gelatin scaffolds. Biomaterials 2009, 30, 4094–4103. [PubMed: 19481080]

(659). Lei B; Shin K-H; Noh D-Y; Jo I-H; Koh Y-H; Choi W-Y; Kim H-E Nanofibrous gelatin-silica hybrid scaffolds mimicking the native extracellular matrix (ECM) using thermally induced phase separation. J. Mater. Chem 2012, 22, 14133–14140.

(660). Barnes CP; Sell SA; Boland ED; Simpson DG; Bowlin GL Nanofiber technology: Designing the next generation of tissue engineering scaffolds. Adv. Drug Deliver. Rev 2007, 59, 1413–1433.

(661). Bhardwaj N; Kundu SC Electrospinning: A fascinating fiber fabrication technique. Biotechnol. Adv 2010, 28, 325–347. [PubMed: 20100560]

(662). Cui H; Webber MJ; Stupp SI Self-assembly of peptide amphiphiles: From molecules to nanostructures to biomaterials. Pept. Sci 2010, 94, 1–18.

(663). Hosseinkhani H; Hong P-D; Yu D-S Self-assembled proteins and peptides for regenerative medicine. Chem. Rev 2013, 113, 4837–4861. [PubMed: 23547530]

(664). Li D; Xia Y Electrospinning of nanofibers: Reinventing the wheel? Adv. Mater. 2004, 16, 1151–1170.

(665). Nerurkar NL; Baker BM; Sen S; Wible EE; Elliott DM; Mauck RL Nanofibrous biologic laminates replicate the form and function of the annulus fibrosus. Nat. Mater. 2009, 8, 986–992. [PubMed: 19855383]

(666). Liu W; Thomopoulos S; Xia Y Electrospun nanofibers for regenerative medicine. Adv. Healthc. Mater. 2012, 1, 10–25. [PubMed: 23184683]

(667). Sun B; Long YZ; Zhang HD; Li MM; Duvail JL; Jiang XY; Yin HL Advances in three-dimensional nanofibrous macrostructures via electrospinning. Prog. Polym. Sci 2014, 39, 862–890.

(668). Zhao G; Zhang X; Lu TJ; Xu F Recent advances in electrospun nanofibrous scaffolds for cardiac tissue engineering. Adv. Func. Mater. 2015, 25, 5726–5738.

(669). Zhang S Fabrication of novel biomaterials through molecular self-assembly. Nat. Biotechnol 2003, 21, 1171–1178. [PubMed: 14520402]

(670). Abou Neel EA; Bozec L; Knowles JC; Syed O; Mudera V; Day R; Hyun JK Collagen — Emerging collagen based therapies hit the patient. Adv. Drug Deliver. Rev 2013, 65, 429–456.

(671). Novak T; Seelbinder B; Twitchell CM; van Donkelaar CC; Voytik-Harbin SL; Neu CP Mechanisms and microenvironment investigation of cellularized high density gradient collagen matrices via densification. Adv. Func. Mater. 2016, 26, 2617–2628.

(672). Antman-Passig M; Shefi O Remote magnetic orientation of 3D collagen hydrogels for directed neuronal regeneration. Nano lett 2016, 16, 2567–2573. [PubMed: 26943183]

(673). Rudisill SG; DiVito MD; Hubel A; Stein A In vitro collagen fibril alignment via incorporation of nanocrystalline cellulose. Acta Biomater 2015, 12, 122–128. [PubMed: 25449923]

(674). Jean A; Engelmayr GC Anisotropic collagen fibrillogenesis within microfabricated scaffolds: Implications for biomimetic tissue engineering. Adv. Healthc. Mater. 2012, 1, 112–116. [PubMed: 23184695]

(675). Guo C; Kaufman LJ Flow and magnetic field induced collagen alignment. Biomaterials 2007, 28, 1105–1114. [PubMed: 17112582]

(676). Huang NF; Okogbaa J; Lee JC; Jha A; Zaitseva TS; Paukshto MV; Sun JS; Punjya N; Fuller GG; Cooke JP The modulation of endothelial cell morphology, function, and survival using

anisotropic nanofibrillar collagen scaffolds. Biomaterials 2013, 34, 4038–4047. [PubMed: 23480958]

(677). Han W; Chen S; Yuan W; Fan Q; Tian J; Wang X; Chen L; Zhang X; Wei W; Liu R; Qu J; Jiao Y; Austin RH; Liu L Oriented collagen fibers direct tumor cell intravasation. Proc. Natl. Acad. Sci. U.S.A 2016, 113, 11208–11213. [PubMed: 27663743]

(678). Schell JY; Wilks BT; Patel M; Franck C; Chalivendra V; Cao X; Shenoy VB; Morgan JR Harnessing cellular-derived forces in self-assembled microtissues to control the synthesis and alignment of ECM. Biomaterials 2016, 77, 120–129. [PubMed: 26610075]

(679). Heher P; Maleiner B; Prüller J; Teuschl AH; Kollmitzer J; Monforte X; Wolbank S; Redl H; Rünzler D; Fuchs C A novel bioreactor for the generation of highly aligned 3D skeletal muscle-like constructs through orientation of fibrin via application of static strain. Acta Biomater 2015, 24, 251–265. [PubMed: 26141153]

(680). Hoogenkamp HR; Bakker G-J; Wolf L; Suurs P; Dunnewind B; Barbut S; Friedl P; van Kuppevelt TH; Daamen WF Directing collagen fibers using counter-rotating cone extrusion. Acta Biomater 2015, 12, 113–121. [PubMed: 25462525]

(681). Liu Z; Zhu Y; Jiao D; Weng Z; Zhang Z; Ritchie RO Enhanced protective role in materials with gradient structural orientations: Lessons from Nature. Acta Biomater 2016, 44, 31–40. [PubMed: 27503833]

(682). Babaei B; Davarian A; Pryse KM; Elson EL; Genin GM Efficient and optimized identification of generalized Maxwell viscoelastic relaxation spectra. J. Mech. Behav. Biomed 2016, 55, 32–41.

(683). Woolfson DN; Mahmoud ZN More than just bare scaffolds: Towards multi-component and decorated fibrous biomaterials. Chem. Soc. Rev 2010, 39, 3464–3479. [PubMed: 20676443]

(684). Luo J; Tong YW Self-assembly of collagen-mimetic peptide amphiphiles into biofunctional nanofiber. ACS Nano 2011, 5, 7739–7747. [PubMed: 21899363]

(685). Vauthey S; Santoso S; Gong H; Watson N; Zhang S Molecular self-assembly of surfactant-like peptides to form nanotubes and nanovesicles. Proc. Natl. Acad. Sci. U.S.A 2002, 99, 5355–5360. [PubMed: 11929973]

(686). Hartgerink JD; Beniash E; Stupp SI Self-assembly and mineralization of peptide-amphiphile nanofibers. Science 2001, 294, 1684–1688. [PubMed: 11721046]

(687). Silva GA; Czeisler C; Niece KL; Beniash E; Harrington DA; Kessler JA; Stupp SI Selective differentiation of neural progenitor cells by high-epitope density nanofibers. Science 2004, 303, 1352. [PubMed: 14739465]

(688). Sur S; Pashuck ET; Guler MO; Ito M; Stupp SI; Launey T A hybrid nanofiber matrix to control the survival and maturation of brain neurons. Biomaterials 2012, 33, 545–555. [PubMed: 22018390]

(689). Chan CK; Kumar TS; Liao S; Murugan R; Ngiam M; Ramakrishnan S Biomimetic nanocomposites for bone graft applications. Nanomedicine 2006, 1, 177–188. [PubMed: 17716107]

(690). Sachlos E; Gotora D; Czernuszka JT Collagen scaffolds reinforced with biomimetic composite nano-sized carbonate-substituted hydroxyapatite crystals and shaped by rapid prototyping to contain internal microchannels. Tissue Eng 2006, 12, 2479–2487. [PubMed: 16995781]

(691). Zhang L; Rodriguez J; Raez J; Myles AJ; Fenniri H; Webster TJ Biologically inspired rosette nanotubes and nanocrystalline hydroxyapatite hydrogel nanocomposites as improved bone substitutes. Nanotechnology 2009, 20, 7480–7480.

(692). Roohani-Esfahani S-I; Nouri-Khorasani S; Lu Z; Appleyard R; Zreiqat H The influence hydroxyapatite nanoparticle shape and size on the properties of biphasic calcium phosphate scaffolds coated with hydroxyapatite–PCL composites. Biomaterials 2010, 31, 5498–5509. [PubMed: 20398935]

(693). Ramon-Azcon J; Ahadian S; Estili M; Liang XB; Ostrovidov S; Kaji H; Shiku H; Ramalingam M; Nakajima K; Sakka Y; Khademhosseini A; Matsue T Dielectrophoretically aligned carbon nanotubes to control electrical and mechanical properties of hydrogels to fabricate contractile muscle myofibers. Adv. Mater. 2013, 25, 4028–4034. [PubMed: 23798469]

(694). Dvir T; Timko BP; Brigham MD; Naik SR; Karajanagi SS; Levy O; Jin HW; Parker KK; Langer R; Kohane DS Nanowired three-dimensional cardiac patches. Nat. Nanotechnol 2011, 6, 720–725. [PubMed: 21946708]

(695). Li YH; Huang GY; Zhang XH; Li BQ; Chen YM; Lu TL; Lu TJ; Xu F Magnetic hydrogels and their potential biomedical applications. Adv. Funct. Mater. 2013, 23, 660–672.

(696). Wang K; Wang X; Han C; Hou W; Wang J; Chen L; Luo Y From micro to macro: The hierarchical design in a micropatterned scaffold for cell assembling and transplantation. Adv. Mater. 2017, 29, 1604600.

(697). Morgan KY; Sklaviadis D; Tochka ZL; Fischer KM; Hearon K; Morgan TD; Langer R; Freed LE Multi-material tissue engineering scaffold with hierarchical pore architecture. Adv. Func. Mater. 2016, 26, 5873–5883.

(698). Oh HH; Ko Y-G; Lu H; Kawazoe N; Chen G Preparation of porous collagen scaffolds with micropatterned structures. Adv. Mater. 2012, 24, 4311–4316. [PubMed: 22730266]

(699). Yang X-Y; Chen L-H; Li Y; Rooke JC; Sanchez C; Su B-L Hierarchically porous materials: Synthesis strategies and structure design. Chem. Soc. Rev 2017, 46, 481–558. [PubMed: 27906387]

(700). Kim D-H; Wong PK; Park J; Levchenko A; Sun Y Microengineered platforms for cell mechanobiology. Annu. Rev. Biomed. Eng 2009, 11, 203–233. [PubMed: 19400708]

(701). Han F; Zhu C; Guo Q; Yang H; Li B Cellular modulation by the elasticity of biomaterials. J. Mater. Chem. B 2016, 4, 9–26.

(702). Trappmann B; Gautrot JE; Connelly JT; Strange DGT; Li Y; Oyen ML; Cohen Stuart MA; Boehm H; Li B; Vogel V; Spatz JP; Watt FM; Huck WTS Extracellular-matrix tethering regulates stem-cell fate. Nat. Mater. 2012, 11, 642–649. [PubMed: 22635042]

(703). Choi CKK; Xu YJ; Wang B; Zhu M; Zhang L; Bian L Substrate coupling strength of integrin-binding ligands modulates adhesion, spreading, and differentiation of human mesenchymal stem cells. Nano lett 2015, 15, 6592–6600. [PubMed: 26390262]

(704). Discher DE; Janmey P; Wang Y.-l. Tissue cells feel and respond to the stiffness of their substrate. Science 2005, 310, 1139–1143. [PubMed: 16293750]

(705). Gilbert PM; Havenstrite KL; Magnusson KEG; Sacco A; Leonardi NA; Kraft P; Nguyen NK; Thrun S; Lutolf MP; Blau HM Substrate elasticity regulates skeletal muscle stem cell self-renewal in culture. Science 2010, 329, 1078–1081. [PubMed: 20647425]

(706). Vogel V; Sheetz M Local force and geometry sensing regulate cell functions. Nat. Rev. Mol. Cell Bio 2006, 7, 265–275. [PubMed: 16607289]

(707). Plotnikov Sergey V.; Pasapera Ana M.; Sabass B; Waterman Clare M. Force fluctuations within focal adhesions mediate ecm-rigidity sensing to guide directed cell migration. Cell 2012, 151, 1513–1527. [PubMed: 23260139]

(708). Swift J; Ivanovska IL; Buxboim A; Harada T; Dingal PCDP; Pinter J; Pajerowski JD; Spinler KR; Shin J-W; Tewari M; Rehfeldt F; Speicher DW; Discher DE Nuclear Lamin-A scales with tissue stiffness and enhances matrix-directed differentiation. Science 2013, 341, 1240104. [PubMed: 23990565]

(709). Yang C; Tibbitt MW; Basta L; Anseth KS Mechanical memory and dosing influence stem cell fate. Nat. Mater. 2014, 13, 645–652. [PubMed: 24633344]

(710). Aizawa Y; Owen SC; Shoichet MS Polymers used to influence cell fate in 3D geometry: New trends. Prog. Polym. Sci 2012, 37, 645–658.

(711). Brown RA; Wiseman M; Chuo CB; Cheema U; Nazhat SN Ultrarapid engineering of biomimetic materials and tissues: Fabrication of nano- and microstructures by plastic compression. Adv. Func. Mater. 2005, 15, 1762–1770.

(712). Levis HJ; Brown RA; Daniels JT Plastic compressed collagen as a biomimetic substrate for human limbal epithelial cell culture. Biomaterials 2010, 31, 7726–7737. [PubMed: 20674002]

(713). Huebsch N; Arany PR; Mao AS; Shvartsman D; Ali OA; Bencherif SA; Rivera-Feliciano J; Mooney DJ Harnessing traction-mediated manipulation of the cell/matrix interface to control stem-cell fate. Nat. Mater. 2010, 9, 518–526. [PubMed: 20418863]

(714). Marquez JP; Elson EL; Genin GM Whole cell mechanics of contractile fibroblasts: relations between effective cellular and extracellular matrix moduli. Philos. T. R. Soc. A 2010, 368, 635–654.

(715). Marquez JP; Genin GM; Pryse KM; Elson EL Cellular and matrix contributions to tissue construct stiffness increase with cellular concentration. Ann. Biomed. Eng 2006, 34, 1475–1482. [PubMed: 16874557]

(716). Marquez JP; Genin GM; Zahalak GI; Elson EL Thin bio-artificial tissues in plane stress: The relationship between cell and tissue strain, and an improved constitutive model. Biophys. J 2005, 88, 765–777. [PubMed: 15596492]

(717). Marquez JP; Genin GM; Zahalak GI; Elson EL The relationship between cell and tissue strain in three-dimensional bio-artificial tissues. Biophys. J. 2005, 88, 778–789. [PubMed: 15596491]

(718). Caliari SR; Vega SL; Kwon M; Soulas EM; Burdick JA Dimensionality and spreading influence MSC YAP/TAZ signaling in hydrogel environments. Biomaterials 2016, 103, 314–323. [PubMed: 27429252]

(719). Doyle AD; Carvajal N; Jin A; Matsumoto K; Yamada KM Local 3D matrix microenvironment regulates cell migration through spatiotemporal dynamics of contractility-dependent adhesions. Nat. Commun 2015, 6, 8720. [PubMed: 26548801]

(720). Li Y; Shi X; Tian L; Sun H; Wu Y; Li X; Li J; Wei Y; Han X; Zhang J; Jia X; Bai R; Jing L; Ding P; Liu H; Han D AuNP–collagen matrix with localized stiffness for cardiac-tissue engineering: enhancing the assembly of intercalated discs by β1-integrin-mediated signaling. Adv. Mater. 2016, 28, 10230–10235. [PubMed: 27723133]

(721). Storm C; Pastore JJ; MacKintosh FC; Lubensky TC; Janmey PA Nonlinear elasticity in biological gels. Nature 2005, 435, 191–194. [PubMed: 15889088]

(722). Motte S; Kaufman LJ Strain stiffening in collagen I networks. Biopolymers 2013, 99, 35–46. [PubMed: 23097228]

(723). Licup AJ; Münster S; Sharma A; Sheinman M; Jawerth LM; Fabry B; Weitz DA; MacKintosh FC Stress controls the mechanics of collagen networks. Proc. Natl. Acad. Sci. U.S.A 2015, 112, 9573–9578. [PubMed: 26195769]

(724). Wen Q; Janmey PA Effects of non-linearity on cell-ECM interactions. Exp. Cell Res 2013, 319, 2481–2489. [PubMed: 23748051]

(725). Hall MS; Alisafaei F; Ban E; Feng X; Hui C-Y; Shenoy VB; Wu M Fibrous nonlinear elasticity enables positive mechanical feedback between cells and ECMs. Proc. Natl. Acad. Sci. U.S.A 2016, 113, 14043–14048. [PubMed: 27872289]

(726). Winer JP; Oake S; Janmey PA Non-linear elasticity of extracellular matrices enables contractile cells to communicate local position and orientation. PLOS ONE 2009, 4, e6382. [PubMed: 19629190]

(727). Petrie RJ; Gavara N; Chadwick RS; Yamada KM Nonpolarized signaling reveals two distinct modes of 3D cell migration. J. Cell Biol 2012, 197, 439. [PubMed: 22547408]

(728). Petrie RJ; Yamada KM At the leading edge of three-dimensional cell migration. J. Cell Sci 2013, 125, 5917–5926.

(729). Kouwer PHJ; Koepf M; Le Sage VAA; Jaspers M; van Buul AM; Eksteen-Akeroyd ZH; Woltinge T; Schwartz E; Kitto HJ; Hoogenboom R; Picken SJ; Nolte RJM; Mendes E; Rowan AE Responsive biomimetic networks from polyisocyanopeptide hydrogels. Nature 2013, 493, 651–655. [PubMed: 23354048]

(730). Jaspers M; Dennison M; Mabesoone MFJ; MacKintosh FC; Rowan AE; Kouwer PHJ Ultra-responsive soft matter from strain-stiffening hydrogels. Nat. Commun 2014, 5, 5808. [PubMed: 25510333]

(731). Muller C; Muller A; Pompe T Dissipative interactions in cell-matrix adhesion. Soft Matter 2013, 9, 6207–6216.

(732). Nekouzadeh A; Pryse KM; Elson EL; Genin GM A simplified approach to quasi-linear viscoelastic modeling. J. Biomech 2007, 40, 3070–3078. [PubMed: 17499254]

(733). Okay O; Oppermann W Polyacrylamide–clay nanocomposite hydrogels: Rheological and light scattering characterization. Macromolecules 2007, 40, 3378–3387.

(734). Chang C-W; van Spreeuwel A; Zhang C; Varghese S PEG/clay nanocomposite hydrogel: A mechanically robust tissue engineering scaffold. Soft Matter 2010, 6, 5157–5164.

(735). Park YD; Tirelli N; Hubbell JA Photopolymerized hyaluronic acid-based hydrogels and interpenetrating networks. Biomaterials 2003, 24, 893–900. [PubMed: 12504509]

(736). Wong Po Foo CTS; Lee JS; Mulyasasmita W; Parisi-Amon A; Heilshorn SC Two-component protein-engineered physical hydrogels for cell encapsulation. Proc. Natl. Acad. Sci. U.S.A 2009, 106, 22067–22072. [PubMed: 20007785]

(737). Zhao X; Huebsch N; Mooney DJ; Suo Z Stress-relaxation behavior in gels with ionic and covalent crosslinks. J. Appl. Phys 2010, 107, 063509.

(738). Schultz KM; Kyburz KA; Anseth KS Measuring dynamic cell–material interactions and remodeling during 3D human mesenchymal stem cell migration in hydrogels. Proc. Natl. Acad. Sci. U.S.A 2015, 112, E3757–E3764. [PubMed: 26150508]

(739). Cameron AR; Frith JE; Gomez GA; Yap AS; Cooper-White JJ The effect of time-dependent deformation of viscoelastic hydrogels on myogenic induction and Rac1 activity in mesenchymal stem cells. Biomaterials 2014, 35, 1857–1868. [PubMed: 24331708]

(740). Chaudhuri O; Gu L; Darnell M; Klumpers D; Bencherif SA; Weaver JC; Huebsch N; Mooney DJ Substrate stress relaxation regulates cell spreading. Nat. Commun 2015, 6, 6365.

(741). McKinnon DD; Domaille DW; Cha JN; Anseth KS Biophysically defined and cytocompatible covalently adaptable networks as viscoelastic 3d cell culture systems. Adv. Mater. 2014, 26, 865–872. [PubMed: 24127293]

(742). McKinnon DD; Domaille DW; Brown TE; Kyburz KA; Kiyotake E; Cha JN; Anseth KS Measuring cellular forces using bis-aliphatic hydrazone crosslinked stress-relaxing hydrogels. Soft Matter 2014, 10, 9230–9236. [PubMed: 25265090]

(743). Münster S; Jawerth LM; Leslie BA; Weitz JI; Fabry B; Weitz DA Strain history dependence of the nonlinear stress response of fibrin and collagen networks. Proc. Natl. Acad. Sci. U.S.A 2013, 110, 12197–12202. [PubMed: 23754380]

(744). Nam S; Hu KH; Butte MJ; Chaudhuri O Strain-enhanced stress relaxation impacts nonlinear elasticity in collagen gels. Proc. Natl. Acad. Sci. U.S.A 2016, 113, 5492–5497. [PubMed: 27140623]

(745). Sun TL; Kurokawa T; Kuroda S; Ihsan AB; Akasaki T; Sato K; Haque MA; Nakajima T; Gong JP Physical hydrogels composed of polyampholytes demonstrate high toughness and viscoelasticity. Nat. Mater. 2013, 12, 932–937. [PubMed: 23892784]

(746). Xu D; Huang J; Zhao D; Ding B; Zhang L; Cai J High-flexibility, high-toughness double-cross-linked chitin hydrogels by sequential chemical and physical cross-linkings. Adv. Mater. 2016, 28, 5844–5849. [PubMed: 27158931]

(747). Zhao D; Huang J; Zhong Y; Li K; Zhang L; Cai J High-strength and high-toughness double-cross-linked cellulose hydrogels: A new strategy using sequential chemical and physical cross-linking. Adv. Func. Mater. 2016, 26, 6279–6287.

(748). Yang Y; Wang X; Yang F; Shen H; Wu D A universal soaking strategy to convert composite hydrogels into extremely tough and rapidly recoverable double-network hydrogels. Adv. Mater. 2016, 28, 7178–7184. [PubMed: 27301068]

(749). Andreu I; Luque T; Sancho A; Pelacho B; Iglesias-García O; Melo E; Farré R; Prósper F; Elizalde MR; Navajas D Heterogeneous micromechanical properties of the extracellular matrix in healthy and infarcted hearts. Acta Biomater 2014, 10, 3235–3242. [PubMed: 24717359]

(750). Wang L; Li Y; Huang G; Zhang X; Pingguan-Murphy B; Gao B; Lu TJ; Xu F Hydrogel-based methods for engineering cellular microenvironment with spatiotemporal gradients. Crit. Rev. Biotechnol 2016, 36, 553–565. [PubMed: 25641330]

(751). Whang M; Kim J Synthetic hydrogels with stiffness gradients for durotaxis study and tissue engineering scaffolds. Tissue Eng. Regen. Med 2016, 13, 126–139. [PubMed: 30603392]

(752). Sunyer R; Conte V; Escribano J; Elosegui-Artola A; Labernadie A; Valon L; Navajas D; García-Aznar JM; Muñoz JJ; Roca-Cusachs P; Trepat X Collective cell durotaxis emerges from long-range intercellular force transmission. Science 2016, 353, 1157. [PubMed: 27609894]

(753). Nemir S; Hayenga HN; West JL PEGDA hydrogels with patterned elasticity: Novel tools for the study of cell response to substrate rigidity. Biotechnol. Bioeng 2010, 105, 636–644. [PubMed: 19816965]

(754). Tse JR; Engler AJ Stiffness gradients mimicking in vivo tissue variation regulate mesenchymal stem cell fate. PLOS ONE 2011, 6, e15978. [PubMed: 21246050]

(755). Wong S; Guo W-H; Wang Y-L Fibroblasts probe substrate rigidity with filopodia extensions before occupying an area. Proc. Natl. Acad. Sci. U.S.A 2014, 111, 17176–17181. [PubMed: 25404288]

(756). Samorezov JE; Morlock CM; Alsberg E Dual ionic and photo-crosslinked alginate hydrogels for micropatterned spatial control of material properties and cell behavior. Bioconjugate Chem 2015, 26, 1339–1347.

(757). Hui Z; Xiaokang L; Shan Z; Yang Z; Long Z; Haiyan D; Wei S; Yanan D Microengineered in vitro model of cardiac fibrosis through modulating myofibroblast mechanotransduction. Biofabrication 2014, 6, 045009. [PubMed: 25378063]

(758). Yang C; DelRio FW; Ma H; Killaars AR; Basta LP; Kyburz KA; Anseth KS Spatially patterned matrix elasticity directs stem cell fate. Proc. Natl. Acad. Sci. U.S.A 2016, 113, E4439–E4445. [PubMed: 27436901]

(759). Kobel S; Lutolf MP Biomaterials meet microfluidics: building the next generation of artificial niches. Curr. Opin. Biotech 2011, 22, 690–697. [PubMed: 21821410]

(760). Colosi C; Shin SR; Manoharan V; Massa S; Costantini M; Barbetta A; Dokmeci MR; Dentini M; Khademhosseini A Microfluidic bioprinting of heterogeneous 3d tissue constructs using low-viscosity bioink. Adv. Mater. 2015, 28, 677–684. [PubMed: 26606883]

(761). Polacheck WJ; Li R; Uzel SGM; Kamm RD Microfluidic platforms for mechanobiology. Lab Chip 2013, 13, 2252–2267. [PubMed: 23649165]

(762). Du YN; Hancock MJ; He JK; Villa-Uribe JL; Wang B; Cropek DM; Khademhosseini A Convection-driven generation of long-range material gradients. Biomaterials 2010, 31, 2686–2694. [PubMed: 20035990]

(763). Choi JK; Agarwal P; Huang H; Zhao S; He X The crucial role of mechanical heterogeneity in regulating follicle development and ovulation with engineered ovarian microtissue. Biomaterials 2014, 35, 5122–5128. [PubMed: 24702961]

(764). Dingal PCDP; Bradshaw AM; Cho S; Raab M; Buxboim A; Swift J; Discher DE Fractal heterogeneity in minimal matrix models of scars modulates stiff-niche stem-cell responses via nuclear exit of a mechanorepressor. Nat. Mater. 2015, 14, 951–960. [PubMed: 26168347]

(765). Han WM; Heo S-J; Driscoll TP; Delucca JF; McLeod CM; Smith LJ; Duncan RL; Mauck RL; Elliott DM Microstructural heterogeneity directs micromechanics and mechanobiology in native and engineered fibrocartilage. Nat. Mater. 2016, 15, 477–484. [PubMed: 26726994]

(766). Choi YS; Vincent LG; Lee AR; Kretchmer KC; Chirasatitsin S; Dobke MK; Engler AJ The alignment and fusion assembly of adipose-derived stem cells on mechanically patterned matrices. Biomaterials 2012, 33, 6943–6951. [PubMed: 22800539]

(767). Tseng P; Di Carlo D Substrates with patterned extracellular matrix and subcellular stiffness gradients reveal local biomechanical responses. Adv. Mater. 2014, 26, 1242–1247. [PubMed: 24323894]

(768). Millon LE; Mohammadi H; Wan WK Anisotropic polyvinyl alcohol hydrogel for cardiovascular applications. J. Biomed. Mater. Res. B 2006, 79B, 305–311.

(769). Hudson SD; Hutter JL; Nieh M-P; Pencer J; Millon LE; Wan W Characterization of anisotropic poly(vinyl alcohol) hydrogel by small- and ultra-small-angle neutron scattering. J. Chem. Phys 2009, 130, 034903. [PubMed: 19173539]

(770). Oh SH; An DB; Kim TH; Lee JH Wide-range stiffness gradient PVA/HA hydrogel to investigate stem cell differentiation behavior. Acta Biomater 2016, 35, 23–31. [PubMed: 26883774]

(771). Alapan Y; Younesi M; Akkus O; Gurkan UA Anisotropically stiff 3D micropillar niche induces extraordinary cell alignment and elongation. Adv. Healthc. Mater. 2016, 5, 1884–1892. [PubMed: 27191679]

(772). Deymier AC; An Y; Boyle JJ; Schwartz AG; Birman V; Genin GM; Thomopoulos S; Barber AH Micro-mechanical properties of the tendon-to-bone attachment. Acta Biomater 2017, 56, 25–35. [PubMed: 28088669]

(773). Genin GM; Thomopoulos S The tendon-to-bone attachment: Unification through disarray. Nat. Mater. 2017, 16, 607–608. [PubMed: 28541313]

(774). Rossetti L; Kuntz LA; Kunold E; Schock J; Muller KW; Grabmayr H; Stolberg-Stolberg J; Pfeiffer F; Sieber SA; Burgkart R; Bausch AR The microstructure and micromechanics of the tendon-bone insertion. Nat. Mater 2017, 16, 664–670. [PubMed: 28250445]

(775). Berry MF; Engler AJ; Woo YJ; Pirolli TJ; Bish LT; Jayasankar V; Morine KJ; Gardner TJ; Discher DE; Sweeney HL Mesenchymal stem cell injection after myocardial infarction improves myocardial compliance. Am. J. Physiol. Heart. Circ. Physiol 2006, 290, H2196–2203. [PubMed: 16473959]

(776). Jansen Karin A.; Bacabac Rommel G.; Piechocka Izabela K.; Koenderink Gijsje H. Cells actively stiffen fibrin networks by generating contractile stress. Biophys. J 2013, 105, 2240–2251. [PubMed: 24268136]

(777). Georges PC; Hui J-J; Gombos Z; McCormick ME; Wang AY; Uemura M; Mick R; Janmey PA; Furth EE; Wells RG Increased stiffness of the rat liver precedes matrix deposition: implications for fibrosis. Am. J. Physiol. Gastr. L. Physiol 2007, 293, G1147–G1154.

(778). Cosgrove BD; Gilbert PM; Porpiglia E; Mourkioti F; Lee SP; Corbel SY; Llewellyn ME; Delp SL; Blau HM Rejuvenation of the muscle stem cell population restores strength to injured aged muscles. Nat. Med 2014, 20, 255–264. [PubMed: 24531378]

(779). Gurtner GC; Werner S; Barrandon Y; Longaker MT Wound repair and regeneration. Nature 2008, 453, 314–321. [PubMed: 18480812]

(780). Liu F; Mih JD; Shea BS; Kho AT; Sharif AS; Tager AM; Tschumperlin DJ Feedback amplification of fibrosis through matrix stiffening and COX-2 suppression. J. Cell Biol 2010, 190, 693–706. [PubMed: 20733059]

(781). Schroer AK; Merryman WD Mechanobiology of myofibroblast adhesion in fibrotic cardiac disease. J. Cell Sci 2015, 128, 1865–1875. [PubMed: 25918124]

(782). Yong KW; Li YH; Huang GY; Lu TJ; Safwani WKZW; Pingguan-Murphy B; Xu F Mechano-regulation of cardiac myofibroblast differentiation: implications for cardiac fibrosis and therapy. Am. J. Physiol. Heart. Circ. Physiol 2015, 309, H532–H542. [PubMed: 26092987]

(783). Levental KR; Yu H; Kass L; Lakins JN; Egeblad M; Erler JT; Fong SFT; Csiszar K; Giaccia A; Weninger W; Yamauchi M; Gasser DL; Weaver VM Matrix crosslinking forces tumor progression by enhancing integrin signaling. Cell 2009, 139, 891–906. [PubMed: 19931152]

(784). Acerbi I; Cassereau L; Dean I; Shi Q; Au A; Park C; Chen YY; Liphardt J; Hwang ES; Weaver VM Human breast cancer invasion and aggression correlates with ECM stiffening and immune cell infiltration. Integr. Biol 2015, 7, 1120–1134.

(785). Bordeleau F; Mason BN; Lollis EM; Mazzola M; Zanotelli MR; Somasegar S; Califano JP; Montague C; LaValley DJ; Huynh J; Mencia-Trinchant N; Negrón Abril YL; Hassane DC; Bonassar LJ; Butcher JT; Weiss RS; Reinhart-King CA Matrix stiffening promotes a tumor vasculature phenotype. Proc. Natl. Acad. Sci. U.S.A 2017, 114, 492–497. [PubMed: 28034921]

(786). Uto K; Tsui JH; DeForest CA; Kim D-H Dynamically tunable cell culture platforms for tissue engineering and mechanobiology. Prog. Polym. Sci 2017, 65, 53–82. [PubMed: 28522885]

(787). Young JL; Engler AJ Hydrogels with time-dependent material properties enhance cardiomyocyte differentiation in vitro. Biomaterials 2011, 32, 1002–1009. [PubMed: 21071078]

(788). Marklein RA; Soranno DE; Burdick JA Magnitude and presentation of mechanical signals influence adult stem cell behavior in 3-dimensional macroporous hydrogels. Soft Matter 2012, 8, 8113–8120.

(789). Liu H-Y; Greene T; Lin T-Y; Dawes CS; Korc M; Lin C-C Enzyme-mediated stiffening hydrogels for probing activation of pancreatic stellate cells. Acta Biomater 2017, 48, 258–269. [PubMed: 27769941]

(790). Guvendiren M; Burdick JA Stiffening hydrogels to probe short- and long-term cellular responses to dynamic mechanics. Nat. Commun 2012, 3, 792. [PubMed: 22531177]

(791). Guvendiren M; Perepelyuk M; Wells RG; Burdick JA Hydrogels with differential and patterned mechanics to study stiffness-mediated myofibroblastic differentiation of hepatic stellate cells. J. Mech. Behav. Biomed 2014, 38, 198–208.

(792). Mabry KM; Lawrence RL; Anseth KS Dynamic stiffening of poly(ethylene glycol)-based hydrogels to direct valvular interstitial cell phenotype in a three-dimensional environment. Biomaterials 2015, 49, 47–56. [PubMed: 25725554]

(793). Moeendarbary E; Weber IP; Sheridan GK; Koser DE; Soleman S; Haenzi B; Bradbury EJ; Fawcett J; Franze K The soft mechanical signature of glial scars in the central nervous system. Nat. Commun 2017, 8, 14787. [PubMed: 28317912]

(794). Frey MT; Wang Y.-l. A photo-modulatable material for probing cellular responses to substrate rigidity. Soft Matter 2009, 5, 1918–1924. [PubMed: 19672325]

(795). Truong VX; Tsang KM; Simon GP; Boyd RL; Evans RA; Thissen H; Forsythe JS Photodegradable gelatin-based hydrogels prepared by bioorthogonal click chemistry for cell encapsulation and release. Biomacromolecules 2015, 16, 2246–2253. [PubMed: 26056855]

(796). Kloxin AM; Tibbitt MW; Kasko AM; Fairbairn JA; Anseth KS Tunable hydrogels for external manipulation of cellular microenvironments through controlled photodegradation. Adv. Mater. 2010, 22, 61–66. [PubMed: 20217698]

(797). Kloxin AM; Benton JA; Anseth KS In situ elasticity modulation with dynamic substrates to direct cell phenotype. Biomaterials 2010, 31, 1–8. [PubMed: 19788947]

(798). Wang H; Haeger SM; Kloxin AM; Leinwand LA; Anseth KS Redirecting valvular myofibroblasts into dormant fibroblasts through light-mediated reduction in substrate modulus. PLOS ONE 2012, 7, e39969. [PubMed: 22808079]

(799). Kirschner CM; Alge DL; Gould ST; Anseth KS Clickable, photodegradable hydrogels to dynamically modulate valvular interstitial cell phenotype. Adv. Healthc. Mater. 2014, 3, 649–657. [PubMed: 24459068]

(800). Wang H; Tibbitt MW; Langer SJ; Leinwand LA; Anseth KS Hydrogels preserve native phenotypes of valvular fibroblasts through an elasticity-regulated PI3K/AKT pathway. Proc. Natl. Acad. Sci. U.S.A 2013, 110, 19336–19341. [PubMed: 24218588]

(801). Dixon JE; Shah DA; Rogers C; Hall S; Weston N; Parmenter CDJ; McNally D; Denning C; Shakesheff KM Combined hydrogels that switch human pluripotent stem cells from self-renewal to differentiation. Proc. Natl. Acad. Sci. U.S.A 2014, 111, 5580–5585. [PubMed: 24706900]

(802). Gillette BM; Jensen JA; Wang MX; Tchao J; Sia SK Dynamic hydrogels: Switching of 3D microenvironments using two-component naturally derived extracellular matrices. Adv. Mater. 2010, 22, 686–691. [PubMed: 20217770]

(803). Hackelbusch S; Rossow T; Steinhilber D; Weitz DA; Seiffert S Hybrid microgels with thermo-tunable elasticity for controllable cell confinement. Adv. Healthc. Mater. 2015, 4, 1841–1848. [PubMed: 26088728]

(804). Yoshikawa HY; Rossetti FF; Kaufmann S; Kaindl T; Madsen J; Engel U; Lewis AL; Armes SP; Tanaka M Quantitative evaluation of mechanosensing of cells on dynamically tunable hydrogels. J. Am. Chem. Soc 2011, 133, 1367–1374. [PubMed: 21218794]

(805). Jiang FX; Yurke B; Schloss RS; Firestein BL; Langrana NA The relationship between fibroblast growth and the dynamic stiffnesses of a DNA crosslinked hydrogel. Biomaterials 2010, 31, 1199–1212. [PubMed: 19931905]

(806). Jiang FX; Yurke B; Schloss RS; Firestein BL; Langrana NA Effect of dynamic stiffness of the substrates on neurite outgrowth by using a DNA-crosslinked hydrogel. Tissue Eng. Part A 2010, 16, 1873–1889. [PubMed: 20067396]

(807). Previtera M; Trout K; Verma D; Chippada U; Schloss R; Langrana N Fibroblast morphology on dynamic softening of hydrogels. Ann. Biomed. Eng 2012, 40, 1061–1072. [PubMed: 22160600]

(808). Shih H; Lin C-C Tuning stiffness of cell-laden hydrogel via host-guest interactions. J. Mater. Chem. B 2016, 4, 4969–4974.

(809). Stowers RS; Allen SC; Suggs LJ Dynamic phototuning of 3D hydrogel stiffness. Proc. Natl. Acad. Sci. U.S.A 2015, 112, 1953–1958. [PubMed: 25646417]

(810). Rosales AM; Anseth KS The design of reversible hydrogels to capture extracellular matrix dynamics. Nat. Rev. Mater. 2016, 1, 15012. [PubMed: 29214058]

(811). Wei Z; Zhao J; Chen YM; Zhang P; Zhang Q Self-healing polysaccharide-based hydrogels as injectable carriers for neural stem cells. Sci. Rep 2016, 6, 37841. [PubMed: 27897217]

(812). Wei Z; Yang JH; Liu ZQ; Xu F; Zhou JX; Zrínyi M; Osada Y; Chen YM Novel biocompatible polysaccharide-based self-healing hydrogel. Adv. Func. Mater. 2015, 25, 1352–1359.

(813). Wei Z; Yang JH; Zhou J; Xu F; Zrinyi M; Dussault PH; Osada Y; Chen YM Self-healing gels based on constitutional dynamic chemistry and their potential applications. Chem. Soc. Rev 2014.

(814). Schiller HB; Fässler R Mechanosensitivity and compositional dynamics of cell–matrix adhesions. Embo Rep 2013, 14, 509–519. [PubMed: 23681438]

(815). Wei WC; Lin HH; Shen MR; Tang MJ Mechanosensing machinery for cells under low substratum rigidity. Am. J. Physiol. Cell Physiol 2008, 295, C1579. [PubMed: 18923058]

(816). Wang N; Tytell JD; Ingber DE Mechanotransduction at a distance: Mechanically coupling the extracellular matrix with the nucleus. Nat. Rev. Mol. Cell Bio 2009, 10, 75–82. [PubMed: 19197334]

(817). Feng X-Q; Lee PVS; Lim CT Preface: molecular, cellular, and tissue mechanobiology. Acta Mechanica Sinica 2017, 33, 219–221.

(818). Giannone G; Sheetz MP Substrate rigidity and force define form through tyrosine phosphatase and kinase pathways. Trends Cell Biol 2006, 16, 213–223. [PubMed: 16529933]

(819). Jin H; Zhang Y; Jing D; Yu S; Ge T; Huang S; Zhao Z Mechanobiology of mesenchymal stem cells: A new perspective into the mechanically induced MSC fate. Acta Biomater 2015, 20, 1–9. [PubMed: 25871537]

(820). Cho S; Irianto J; Discher DE Mechanosensing by the nucleus: From pathways to scaling relationships. J. Cell Biol 2017, 216, 305–315. [PubMed: 28043971]

(821). Östlund C; Folker ES; Choi JC; Gomes ER; Gundersen GG; Worman HJ Dynamics and molecular interactions of linker of nucleoskeleton and cytoskeleton (LINC) complex proteins. J. Cell Sci 2009, 122, 4099. [PubMed: 19843581]

(822). Changede R; Sheetz M Integrin and cadherin clusters: A robust way to organize adhesions for cell mechanics. Bioessays 2016, 39, 1600123.

(823). Cho S; Irianto J; Discher DE Mechanosensing by the nucleus: From pathways to scaling relationships. Journal of Cell Biology 2017.

(824). Enyedi B; Niethammer P Nuclear membrane stretch and its role in mechanotransduction. Nucleus 2017, 8, 156–161. [PubMed: 28112995]

(825). Discher DE; Smith L; Cho S; Colasurdo M; García AJ; Safran S Matrix Mechanosensing: From Scaling Concepts in ‘Omics Data to Mechanisms in the Nucleus, Regeneration, and Cancer. Annu. Rev. Biophys 2017, 46, 295–315. [PubMed: 28532215]

(826). Nicodemus GD; Bryant SJ Cell encapsulation in biodegradable hydrogels for tissue engineering applications. Tissue Eng. Part B Rev 2008, 14, 149–165. [PubMed: 18498217]

(827). Li YL; Rodrigues J; Tomas H Injectable and biodegradable hydrogels: Gelation, biodegradation and biomedical applications. Chem. Soc. Rev 2012, 41, 2193–2221. [PubMed: 22116474]

(828). Bratt-Leal AM; Carpenedo RL; Ungrin MD; Zandstra PW; McDevitt TC Incorporation of biomaterials in multicellular aggregates modulates pluripotent stem cell differentiation. Biomaterials 2011, 32, 48–56. [PubMed: 20864164]

(829). Barradas AMC; Fernandes HAM; Groen N; Chai YC; Schrooten J; van de Peppel J; van Leeuwen JPTM; van Blitterswijk CA; de Boer J A calcium-induced signaling cascade leading to osteogenic differentiation of human bone marrow-derived mesenchymal stromal cells. Biomaterials 2012, 33, 3205–3215. [PubMed: 22285104]

(830). Shih Y-RV; Hwang Y; Phadke A; Kang H; Hwang NS; Caro EJ; Nguyen S; Siu M; Theodorakis EA; Gianneschi NC; Vecchio KS; Chien S; Lee OK; Varghese S Calcium phosphate-bearing matrices induce osteogenic differentiation of stem cells through adenosine signaling. Proc. Natl. Acad. Sci. U.S.A 2014, 111, 990–995. [PubMed: 24395775]

(831). O’Reilly MS; Boehm T; Shing Y; Fukai N; Vasios G; Lane WS; Flynn E; Birkhead JR; Olsen BR; Folkman J Endostatin: An endogenous inhibitor of angiogenesis and tumor growth. Cell 1997, 88, 277–285. [PubMed: 9008168]

(832). Sudhakar A; Sugimoto H; Yang C; Lively J; Zeisberg M; Kalluri R Human tumstatin and human endostatin exhibit distinct antiangiogenic activities mediated by αvβ3 and α5β1 integrins. Proc. Natl. Acad. Sci. U.S.A 2003, 100, 4766–4771. [PubMed: 12682293]

(833). Lampe KJ; Bjugstad KB; Mahoney MJ Impact of degradable macromer content in a poly(ethylene glycol) hydrogel on neural cell metabolic activity, redox state, proliferation, and differentiatio. Tissue Eng. Part A 2010, 16, 1857–1866. [PubMed: 20067398]

(834). Lampe KJ; Namba RM; Silverman TR; Bjugstad KB; Mahoney MJ Impact of lactic acid on cell proliferation and free radical-induced cell death in monolayer cultures of neural precursor cells. Biotechnol. Bioeng 2009, 103, 1214–1223. [PubMed: 19408314]

(835). Fonseca KB; Granja PL; Barrias CC Engineering proteolytically-degradable artificial extracellular matrices. Prog. Polym. Sci 2014, 39, 2010–2029.

(836). Kopeček J; Kopečková P HPMA copolymers: Origins, early developments, present, and future. Adv. Drug Deliver. Rev 2010, 62, 122–149.

(837). Lutolf MP; Lauer-Fields JL; Schmoekel HG; Metters AT; Weber FE; Fields GB; Hubbell JA Synthetic matrix metalloproteinase-sensitive hydrogels for the conduction of tissue regeneration: Engineering cell-invasion characteristics. Proc. Natl. Acad. Sci. U.S.A 2003, 100, 5413–5418. [PubMed: 12686696]

(838). Lutolf MP; Raeber GP; Zisch AH; Tirelli N; Hubbell JA Cell-responsive synthetic hydrogels. Adv. Mater. 2003, 15, 888–892.

(839). Lutolf MP; Weber FE; Schmoekel HG; Schense JC; Kohler T; Muller R; Hubbell JA Repair of bone defects using synthetic mimetics of collagenous extracellular matrices. Nat. Biotechnol 2003, 21, 513–518. [PubMed: 12704396]

(840). Phelps EA; Landázuri N; Thulé PM; Taylor WR; García AJ Bioartificial matrices for therapeutic vascularization. Proc. Natl. Acad. Sci. U.S.A 2010, 107, 3323–3328. [PubMed: 20080569]

(841). Anderson SB; Lin C-C; Kuntzler DV; Anseth KS The performance of human mesenchymal stem cells encapsulated in cell-degradable polymer-peptide hydrogels. Biomaterials 2011, 32, 3564–3574. [PubMed: 21334063]

(842). Patterson J; Hubbell JA Enhanced proteolytic degradation of molecularly engineered PEG hydrogels in response to MMP-1 and MMP-2. Biomaterials 2010, 31, 7836–7845. [PubMed: 20667588]

(843). Aimetti AA; Tibbitt MW; Anseth KS Human neutrophil elastase responsive delivery from poly(ethylene glycol) hydrogels. Biomacromolecules 2009, 10, 1484–1489. [PubMed: 19408953]

(844). Aimetti AA; Machen AJ; Anseth KS Poly(ethylene glycol) hydrogels formed by thiol-ene photopolymerization for enzyme-responsive protein delivery. Biomaterials 2009, 30, 6048–6054. [PubMed: 19674784]

(845). Patterson J; Hubbell JA SPARC-derived protease substrates to enhance the plasmin sensitivity of molecularly engineered PEG hydrogels. Biomaterials 2011, 32, 1301–1310. [PubMed: 21040970]

(846). Jo YS; Rizzi SC; Ehrbar M; Weber FE; Hubbell JA; Lutolf MP Biomimetic PEG hydrogels crosslinked with minimal plasmin-sensitive tri-amino acid peptides. J. Biomed. Mater. Res. A 2010, 93A, 870–877.

(847). Khetan S; Katz JS; Burdick JA Sequential crosslinking to control cellular spreading in 3-dimensional hydrogels. Soft Matter 2009, 5, 1601–1606.

(848). Khetan S; Burdick JA Patterning network structure to spatially control cellular remodeling and stem cell fate within 3-dimensional hydrogels. Biomaterials 2010, 31, 8228–8234. [PubMed: 20674004]

(849). Hanjaya-Putra D; Wong KT; Hirotsu K; Khetan S; Burdick JA; Gerecht S Spatial control of cell-mediated degradation to regulate vasculogenesis and angiogenesis in hyaluronan hydrogels. Biomaterials 2012, 33, 6123–6131. [PubMed: 22672833]

(850). Parmar PA; Skaalure SC; Chow LW; St-Pierre J-P; Stoichevska V; Peng YY; Werkmeister JA; Ramshaw JAM; Stevens MM Temporally degradable collagen–mimetic hydrogels tuned to chondrogenesis of human mesenchymal stem cells. Biomaterials 2016, 99, 56–71. [PubMed: 27214650]

(851). Kerkelä E; Saarialho-Kere U Matrix metalloproteinases in tumor progression: focus on basal and squamous cell skin cancer. Exp. Dermatol 2003, 12, 109–125. [PubMed: 12702139]

(852). Tan J-X; Wang X-Y; Li H-Y; Su X-L; Wang L; Ran L; Zheng K; Ren G-S HYAL1 overexpression is correlated with the malignant behavior of human breast cancer. Int. J. Cancer 2011, 128, 1303–1315. [PubMed: 20473947]

(853). Spinale FG Myocardial matrix remodeling and the matrix metalloproteinases: Influence on cardiac form and function. Physiol. Rev 2007, 87, 1285–1342. [PubMed: 17928585]

(854). Burrage PS; Mix KS; Brinckerhoff CE In Frontiers in Bioscience: A Journal and Virtual Library, 2006; Vol. 11.

(855). Lee F; Chung JE; Kurisawa M An injectable hyaluronic acid–tyramine hydrogel system for protein delivery. J. Control. Release 2009, 134, 186–193. [PubMed: 19121348]

(856). Tauro JR; Gemeinhart RA Matrix metalloprotease triggered delivery of cancer chemotherapeutics from hydrogel matrixes. Bioconjugate Chem 2005, 16, 1133–1139.

(857). Foster GA; Headen DM; González-García C; Salmerón-Sánchez M; Shirwan H; García AJ Protease-degradable microgels for protein delivery for vascularization. Biomaterials 2017, 113, 170–175. [PubMed: 27816000]

(858). Zhang Z; Ni J; Chen L; Yu L; Xu J; Ding J Biodegradable and thermoreversible PCLA–PEG–PCLA hydrogel as a barrier for prevention of post-operative adhesion. Biomaterials 2011, 32, 4725–4736. [PubMed: 21482434]

(859). Wang F; Li Z; Khan M; Tamama K; Kuppusamy P; Wagner WR; Sen CK; Guan J Injectable, rapid gelling and highly flexible hydrogel composites as growth factor and cell carriers. Acta Biomater 2010, 6, 1978–1991. [PubMed: 20004745]

(860). Galperin A; Long TJ; Ratner BD Degradable, thermo-sensitive poly(N-isopropyl acrylamide)-based scaffolds with controlled porosity for tissue engineering applications. Biomacromolecules 2010, 11, 2583–2592. [PubMed: 20836521]

(861). Patenaude M; Hoare T Injectable, degradable thermoresponsive poly(N-isopropylacrylamide) hydrogels. ACS Macro Lett 2012, 1, 409–413.

(862). Boontheekul T; Kong H-J; Mooney DJ Controlling alginate gel degradation utilizing partial oxidation and bimodal molecular weight distribution. Biomaterials 2005, 26, 2455–2465. [PubMed: 15585248]

(863). Ashton RS; Banerjee A; Punyani S; Schaffer DV; Kane RS Scaffolds based on degradable alginate hydrogels and poly(lactide-co-glycolide) microspheres for stem cell culture. Biomaterials 2007, 28, 5518–5525. [PubMed: 17881048]

(864). Boontheekul T; Hill EE; Kong H-J; Mooney DJ Regulating myoblast phenotype through controlled gel stiffness and degradation. Tissue Eng 2007, 13, 1431–1442. [PubMed: 17561804]

(865). Lee KY; Mooney DJ Alginate: Properties and biomedical applications. Prog. Polym. Sci 2012, 37, 106–126. [PubMed: 22125349]

(866). Ruvinov E; Cohen S Alginate biomaterial for the treatment of myocardial infarction: progress, translational strategies, and clinical outlook: from ocean algae to patient bedside. Adv. Drug Deliver. Rev 2016, 96, 54–76.

(867). Patterson J; Siew R; Herring SW; Lin ASP; Guldberg R; Stayton PS Hyaluronic acid hydrogels with controlled degradation properties for oriented bone regeneration. Biomaterials 2010, 31, 6772–6781. [PubMed: 20573393]

(868). Rydholm AE; Anseth KS; Bowman CN Effects of neighboring sulfides and pH on ester hydrolysis in thiol–acrylate photopolymers. Acta Biomater 2007, 3, 449–455. [PubMed: 17276150]

(869). Pasparakis G; Manouras T; Argitis P; Vamvakaki M Photodegradable polymers for biotechnological applications. Macromol. Rapid Comm 2012, 33, 183–198.

(870). Bao C; Zhu L; Lin Q; Tian H Building biomedical materials using photochemical bond cleavage. Adv. Mater. 2015, 27, 1647–1662. [PubMed: 25655424]

(871). Tibbitt MW; Kloxin AM; Dyamenahalli KU; Anseth KS Controlled two-photon photodegradation of PEG hydrogels to study and manipulate subcellular interactions on soft materials. Soft Matter 2010, 6, 5100–5108. [PubMed: 21984881]

(872). You J; Haque A; Shin D-S; Son KJ; Siltanen C; Revzin A Bioactive photodegradable hydrogel for cultivation and retrieval of embryonic stem cells. Adv. Func. Mater. 2015, 25, 4650–4656.

(873). Shin D-S; You J; Rahimian A; Vu T; Siltanen C; Ehsanipour A; Stybayeva G; Sutcliffe J; Revzin A Photodegradable hydrogels for capture, detection, and release of live cells. Angew. Chem. Int. Edit 2014, 53, 8221–8224.

(874). Griffin DR; Kasko AM Photoselective delivery of model therapeutics from hydrogels. ACS Macro Lett 2012, 1, 1330–1334. [PubMed: 25285242]

(875). Griffin DR; Schlosser JL; Lam SF; Nguyen TH; Maynard HD; Kasko AM Synthesis of photodegradable macromers for conjugation and release of bioactive molecules. Biomacromolecules 2013, 14, 1199–1207. [PubMed: 23506440]

(876). Griffin DR; Kasko AM Photodegradable macromers and hydrogels for live cell encapsulation and release. J. Am. Chem. Soc 2012, 134, 13103–13107. [PubMed: 22765384]

(877). Fairbanks BD; Singh SP; Bowman CN; Anseth KS Photodegradable, photoadaptable hydrogels via radical-mediated disulfide fragmentation reaction. Macromolecules 2011, 44, 2444–2450. [PubMed: 21512614]

(878). Peng K; Tomatsu I; van den Broek B; Cui C; Korobko AV; van Noort J; Meijer AH; Spaink HP; Kros A Dextran based photodegradable hydrogels formed via a Michael addition. Soft Matter 2011, 7, 4881–4887.

(879). Fomina N; McFearin CL; Sermsakdi M; Morachis JM; Almutairi A Low power, biologically benign NIR light triggers polymer disassembly. Macromolecules 2011, 44, 8590–8597. [PubMed: 22096258]

(880). Zhang J; Skardal A; Prestwich GD Engineered extracellular matrices with cleavable crosslinkers for cell expansion and easy cell recovery. Biomaterials 2008, 29, 4521–4531. [PubMed: 18768219]

(881). Buwalda SJ; Calucci L; Forte C; Dijkstra PJ; Feijen J Stereocomplexed 8-armed poly(ethylene glycol)–poly(lactide) star block copolymer hydrogels: Gelation mechanism, mechanical properties and degradation behavior. Polymer 2012, 53, 2809–2817.

(882). Hu J; Chen Y; Li Y; Zhou Z; Cheng Y A thermo-degradable hydrogel with light-tunable degradation and drug release. Biomaterials 2017, 112, 133–140. [PubMed: 27760397]

(883). Koehler KC; Alge DL; Anseth KS; Bowman CN A Diels–Alder modulated approach to control and sustain the release of dexamethasone and induce osteogenic differentiation of human mesenchymal stem cells. Biomaterials 2013, 34, 4150–4158. [PubMed: 23465826]

(884). Sanyal A Diels–alder cycloaddition-cycloreversion: A powerful combo in materials design. Macromol. Chem. Phys 2010, 211, 1417–1425.

(885). Singh S; Topuz F; Hahn K; Albrecht K; Groll J Embedding of active proteins and living cells in redox-sensitive hydrogels and nanogels through enzymatic cross-linking. Angew. Chem. Int. Edit 2013, 52, 3000–3003.

(886). Choh S-Y; Cross D; Wang C Facile synthesis and characterization of disulfide-cross-linked hyaluronic acid hydrogels for protein delivery and cell encapsulation. Biomacromolecules 2011, 12, 1126–1136. [PubMed: 21384907]

(887). Ossipov D; Kootala S; Yi Z; Yang X; Hilborn J Orthogonal chemoselective assembly of hyaluronic acid networks and nanogels for drug delivery. Macromolecules 2013, 46, 4105–4113.

(888). Baldwin AD; Kiick KL Tunable degradation of maleimide–thiol adducts in reducing environments. Bioconjugate Chem 2011, 22, 1946–1953.

(889). Baldwin AD; Kiick KL Reversible maleimide-thiol adducts yield glutathione-sensitive poly(ethylene glycol)-heparin hydrogels. Polym. Chem 2013, 4, 133–143. [PubMed: 23766781]

(890). Traverso N; Ricciarelli R; Nitti M; Marengo B; Furfaro AL; Pronzato MA; Marinari UM; Domenicotti C Role of glutathione in cancer progression and chemoresistance. Oxid Med. Cell Longev 2013, 2013, 972913. [PubMed: 23766865]

(891). Wang H; Heilshorn SC Adaptable hydrogel networks with reversible linkages for tissue engineering. Adv. Mater. 2015, DOI: 10.1002/adma.201501558.

(892). Tong X; Yang F Sliding hydrogels with mobile molecular ligands and crosslinks as 3D stem cell niche. Adv. Mater. 2016, 28, 7257–7263. [PubMed: 27305637]

(893). Bardsley K; Wimpenny I; Wechsler R; Shachaf Y; Yang Y; El Haj AJ Defining a turnover index for the correlation of biomaterial degradation and cell based extracellular matrix synthesis using fluorescent tagging techniques. Acta Biomater 2016, 45, 133–142. [PubMed: 27592815]

(894). He M; Li J; Tan S; Wang R; Zhang Y Photodegradable supramolecular hydrogels with fluorescence turn-on reporter for photomodulation of cellular microenvironments. J. Am. Chem. Soc 2013, 135, 18718–18721. [PubMed: 24106809]

(895). Schultz KM; Anseth KS Monitoring degradation of matrix metalloproteinases-cleavable PEG hydrogels via multiple particle tracking microrheology. Soft Matter 2013, 9, 1570–1579.

(896). Leight JL; Alge DL; Maier AJ; Anseth KS Direct measurement of matrix metalloproteinase activity in 3D cellular microenvironments using a fluorogenic peptide substrate. Biomaterials 2013, 34, 7344–7352. [PubMed: 23830581]

(897). Mihic A; Cui Z; Wu J; Vlacic G; Miyagi Y; Li S-H; Lu S; Sung H-W; Weisel RD; Li R-K A conductive polymer hydrogel supports cell electrical signaling and improves cardiac function after implantation into myocardial infarct. Circulation 2015, 132, 772. [PubMed: 26304669]

(898). Shin SR; Jung SM; Zalabany M; Kim K; Zorlutuna P; Kim SB; Nikkhah M; Khabiry M; Azize M; Kong J; Wan KT; Palacios T; Dokmeci MR; Bae H; Tang XW; Khademhosseini A Carbon-nanotube-embedded hydrogel sheets for engineering cardiac constructs and bioactuators. ACS Nano 2013, 7, 2369–2380. [PubMed: 23363247]

(899). Annabi N; Shin SR; Tamayol A; Miscuglio M; Bakooshli MA; Assmann A; Mostafalu P; Sun J-Y; Mithieux S; Cheung L; Tang X; Weiss AS; Khademhosseini A Highly elastic and conductive human-based protein hybrid hydrogels. Adv. Mater. 2016, 28, 40–49. [PubMed: 26551969]

(900). Shirakawa H; Louis EJ; MacDiarmid AG; Chiang CK; Heeger AJ Synthesis of electrically conducting organic polymers: halogen derivatives of polyacetylene, (CH). J. Chem. Soc., Chem. Commun 1977, 578–580.

(901). Guo B; Glavas L; Albertsson A-C Biodegradable and electrically conducting polymers for biomedical applications. Prog. Polym. Sci 2013, 38, 1263–1286.

(902). Qazi TH; Rai R; Boccaccini AR Tissue engineering of electrically responsive tissues using polyaniline based polymers: A review. Biomaterials 2014, 35, 9068–9086. [PubMed: 25112936]

(903). Wong JY; Langer R; Ingber DE Electrically conducting polymers can noninvasively control the shape and growth of mammalian cells. Proc. Natl. Acad. Sci. U.S.A 1994, 91, 3201–3204. [PubMed: 8159724]

(904). Guimard NK; Gomez N; Schmidt CE Conducting polymers in biomedical engineering. Prog. Polym. Sci 2007, 32, 876–921.

(905). Balint R; Cassidy NJ; Cartmell SH Conductive polymers: Towards a smart biomaterial for tissue engineering. Acta Biomater 2014, 10, 2341–2353. [PubMed: 24556448]

(906). Hsiao C-W; Bai M-Y; Chang Y; Chung M-F; Lee T-Y; Wu C-T; Maiti B; Liao Z-X; Li R-K; Sung H-W Electrical coupling of isolated cardiomyocyte clusters grown on aligned conductive nanofibrous meshes for their synchronized beating. Biomaterials 2013, 34, 1063–1072. [PubMed: 23164424]

(907). Xie J; MacEwan MR; Willerth SM; Li X; Moran DW; Sakiyama-Elbert SE; Xia Y Conductive core–sheath nanofibers and their potential application in neural tissue engineering. Adv. Func. Mater. 2009, 19, 2312–2318.

(908). Xie M; Wang L; Guo B; Wang Z; Chen YE; Ma PX Ductile electroactive biodegradable hyperbranched polylactide copolymers enhancing myoblast differentiation. Biomaterials 2015, 71, 158–167. [PubMed: 26335860]

(909). Xie M; Wang L; Ge J; Guo B; Ma PX Strong electroactive biodegradable shape memory polymer networks based on star-shaped polylactide and aniline trimer for bone tissue engineering. ACS Appl. Mater. Inter 2015, 7, 6772–6781.

(910). Chen J; Ge J; Guo B; Gao K; Ma PX Nanofibrous polylactide composite scaffolds with electroactivity and sustained release capacity for tissue engineering. J. Mater. Chem. B 2016, 4, 2477–2485.

(911). Liu Y; Hu J; Zhuang X; Zhang P; Wei Y; Wang X; Chen X Synthesis and characterization of novel biodegradable and electroactive hydrogel based on aniline oligomer and gelatin. Macromol Biosci 2012, 12, 241–250. [PubMed: 22028067]

(912). Li L; Ge J; Guo B; Ma PX In situ forming biodegradable electroactive hydrogels. Polym. Chem 2014, 5, 2880–2890.

(913). Wu Y; Chen YX; Yan J; Quinn D; Dong P; Sawyer SW; Soman P Fabrication of conductive gelatin methacrylate–polyaniline hydrogels. Acta Biomater 2016, 33, 122–130. [PubMed: 26821341]

(914). Abidian MR; Daneshvar ED; Egeland BM; Kipke DR; Cederna PS; Urbanchek MG Hybrid conducting polymer–hydrogel conduits for axonal growth and neural tissue engineering. Adv. Healthc. Mater. 2012, 1, 762–767. [PubMed: 23184828]

(915). Shi Z; Gao H; Feng J; Ding B; Cao X; Kuga S; Wang Y; Zhang L; Cai J In situ synthesis of robust conductive cellulose/polypyrrole composite aerogels and their potential application in nerve regeneration. Angew. Chem. Int. Edit 2014, 53, 5380–5384.

(916). Sirivisoot S; Pareta R; Harrison BS Protocol and cell responses in three-dimensional conductive collagen gel scaffolds with conductive polymer nanofibres for tissue regeneration. Interface Focus 2014, 4, 20130050. [PubMed: 24501678]

(917). Guiseppi-Elie A Electroconductive hydrogels: Synthesis, characterization and biomedical applications. Biomaterials 2010, 31, 2701–2716. [PubMed: 20060580]

(918). Cobley CM; Chen J; Cho EC; Wang LV; Xia Y Gold nanostructures: A class of multifunctional materials for biomedical applications. Chem. Soc. Rev 2011, 40, 44–56. [PubMed: 20818451]

(919). Dykman L; Khlebtsov N Gold nanoparticles in biomedical applications: recent advances and perspectives. Chem. Soc. Rev 2012, 41, 2256–2282. [PubMed: 22130549]

(920). You J-O; Rafat M; Ye GJC; Auguste DT Nanoengineering the heart: Conductive scaffolds enhance connexin 43 expression. Nano lett 2011, 11, 3643–3648. [PubMed: 21800912]

(921). Orza A; Soritau O; Olenic L; Diudea M; Florea A; Rus Ciuca D; Mihu C; Casciano D; Biris AS Electrically conductive gold-coated collagen nanofibers for placental-derived mesenchymal stem cells enhanced differentiation and proliferation. ACS Nano 2011, 5, 4490–4503. [PubMed: 21609025]

(922). You J-O; Auguste DT Conductive, physiologically responsive hydrogels. Langmuir 2010, 26, 4607–4612. [PubMed: 20199077]

(923). Shevach M; Fleischer S; Shapira A; Dvir T Gold nanoparticle-decellularized matrix hybrids for cardiac tissue engineering. Nano lett 2014, 14, 5792–5796. [PubMed: 25176294]

(924). Navaei A; Saini H; Christenson W; Sullivan RT; Ros R; Nikkhah M Gold nanorod-incorporated gelatin-based conductive hydrogels for engineering cardiac tissue constructs. Acta Biomater 2016, 41, 133–146. [PubMed: 27212425]

(925). Zhu K; Shin SR; van Kempen T; Li Y-C; Ponraj V; Nasajpour A; Mandla S; Hu N; Liu X; Leijten J; Lin Y-D; Hussain MA; Zhang YS; Tamayol A; Khademhosseini A Gold nanocomposite bioink for printing 3D cardiac constructs. Adv. Func. Mater. 2017, 27, DOI: 10.1002/adfm.201605352.

(926). Kharaziha M; Shin SR; Nikkhah M; Topkaya SN; Masoumi N; Annabi N; Dokmeci MR; Khademhosseini A Tough and flexible CNT–polymeric hybrid scaffolds for engineering cardiac constructs. Biomaterials 2014, 35, 7346–7354. [PubMed: 24927679]

(927). Pok S; Vitale F; Eichmann SL; Benavides OM; Pasquali M; Jacot JG Biocompatible carbon nanotube–chitosan scaffold matching the electrical conductivity of the heart. ACS Nano 2014, 8, 9822–9832. [PubMed: 25233037]

(928). Li X; Zhou J; Liu Z; Chen J; Lü S; Sun H; Li J; Lin Q; Yang B; Duan C; Xing M; Wang C A PNIPAAm-based thermosensitive hydrogel containing SWCNTs for stem cell transplantation in myocardial repair. Biomaterials 2014, 35, 5679–5688. [PubMed: 24746964]

(929). Lee JH; Lee J-Y; Yang SH; Lee E-J; Kim H-W Carbon nanotube–collagen three-dimensional culture of mesenchymal stem cells promotes expression of neural phenotypes and secretion of neurotrophic factors. Acta Biomater 2014, 10, 4425–4436. [PubMed: 24954912]

(930). Cho Y; Ben Borgens R Electrically controlled release of the nerve growth factor from a collagen-carbon nanotube composite for supporting neuronal growth. J. Mater. Chem. B 2013, 1, 4166–4170.

(931). Shin SR; Bae H; Cha JM; Mun JY; Chen Y-C; Tekin H; Shin H; Farshchi S; Dokmeci MR; Tang S; Khademhosseini A Carbon nanotube reinforced hybrid microgels as scaffold materials for cell encapsulation. ACS Nano 2012, 6, 362–372. [PubMed: 22117858]

(932). Ahadian S; Ramón-Azcón J; Estili M; Liang X; Ostrovidov S; Shiku H; Ramalingam M; Nakajima K; Sakka Y; Bae H; Matsue T; Khademhosseini A Hybrid hydrogels containing vertically aligned carbon nanotubes with anisotropic electrical conductivity for muscle myofiber fabrication. Sci. Rep 2014, 4, 4271. [PubMed: 24642903]

(933). Shin SR; Shin C; Memic A; Shadmehr S; Miscuglio M; Jung HY; Jung SM; Bae H; Khademhosseini A; Tang X; Dokmeci MR Aligned carbon nanotube–based flexible gel substrates for engineering biohybrid tissue actuators. Adv. Func. Mater. 2015, 25, 4486–4495.

(934). Martins AM; Eng G; Caridade SG; Mano JF; Reis RL; Vunjak-Novakovic G Electrically conductive chitosan/carbon scaffolds for cardiac tissue engineering. Biomacromolecules 2014, 15, 635–643. [PubMed: 24417502]

(935). Sayyar S; Murray E; Thompson BC; Chung J; Officer DL; Gambhir S; Spinks GM; Wallace GG Processable conducting graphene/chitosan hydrogels for tissue engineering. J. Mater. Chem. B 2015, 3, 481–490.

(936). Liu X; Miller Ii AL; Park S; Waletzki BE; Terzic A; Yaszemski MJ; Lu L Covalent crosslinking of graphene oxide and carbon nanotube into hydrogels enhances nerve cell responses. J. Mater. Chem. B 2016, 4, 6930–6941.

(937). Jo H; Sim M; Kim S; Yang S; Yoo Y; Park J-H; Yoon TH; Kim M-G; Lee JY Electrically conductive graphene/polyacrylamide hydrogels produced by mild chemical reduction for enhanced myoblast growth and differentiation. Acta Biomater 2017, 48, 100–109. [PubMed: 27989919]

(938). Firme Iii CP; Bandaru PR Toxicity issues in the application of carbon nanotubes to biological systems. Nanomed-Nanotechnol 2010, 6, 245–256.

(939). Gurunathan S; Kim J-H Synthesis, toxicity, biocompatibility, and biomedical applications of graphene and graphene-related materials. Int. J. Nanomed 2016, 11, 1927–1945.

(940). Feiner R; Engel L; Fleischer S; Malki M; Gal I; Shapira A; Shacham-Diamand Y; Dvir T Engineered hybrid cardiac patches with multifunctional electronics for online monitoring and regulation of tissue function. Nat. Mater. 2016, 15, 679–685. [PubMed: 26974408]

(941). Tian B; Liu J; Dvir T; Jin L; Tsui JH; Qing Q; Suo Z; Langer R; Kohane DS; Lieber CM Macroporous nanowire nanoelectronic scaffolds for synthetic tissues. Nat. Mater. 2012, 11, 986–994. [PubMed: 22922448]

(942). Duan X; Fu T-M; Liu J; Lieber CM Nanoelectronics-biology frontier: From nanoscopic probes for action potential recording in live cells to three-dimensional cyborg tissues. Nano Today 2013, 8, 351–373. [PubMed: 24073014]

(943). Lind JU; Busbee TA; Valentine AD; Pasqualini FS; Yuan H; Yadid M; Park S-J; Kotikian A; Nesmith AP; Campbell PH; Vlassak JJ; Lewis JA; Parker KK Instrumented cardiac microphysiological devices via multimaterial three-dimensional printing. Nat. Mater. 2016, Doi: 10.1038/nmat4782.

(944). Guarino V; Alvarez-Perez MA; Borriello A; Napolitano T; Ambrosio L Conductive PANi/PEGDA macroporous hydrogels for nerve regeneration. Adv. Healthc. Mater. 2013, 2, 218–227. [PubMed: 23184787]

(945). Xu D; Fan L; Gao L; Xiong Y; Wang Y; Ye Q; Yu A; Dai H; Yin Y; Cai J; Zhang L Micro-nanostructured polyaniline assembled in cellulose matrix via interfacial polymerization for applications in nerve regeneration. ACS Appl. Mater. Inter 2016, 8, 17090–17097.

(946). Zhao X; Li P; Guo B; Ma PX Antibacterial and conductive injectable hydrogels based on quaternized chitosan-graft-polyaniline/oxidized dextran for tissue engineering. Acta Biomater 2015, 26, 236–248. [PubMed: 26272777]

(947). Zhao X; Wu H; Guo B; Dong R; Qiu Y; Ma PX Antibacterial anti-oxidant electroactive injectable hydrogel as self-healing wound dressing with hemostasis and adhesiveness for cutaneous wound healing. Biomaterials 2017, 122, 34–47. [PubMed: 28107663]

(948). Sun KH; Liu Z; Liu C; Yu T; Shang T; Huang C; Zhou M; Liu C; Ran F; Li Y; Shi Y; Pan L Evaluation of in vitro and in vivo biocompatibility of a myo-inositol hexakisphosphate gelated polyaniline hydrogel in a rat model. Sci. Rep 2016, 6, 23931. [PubMed: 27073144]

(949). Runge MB; Dadsetan M; Baltrusaitis J; Ruesink T; Lu L; Windebank AJ; Yaszemski MJ Development of electrically conductive oligo(polyethylene glycol) fumarate-polypyrrole hydrogels for nerve regeneration. Biomacromolecules 2010, 11, 2845–2853. [PubMed: 20942380]

(950). Yang S; Jang L; Kim S; Yang J; Yang K; Cho SW; Lee JY Polypyrrole/alginate hybrid hydrogels: Electrically conductive and soft biomaterials for human mesenchymal stem cell culture and potential neural tissue engineering applications. Macromol Biosci 2016, 16, 1653–1661. [PubMed: 27455895]

(951). Yang J; Choe G; Yang S; Jo H; Lee JY Polypyrrole-incorporated conductive hyaluronic acid hydrogels. Biomaterials Research 2016, 20, 31. [PubMed: 27708859]

(952). Ketabat F; Karkhaneh A; Mehdinavaz Aghdam R; Hossein Ahmadi Tafti S Injectable conductive collagen/alginate/polypyrrole hydrogels as a biocompatible system for biomedical applications. J. Biomater. Sci. Polym. Ed 2017, 28, 794–805. [PubMed: 28278043]

(953). Kotanen CN; Tlili C; Guiseppi-Elie A Bioactive electroconductive hydrogels: the effects of electropolymerization charge density on the storage stability of an enzyme-based biosensor. Applied Biochemistry and Biotechnology 2012, 166, 878–888. [PubMed: 22212391]

(954). Chansai P; Sirivat A; Niamlang S; Chotpattananont D; Viravaidya-Pasuwat K Controlled transdermal iontophoresis of sulfosalicylic acid from polypyrrole/poly(acrylic acid) hydrogel. Int. J. Pharmaceut 2009, 381, 25–33.

(955). Hassarati RT; Marcal H; John L; Foster R; Green RA Biofunctionalization of conductive hydrogel coatings to support olfactory ensheathing cells at implantable electrode interfaces. J. Biomed. Mater. Res. B 2016, 104, 712–722.

(956). Green RA; Lim KS; Henderson WC; Hassarati RT; Martens PJ; Lovell NH; Poole-Warren LA Living electrodes: Tissue engineering the neural interface. EMBS 2013, 2013, 6957–6960.

(957). Hassarati RT; Foster LJ; Green RA Influence of biphasic stimulation on olfactory ensheathing cells for neuroprosthetic devices. Frontiers in Neuroscience 2016, 10, 432. [PubMed: 27757072]

(958). Mario Cheong GL; Lim KS; Jakubowicz A; Martens PJ; Poole-Warren LA; Green RA Conductive hydrogels with tailored bioactivity for implantable electrode coatings. Acta Biomater 2014, 10, 1216–1226. [PubMed: 24365707]

(959). Green RA; Hassarati RT; Goding JA; Baek S; Lovell NH; Martens PJ; Poole-Warren LA Conductive hydrogels: Mechanically robust hybrids for use as biomaterials. Macromol Biosci 2012, 12, 494–501. [PubMed: 22344960]

(960). Chen C; Chen X; Zhang H; Zhang Q; Wang L; Li C; Dai B; Yang J; Liu J; Sun D Electrically-responsive core-shell hybrid microfibers for controlled drug release and cell culture. Acta Biomater 2017, DOI: 10.1016/j.actbio.2017.1004.1005.

(961). Dong R; Zhao X; Guo B; Ma PX Self-healing conductive injectable hydrogels with antibacterial activity as cell delivery carrier for cardiac cell therapy. ACS Appl. Mater. Inter 2016, 8, 17138–17150.

(962). Wang Q; Wang Q; Teng W Injectable, degradable, electroactive nanocomposite hydrogels containing conductive polymer nanoparticles for biomedical applications. Int. J. Nanomed 2016, 11, 131–144.

(963). Sherrell PC; Cieslar-Pobuda A; Ejneby MS; Sammalisto L; Gelmi A; de Muinck E; Brask J; Los MJ; Rafat M Rational design of a conductive collagen heart patch. Macromol Biosci 2017, DOI: 10.1002/mabi.201600446.

(964). Zhou J; Chen J; Sun H; Qiu X; Mou Y; Liu Z; Zhao Y; Li X; Han Y; Duan C; Tang R; Wang C; Zhong W; Liu J; Luo Y; Xing M; Wang C Engineering the heart: Evaluation of conductive nanomaterials for improving implant integration and cardiac function. Sci. Rep 2014, 4, 3733. [PubMed: 24429673]

(965). Koppes AN; Keating KW; McGregor AL; Koppes RA; Kearns KR; Ziemba AM; McKay CA; Zuidema JM; Rivet CJ; Gilbert RJ; Thompson DM Robust neurite extension following

exogenous electrical stimulation within single walled carbon nanotube-composite hydrogels. Acta Biomater 2016, 39, 34–43. [PubMed: 27167609]

(966). Behan BL; DeWitt DG; Bogdanowicz DR; Koppes AN; Bale SS; Thompson DM Single-walled carbon nanotubes alter Schwann cell behavior differentially within 2D and 3D environments. J. Biomed. Mater. Res. A 2011, 96, 46–57. [PubMed: 20949573]

(967). Arslantunali D; Budak G; Hasirci V Multiwalled CNT-pHEMA composite conduit for peripheral nerve repair. J. Biomed. Mater. Res. A 2014, 102, 828–841. [PubMed: 23554154]

(968). Liu XW; Huang YX; Sun XF; Sheng GP; Zhao F; Wang SG; Yu HQ Conductive carbon nanotube hydrogel as a bioanode for enhanced microbial electrocatalysis. ACS Appl. Mater. Inter 2014, 6, 8158–8164.

(969). Bao R; Tan B; Liang S; Zhang N; Wang W; Liu W A pi-pi conjugation-containing soft and conductive injectable polymer hydrogel highly efficiently rebuilds cardiac function after myocardial infarction. Biomaterials 2017, 122, 63–71. [PubMed: 28107665]

(970). Jo H; Sim M; Kim S; Yang S; Yoo Y; Park JH; Yoon TH; Kim MG; Lee JY Electrically conductive graphene/polyacrylamide hydrogels produced by mild chemical reduction for enhanced myoblast growth and differentiation. Acta Biomater 2017, 48, 100–109. [PubMed: 27989919]

(971). Han L; Lu X; Wang M; Gan D; Deng W; Wang K; Fang L; Liu K; Chan CW; Tang Y; Weng LT; Yuan H A mussel-inspired conductive, self-adhesive, and self-healable tough hydrogel as cell stimulators and implantable bioelectronics. Small 2017, 13, 1601916.

(972). Meng X; Stout DA; Sun L; Beingessner RL; Fenniri H; Webster TJ Novel injectable biomimetic hydrogels with carbon nanofibers and self assembled rosette nanotubes for myocardial applications. J. Biomed. Mater. Res. A 2013, 101, 1095–1102. [PubMed: 23008178]

(973). Liu X; Miller AL 2nd; Park S; Waletzki BE; Zhou Z; Terzic A; Lu L Functionalized carbon nanotube and graphene oxide embedded electrically conductive hydrogel synergistically stimulates nerve cell differentiation. ACS Appl. Mater. Inter 2017, 9, 14677–14690.

(974). Baei P; Jalili-Firoozinezhad S; Rajabi-Zeleti S; Tafazzoli-Shadpour M; Baharvand H; Aghdami N Electrically conductive gold nanoparticle-chitosan thermosensitive hydrogels for cardiac tissue engineering. Materials Science & Engineering C-Materials for Biological Applications 2016, 63, 131–141.

(975). Navaei A; Saini H; Christenson W; Sullivan RT; Ros R; Nikkhah M Gold nanorod-incorporated gelatin-based conductive hydrogels for engineering cardiac tissue constructs. Acta biomaterialia 2016, 41, 133–146. [PubMed: 27212425]

(976). Wang XT; Boire TC; Bronikowski C; Zachman AL; Crowder SW; Sung HJ Decoupling polymer properties to elucidate mechanisms governing cell behavior. Tissue Eng. Part B Rev 2012, 18, 396–404. [PubMed: 22536977]

(977). Fu J; Wang Y-K; Yang MT; Desai RA; Yu X; Liu Z; Chen CS Mechanical regulation of cell function with geometrically modulated elastomeric substrates. Nat. Meth 2010, 7, 733–736.

(978). Lee MK; Rich MH; Baek K; Lee J; Kong H Bioinspired tuning of hydrogel permeability-rigidity dependency for 3D cell culture. Sci. Rep 2015, 5, 8948. [PubMed: 25752700]

(979). Peyton SR; Kalcioglu ZI; Cohen JC; Runkle AP; Van Vliet KJ; Lauffenburger DA; Griffith LG Marrow-derived stem cell motility in 3D synthetic scaffold is governed by geometry along with adhesivity and stiffness. Biotechnol. Bioeng 2011, 108, 1181–1193. [PubMed: 21449030]

(980). Kim J; Staunton JR; Tanner K Independent control of topography for 3D patterning of the ecm microenvironment. Adv. Mater 2015, 28, 132–137. [PubMed: 26551393]

(981). Joaquin D; Grigola M; Kwon G; Blasius C; Han Y; Perlitz D; Jiang J; Ziegler Y; Nardulli A; Hsia KJ Cell migration and organization in three-dimensional in vitro culture driven by stiffness gradient. Biotechnol. Bioeng 2016, 113, 2496–2506. [PubMed: 27183296]

(982). Li Z; Gong Y; Sun S; Du Y; Lü D; Liu X; Long M Differential regulation of stiffness, topography, and dimension of substrates in rat mesenchymal stem cells. Biomaterials 2013, 34, 7616–7625. [PubMed: 23863454]

(983). Peyton SR; Raub CB; Keschrumrus VP; Putnam AJ The use of poly(ethylene glycol) hydrogels to investigate the impact of ECM chemistry and mechanics on smooth muscle cells. Biomaterials 2006, 27, 4881–4893. [PubMed: 16762407]

(984). Ye K; Wang X; Cao L; Li S; Li Z; Yu L; Ding J Matrix stiffness and nanoscale spatial organization of cell-adhesive ligands direct stem cell fate. Nano lett 2015, 15, 4720–4729. [PubMed: 26027605]

(985). Hoffmann JC; West JL Three-dimensional photolithographic micropatterning: a novel tool to probe the complexities of cell migration. Integr. Biol 2013, 5, 817–827.

(986). Ananthanarayanan B; Kim Y; Kumar S Elucidating the mechanobiology of malignant brain tumors using a brain matrix-mimetic hyaluronic acid hydrogel platform. Biomaterials 2011, 32, 7913–7923. [PubMed: 21820737]

(987). Cha C; Kohman RH; Kong H Biodegradable polymer crosslinker: Independent control of stiffness, toughness, and hydrogel degradation rate. Adv. Func. Mater. 2009, 19, 3056–3062.

(988). Cha C; Kim SY; Cao L; Kong H Decoupled control of stiffness and permeability with a cell-encapsulating poly(ethylene glycol) dimethacrylate hydrogel. Biomaterials 2010, 31, 4864–4871. [PubMed: 20347136]

(989). Cha C; Jeong JH; Shim J; Kong H Tuning the dependency between stiffness and permeability of a cell encapsulating hydrogel with hydrophilic pendant chains. Acta Biomater 2011, 7, 3719–3728. [PubMed: 21704737]

(990). Scott RA; Elbert DL; Willits RK Modular poly(ethylene glycol) scaffolds provide the ability to decouple the effects of stiffness and protein concentration on PC12 cells. Acta Biomater 2011, 7, 3841–3849. [PubMed: 21787889]

(991). Gill BJ; Gibbons DL; Roudsari LC; Saik JE; Rizvi ZH; Roybal JD; Kurie JM; West JL A synthetic matrix with independently tunable biochemistry and mechanical properties to study epithelial morphogenesis and EMT in a lung adenocarcinoma model. Cancer Res 2012, 72, 6013–6023. [PubMed: 22952217]

(992). Yong KW; Li Y; Liu F; Bin G; Lu TJ; Wan Abas WAB; Wan Safwani WKZ; Pingguan-Murphy B; Ma Y; Xu F; Huang G Paracrine effects of adipose-derived stem cells on matrix stiffness-induced cardiac myofibroblast differentiation via angiotensin II Type 1 Receptor and Smad7. Sci. Rep 2016, 6, 33067. [PubMed: 27703175]

(993). Lang NR; Skodzek K; Hurst S; Mainka A; Steinwachs J; Schneider J; Aifantis KE; Fabry B Biphasic response of cell invasion to matrix stiffness in three-dimensional biopolymer networks. Acta Biomater 2015, 13, 61–67. [PubMed: 25462839]

(994). Mason BN; Starchenko A; Williams RM; Bonassar LJ; Reinhart-King CA Tuning three-dimensional collagen matrix stiffness independently of collagen concentration modulates endothelial cell behavior. Acta Biomater 2013, 9, 4635–4644. [PubMed: 22902816]

(995). Au SH; Storey BD; Moore JC; Tang Q; Chen Y-L; Javaid S; Sarioglu AF; Sullivan R; Madden MW; O'Keefe R; Haber DA; Maheswaran S; Langenau DM; Stott SL; Toner M Clusters of circulating tumor cells traverse capillary-sized vessels. Proc. Natl. Acad. Sci. U.S.A 2016, 113, 4947–4952. [PubMed: 27091969]

(996). Byun S; Son S; Amodei D; Cermak N; Shaw J; Kang JH; Hecht VC; Winslow MM; Jacks T; Mallick P; Manalis SR Characterizing deformability and surface friction of cancer cells. Proc. Natl. Acad. Sci. U.S.A 2013, 110, 7580–7585. [PubMed: 23610435]

(997). Darling EM; Carlo DD High-throughput assessment of cellular mechanical properties. Annu. Rev. Biomed. Eng 2015, 17, 35–62. [PubMed: 26194428]

(998). Masaeli M; Gupta D; O'Byrne S; Tse HTK; Gossett DR; Tseng P; Utada AS; Jung H-J; Young S; Clark AT; Di Carlo D Multiparameter mechanical and morphometric screening of cells. Sci. Rep 2016, 6, 37863. [PubMed: 27910869]

(999). Che J; Yu V; Garon EB; Goldman J; Di Carlo D Biophysical isolation and identification of circulating tumor cells. Lab Chip 2017.

(1000). Sarioglu AF; Aceto N; Kojic N; Donaldson MC; Zeinali M; Hamza B; Engstrom A; Zhu H; Sundaresan TK; Miyamoto DT; Luo X; Bardia A; Wittner BS; Ramaswamy S; Shioda T; Ting DT; Stott SL; Kapur R; Maheswaran S; Haber DA; Toner M A microfluidic device for label-free, physical capture of circulating tumor cell clusters. Nat. Meth 2015, 12, 685–691.

(1001). Gossett DR; Tse HTK; Lee SA; Ying Y; Lindgren AG; Yang OO; Rao J; Clark AT; Di Carlo D Hydrodynamic stretching of single cells for large population mechanical phenotyping. Proc. Natl. Acad. Sci. U.S.A 2012, 109, 7630–7635. [PubMed: 22547795]

(1002). Dudani JS; Gossett DR; Tse HTK; Di Carlo D Pinched-flow hydrodynamic stretching of single-cells. Lab Chip 2013, 13, 3728–3734. [PubMed: 23884381]

(1003). Kourouklis AP; Kaylan KB; Underhill GH Substrate stiffness and matrix composition coordinately control the differentiation of liver progenitor cells. Biomaterials 2016, 99, 82–94. [PubMed: 27235994]

(1004). Hartman CD; Isenberg BC; Chua SG; Wong JY Vascular smooth muscle cell durotaxis depends on extracellular matrix composition. Proc. Natl. Acad. Sci. U.S.A 2016, 113, 11190–11195. [PubMed: 27647912]

(1005). Zustiak SP; Dadhwal S; Medina C; Steczina S; Chehreghanianzabi Y; Ashraf A; Asuri P Three-dimensional matrix stiffness and adhesive ligands affect cancer cell response to toxins. Biotechnol. Bioeng 2016, 113, 443–452. [PubMed: 26184715]

(1006). Onoe H; Okitsu T; Itou A; Kato-Negishi M; Gojo R; Kiriya D; Sato K; Miura S; Iwanaga S; Kuribayashi-Shigetomi K; Matsunaga YT; Shimoyama Y; Takeuchi S Metre-long cell-laden microfibres exhibit tissue morphologies and functions. Nature materials 2013, 12, 584–590. [PubMed: 23542870]

(1007). O'Neill HS; Gallagher LB; O'Sullivan J; Whyte W; Curley C; Dolan E; Hameed A; O'Dwyer J; Payne C; O'Reilly D; Ruiz-Hernandez E; Roche ET; O'Brien FJ; Cryan SA; Kelly H; Murphy B; Duffy GP Biomaterial-enhanced cell and drug delivery: Lessons learned in the cardiac field and future perspectives. Adv. Mater 2016, 28, 5648–5661. [PubMed: 26840955]

(1008). Pradhan S; Hassani I; Clary JM; Lipke EA Polymeric biomaterials for in vitro cancer tissue engineering and drug testing applications. Tissue Eng. Part B Rev 2016, 22, 470–484. [PubMed: 27302080]

(1009). Bajaj P; Schweller RM; Khademhosseini A; West JL; Bashir R 3D biofabrication strategies for tissue engineering and regenerative medicine. Annu. Rev. Biomed. Eng 2013, 16, 247–276.

(1010). Wong VW; Levi B; Rajadas J; Longaker MT; Gurtner GC Stem Cell Niches for Skin Regeneration. Int. J. Biomater 2012, 2012, 926059. [PubMed: 22701121]

(1011). MacNeil S Biomaterials for tissue engineering of skin. Mater. Today 2008, 11, 26–35.

(1012). MacNeil S Progress and opportunities for tissue-engineered skin. Nature 2007, 445, 874–880. [PubMed: 17314974]

(1013). Webber MJ; Khan OF; Sydlik SA; Tang BC; Langer R A perspective on the clinical translation of scaffolds for tissue engineering. Ann. Biomed. Eng 2015, 43, 641–656. [PubMed: 25201605]

(1014). Zhao X; Lang Q; Yildirimer L; Lin ZY; Cui W; Annabi N; Ng KW; Dokmeci MR; Ghaemmaghami AM; Khademhosseini A Photocrosslinkable gelatin hydrogel for epidermal tissue engineering. Adv. Healthc. Mater. 2016, 5, 108–118. [PubMed: 25880725]

(1015). Yildirimer L; Thanh NT; Seifalian AM Skin regeneration scaffolds: A multimodal bottom-up approach. Trends Biotechnol 2012, 30, 638648.

(1016). Nicholas MN; Yeung J Current status and future of skin substitutes for chronic wound healing. J. Cutan. Med. Surg 2017, 21, 23–30. [PubMed: 27530398]

(1017). Zhou H; You C; Wang X; Jin R; Wu P; Li Q; Han C The progress and challenges for dermal regeneration in tissue engineering. J. Biomed. Mater. Res. A 2017, 105, 1208–1218. [PubMed: 28063210]

(1018). Dias JR; Granja PL; Bártolo PJ Advances in electrospun skin substitutes. Prog. Mater. Sci 2016, 84, 314–334.

(1019). Ng WL; Wang S; Yeong WY; Naing MW Skin bioprinting: Impending reality or fantasy? Trends Biotechnol 2016, 34, 689–699. [PubMed: 27167724]

(1020). Pereira RF; Barrias CC; Granja PL; Bartolo PJ Advanced biofabrication strategies for skin regeneration and repair. Nanomedicine 2013, 8, 603–621. [PubMed: 23560411]

(1021). Sun BK; Siprashvili Z; Khavari PA Advances in skin grafting and treatment of cutaneous wounds. Science 2014, 346, 941–945. [PubMed: 25414301]

(1022). Madaghiele M; Demitri C; Sannino A; Ambrosio L Polymeric hydrogels for burn wound care: Advanced skin wound dressings and regenerative templates. Burns & Trauma 2014, 2, 153–161. [PubMed: 27602378]

(1023). Frueh FS; Menger MD; Lindenblatt N; Giovanoli P; Laschke MW Current and emerging vascularization strategies in skin tissue engineering. Crit. Rev. Biotechnol 2016, 1–13. [PubMed: 23883073]

(1024). Prabhakaran MP; Venugopal J; Kai D; Ramakrishna S Biomimetic material strategies for cardiac tissue engineering. Mater. Sci. Eng. C Mater. Biol. Appl 2011, 31, 503–513.

(1025). Davis ME; Hsieh PCH; Grodzinsky AJ; Lee RT Customdesign of the cardiac microenvironment with biomaterials. Circ. Res 2005, 97, 8–15. [PubMed: 16002755]

(1026). Rane AA; Christman KL Biomaterials for the treatment of myocardial infarction: A 5-year update. J. Am. Coll. Cardiol 2011, 58, 2615–2629. [PubMed: 22152947]

(1027). Melkoumian Z; Weber JL; Weber DM; Fadeev AG; Zhou Y; Dolley-Sonneville P; Yang J; Qiu L; Priest CA; Shogbon C Synthetic peptide-acrylate surfaces for long-term self-renewal and cardiomyocyte differentiation of human embryonic stem cells. Nat. Biotechnol 2010, 28, 606–610. [PubMed: 20512120]

(1028). Park J; Park S; Ryu S; Bhang SH; Kim J; Yoon JK; Park YH; Cho SP; Lee S; Hong BH Graphene-regulated cardiomyogenic differentiation process of mesenchymal stem cells by enhancing the expression of extracellular matrix proteins and cell signaling molecules. Adv. Healthc. Mater 2014, 3, 176–181. [PubMed: 23949999]

(1029). Higuchi A; Ling Q-D; Ko Y-A; Chang Y; Umezawa A Biomaterials for the feeder-free culture of human embryonic stem cells and induced pluripotent stem cells. Chem. Rev 2011, 111, 3021–3035. [PubMed: 21344932]

(1030). Kraehenbuehl TP; Zammaretti P; Aj VDV; Schoenmakers RG; Lutolf MP; Jaconi ME; Hubbell JA Three-dimensional extracellular matrix-directed cardioprogenitor differentiation: systematic modulation of a synthetic cell-responsive PEG-hydrogel. Biomaterials 2008, 29, 2757. [PubMed: 18396331]

(1031). Zhao S; Xu Z; Wang H; Reese BE; Gushchina LV; Jiang M; Agarwal P; Xu J; Zhang M; Shen R; Liu Z; Weisleder N; He X Bioengineering of injectable encapsulated aggregates of pluripotent stem cells for therapy of myocardial infarction. Nat. Commun 2016, 7, 13306. [PubMed: 27786170]

(1032). Bratt-Leal AM; Carpenedo RL; McDevitt TC Engineering the embryoid body microenvironment to direct embryonic stem cell differentiation. Biotechnol. Progr 2009, 25, 43–51.

(1033). Sahoo S; Ang LT; Goh CH; Toh SL Growth factor delivery through electrospun nanofibers in scaffolds for tissue engineering applications. J. Biomed. Mater. Res. A 2010, 93A, 1539–1550.

(1034). Pisano F; Mura M; Cervio E; Danieli P; Malpasso G; Ciuffreda MC; Gnecchi M Overexpression of growth factors to improve cardiac differentiation of human mesenchymal stem cells derived from the amniotic membrane. Eur. Heart. J 2013, 34, P5692–P5692.

(1035). Serena E; Figallo E; Tandon N; Cannizzaro C; Gerecht S; Elvassore N; Vunjaknovakovic G Electrical stimulation of human embryonic stem cells: Cardiac differentiation and the generation of reactive oxygen species. Exp. Cell Res 2011, 315, 3611–3619.

(1036). Limpitikul W; Christoforou N; Thompson SA; Gearhart JD; Tung L; Lipke EA Influence of electromechanical activity on cardiac differentiation of mouse embryonic stem cells. Cardiovasc. Eng. Technol 2010, 1, 179–193. [PubMed: 29057018]

(1037). Kim DH; Kim P; Song I; Cha JM; Lee SH; Kim B; Suh KY Guided three-dimensional growth of functional cardiomyocytes on polyethylene glycol nanostructures. Langmuir the ACS Journal of Surfaces & Colloids 2006, 22, 5419–5426. [PubMed: 16732672]

(1038). Badie N; Scull JA; Klinger RY; Krol A; Bursac N Conduction block in micropatterned cardiomyocyte cultures replicating the structure of ventricular cross-sections. Cardiovasc. Res 2012, 93, 263–271. [PubMed: 22072633]

(1039). Zhang B; Xiao Y; Hsieh A; Thavandiran N; Radisic M Micro- and nanotechnology in cardiovascular tissue engineering. Nanotechnology 2011, 22, 494003. [PubMed: 22101261]

(1040). Hosseinkhani H; Hosseinkhani M; Hattori S; Matsuoka R; Kawaguchi N Micro and nano-scale in vitro 3D culture system for cardiac stem cells. J. Biomed. Mater. Res. A 2010, 94a, 1–8.

(1041). Luna JI; Ciriza J; Garciaojeda ME; Kong M; Herren A; Lieu DK; Li RA; Fowlkes CC; Khine M; Mccloskey KE Multiscale biomimetic topography for the alignment of neonatal and embryonic stem cell-derived heart cells. Tissue Eng. Part C Meth 2011, 17, 579–588.

(1042). Szentivanyi A; Chakradeo T; Zernetsch H; Glasmacher B Electrospun cellular microenvironments: Understanding controlled release and scaffold structure. Adv. Drug Deliver. Rev 2011, 63, 209–220.

(1043). Gupta MK; Walthall JM; Raghav V; Crowder SW; Dae Kwang J; Yu SS; Feaster TK; Xintong W; Giorgio TD; Hong CC Combinatorial polymer electrospun matrices promote physiologically-relevant cardiomyogenic stem cell differentiation. PLOS ONE 2011, 6, e28935. [PubMed: 22216144]

(1044). Badrossamay MR; McIlwee HA; Goss JA; Parker KK Nanofiber assembly by rotary jet-spinning. Nano lett 2010, 10, 2257–2261. [PubMed: 20491499]

(1045). Davis ME; Hsieh PC; Takahashi T; Song Q; Zhang S; Kamm RD; Grodzinsky AJ; Anversa P; Lee RT Local myocardial insulin-like growth factor 1 (IGF-1) delivery with biotinylated peptide nanofibers improves cell therapy for myocardial infarction. Proc. Natl. Acad. Sci. U.S.A 2006, 103, 8155–8160. [PubMed: 16698918]

(1046). Webber MJ; Tongers J; Newcomb CJ; Marquardt KT; Bauersachs J; Losordo DW; Stupp SI Supramolecular nanostructures that mimic VEGF as a strategy for ischemic tissue repair. Proc. Natl. Acad. Sci. U.S.A 2011, 108, 13438–13443. [PubMed: 21808036]

(1047). Shin Y; Yang K; Han S; Park H-J; Seok Heo Y; Cho S-W; Chung S Reconstituting vascular microenvironment of neural stem cell niche in three-dimensional extracellular matrix. Adv. Healthc. Mater. 2014, 3, 1457–1464. [PubMed: 24523050]

(1048). Yao S; Liu X; Wang X; Merolli A; Chen X; Cui F Directing neural stem cell fate with biomaterial parameters for injured brain regeneration. Prog. Nat. Sci 2013, 23, 103–112.

(1049). Li X; Liu S; Zhao Y; Li J; Ding W; Han S; Chen B; Xiao Z; Dai J Training neural stem cells on functional collagen scaffolds for severe spinal cord injury repair. Adv. Func. Mater. 2016, 26, 5835–5847.

(1050). Trumble TE; Shon FG The physiology of nerve transplantation. Hand Clin 2000, 16, 105–122. [PubMed: 10696580]

(1051). Evans PJ; Midha R; Mackinnon SE The peripheral nerve allograft: A comprehensive review of regeneration and neuroimmunology. Prog. Neurobiol 1994, 43, 187–233. [PubMed: 7816927]

(1052). Fawcett JW; Asher RA The glial scar and central nervous system repair. Brain Res. Bull. 1999, 49, 377–391. [PubMed: 10483914]

(1053). Bellamkonda R; Ranieri J; Aebischer P Laminin oligopeptide derivatized agarose gels allow three-dimensional neurite extension in vitro. J. Neurosci. Res 1995, 41, 501–509. [PubMed: 7473881]

(1054). Plant GW; Woerly S; Harvey AR Hydrogels containing peptide or aminosugar sequences implanted into the rat brain: influence on cellular migration and axonal growth. Exp. Neurol 1997, 143, 287–299. [PubMed: 9056391]

(1055). Woerly S; Pinet E; De Robertis L; Van Diep D; Bousmina M Spinal cord repair with PHPMA hydrogel containing RGD peptides (NeuroGel™). Biomaterials 2001, 22, 1095–1111. [PubMed: 11352090]

(1056). Banerjee A; Arha M; Choudhary S; Ashton RS; Bhatia SR; Schaffer DV; Kane RS The influence of hydrogel modulus on the proliferation and differentiation of encapsulated neural stem cells. Biomaterials 2009, 30, 4695–4699. [PubMed: 19539367]

(1057). Saha K; Keung AJ; Irwin EF; Li Y; Little L; Schaffer DV; Healy KE Substrate modulus directs neural stem cell behavior. Biophys. J 2008, 95, 4426–4438. [PubMed: 18658232]

(1058). Yang F; Murugan R; Wang S; Ramakrishna S Electrospinning of nano/micro scale poly(l-lactic acid) aligned fibers and their potential in neural tissue engineering. Biomaterials 2005, 26, 2603–2610. [PubMed: 15585263]

(1059). Lim SH; Liu XY; Song H; Yarema KJ; Mao H-Q The effect of nanofiber-guided cell alignment on the preferential differentiation of neural stem cells. Biomaterials 2010, 31, 9031–9039. [PubMed: 20797783]

(1060). Bakhru S; Nain AS; Highley C; Wang J; Campbell P; Amon C; Zappe S Direct and cell signaling-based, geometry-induced neuronal differentiation of neural stem cells. Integr. Biol 2011, 3, 1207–1214.

(1061). Zhang Z; Yao S; Xie S; Wang X; Chang F; Luo J; Wang J; Fu J Effect of hierarchically aligned fibrin hydrogel in regeneration of spinal cord injury demonstrated by tractography: A pilot study. Sci. Rep 2017, 7, 40017. [PubMed: 28067245]

(1062). Kim SH; Im S-K; Oh S-J; Jeong S; Yoon E-S; Lee CJ; Choi N; Hur E-M Anisotropically organized three-dimensional culture platform for reconstruction of a hippocampal neural network. Nat. Commun 2017, 8, 14346. [PubMed: 28146148]

(1063). Onoe H; Kato-Negishi M; Itou A; Takeuchi S Differentiation induction of mouse neural stem cells in hydrogel tubular microenvironments with controlled tube dimensions. Adv. Healthc. Mater. 2016, 5, 1104–1111. [PubMed: 26919482]

(1064). Yao S; Liu X; Yu S; Wang X; Zhang S; Wu Q; Sun X; Mao H Co-effects of matrix low elasticity and aligned topography on stem cell neurogenic differentiation and rapid neurite outgrowth. Nanoscale 2016, 8, 10252–10265. [PubMed: 27124547]

(1065). McCreedy DA; Sakiyama-Elbert SE Combination therapies in the CNS: Engineering the environment. Neurosci. Lett 2012, 519, 115–121. [PubMed: 22343313]

(1066). Huang BJ; Hu JC; Athanasiou KA Cell-based tissue engineering strategies used in the clinical repair of articular cartilage. Biomaterials 2016, 98, 1–22. [PubMed: 27177218]

(1067). Liu Y; Zhang L; Zhou G; Li Q; Liu W; Yu Z; Luo X; Jiang T; Zhang W; Cao Y In vitro engineering of human ear-shaped cartilage assisted with CAD/CAM technology. Biomaterials 2010, 31, 2176–2183. [PubMed: 20022366]

(1068). Vinatier C; Mrugala D; Jorgensen C; Guicheux J; Noël D Cartilage engineering: A crucial combination of cells, biomaterials and biofactors. Trends Biotechnol 2009, 27, 307–314. [PubMed: 19329205]

(1069). Vinatier C; Guicheux J Cartilage tissue engineering: From biomaterials and stem cells to osteoarthritis treatments. Ann. Phys. Rehabil. Med 2016, 59, 139–144. [PubMed: 27079583]

(1070). Xue J; Feng B; Zheng R; Lu Y; Zhou G; Liu W; Cao Y; Zhang Y; Zhang WJ Engineering ear-shaped cartilage using electrospun fibrous membranes of gelatin/polycaprolactone. Biomaterials 2013, 34, 2624–2631. [PubMed: 23352044]

(1071). Puppi D; Chiellini F; Piras AM; Chiellini E Polymeric materials for bone and cartilage repair. Prog. Polym. Sci 2010, 35, 403–440.

(1072). Zheng R; Duan H; Xue J; Liu Y; Feng B; Zhao S; Zhu Y; Liu Y; He A; Zhang W; Liu W; Cao Y; Zhou G The influence of gelatin/PCL ratio and 3-D construct shape of electrospun membranes on cartilage regeneration. Biomaterials 2014, 35, 152–164. [PubMed: 24135269]

(1073). Raghothaman D; Leong MF; Lim TC; Toh JKC; Wan ACA; Yang Z; Lee EH Engineering cell matrix interactions in assembled polyelectrolyte fiber hydrogels for mesenchymal stem cell chondrogenesis. Biomaterials 2014, 35, 2607–2616. [PubMed: 24388815]

(1074). Spiller KL; Maher SA; Lowman AM Hydrogels for the repair of articular cartilage defects. Tissue Eng. Part B Rev 2011, 17, 281–299. [PubMed: 21510824]

(1075). Demoor M; Ollitrault D; Gomez-Leduc T; Bouyoucef M; Hervieu M; Fabre H; Lafont J; Denoix J-M; Audigié F; Mallein-Gerin F; Legendre F; Galera P Cartilage tissue engineering: Molecular control of chondrocyte differentiation for proper cartilage matrix reconstruction. BBA-Gen. Subjects 2014, 1840, 2414–2440.

(1076). Sadtler K; Singh A; Wolf MT; Wang X; Pardoll DM; Elisseeff JH Design, clinical translation and immunological response of biomaterials in regenerative medicine. Nat. Rev. Mater. 2016, 1, 16040.

(1077). Wang L-S; Du C; Toh WS; Wan ACA; Gao SJ; Kurisawa M Modulation of chondrocyte functions and stiffness-dependent cartilage repair using an injectable enzymatically crosslinked hydrogel with tunable mechanical properties. Biomaterials 2014, 35, 2207–2217. [PubMed: 24333028]

(1078). Bhardwaj N; Devi D; Mandal BB Tissue-engineered cartilage: The crossroads of biomaterials, cells and stimulating factors. Macromol Biosci 2015, 15, 153–182. [PubMed: 25283763]

(1079). Huey DJ; Hu JC; Athanasiou KA Unlike bone, cartilage regeneration remains elusive. Science 2012, 338, 917–921. [PubMed: 23161992]

(1080). Camarero-Espinosa S; Rothen-Rutishauser B; Weder C; Foster EJ Directed cell growth in multi-zonal scaffolds for cartilage tissue engineering. Biomaterials 2016, 74, 42–52. [PubMed: 26447554]

(1081). Bhumiratana S; Eton RE; Oungoulian SR; Wan LQ; Ateshian GA; Vunjak-Novakovic G Large, stratified, and mechanically functional human cartilage grown in vitro by mesenchymal condensation. Proc. Natl. Acad. Sci. U.S.A 2014, 111, 6940–6945. [PubMed: 24778247]

(1082). Zhao X; Liu S; Yildirimer L; Zhao H; Ding R; Wang H; Cui W; Weitz D Injectable stem cell-laden photocrosslinkable microspheres fabricated using microfluidics for rapid generation of osteogenic tissue constructs. Adv. Func. Mater. 2016, 26, 2809–2819.

(1083). Chen XD; Dusevich V; Feng JQ; Manolagas SC; Jilka RL Extracellular matrix made by bone marrow cells facilitates expansion of marrow-derived mesenchymal progenitor cells and prevents their differentiation into osteoblasts. J. Bone Miner. Res 2007, 22, 1943–1956. [PubMed: 17680726]

(1084). Bitar M; Brown RA; Salih V; Kidane AG; Knowles JC; Nazhat SN Effect of cell density on osteoblastic differentiation and matrix degradation of biomimetic dense collagen scaffolds. Biomacromolecules 2007, 9, 129–135. [PubMed: 18095652]

(1085). Fernandez-Yague MA; Abbah SA; McNamara L; Zeugolis DI; Pandit A; Biggs MJ Biomimetic approaches in bone tissue engineering: Integrating biological and physicomechanical strategies. Adv. Drug Deliver. Rev 2015, 84, 1–29.

(1086). Chen R; Wang J; Liu C Biomaterials act as enhancers of growth factors in bone regeneration. Adv. Func. Mater. 2016, 26, 8810–8823.

(1087). Shin H; Jo S; Mikos AG Modulation of marrow stromal osteoblast adhesion on biomimetic oligo [poly (ethylene glycol) fumarate] hydrogels modified with Arg-Gly-Asp peptides and a poly (ethylene glycol) spacer. J. Biomed. Mater. Res 2002, 61, 169–179. [PubMed: 12061329]

(1088). Dalton BA; McFarland CD; Underwood PA; Steele JG Role of the heparin binding domain of fibronectin in attachment and spreading of human bone-derived cells. J. Cell Sci 1995, 108, 2083–2092. [PubMed: 7657726]

(1089). Martino MM; Briquez PS; Ranga A; Lutolf MP; Hubbell JA Heparin-binding domain of fibrin (ogen) binds growth factors and promotes tissue repair when incorporated within a synthetic matrix. Proceedings of the National Academy of Sciences 2013, 110, 4563–4568.

(1090). Wu S; Liu X; Yeung KWK; Liu C; Yang X Biomimetic porous scaffolds for bone tissue engineering. Mater. Sci. Eng. R Rep 2014, 80, 1–36.

(1091). Karageorgiou V; Kaplan D Porosity of 3D biomaterial scaffolds and osteogenesis. Biomaterials 2005, 26, 5474–5491. [PubMed: 15860204]

(1092). Oh SH; Park IK; Kim JM; Lee JH In vitro and in vivo characteristics of PCL scaffolds with pore size gradient fabricated by a centrifugation method. Biomaterials 2007, 28, 1664–1671. [PubMed: 17196648]

(1093). Nguyen LH; Annabi N; Nikkhah M; Bae H; Binan L; Park S; Kang Y; Yang Y; Khademhosseini A Vascularized bone tissue engineering: Approaches for potential improvement. Tissue Eng. Part B Rev 2012, 18, 363–382. [PubMed: 22765012]

(1094). Andrea Di L; Alessia L; Giuseppe C; Carlos M; Clemens van B; Lorenzo M Toward mimicking the bone structure: Design of novel hierarchical scaffolds with a tailored radial porosity gradient. Biofabrication 2016, 8, 045007. [PubMed: 27725338]

(1095). Gómez S; Vlad MD; López J; Fernández E Design and properties of 3D scaffolds for bone tissue engineering. Acta Biomater 2016, 42, 341–350. [PubMed: 27370904]

(1096). Bose S; Roy M; Bandyopadhyay A Recent advances in bone tissue engineering scaffolds. Trends Biotechnol 2012, 30, 546–554. [PubMed: 22939815]

(1097). Bose S; Vahabzadeh S; Bandyopadhyay A Bone tissue engineering using 3D printing. Mater. Today 2013, 16, 496–504.

(1098). Abou Neel EA; Chrzanowski W; Salih VM; Kim HW; Knowles JC Tissue engineering in dentistry. J. Dent 2014, 42, 915–928. [PubMed: 24880036]

(1099). Horst OV; Chavez MG; Jheon AH; Desai T; Klein OD Stem cell and biomaterials research in dental tissue engineering and regeneration. Dent. Clin. North Am 2012, 56, 495–520. [PubMed: 22835534]

(1100). Grasman JM; Zayas MJ; Page RL; Pins GD Biomimetic scaffolds for regeneration of volumetric muscle loss in skeletal muscle injuries. Acta Biomater 2015, 25, 2–15. [PubMed: 26219862]

(1101). Quarta M; Brett JO; DiMarco R; De Morree A; Boutet SC; Chacon R; Gibbons MC; Garcia VA; Su J; Shrager JB; Heilshorn S; Rando TA An artificial niche preserves the quiescence of muscle stem cells and enhances their therapeutic efficacy. Nat. Biotechnol 2016, 34, 752–759. [PubMed: 27240197]

(1102). Pumberger M; Qazi TH; Ehrentraut MC; Textor M; Kueper J; Stoltenburg-Didinger G; Winkler T; von Roth P; Reinke S; Borselli C; Perka C; Mooney DJ; Duda GN; Geißler S Synthetic niche to modulate regenerative potential of MSCs and enhance skeletal muscle regeneration. Biomaterials 2016, 99, 95–108. [PubMed: 27235995]

(1103). Thomopoulos S; Birman V; Genin GM Structural interfaces and attachments in biology; Springer, 2013.

(1104). Smith L; Xia Y; Galatz LM; Genin GM; Thomopoulos S Tissue-engineering strategies for the tendon/ligament-to-bone insertion. Connect. Tissue. Res 2012, 53, 95–105. [PubMed: 22185608]

(1105). Lu HH; Thomopoulos S Functional attachment of soft tissues to bone: development, healing, and tissue engineering. Annu. Rev. Biomed. Eng 2013, 15, 201–226. [PubMed: 23642244]

(1106). Thomopoulos S; Genin GM; Galatz LM The development and morphogenesis of the tendon-to-bone insertion - what development can teach us about healing. J. Musculoskelet. Neuronal Interact 2010, 10, 35–45. [PubMed: 20190378]

(1107). Liu W; Zhang Y; Thomopoulos S; Xia Y Generation of controllable gradients in cell density. Angew. Chem. Int. Edit 2013, 52, 429–432.

(1108). Thomopoulos S; Das R; Birman V; Smith L; Ku K; Elson EL; Pryse KM; Marquez JP; Genin GM Fibrocartilage tissue engineering: the role of the stress environment on cell morphology and matrix expression. Tissue Eng. Part A 2010, 17, 1039–1053.

(1109). Pashuck ET; Stevens MM Designing regenerative biomaterial therapies for the clinic. Sci. Transl. Med 2012, 4, 160sr164–160sr164.

(1110). Sarkar K; Xue Y; Sant S In The Immune Response to Implanted Materials and Devices: The Impact of the Immune System on the Success of an Implant; Corradetti B, Ed.; Springer International Publishing: Cham, 2017.

(1111). Singh A Biomaterials innovation for next generation ex vivo immune tissue engineering. Biomaterials 2017, 130, 104–110. [PubMed: 28335993]

(1112). Lynn AK; Yannas IV; Bonfield W Antigenicity and immunogenicity of collagen. J. Biomed. Mater. Res. B 2004, 71B, 343–354.

(1113). Parenteau-Bareil R; Gauvin R; Berthod F Collagen-based biomaterials for tissue engineering applications. Materials 2010, 3, 1863.

(1114). Ménard M; Dusseault J; Langlois G; Baille WE; Tam KS; Yahia LH; Zhu XX; Hallé J-P Role of protein contaminants in the immunogenicity of alginates. J. Biomed. Mater. Res. B 2010, 93B, 333–340.

(1115). Franz S; Rammelt S; Scharnweber D; Simon JC Immune responses to implants – A review of the implications for the design of immunomodulatory biomaterials. Biomaterials 2011, 32, 6692–6709. [PubMed: 21715002]

(1116). Zhang L; Cao Z; Bai T; Carr L; Ella-Menye J-R; Irvin C; Ratner BD; Jiang S Zwitterionic hydrogels implanted in mice resist the foreign-body reaction. Nat. Biotechnol 2013, 31, 553–556. [PubMed: 23666011]

(1117). Hezi-Yamit A; Sullivan C; Wong J; David L; Chen M; Cheng P; Shumaker D; Wilcox JN; Udipi K Impact of polymer hydrophilicity on biocompatibility: Implication for DES polymer design. J. Biomed. Mater. Res. A 2009, 90A, 133–141.

(1118). Vegas AJ; Veiseh O; Doloff JC; Ma M; Tam HH; Bratlie K; Li J; Bader AR; Langan E; Olejnik K; Fenton P; Kang JW; Hollister-Locke J; Bochenek MA; Chiu A; Siebert S; Tang K; Jhunjhunwala S; Aresta-Dasilva S; Dholakia N; Thakrar R; Vietti T; Chen M; Cohen J;

Siniakowicz K; Qi M; McGarrigle J; Lyle S; Harlan DM; Greiner DL; Oberholzer J; Weir GC; Langer R; Anderson DG Combinatorial hydrogel library enables identification of materials that mitigate the foreign body response in primates. Nat. Biotechnol 2016, 34, 345–352. [PubMed: 26807527]

(1119). Vasconcelos DP; Costa M; Amaral IF; Barbosa MA; Águas AP; Barbosa JN Development of an immunomodulatory biomaterial: Using resolvin D1 to modulate inflammation. Biomaterials 2015, 53, 566–573. [PubMed: 25890752]

(1120). Browne S; Pandit A Biomaterial-mediated modification of the local inflammatory environment. Front. Biotechnol. Bioeng 2015, 3, DOI: 10.3389/fbioe.2015.00067.

(1121). Zakrzewski JL; van den Brink MRM; Hubbell JA Overcoming immunological barriers in regenerative medicine. Nat. Biotechnol 2014, 32, 786–794. [PubMed: 25093888]

(1122). Wei M; Gao Y; Li X; Serpe MJ Stimuli-responsive polymers and their applications. Polym. Chem 2017, 8, 127–143.

(1123). Lim HL; Hwang Y; Kar M; Varghese S Smart hydrogels as functional biomimetic systems. Biomater. Sci 2014, 2, 603–618.

(1124). Roy D; Cambre JN; Sumerlin BS Future perspectives and recent advances in stimuli-responsive materials. Prog. Polym. Sci 2010, 35, 278–301.

(1125). Wilson AN; Guiseppi-Elie A Bioresponsive hydrogels. Adv. Healthc. Mater. 2013, 2, 520–532. [PubMed: 23233355]

(1126). Miyata T; Asami N; Uragami T A reversibly antigen-responsive hydrogel. Nature 1999, 399, 766–769. [PubMed: 10391240]

(1127). Miyata T; Asami N; Uragami T Structural design of stimuli-responsive bioconjugated hydrogels that respond to a target antigen. J. Polym. Sci. Polym. Phys 2009, 47, 2144–2157.

(1128). Singh A; Peppas NA Hydrogels and scaffolds for immunomodulation. Adv. Mater. 2014, 26, 6530–6541. [PubMed: 25155610]

(1129). Dondossola E; Holzapfel BM; Alexander S; Filippini S; Hutmacher DW; Friedl P Examination of the foreign body response to biomaterials by nonlinear intravital microscopy. Nature Biomedical Engineering 2016, 1, 0007.

(1130). Grainger DW All charged up about implanted biomaterials. Nat. Biotechnol 2013, 31, 507–509. [PubMed: 23752436]

(1131). Picollet-D'hahan N; Dolega ME; Liguori L; Marquette C; Le Gac S; Gidrol X; Martin DK A 3D toolbox to enhance physiological relevance of human tissue models. Trends Biotechnol 2016, 34, 757–769. [PubMed: 27497676]

(1132). Kinney MA; Hookway TA; Wang Y; McDevitt TC Engineering three-dimensional stem cell morphogenesis for the development of tissue models and scalable regenerative therapeutics. Ann. Biomed. Eng 2013, 42, 352–367. [PubMed: 24297495]

(1133). Esch EW; Bahinski A; Huh D Organs-on-chips at the frontiers of drug discovery. Nat. Rev. Drug Discov 2015, 14, 248–260. [PubMed: 25792263]

(1134). Huh D; Hamilton GA; Ingber DE From 3D cell culture to organs-on-chips. Trends Cell Biol 2011, 21, 745–754. [PubMed: 22033488]

(1135). Verhulsel M; Vignes M; Descroix S; Malaquin L; Vignjevic DM; Viovy J-L A review of microfabrication and hydrogel engineering for micro-organs on chips. Biomaterials 2014, 35, 1816–1832. [PubMed: 24314552]

(1136). Bhatia SN; Ingber DE Microfluidic organs-on-chips. Nat. Biotechnol 2014, 32, 760–772. [PubMed: 25093883]

(1137). Zhang YS; Aleman J; Arneri A; Bersini S; Piraino F; Shin SR; Dokmeci MR; Khademhosseini A From cardiac tissue engineering to heart-on-a-chip: Beating challenges. Biomed. Mater. 2015, 10, 034006. [PubMed: 26065674]

(1138). Huh D; Matthews BD; Mammoto A; Montoya-Zavala M; Hsin HY; Ingber DE Reconstituting Organ-Level Lung Functions on a Chip. Science 2010, 328, 1662–1668. [PubMed: 20576885]

(1139). Khetani SR; Berger DR; Ballinger KR; Davidson MD; Lin C; Ware BR Microengineered liver tissues for drug testing. J. Lab. Autom 2015, 20, 216–250. [PubMed: 25617027]

(1140). Kim S; LesherPerez SC; Yamanishi C; Labuz JM; Leung B; Takayama S Pharmacokinetic profile that reduces nephrotoxicity of gentamicin in a perfused kidney-on-a-chip. Biofabrication 2016, 8, 015021. [PubMed: 27011358]

(1141). Zheng W; Huang R; Jiang B; Zhao Y; Zhang W; Jiang X An early-stage atherosclerosis research model based on microfluidics. Small 2016, 12, 2022–2034. [PubMed: 26890624]

(1142). Al-Saffar A; da Costa AN; Delaunois A; Leishman DJ; Marks L; Rosseels M-L; Valentin J-P In Principles of Safety Pharmacology; Springer, 2015.

(1143). Sabhachandani P; Motwani V; Cohen N; Sarkar S; Torchilin V; Konry T Generation and functional assessment of 3D multicellular spheroids in droplet based microfluidics platform. Lab Chip 2016, 16, 497–505. [PubMed: 26686985]

(1144). Singelyn JM; DeQuach JA; Seif-Naraghi SB; Littlefield RB; Schup-Magoffin PJ; Christman KL Naturally derived myocardial matrix as an injectable scaffold for cardiac tissue engineering. Biomaterials 2009, 30, 5409–5416. [PubMed: 19608268]

(1145). Valencia PM; Farokhzad OC; Karnik R; Langer R Microfluidic technologies for accelerating the clinical translation of nanoparticles. Nat. Nanotechnol 2012, 7, 623–629. [PubMed: 23042546]

(1146). Masumoto H; Ikuno T; Takeda M; Fukushima H; Marui A; Katayama S; Shimizu T; Ikeda T; Okano T; Sakata R; Yamashita JK Human iPS cell-engineered cardiac tissue sheets with cardiomyocytes and vascular cells for cardiac regeneration. Sci. Rep 2014, 4, 6716. [PubMed: 25336194]

(1147). Infanger DW; Lynch ME; Fischbach C Engineered culture models for studies of tumor-microenvironment interactions. Annu. Rev. Biomed. Eng 2013, 15, 29–53. [PubMed: 23642249]

(1148). Bussek A; Schmidt M; Bauriedl J; Ravens U; Wettwer E; Lohmann H Cardiac tissue slices with prolonged survival for in vitro drug safety screening. J. Pharmacol. Tox. Met 2012, 66, 145–151.

(1149). van Spreeuwel A; Bax N; Bastiaens A; Foolen J; Loerakker S; Borochin M; Van Der Schaft D; Chen C; Baaijens F; Bouten C The influence of matrix (an) isotropy on cardiomyocyte contraction in engineered cardiac microtissues. Integr. Biol 2014, 6, 422–429.

(1150). Wakatsuki T; Kolodney MS; Zahalak GI; Elson EL Cell mechanics studied by a reconstituted model tissue. Biophys. J. 2000, 79, 2353–2368. [PubMed: 11053115]

(1151). Annabi N; Tsang K; Mithieux SM; Nikkhah M; Ameri A; Khademhosseini A; Weiss AS Highly elastic micropatterned hydrogel for engineering functional cardiac tissue. Adv. Func. Mater. 2013, 23, 4950–4959.

(1152). Thavandiran N; Dubois N; Mikryukov A; Massé S; Beca B; Simmons CA; Deshpande VS; McGarry JP; Chen CS; Nanthakumar K; Keller GM; Radisic M; Zandstra PW Design and formulation of functional pluripotent stem cell-derived cardiac microtissues. Proc. Natl. Acad. Sci. U.S.A 2013, 110, E4698–E4707. [PubMed: 24255110]

(1153). Legant WR; Miller JS; Blakely BL; Cohen DM; Genin GM; Chen CS Measurement of mechanical tractions exerted by cells in three-dimensional matrices. Nat. Meth 2010, 7, 969–971.

(1154). Asnes CF; Marquez JP; Elson EL; Wakatsuki T Reconstitution of the Frank-Starling mechanism in engineered heart tissues. Biophys. J. 2006, 91, 1800–1810. [PubMed: 16782784]

(1155). Wang L; Xu C; Zhu Y; Yu Y; Sun N; Zhang X; Feng K; Qin J Human induced pluripotent stem cell-derived beating cardiac tissues on paper. Lab Chip 2015, 15, 4283–4290. [PubMed: 26430714]

(1156). Ng K; Gao B; Yong KW; Li Y; Shi M; Zhao X; Li Z; Zhang X; Pingguan-Murphy B; Yang H; Xu F Paper-based cell culture platform and its emerging biomedical applications. Mater. Today 2016, 20, 32–44

(1157). Mosadegh B; Dabiri BE; Lockett MR; Derda R; Campbell P; Parker KK; Whitesides GM Three-dimensional paper-based model for cardiac ischemia. Adv. Healthc. Mater. 2014, 3, 1036–1043. [PubMed: 24574054]

(1158). Annabi N; Selimović Š; Cox JPA; Ribas J; Bakooshli MA; Heintze D; Weiss AS; Cropek D; Khademhosseini A Hydrogel-coated microfluidic channels for cardiomyocyte culture. Lab Chip 2013, 13, 3569–3577. [PubMed: 23728018]

(1159). Bergström G; Christoffersson J; Schwanke K; Zweigerdt R; Mandenius C-F Stem cell derived in vivo-like human cardiac bodies in a microfluidic device for toxicity testing by beating frequency imaging. Lab Chip 2015, 15, 3242–3249. [PubMed: 26135270]

(1160). Douville NJ; Zamankhan P; Tung Y-C; Li R; Vaughan BL; Tai C-F; White J; Christensen PJ; Grotberg JB; Takayama S Combination of fluid and solid mechanical stresses contribute to cell death and detachment in a microfluidic alveolar model. Lab Chip 2011, 11, 609–619. [PubMed: 21152526]

(1161). Huh D; Leslie DC; Matthews BD; Fraser JP; Jurek S; Hamilton GA; Thorneloe KS; McAlexander MA; Ingber DE A human disease model of drug toxicity–induced pulmonary edema in a lung-on-a-chip microdevice. Sci. Transl. Med 2012, 4, 159ra147.

(1162). Kaplowitz N Idiosyncratic drug hepatotoxicity. Nat. Rev. Drug Discov 2005, 4, 489–499. [PubMed: 15931258]

(1163). Wang J; Chen F; Liu L; Qi C; Wang B; Yan X; Huang C; Hou W; Zhang MQ; Chen Y Engineering EMT using 3D micro-scaffold to promote hepatic functions for drug hepatotoxicity evaluation. Biomaterials 2016, 91, 11–22. [PubMed: 26994875]

(1164). Khetani SR; Bhatia SN Microscale culture of human liver cells for drug development. Nat. Biotechnol. 2008, 26, 120–126. [PubMed: 18026090]

(1165). Dragoni S; Franco G; Regoli M; Bracciali M; Morandi V; Sgaragli G; Bertelli E; Valoti M Gold nanoparticles uptake and cytotoxicity assessed on rat liver precision cut slices. Toxicol. Sci 2012, kfs150.

(1166). Leite SB; Wilk-Zasadna I; Comenges JMZ; Airola E; Reis-Fernandes MA; Mennecozzi M; Guguen-Guillouzo C; Chesne C; Gouillou C; Alves PM 3D HepaRG Model as an attractive tool for toxicity testing. Toxicol. Sci 2012, kfs232.

(1167). Tostões RM; Leite SB; Serra M; Jensen J; Björquist P; Carrondo MJ; Brito C; Alves PM Human liver cell spheroids in extended perfusion bioreactor culture for repeated-dose drug testing. Hepatology 2012, 55, 1227–1236. [PubMed: 22031499]

(1168). Wong SF; Choi YY; Kim DS; Chung BG; Lee S-H Concave microwell based size-controllable hepatosphere as a three-dimensional liver tissue model. Biomaterials 2011, 32, 8087–8096. [PubMed: 21813175]

(1169). Bhise NS; Manoharan V; Massa S; Tamayol A; Ghaderi M; Miscuglio M; Lang Q; Zhang YS; Shin SR; Calzone G A liver-on-a-chip platform with bioprinted hepatic spheroids. Biofabrication 2016, 8, 014101. [PubMed: 26756674]

(1170). Bhise NS; Ribas J; Manoharan V; Zhang YS; Polini A; Massa S; Dokmeci MR; Khademhosseini A Organ-on-a-chip platforms for studying drug delivery systems. J. Control. Release 2014, 190, 82–93. [PubMed: 24818770]

(1171). Wagner I; Materne E-M; Brincker S; Süßbier U; Frädrich C; Busek M; Sonntag F; Sakharov DA; Trushkin EV; Tonevitsky AG A dynamic multi-organ-chip for long-term cultivation and substance testing proven by 3D human liver and skin tissue co-culture. Lab Chip 2013, 13, 3538–3547. [PubMed: 23648632]

(1172). Ploss A; Khetani SR; Jones CT; Syder AJ; Trehan K; Gaysinskaya VA; Mu K; Ritola K; Rice CM; Bhatia SN Persistent hepatitis C virus infection in microscale primary human hepatocyte cultures. Proc. Natl. Acad. Sci. U.S.A 2010, 107, 3141–3145. [PubMed: 20133632]

(1173). Heldin C-H; Rubin K; Pietras K; Östman A High interstitial fluid pressure—an obstacle in cancer therapy. Nat. Rev. Cancer 2004, 4, 806–813. [PubMed: 15510161]

(1174). Bhise NS; Shmueli RB; Sunshine JC; Tzeng SY; Green JJ Drug delivery strategies for therapeutic angiogenesis and antiangiogenesis. Expert Opin. Drug Del 2011, 8, 485–504.

(1175). Loessner D; Holzapfel BM; Clements JA Engineered microenvironments provide new insights into ovarian and prostate cancer progression and drug responses. Adv. Drug Deliver. Rev 2014, 79–80, 193–213.

(1176). Alemany-Ribes M; Semino CE Bioengineering 3D environments for cancer models. Adv. Drug Deliver. Rev 2014, 79–80, 40–49.

(1177). Fong ELS; Harrington DA; Farach-Carson MC; Yu H Heralding a new paradigm in 3D tumor modeling. Biomaterials 2016, 108, 197–213. [PubMed: 27639438]

(1178). Gonzalez-Rodriguez D; Guevorkian K; Douezan S; Brochard-Wyart F Soft matter models of developing tissues and tumors. Science 2012, 338, 910–917. [PubMed: 23161991]

(1179). Rodenhizer D; Gaude E; Cojocari D; Mahadevan R; Frezza C; Wouters BG; McGuigan AP A three-dimensional engineered tumour for spatial snapshot analysis of cell metabolism and phenotype in hypoxic gradients. Nat. Mater. 2016, 15, 227–234. [PubMed: 26595121]

(1180). Albanese A; Lam AK; Sykes EA; Rocheleau JV; Chan WC Tumour-on-a-chip provides an optical window into nanoparticle tissue transport. Nat. Commun 2013, 4, 2718. [PubMed: 24177351]

(1181). Lei Y; Li J; Wang N; Yang X; Hamada Y; Li Q; Zheng W; Jiang X An on-chip model for investigating the interaction between neurons and cancer cells. Integr. Biol 2016, 8, 359–367.

(1182). Chaudhuri PK; Warkiani ME; Jing T; Lim CT Microfluidics for research and applications in oncology. Analyst 2016, 141, 504–524. [PubMed: 26010996]

(1183). Wlodkowic D; Cooper JM Tumors on chips: oncology meets microfluidics. Curr. Opin. Chem. Biol 2010, 14, 556–567. [PubMed: 20832352]

(1184). Kim S; Chung M; Jeon NL Three-dimensional biomimetic model to reconstitute sprouting lymphangiogenesis in vitro. Biomaterials 2016, 78, 115–128. [PubMed: 26691234]

(1185). Fan Y; Nguyen DT; Akay Y; Xu F; Akay M Engineering a brain cancer chip for high-throughput drug screening. Sci. Rep 2016, 6, 25062. [PubMed: 27151082]

(1186). Aung A; Theprungsirikul J; Lim HL; Varghese S Chemotaxis-driven assembly of endothelial barrier in a tumor-on-a-chip platform. Lab Chip 2016, 16, 1886–1898. [PubMed: 27097908]

(1187). Aung A; Bhullar IS; Theprungsirikul J; Davey SK; Lim HL; Chiu Y-J; Ma X; Dewan S; Lo Y-H; McCulloch A; Varghese S 3D cardiac utissues within a microfluidic device with real-time contractile stress readout. Lab Chip 2016, 16, 153–162. [PubMed: 26588203]

(1188). Knowlton S; Onal S; Yu CH; Zhao JJ; Tasoglu S Bioprinting for cancer research. Trends Biotechnol 2015, 33, 504–513. [PubMed: 26216543]

(1189). Pamies D; Hartung T; Hogberg HT Biological and medical applications of a brain-on-a-chip. Exp. Biol. Med 2014, 239, 1096–1107.

(1190). Karimi M; Bahrami S; Mirshekari H; Basri SMM; Nik AB; Aref AR; Akbari M; Hamblin MR Microfluidic systems for stem cell-based neural tissue engineering. Lab Chip 2016, 16, 2551–2571. [PubMed: 27296463]

(1191). Zheng Y; Chen JM; Craven M; Choi NW; Totorica S; Diaz-Santana A; Kermani P; Hempstead B; Fischbach-Teschl C; Lopez JA; Stroock AD In vitro microvessels for the study of angiogenesis and thrombosis. Proc. Natl. Acad. Sci. U.S.A 2012, 109, 9342–9347. [PubMed: 22645376]

(1192). Sakar MS; Neal D; Boudou T; Borochin MA; Li Y; Weiss R; Kamm RD; Chen CS; Asada HH Formation and optogenetic control of engineered 3D skeletal muscle bioactuators. Lab Chip 2012, 12, 4976–4985. [PubMed: 22976544]

(1193). Naeye B; Deschout H; Caveliers V; Descamps B; Braeckmans K; Vanhove C; Demeester J; Lahoutte T; De Smedt SC; Raemdonck K In vivo disassembly of IV administered siRNA matrix nanoparticles at the renal filtration barrier. Biomaterials 2013, 34, 2350–2358. [PubMed: 23261216]

(1194). Wilmer MJ; Ng CP; Lanz HL; Vulto P; Suter-Dick L; Masereeuw R Kidney-on-a-chip technology for drug-induced nephrotoxicity screening. Trends Biotechnol 2016, 34, 156–170. [PubMed: 26708346]

(1195). Kim HJ; Huh D; Hamilton G; Ingber DE Human gut-on-a-chip inhabited by microbial flora that experiences intestinal peristalsis-like motions and flow. Lab Chip 2012, 12, 2165–2174. [PubMed: 22434367]

(1196). Kim HJ; Ingber DE Gut-on-a-Chip microenvironment induces human intestinal cells to undergo villus differentiation. Integr. Biol 2013, 5, 1130–1140.

(1197). Mohammadi MH; Heidary Araghi B; Beydaghi V; Geraili A; Moradi F; Jafari P; Janmaleki M; Valente KP; Akbari M; Sanati-Nezhad A Skin diseases modeling using combined tissue engineering and microfluidic technologies. Adv. Healthc. Mater. 2016, 5, 2459–2480. [PubMed: 27548388]

(1198). Moraes C; Labuz JM; Leung BM; Inoue M; Chun T-H; Takayama S On being the right size: scaling effects in designing a human-on-a-chip. Integr. Biol 2013, 5, 1149–1161.

(1199). Abaci HE; Shuler ML Human-on-a-chip design strategies and principles for physiologically based pharmacokinetics/pharmacodynamics modeling. Integr. Biol 2015, 7, 383–391.

(1200). Robinton DA; Daley GQ The promise of induced pluripotent stem cells in research and therapy. Nature 2012, 481, 295–305. [PubMed: 22258608]

(1201). Tang J; Shen D; Caranasos TG; Wang Z; Vandergriff AC; Allen TA; Hensley MT; Dinh P-U; Cores J; Li T-S; Zhang J; Kan Q; Cheng K Therapeutic microparticles functionalized with biomimetic cardiac stem cell membranes and secretome. Nat. Commun 2017, 8, 13724. [PubMed: 28045024]

(1202). Avior Y; Sagi I; Benvenisty N Pluripotent stem cells in disease modelling and drug discovery. Nat. Rev. Mol. Cell Bio 2016, 17, 170–182. [PubMed: 26818440]

(1203). Desbordes SC; Studer L Adapting human pluripotent stem cells to high-throughput and high-content screening. Nat. Protoc 2013, 8, 111–130. [PubMed: 23257981]

(1204). Serra M; Brito C; Correia C; Alves PM Process engineering of human pluripotent stem cells for clinical application. Trends Biotechnol 2012, 30, 350–359. [PubMed: 22541338]

(1205). Deng Y; Yang Z; Terry T; Pan S; Woodside DG; Wang J; Ruan K; Willerson JT; Dixon RAF; Liu Q Prostacyclin-producing human mesenchymal cells target H19 lncRNA to augment endogenous progenitor function in hindlimb ischaemia. Nat. Commun 2016, 7, 11276. [PubMed: 27080438]

(1206). Manufacturing and banking of mesenchymal stem cells. Expert Opinion on Biological Therapy 2013, 13, 673–691. [PubMed: 23339745]

(1207). Lei Y; Schaffer DV A fully defined and scalable 3D culture system for human pluripotent stem cell expansion and differentiation. Proc. Natl. Acad. Sci. U.S.A 2013, 110, E5039–E5048. [PubMed: 24248365]

(1208). Ma T; Tsai A-C; Liu Y Biomanufacturing of human mesenchymal stem cells in cell therapy: Influence of microenvironment on scalable expansion in bioreactors. Biochem. Eng. J 2016, 108, 44–50.

(1209). Villa-Diaz LG; Ross AM; Lahann J; Krebsbach PH Concise Review: The evolution of human pluripotent stem cell culture: From feeder cells to synthetic coatings. Stem Cells 2013, 31, 1–7. [PubMed: 23081828]

(1210). Steiner D; Khaner H; Cohen M; Even-Ram S; Gil Y; Itsykson P; Turetsky T; Idelson M; Aizenman E; Ram R; Berman-Zaken Y; Reubinoff B Derivation, propagation and controlled differentiation of human embryonic stem cells in suspension. Nat. Biotechnol 2010, 28, 361–364. [PubMed: 20351691]

(1211). Chen AK-L; Chen X; Choo ABH; Reuveny S; Oh SKW Critical microcarrier properties affecting the expansion of undifferentiated human embryonic stem cells. Stem Cell Res 2011, 7, 97–111. [PubMed: 21763618]

(1212). Serra M; Correia C; Malpique R; Brito C; Jensen J; Bjorquist P; Carrondo MJT; Alves PM Microencapsulation Technology: A Powerful Tool for Integrating Expansion and Cryopreservation of Human Embryonic Stem Cells. PLOS ONE 2011, 6, e23212. [PubMed: 21850261]

(1213). McDevitt TC; Palecek SP Innovation in the culture and derivation of pluripotent human stem cells. Curr. Opin. Biotech 2008, 19, 527–533. [PubMed: 18760357]

(1214). Burdick JA; Vunjak-Novakovic G Engineered microenvironments for controlled stem cell differentiation. Tissue Eng. Part A 2009, 15, 205–219. [PubMed: 18694293]

(1215). Leung HW; Chen A; Choo ABH; Reuveny S; Oh SKW Agitation can Induce Differentiation of Human Pluripotent Stem Cells in Microcarrier Cultures. Tissue Engineering Part C-Methods 2011, 17, 165–172. [PubMed: 20698747]

(1216). Serra M; Correia C; Malpique R; Brito C; Jensen J; Bjorquist P; Carrondo MJT; Alves PM Microencapsulation Technology: A Powerful Tool for Integrating Expansion and Cryopreservation of Human Embryonic Stem Cells. Plos One 2011, 6.

(1217). Chayosumrit M; Tuch B; Sidhu K Alginate microcapsule for propagation and directed differentiation of hESCs to definitive endoderm. Biomaterials 2010, 31, 505–514. [PubMed: 19833385]

(1218). Yin X; Mead Benjamin E.; Safaee H; Langer R; Karp Jeffrey M.; Levy O Engineering stem cell organoids. Cell Stem Cell 2016, 18, 25–38. [PubMed: 26748754]

(1219). Tamura A; Kobayashi J; Yamato M; Okano T Thermally responsive microcarriers with optimal poly(N-isopropylacrylamide) grafted density for facilitating cell adhesion/detachment in suspension culture. Acta Biomater 2012, 8, 3904–3913. [PubMed: 22813847]

(1220). Kinney MA; Sargent CY; McDevitt TC The multiparametric effects of hydrodynamic environments on stem cell culture. Tissue Eng. Part B Rev 2011, 17, 249–262. [PubMed: 21491967]

(1221). Fernandes AM; Marinho PAN; Sartore RC; Paulsen BS; Mariante RM; Castilho LR; Rehen SK Successful scale-up of human embryonic stem cell production in a stirred microcarrier culture system. Braz. J. Med. Biol. Res 2009, 42, 515–522. [PubMed: 19448900]

(1222). Liu N; Zang R; Yang S-T; Li Y Stem cell engineering in bioreactors for large-scale bioprocessing. Eng. Life. Sci 2014, 14, 4–15.

(1223). Purwada A; Roy K; Singh A Engineering vaccines and niches for immune modulation. Acta Biomater 2014, 10, 1728–1740. [PubMed: 24373907]

(1224). Paulis LE; Mandal S; Kreutz M; Figdor CG Dendritic cell-based nanovaccines for cancer immunotherapy. Curr. Opin. Immunol 2013, 25, 389–395. [PubMed: 23571027]

(1225). Silva JM; Videira M; Gaspar R; Préat V; Florindo HF Immune system targeting by biodegradable nanoparticles for cancer vaccines. J. Control. Release 2013, 168, 179–199. [PubMed: 23524187]

(1226). Mellman I; Coukos G; Dranoff G Cancer immunotherapy comes of age. Nature 2011, 480, 480–489. [PubMed: 22193102]

(1227). Hotaling NA; Tang L; Irvine DJ; Babensee JE Biomaterial strategies for immunomodulation. Annu. Rev. Biomed. Eng 2015, 17, 317–349. [PubMed: 26421896]

(1228). Li WA; Mooney DJ Materials based tumor immunotherapy vaccines. Curr. Opin. Immunol 2013, 25, 238–245. [PubMed: 23337254]

(1229). Wang C; Ye Y; Hu Q; Bellotti A; Gu Z Tailoring Biomaterials for Cancer Immunotherapy: Emerging Trends and Future Outlook. Adv. Mater 2017, 29, 1606036.

(1230). Hori Y; Winans AM; Huang CC; Horrigan EM; Irvine DJ Injectable dendritic cell-carrying alginate gels for immunization and immunotherapy. Biomaterials 2008, 29, 3671–3682. [PubMed: 18565578]

(1231). Suematsu S; Watanabe T Generation of a synthetic lymphoid tissue-like organoid in mice. Nat. Biotechnol 2004, 22, 1539–1545. [PubMed: 15568019]

(1232). Kumamoto T; Huang EK; Paek HJ; Morita A; Matsue H; Valentini RF; Takashima A Induction of tumor-specific protective immunity by in situ Langerhans cell vaccine. Nat. Biotechnol 2002, 20, 64–69. [PubMed: 11753364]

(1233). Ali OA; Huebsch N; Cao L; Dranoff G; Mooney DJ Infection-mimicking materials to program dendritic cells in situ. Nat. Mater. 2009, 8, 151–158. [PubMed: 19136947]

(1234). Ali OA; Emerich D; Dranoff G; Mooney DJ In situ regulation of DC subsets and T cells mediates tumor regression in mice. Sci. Transl. Med 2009, 1, 8ra19.

(1235). Singh A; Suri S; Roy K In-situ crosslinking hydrogels for combinatorial delivery of chemokines and siRNA–DNA carrying microparticles to dendritic cells. Biomaterials 2009, 30, 5187–5200. [PubMed: 19560815]

(1236). Lee TT; García JR; Paez JI; Singh A; Phelps EA; Weis S; Shafiq Z; Shekaran A; del Campo A; García AJ Light-triggered in vivo activation of adhesive peptides regulates cell adhesion, inflammation and vascularization of biomaterials. Nat. Mater. 2015, 14, 352–360. [PubMed: 25502097]

(1237). Indolfi L; Baker AB; Edelman ER The role of scaffold microarchitecture in engineering endothelial cell immunomodulation. Biomaterials 2012, 33, 7019–7027. [PubMed: 22796162]

(1238). Delcassian D; Sattler S; Dunlop IE T cell immunoengineering with advanced biomaterials. Integr. Biol 2017, 9, 211–222.

(1239). Vishwakarma A; Bhise NS; Evangelista MB; Rouwkema J; Dokmeci MR; Ghaemmaghami AM; Vrana NE; Khademhosseini A Engineering immunomodulatory biomaterials to tune the inflammatory response. Trends Biotechnol 2016, 34, 470–482. [PubMed: 27138899]

(1240). Ali OA; Tayalia P; Shvartsman D; Lewin S; Mooney DJ Inflammatory cytokines presented from polymer matrices differentially generate and activate DCs in situ. Adv. Func. Mater. 2013, 23, 4621–4628.

(1241). Ballotta V; Driessen-Mol A; Bouten CVC; Baaijens FPT Strain-dependent modulation of macrophage polarization within scaffolds. Biomaterials 2014, 35, 4919–4928. [PubMed: 24661551]

(1242). McWhorter FY; Davis CT; Liu WF Physical and mechanical regulation of macrophage phenotype and function. Cell. Mol. Life Sci 2015, 72, 1303–1316. [PubMed: 25504084]

(1243). Yu Y; Wu R-X; Yin Y; Chen F-M Directing immunomodulation using biomaterials for endogenous regeneration. J. Mater. Chem. B 2016, 4, 569–584.

(1244). Apoorva FNU; Tian YF; Pierpont TM; Bassen DM; Cerchietti L; Butcher JT; Weiss RS; Singh A Lymph node stiffness-mimicking hydrogels regulate human B-cell lymphoma growth and cell surface receptor expression in a molecular subtype-specific manner. J. Biomed. Mater. Res. A 2017, 105, 1833–1844. [PubMed: 28177577]

(1245). Hori Y; Winans AM; Irvine DJ Modular injectable matrices based on alginate solution/microsphere mixtures that gel in situ and co-deliver immunomodulatory factors. Acta Biomater 2009, 5, 969–982. [PubMed: 19117820]

(1246). Singh A; Agarwal R; Diaz-Ruiz CA; Willett NJ; Wang P; Lee LA; Wang Q; Guldberg RE; García AJ Nanoengineered particles for enhanced intra-articular retention and delivery of proteins. Adv. Healthc. Mater. 2014, 3, 1562–1567. [PubMed: 24687997]

(1247). Purwada A; Tian YF; Huang W; Rohrbach KM; Deol S; August A; Singh A Self-assembly protein nanogels for safer cancer immunotherapy. Adv. Healthc. Mater. 2016, 5, 1413–1419. [PubMed: 27100566]

(1248). Tahara Y; Akiyoshi K Current advances in self-assembled nanogel delivery systems for immunotherapy. Adv. Drug Deliver. Rev 2015, 95, 65–76.

(1249). Purwada A; Shah SB; Beguelin W; Melnick AM; Singh A Modular immune organoids with integrin ligand specificity differentially regulate ex vivo B cell activation. ACS Biomater. Sci. Eng 2017, 3, 214–225.

(1250). Purwada A; Singh A Immuno-engineered organoids for regulating the kinetics of B-cell development and antibody production. Nat. Protoc 2017, 12, 168–182. [PubMed: 28005068]

(1251). Purwada A; Jaiswal MK; Ahn H; Nojima T; Kitamura D; Gaharwar AK; Cerchietti L; Singh A Ex vivo engineered immune organoids for controlled germinal center reactions. Biomaterials 2015, 63, 24–34. [PubMed: 26072995]

(1252). Tian YF; Ahn H; Schneider RS; Yang SN; Roman-Gonzalez L; Melnick AM; Cerchietti L; Singh A Integrin-specific hydrogels as adaptable tumor organoids for malignant B and T cells. Biomaterials 2015, 73, 110–119. [PubMed: 26406451]

(1253). Singh A; Qin H; Fernandez I; Wei J; Lin J; Kwak LW; Roy K An injectable synthetic immune-priming center mediates efficient T-cell class switching and T-helper 1 response against B cell lymphoma. J. Control. Release 2011, 155, 184–192. [PubMed: 21708196]

(1254). Pradhan P; Qin H; Leleux JA; Gwak D; Sakamaki I; Kwak LW; Roy K The effect of combined IL10 siRNA and CpG ODN as pathogen-mimicking microparticles on Th1/Th2 cytokine balance in dendritic cells and protective immunity against B cell lymphoma. Biomaterials 2014, 35, 5491–5504. [PubMed: 24720881]

(1255). Hori Y; Stern PJ; Hynes RO; Irvine DJ Engulfing tumors with synthetic extracellular matrices for cancer immunotherapy. Biomaterials 2009, 30, 6757–6767. [PubMed: 19766305]

(1256). Li Y; Fang M; Zhang J; Wang J; Song Y; Shi J; Li W; Wu G; Ren J; Wang Z Hydrogel dual delivered celecoxib and anti-PD-1 synergistically improve antitumor immunity. Oncoimmunology 2016, 5, e1074374. [PubMed: 27057439]

(1257). Roy K; Wang D; Hedley ML; Barman SP Gene delivery with in-situ crosslinking polymer networks generates long-term systemic protein expression. Mol. Ther 2003, 7, 401–408. [PubMed: 12668136]

(1258). Stephan SB; Taber AM; Jileaeva I; Pegues EP; Sentman CL; Stephan MT Biopolymer implants enhance the efficacy of adoptive T-cell therapy. Nat. Biotechnol 2015, 33, 97–101. [PubMed: 25503382]

(1259). Gübeli RJ; Schöneweis K; Huzly D; Ehrbar M; Hamri GC-E; El-Baba MD; Urban S; Weber W Pharmacologically triggered hydrogel for scheduling hepatitis B vaccine administration. Sci. Rep 2013, 3, 2610. [PubMed: 24018943]

(1260). Stachowiak AN; Irvine DJ Inverse opal hydrogel-collagen composite scaffolds as a supportive microenvironment for immune cell migration. J. Biomed. Mater. Res. A 2008, 85A, 815–828.

(1261). Singh A; Nie H; Ghosn B; Qin H; Kwak LW; Roy K Efficient modulation of T-cell response by dual-mode, single-carrier delivery of cytokine-targeted siRNA and DNA vaccine to antigen-presenting cells. Mol. Ther 2008, 16, 2011–2021. [PubMed: 18813280]

(1262). Spiller KL; Nassiri S; Witherel CE; Anfang RR; Ng J; Nakazawa KR; Yu T; Vunjak-Novakovic G Sequential delivery of immunomodulatory cytokines to facilitate the M1-to-M2 transition of macrophages and enhance vascularization of bone scaffolds. Biomaterials 2015, 37, 194–207. [PubMed: 25453950]

(1263). Sexton A; Whitney PG; Chong S-F; Zelikin AN; Johnston APR; De Rose R; Brooks AG; Caruso F; Kent SJ A Protective vaccine delivery system for in vivo T cell stimulation using nanoengineered polymer hydrogel capsules. ACS Nano 2009, 3, 3391–3400. [PubMed: 19824668]

(1264). Monette A; Ceccaldi C; Assaad E; Lerouge S; Lapointe R Chitosan thermogels for local expansion and delivery of tumor-specific T lymphocytes towards enhanced cancer immunotherapies. Biomaterials 2016, 75, 237–249. [PubMed: 26513416]

(1265). Park J; Wrzesinski SH; Stern E; Look M; Criscione J; Ragheb R; Jay SM; Demento SL; Agawu A; Licona Limon P; Ferrandino AF; Gonzalez D; Habermann A; Flavell RA; Fahmy TM Combination delivery of TGF-β inhibitor and IL-2 by nanoscale liposomal polymeric gels enhances tumour immunotherapy. Nat. Mater. 2012, 11, 895–905. [PubMed: 22797827]

(1266). Chevallay B; Herbage D Collagen-based biomaterials as 3D scaffold for cell cultures: applications for tissue engineering and gene therapy. Med. Biol. Eng. Comput 2000, 38, 211–218. [PubMed: 10829416]

(1267). Verma IM Gene therapy that works. Science 2013, 341, 853–855. [PubMed: 23970689]

(1268). Zhang XJ; Li Y; Chen YE; Chen JH; Ma PX Cell-free 3D scaffold with two-stage delivery of miRNA-26a to regenerate critical-sized bone defects. Nature Communications 2016, 7.

(1269). Aagaard L; Rossi JJ RNAi therapeutics: Principles, prospects and challenges. Adv. Drug Deliver. Rev 2007, 59, 75–86.

(1270). Yin PT; Shah BP; Lee K-B Combined magnetic nanoparticle-based microrna and hyperthermia therapy to enhance apoptosis in brain cancer cells. Small 2014, 10, 4106–4112. [PubMed: 24947843]

(1271). Endo-Takahashi Y; Negishi Y; Nakamura A; Ukai S; Ooaku K; Oda Y; Sugimoto K; Moriyasu F; Takagi N; Suzuki R; Maruyama K; Aramaki Y Systemic delivery of miR-126 by miRNA-loaded Bubble liposomes for the treatment of hindlimb ischemia. Sci. Rep 2014, 4, 3883. [PubMed: 24457599]

(1272). Jin G; Feng G; Qin W; Tang BZ; Liu B; Li K Multifunctional organic nanoparticles with aggregation-induced emission (AIE) characteristics for targeted photodynamic therapy and RNA interference therapy. Chem. Commun 2016, 52, 2752–2755.

(1273). Zhao J; Mi Y; Feng S-S Targeted co-delivery of docetaxel and siPlk1 by herceptin-conjugated vitamin E TPGS based immunomicelles. Biomaterials 2013, 34, 3411–3421. [PubMed: 23375951]

(1274). Guo P The emerging field of RNA nanotechnology. Nat. Nanotechnol 2010, 5, 833–842. [PubMed: 21102465]

(1275). Sakurai H; Kawabata K; Sakurai F; Nakagawa S; Mizuguchi H Innate immune response induced by gene delivery vectors. Int. J. Pharmaceut 2008, 354, 9–15.

(1276). Kim Y-M; Park M-R; Song S-C Injectable polyplex hydrogel for localized and long-term delivery of siRNA. ACS Nano 2012, 6, 5757–5766. [PubMed: 22663194]

(1277). Hu Y; Atukorale PU; Lu JJ; Moon JJ; Um SH; Cho EC; Wang Y; Chen J; Irvine DJ Cytosolic delivery mediated via electrostatic surface binding of protein, virus, or siRNA cargos to pH-responsive core–shell gel particles. Biomacromolecules 2009, 10, 756–765. [PubMed: 19239276]

(1278). Dunn SS; Tian S; Blake S; Wang J; Galloway AL; Murphy A; Pohlhaus PD; Rolland JP; Napier ME; DeSimone JM Reductively responsive siRNA-conjugated hydrogel nanoparticles for gene silencing. J. Am. Chem. Soc 2012, 134, 7423–7430. [PubMed: 22475061]

(1279). Samal SK; Dash M; Van Vlierberghe S; Kaplan DL; Chiellini E; van Blitterswijk C; Moroni L; Dubruel P Cationic polymers and their therapeutic potential. Chem. Soc. Rev 2012, 41, 7147–7194. [PubMed: 22885409]

(1280). Paul A; Hasan A; Kindi HA; Gaharwar AK; Rao VTS; Nikkhah M; Shin SR; Krafft D; Dokmeci MR; Shum-Tim D; Khademhosseini A Injectable graphene oxide/hydrogel-based angiogenic gene delivery system for vasculogenesis and cardiac repair. ACS Nano 2014, 8, 8050–8062. [PubMed: 24988275]

(1281). Nelson CE; Kintzing JR; Hanna A; Shannon JM; Gupta MK; Duvall CL Balancing cationic and hydrophobic content of PEGylated siRNA polyplexes enhances endosome escape, stability, blood circulation time, and bioactivity in vivo. ACS Nano 2013, 7, 8870–8880. [PubMed: 24041122]

(1282). Li H; Yu SS; Miteva M; Nelson CE; Werfel T; Giorgio TD; Duvall CL Matrix metalloproteinase responsive, proximity-activated polymeric nanoparticles for siRNA delivery. Adv. Func. Mater. 2013, 23, 3040–3052.

(1283). Zhao J; Jin G; Weng G; Li J; Zhu J; Zhao J Recent advances in activatable fluorescence imaging probes for tumor imaging. Drug discovery today 2017.

(1284). Nelson CE; Kim AJ; Adolph EJ; Gupta MK; Yu F; Hocking KM; Davidson JM; Guelcher SA; Duvall CL Tunable delivery of siRNA from a biodegradable scaffold to promote angiogenesis in vivo. Adv. Mater. 2014, 26, 607–614. [PubMed: 24338842]

(1285). De Laporte L; Shea LD Matrices and scaffolds for DNA delivery in tissue engineering. Adv. Drug Deliver. Rev 2007, 59, 292–307.

(1286). Altschuler SJ; Wu LF Cellular heterogeneity: Do differences make a difference? Cell 2010, 141, 559–563. [PubMed: 20478246]

(1287). Amir E.-a. D.; Davis KL; Tadmor MD; Simonds EF; Levine JH; Bendall SC; Shenfeld DK; Krishnaswamy S; Nolan GP; Pe'er D viSNE enables visualization of high dimensional single-cell data and reveals phenotypic heterogeneity of leukemia. Nat. Biotechnol 2013, 31, 545–552. [PubMed: 23685480]

(1288). Smallwood SA; Lee HJ; Angermueller C; Krueger F; Saadeh H; Peat J; Andrews SR; Stegle O; Reik W; Kelsey G Single-cell genome-wide bisulfite sequencing for assessing epigenetic heterogeneity. Nat. Meth 2014, 11, 817–820.

(1289). Navin N; Kendall J; Troge J; Andrews P; Rodgers L; McIndoo J; Cook K; Stepansky A; Levy D; Esposito D; Muthuswamy L; Krasnitz A; McCombie WR; Hicks J; Wigler M Tumour evolution inferred by single-cell sequencing. Nature 2011, 472, 90–94. [PubMed: 21399628]

(1290). Xu X; Hou Y; Yin X; Bao L; Tang A; Song L; Li F; Tsang S; Wu K; Wu H; He W; Zeng L; Xing M; Wu R; Jiang H; Liu X; Cao D; Guo G; Hu X; Gui Y; Li Z; Xie W; Sun X; Shi M; Cai Z; Wang B; Zhong M; Li J; Lu Z; Gu N; Zhang X; Goodman L; Bolund L; Wang J; Yang H; Kristiansen K; Dean M; Li Y; Wang J Single-cell exome sequencing reveals single-nucleotide mutation characteristics of a kidney tumor. Cell 2012, 148, 886–895. [PubMed: 22385958]

(1291). Moignard V; Macaulay IC; Swiers G; Buettner F; Schütte J; Calero-Nieto FJ; Kinston S; Joshi A; Hannah R; Theis FJ; Jacobsen SE; de Bruijn MF; Göttgens B Characterization of transcriptional networks in blood stem and progenitor cells using high-throughput single-cell gene expression analysis. Nat. Cell Biol 2013, 15, 363–372. [PubMed: 23524953]

(1292). Klein Allon M.; Mazutis L; Akartuna I; Tallapragada N; Veres A; Li V; Peshkin L; Weitz David A.; Kirschner Marc W. Droplet barcoding for single-cell transcriptomics applied to embryonic stem cells. Cell 2015, 161, 1187–1201. [PubMed: 26000487]

(1293). Fritzsch FSO; Dusny C; Frick O; Schmid A Single-cell analysis in biotechnology, systems biology, and biocatalysis. Annu. Rev. Chem. Biomol 2012, 3, 129–155.

(1294). Chattopadhyay PK; Gierahn TM; Roederer M; Love JC Single-cell technologies for monitoring immune systems. Nat. Immunol 2014, 15, 128–135. [PubMed: 24448570]

(1295). Yin H; Marshall D Microfluidics for single cell analysis. Curr. Opin. Biotech 2012, 23, 110–119. [PubMed: 22133547]

(1296). Lecault V; White AK; Singhal A; Hansen CL Microfluidic single cell analysis: from promise to practice. Curr. Opin. Chem. Biol 2012, 16, 381–390. [PubMed: 22525493]

(1297). Weaver WM; Tseng P; Kunze A; Masaeli M; Chung AJ; Dudani JS; Kittur H; Kulkarni RP; Di Carlo D Advances in high-throughput single-cell microtechnologies. Curr. Opin. Biotech 2014, 25, 114–123. [PubMed: 24484889]

(1298). Groen N; Guvendiren M; Rabitz H; Welsh WJ; Kohn J; de Boer J Stepping into the omics era: Opportunities and challenges for biomaterials science and engineering. Acta Biomater 2016, 34, 133–142. [PubMed: 26876875]

(1299). Guerette PA; Hoon S; Seow Y; Raida M; Masic A; Wong FT; Ho VHB; Kong KW; Demirel MC; Pena-Francesch A; Amini S; Tay GZ; Ding D; Miserez A Accelerating the design of biomimetic materials by integrating RNA-seq with proteomics and materials science. Nat. Biotechnol 2013, 31, 908–915. [PubMed: 24013196]

(1300). Cranford SW; de Boer J; van Blitterswijk C; Buehler MJ Materiomics: An -omics approach to biomaterials research. Adv. Mater. 2013, 25, 802–824. [PubMed: 23297023]

(1301). Rasi Ghaemi S; Harding FJ; Delalat B; Gronthos S; Voelcker NH Exploring the mesenchymal stem cell niche using high throughput screening. Biomaterials 2013, 34, 7601–7615. [PubMed: 23871539]

(1302). Oliveira MB; Mano JF High-throughput screening for integrative biomaterials design: exploring advances and new trends. Trends Biotechnol 2014, 32, 627–636. [PubMed: 25450043]

(1303). Patel AK; Tibbitt MW; Celiz AD; Davies MC; Langer R; Denning C; Alexander MR; Anderson DG High throughput screening for discovery of materials that control stem cell fate. Curr. Opin. Solid State Mater. Sci 2016, 20, 202–211.

(1304). Mei Y; Saha K; Bogatyrev SR; Yang J; Hook AL; Kalcioglu ZI; Cho S-W; Mitalipova M; Pyzocha N; Rojas F; Van Vliet KJ; Davies MC; Alexander MR; Langer R; Jaenisch R; Anderson DG Combinatorial development of biomaterials for clonal growth of human pluripotent stem cells. Nat. Mater. 2010, 9, 768–778. [PubMed: 20729850]

(1305). Gobaa S; Hoehnel S; Roccio M; Negro A; Kobel S; Lutolf MP Artificial niche microarrays for probing single stem cell fate in high throughput. Nat. Meth 2011, 8, 949–955.

(1306). Ranga A; Gobaa S; Okawa Y; Mosiewicz K; Negro A; Lutolf MP 3D niche microarrays for systems-level analyses of cell fate. Nat. Commun 2014, 5, 4324. [PubMed: 25027775]

(1307). Li Y; Chen P; Wang Y; Yan S; Feng X; Du W; Koehler SA; Demirci U; Liu B-F Rapid assembly of heterogeneous 3D cell microenvironments in a microgel Array. Adv. Mater. 2016, 28, 3543–3548. [PubMed: 26991071]

(1308). Hou L; Coller J; Natu V; Hastie TJ; Huang NF Combinatorial extracellular matrix microenvironments promote survival and phenotype of human induced pluripotent stem cell-derived endothelial cells in hypoxia. Acta Biomater 2016, 44, 188–199. [PubMed: 27498178]

(1309). Gaharwar AK; Arpanaei A; Andresen TL; Dolatshahi-Pirouz A 3D biomaterial microarrays for regenerative medicine: Current state-of-the-art, emerging directions and future trends. Adv. Mater. 2015, 28, 771–781. [PubMed: 26607415]

(1310). Ranga A; Lutolf MP High-throughput approaches for the analysis of extrinsic regulators of stem cell fate. Curr. Opin. Cell Biol 2012, 24, 236–244. [PubMed: 22301436]

(1311). Floren M; Tan W Three-dimensional, soft neotissue arrays as high throughput platforms for the interrogation of engineered tissue environments. Biomaterials 2015, 59, 39–52. [PubMed: 25956850]

(1312). Mabry KM; Schroeder ME; Payne SZ; Anseth KS Three-dimensional high-throughput cell encapsulation platform to study changes in cell-matrix interactions. ACS Appl. Mater. Inter 2016, 8, 21914–21922.

(1313). Shin J-W; Mooney DJ Extracellular matrix stiffness causes systematic variations in proliferation and chemosensitivity in myeloid leukemias. Proc. Natl. Acad. Sci. U.S.A 2016, 113, 12126–12131. [PubMed: 27790998]

(1314). Marquez JP; Legant W; Lam V; Cayemberg A; Elson E; Wakatsuki T High-throughput measurements of hydrogel tissue construct mechanics. Tissue Eng. Part C Meth 2009, 15, 181–190.

(1315). Han YL; Huang G; Wang L; Fan X; Li F; Wang P; Lu TJ; Xu F High-throughput imaging methodologies for biomechanical testing. Handbook of Imaging in Biological Mechanics 2014, 185.

(1316). Choi M; Choi JW; Kim S; Nizamoglu S; Hahn SK; Yun SH Light-guiding hydrogels for cell-based sensing and optogenetic synthesis in vivo. Nat. Photonics 2013, 7, 987–994. [PubMed: 25346777]

(1317). Kitamura T; Pollard JW; Vendrell M Optical windows for imaging the metastatic tumour microenvironment in vivo. Trends Biotechnol 2017, 35, 5–8. [PubMed: 27238900]

(1318). Smith BR; Gambhir SS Nanomaterials for in vivo imaging. Chem. Rev 2017, 117, 901–986. [PubMed: 28045253]

(1319). Benam KH; Dauth S; Hassell B; Herland A; Jain A; Jang K-J; Karalis K; Kim HJ; MacQueen L; Mahmoodian R; Musah S; Torisawa Y.-s.; van der Meer AD; Villenave R; Yadid M; Parker KK; Ingber DE Engineered in vitro disease models. Annu. Rev. Pathol-Mech 2015, 10, 195–262.

(1320). McCullen SD; Chow AGY; Stevens MM In vivo tissue engineering of musculoskeletal tissues. Curr. Opin. Biotech 2011, 22, 715–720. [PubMed: 21646011]

(1321). Li Q; Ma L; Gao C Biomaterials for in situ tissue regeneration: development and perspectives. J. Mater. Chem. B 2015, 3, 8921–8938.

(1322). Yang J-A; Yeom J; Hwang BW; Hoffman AS; Hahn SK In situ-forming injectable hydrogels for regenerative medicine. Prog. Polym. Sci 2014, 39, 1973–1986.

(1323). Li Y; Liu W; Liu F; Zeng Y; Zuo S; Feng S; Qi C; Wang B; Yan X; Khademhosseini A; Bai J; Du Y Primed 3D injectable microniches enabling low-dosage cell therapy for critical limb ischemia. Proc. Natl. Acad. Sci. U.S.A 2014, 111, 13511–13516. [PubMed: 25197069]

(1324). Srivastava D; DeWitt N In vivo cellular reprogramming: The next generation. Cell 2016, 166, 1386–1396. [PubMed: 27610565]

(1325). Hasan A; Khattab A; Islam MA; Hweij KA; Zeitouny J; Waters R; Sayegh M; Hossain MM; Paul A Injectable hydrogels for cardiac tissue repair after myocardial infarction. Adv. Sci 2015, 2, DOI: 10.1002/advs.201500122.

(1326). Zhao Y; Yan H; Qiao S; Zhang L; Wang T; Meng Q; Chen X; Lin F-H; Guo K; Li C; Tian W Hydrogels bearing bioengineered mimetic embryonic microenvironments for tumor reversion. J. Mater. Chem. B 2016, 4, 6183–6191.

(1327). Jain A; Betancur M; Patel GD; Valmikinathan CM; Mukhatyar VJ; Vakharia A; Pai SB; Brahma B; MacDonald TJ; Bellamkonda RV Guiding intracortical brain tumour cells to an extracortical cytotoxic hydrogel using aligned polymeric nanofibres. Nat. Mater. 2014, 13, 308–316. [PubMed: 24531400]

(1328). Curtarolo S; Hart GLW; Nardelli MB; Mingo N; Sanvito S; Levy O The high-throughput highway to computational materials design. Nat. Mater. 2013, 12, 191–201. [PubMed: 23422720]

(1329). Bian Q; Cahan P Computational tools for stem cell biology. Trends Biotechnol 2016, 34, 993–1009. [PubMed: 27318512]

(1330). Fallas JA; Hartgerink JD Computational design of self-assembling register-specific collagen heterotrimers. Nat. Commun 2012, 3, 1087. [PubMed: 23011141]

(1331). Engler AJ; Humbert PO; Wehrle-Haller B; Weaver VM Multiscale modeling of form and function. Science 2009, 324, 208–212. [PubMed: 19359578]

(1332). Sander EA; Stylianopoulos T; Tranquillo RT; Barocas VH Image-based multiscale modeling predicts tissue-level and network-level fiber reorganization in stretched cell-compacted collagen gels. Proc. Natl. Acad. Sci. U.S.A 2009, 106, 17675–17680. [PubMed: 19805118]

(1333). Chen B; Ji B; Gao H Modeling active mechanosensing in cell–matrix interactions. Annu. Rev. Biophys 2015, 44, 1–32. [PubMed: 26098510]

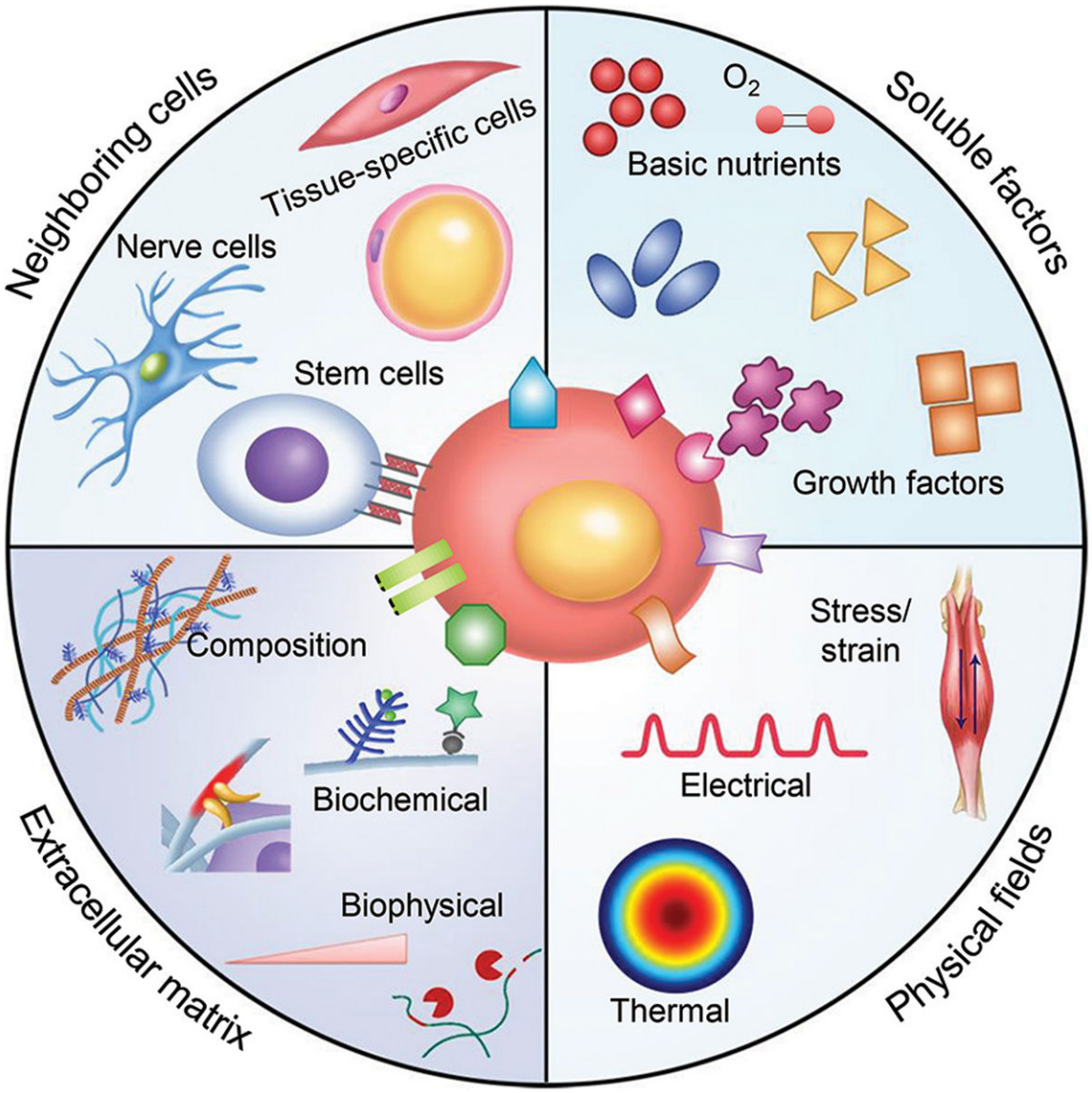

Figure 1.

Schematic illustration of the main components of the cell microenvironment. Key components of the cell microenvironment include neighboring cells, soluble factors, the ECM, and biophysical fields (e.g., stress and stain, electrical, and thermal fields). Among these, the ECM not only serves as a structural support for cells to reside within but also provides diverse biochemical and biophysical cues for regulating cell behaviors.

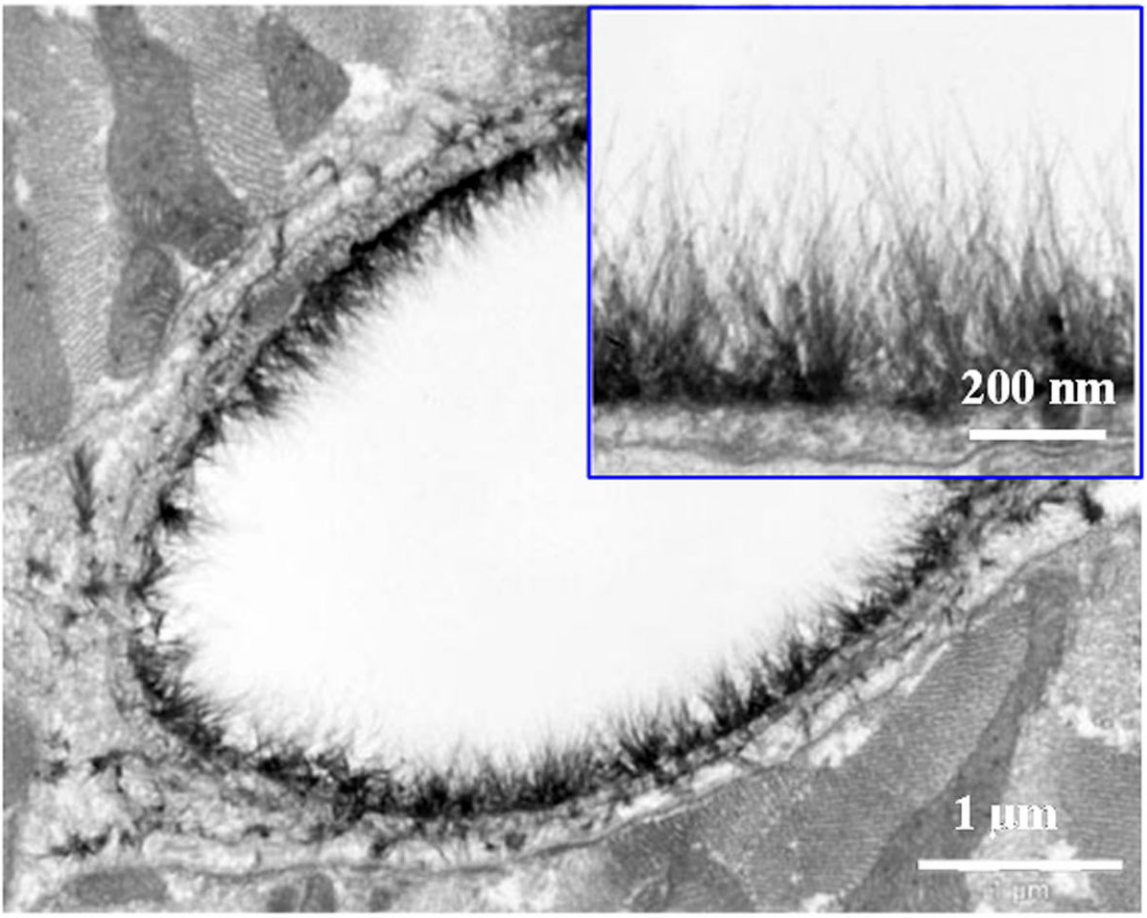

Figure 2.
Electron microscopic overview of a rat left ventricular myocardial capillary. The capillary was stained with Alcian blue 8GX. The inset is a detailed picture of glycocalyx on the capillary. Reprinted with permission from ref 21. Copyright 2003 Wolters Kluwer.

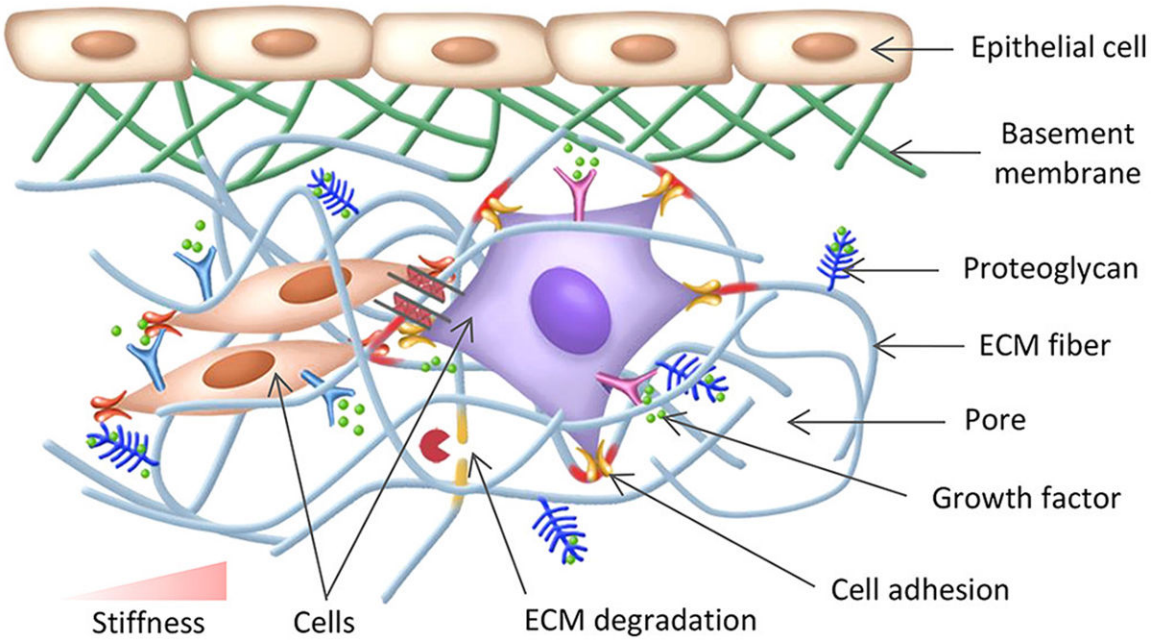

Figure 3.

Schematic representation of cell–ECM interactions. Cells are surrounded by abundant ECM, which provides diverse biochemical cues (e.g., cell adhesion ligands and growth factor immobilization) and biophysical cues (e.g., structural features, mechanical stiffness, and degradation) for guiding cell behaviors.

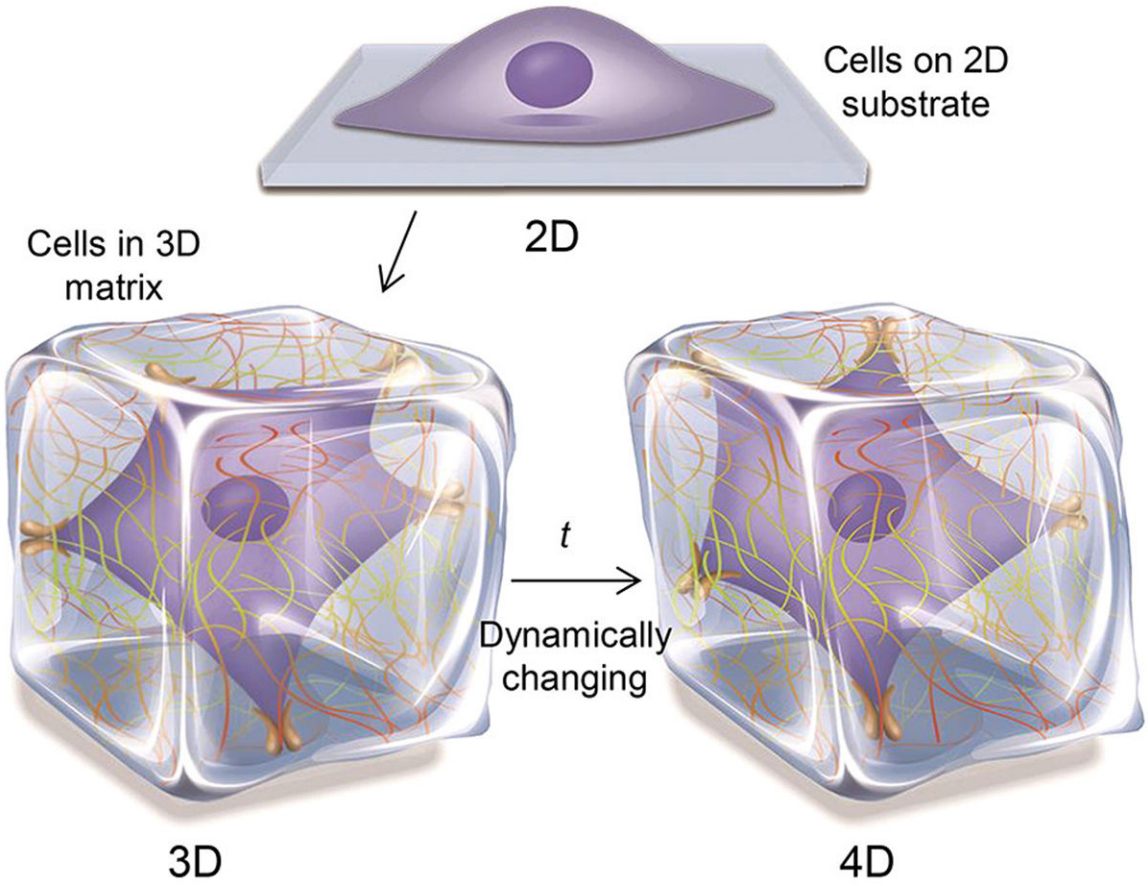

Figure 4.
Schematic of engineering the cell microenvironment from 2D to 3D and 4D.

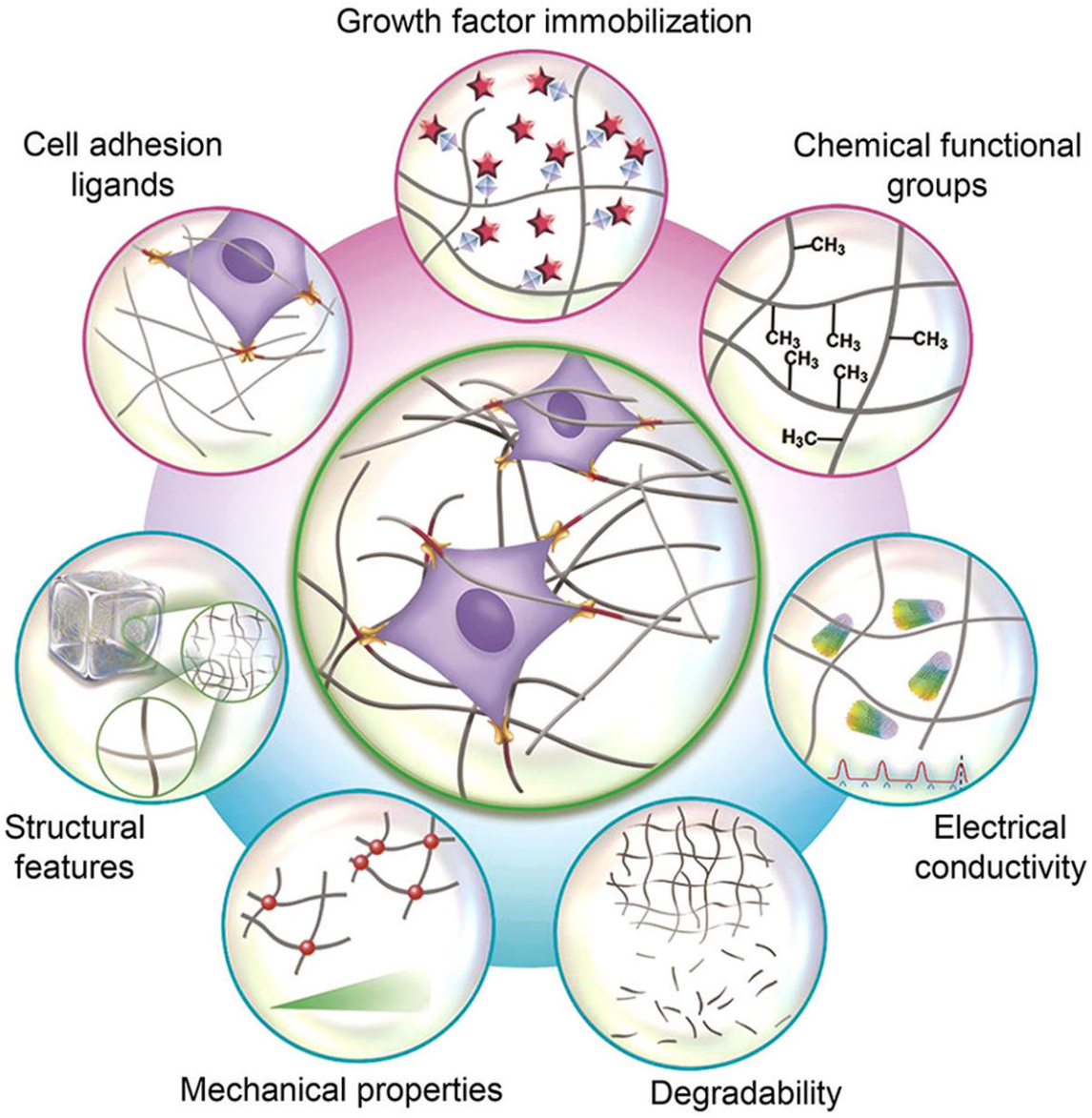

Figure 5.

Biomimetic material design considerations for engineering the 3D cell microenvironment. The design considerations can be generally divided into two classes, i.e., biochemical (e.g., cell adhesion ligands, soluble factor immobilization, and chemical functional groups) and biophysical design considerations (e.g., structural features, mechanical properties, degradability, and electrical conductivity).

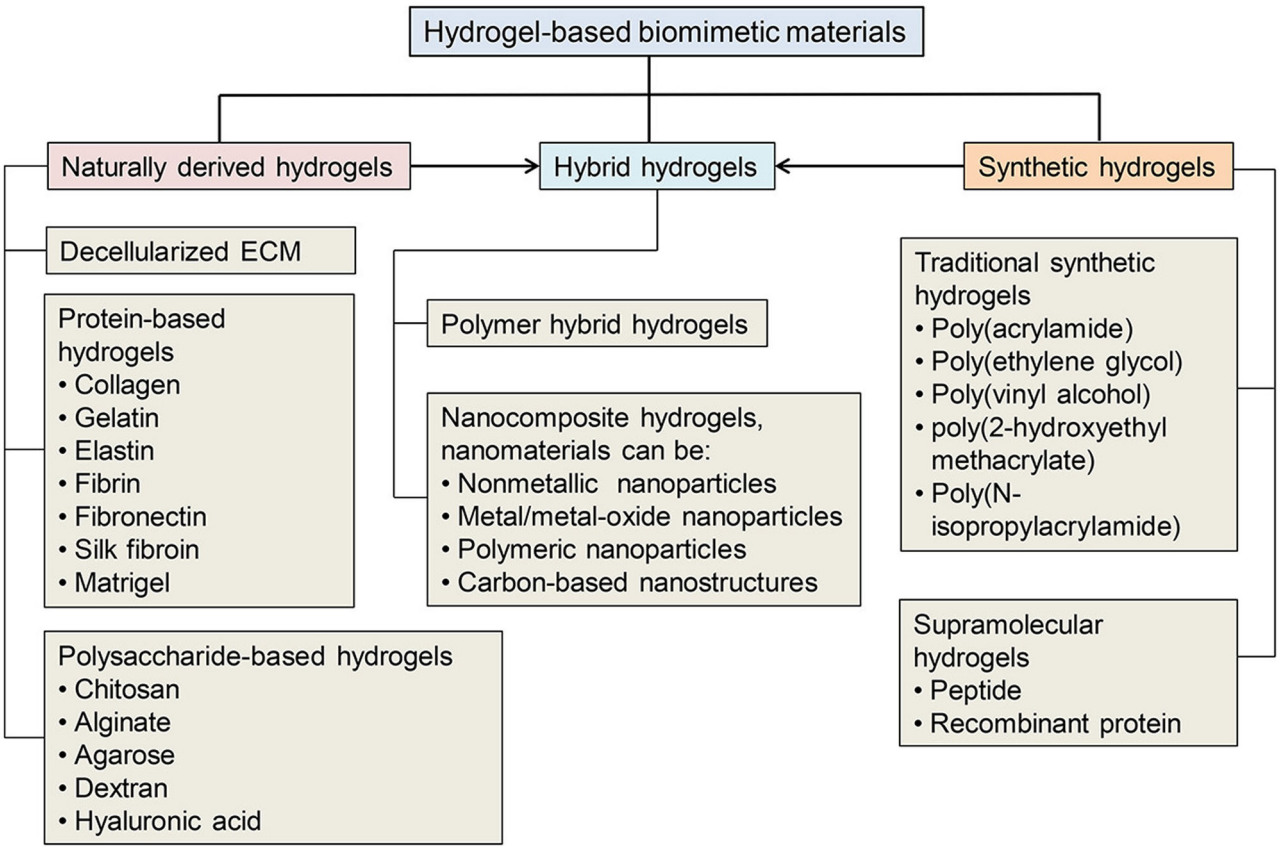

Figure 6.

Classification of hydrogel-based biomimetic materials for engineering the 3D cell microenvironment. Most biomimetic materials used for engineering the 3D cell microenvironment are based on hydrogels, which can be classified into naturally derived, synthetic, and hybrid hydrogels, according to their origins and compositions.

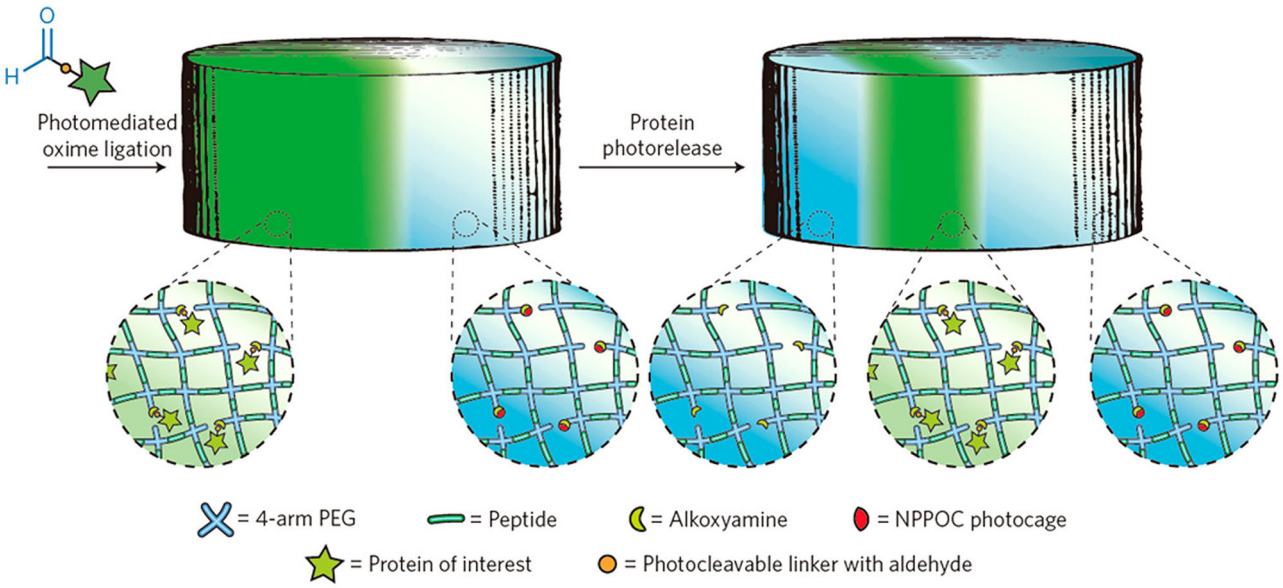

Figure 7.

Photopatterning full-length proteins in hydrogels. The protein of interest is first functionalized with NHS-ortho-nitrobenzyl (o-NB)-CHO and then incorporated into SPAAC-based hydrogels via photomediated oxime ligation. Upon further light exposure, the photoscissile o-NB moieties undergo photocleavage, leading to the removal of linked proteins. Reprinted with permission from ref 419. Copyright 2015 Nature Publishing Group.

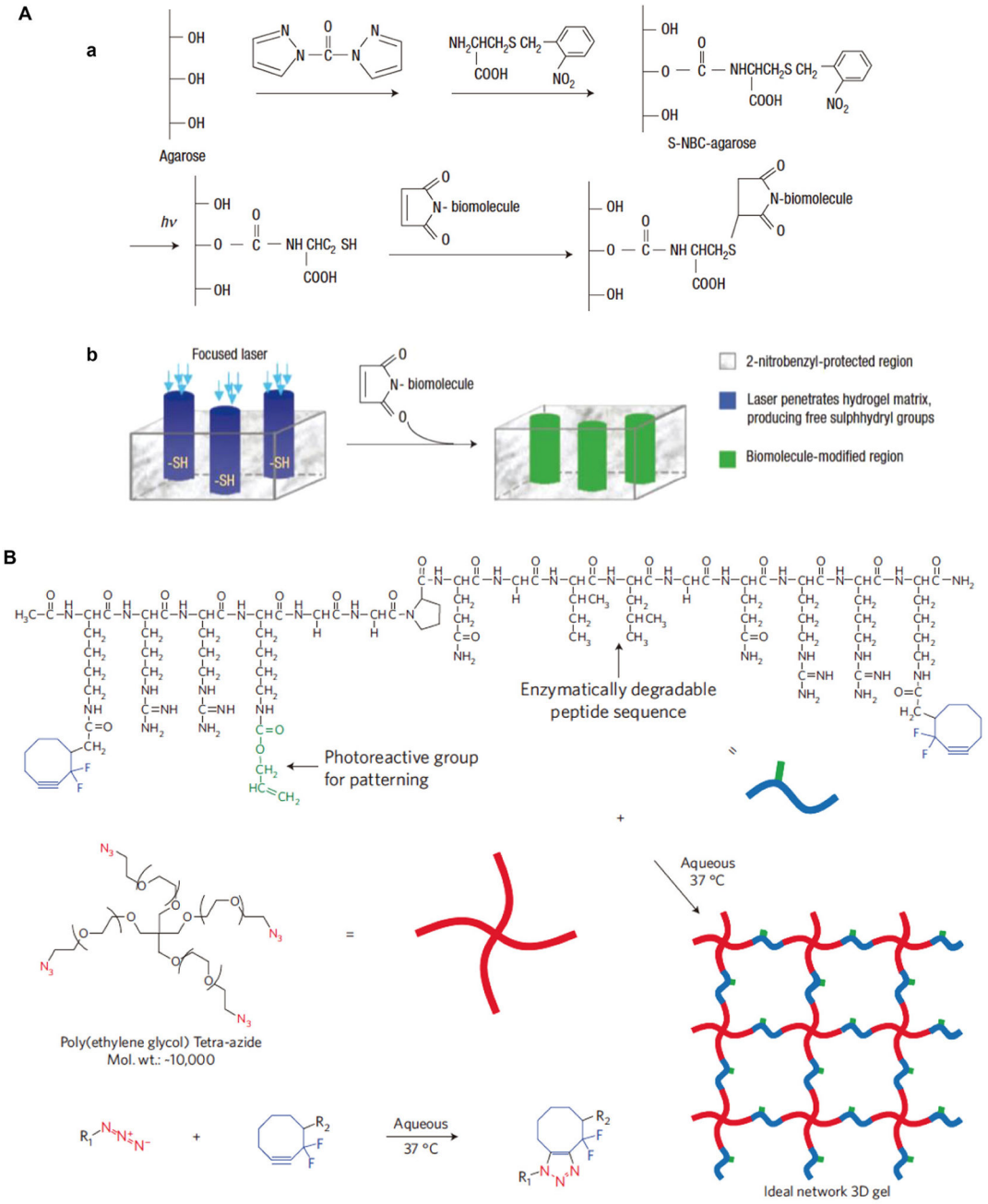

Figure 8.

Photopatterning hydrogels with cell adhesion peptides. (A) Maleimide-functionalized biomolecules (e.g., GRGDS) are incorporated into agarose hydrogels modified with 2-NB-protected cysteine. Reprinted with permission from ref 448. Copyright 2004 Nature Publishing Group. (B) PEG-based hydrogels are prepared through a copper-free SPAAC click reaction. Biochemical molecules (e.g., RGD) can be subsequently patterned in the hydrogels by an orthogonal thiol–ene photocoupling reaction. Reprinted with permission from ref 456. Copyright 2009 Nature Publishing Group.

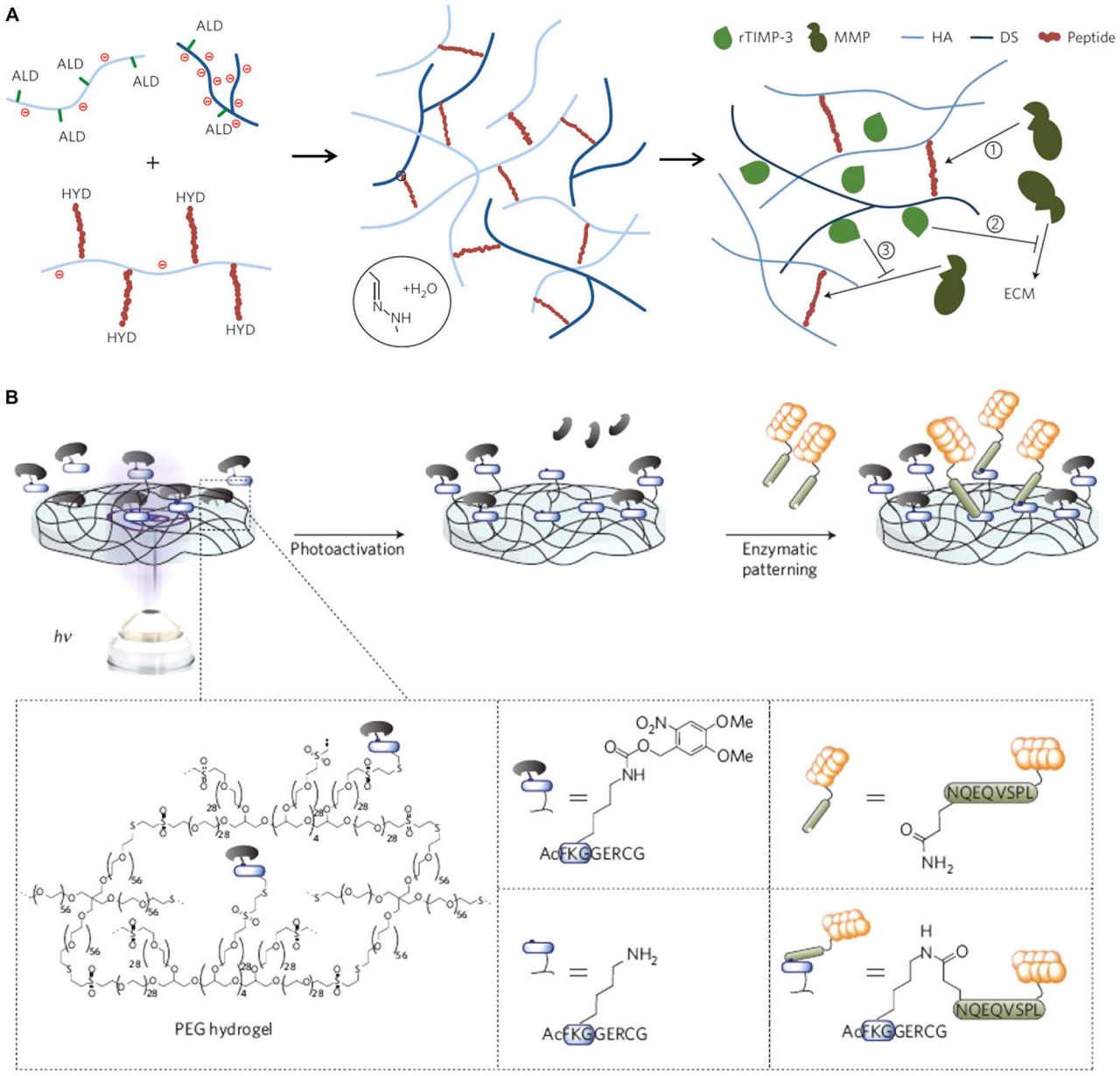

Figure 9.

Growth factor immobilization in hydrogels. (A) HA hydrogels are modified with dextran sulfate (a heparin mimetic) for sequestering rTIMP-3. The hydrogels can release rTIMP-3 in response to locally elevated MMP levels in vivo. Reprinted with permission from ref 490. Copyright 2014 Nature Publishing Group. (B) Enzymatic hydrogel photopatterning with bioactive signaling proteins. Transglutaminase factor XIII is rendered photosensitive by masking its active site with a photolabile cage group and then incorporated into PEG-based hydrogels. Biologically relevant signaling proteins are subsequently patterned into hydrogels through local light-activated enzymatic cross-linking. Reprinted with permission from ref 500. Copyright 2013 Nature Publishing Group.

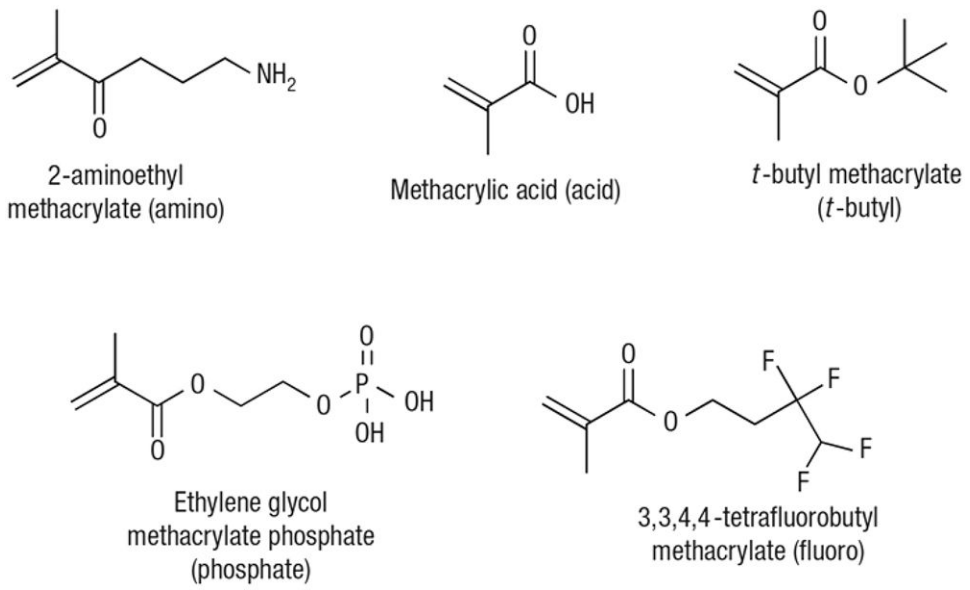

Figure 10.

Small-molecule chemical groups used for modifying PEG hydrogels, including amino, acid, t-butyl, phosphate, and fluoro groups. Reprinted with permission from ref 33. Copyright 2008 Nature Publishing Group.

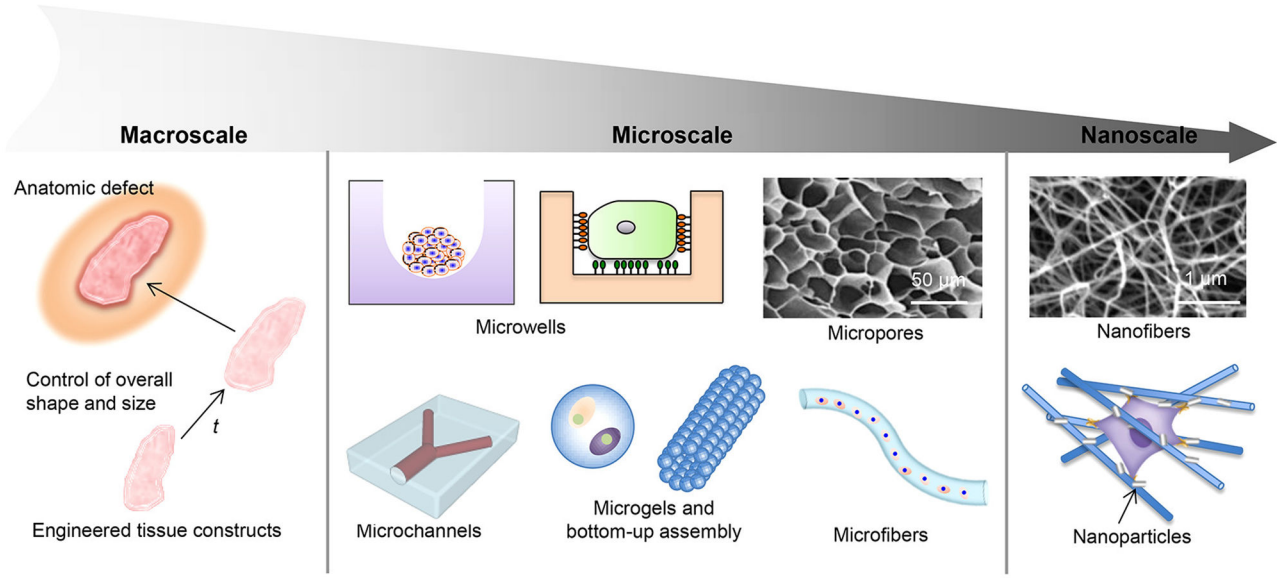

Figure 11.

Schematic of the structural design aspects of biomimetic materials that can be classified as macroscale, microscale, and nanoscale design aspects. Macroscale design is related to external structure characteristics, such as overall shape and size. Microscale design is related to the characteristics of microwells, micropores, microchannels, microgels, and microfibers in hydrogels. Nanoscale design is related to the characteristics of nanofibers and nanoparticles that compose hydrogels.

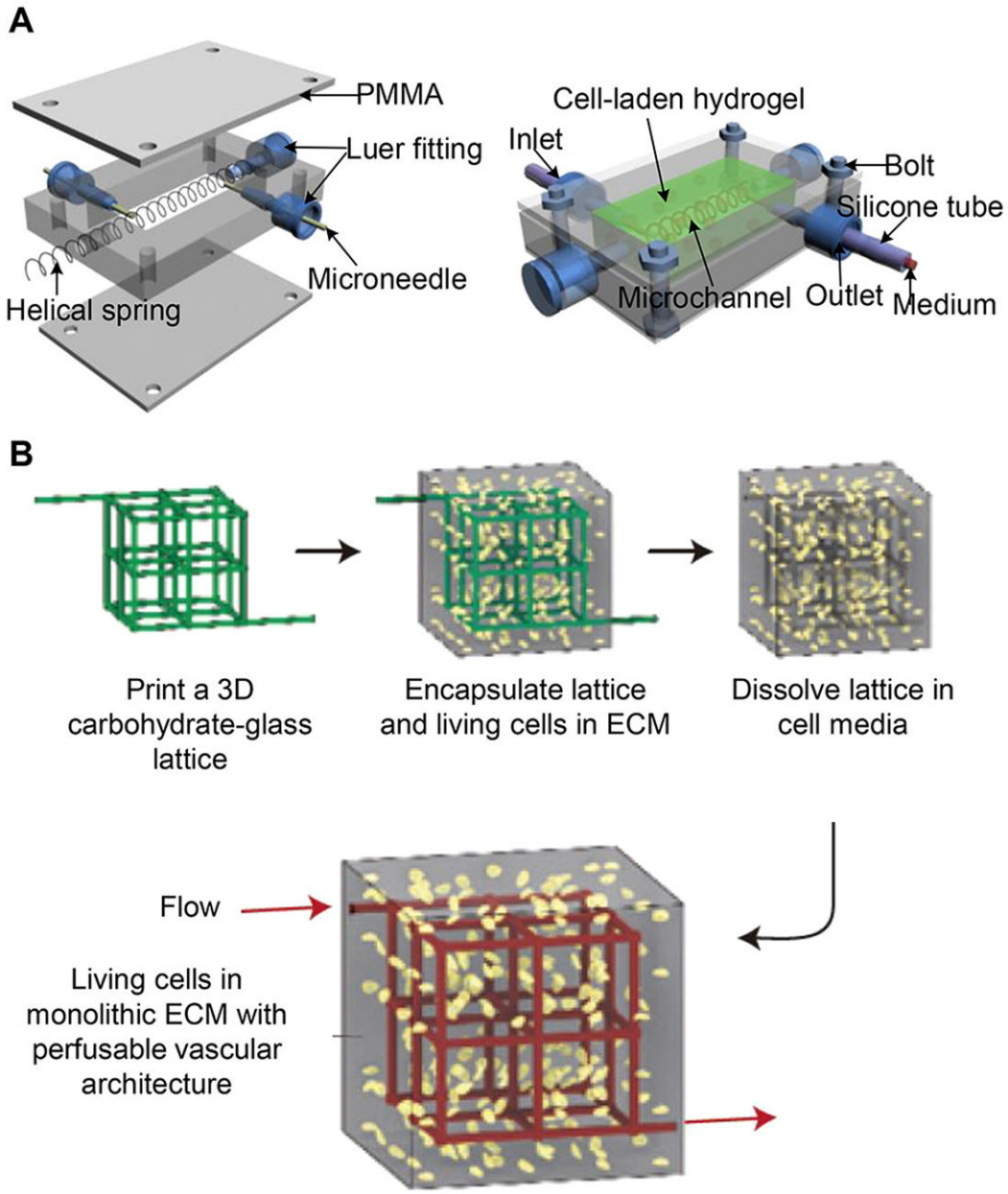

Figure 12.

Fabrication of microfluidic hydrogels for perfusion cell culture. (A) Schematic of the fabrication of microfluidic cell-laden hydrogels using a helical spring as a template. Reprinted with permission from ref 629. Copyright 2012 Wiley Periodicals, Inc. (B) Schematic of the fabrication of microfluidic cell-laden hydrogels based on sacrificial printed carbohydrate-glass fibers. Reprinted with permission from ref 592. Copyright 2012 Nature Publishing Group.

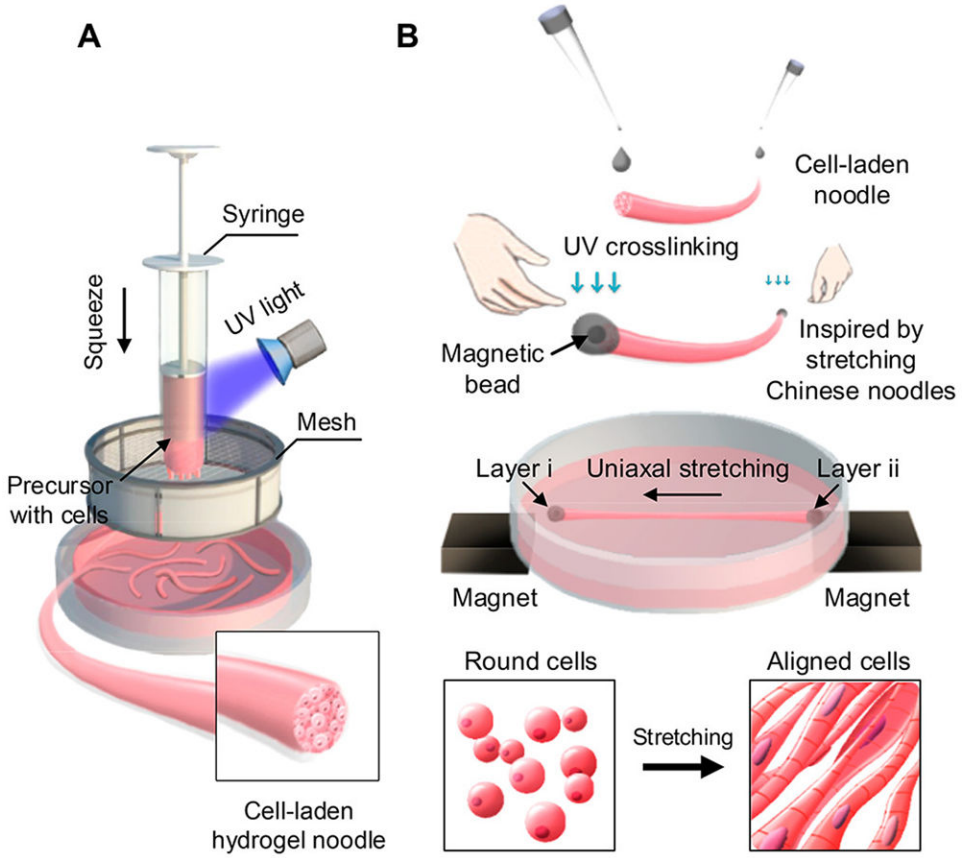

Figure 13.

Chinese-noodle-inspired fabrication of hydrogel microfibers for engineering muscle myofibers. (A) Schematic of the high-throughput generation of cell-laden hydrogel microfibers by squeezing a cell-laden hydrogel block through a sieve. (B) Schematic of the magnetically actuated stretching of cell-laden hydrogel microfibers for generating functional myofibers. Reprinted with permission from ref 646. Copyright 2015 WILEY-VCH Verlag GmbH & Co. KGaA, Weinheim.

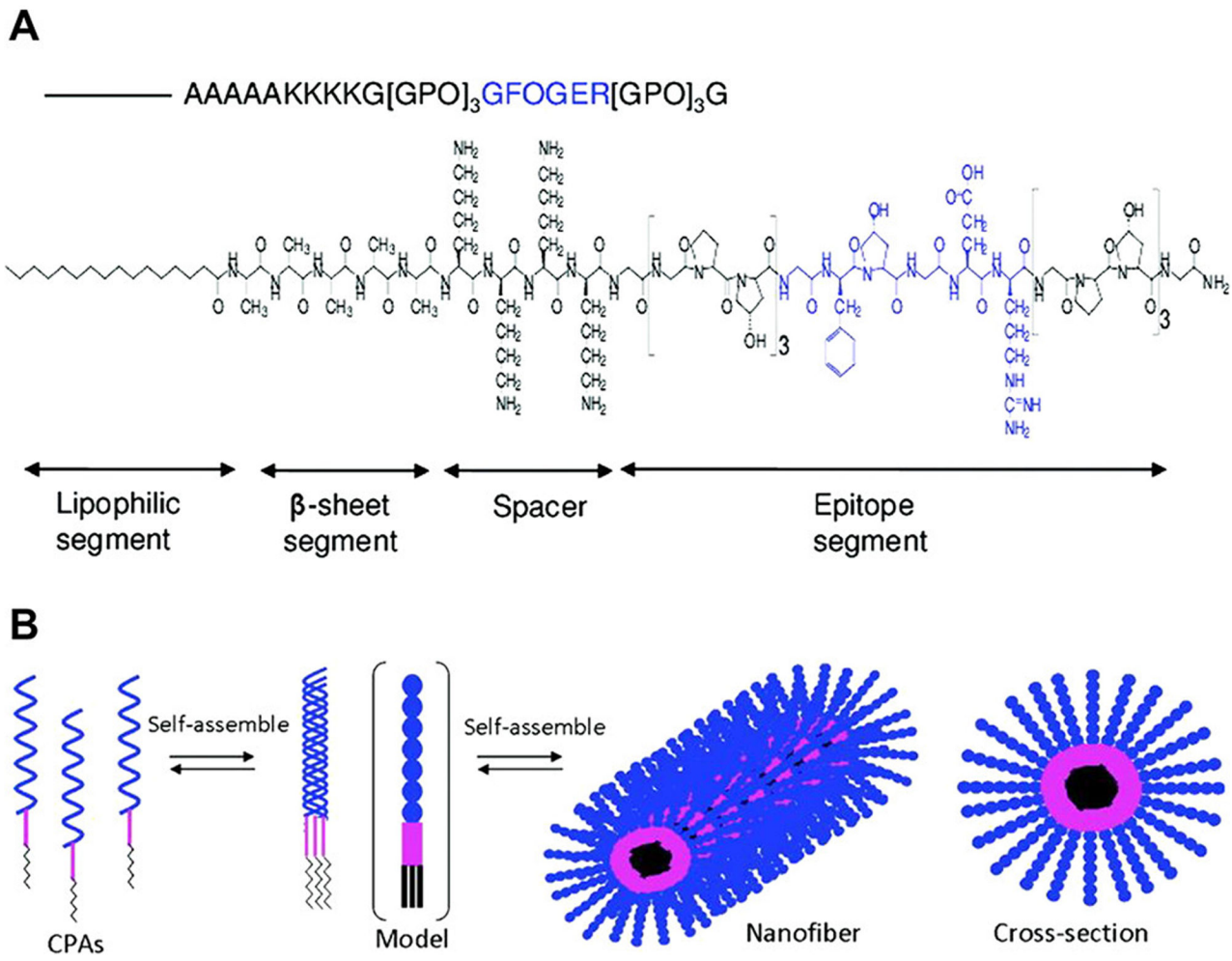

Figure 14.

Generation of nanofibers through the self-assembly of collagen-mimetic peptide amphiphiles. (A) Molecular structure of collagen-mimetic peptide amphiphiles. (B) Self-assembly process. Reprinted with permission from ref 685. Copyright 2011 American Chemical Society.

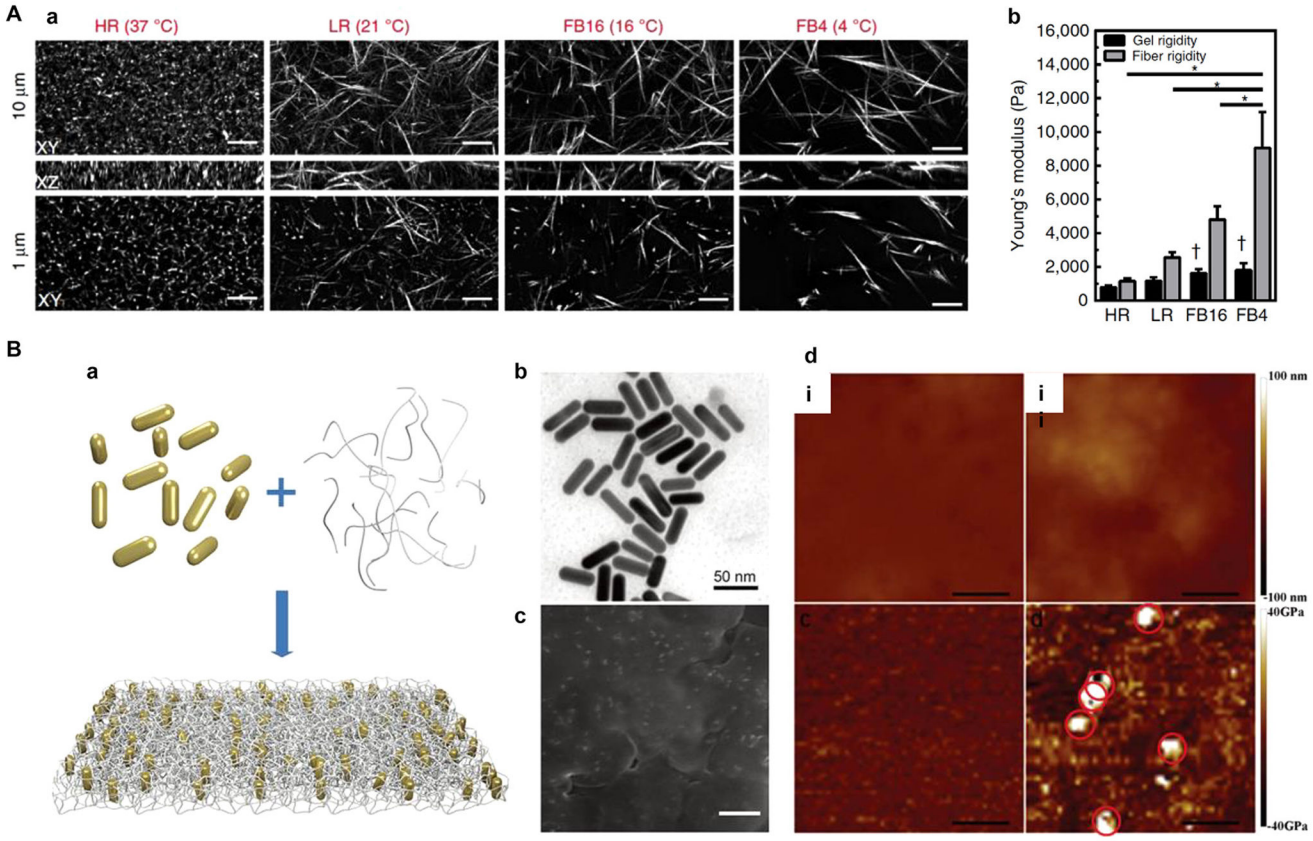

Figure 15.

Control over nanoscale hydrogel mechanics. (A) Decreasing the self-assembly temperature results in collagen fibril bundling and increased fiber diameter (a), which contributes to increased local fiber stiffness (b). Scale bars: μm. Reprinted with permission from ref 720. Copyright 2015 Nature Publishing Group. (B) AuNRs are mixed with collagen to form nanocomposite hydrogels (a–c). The incorporation of AuNRs results in increased nanoscale hydrogel stiffness without impacting the bulk mechanical properties (d). Scale bars: 500 nm for (c, d). Reprinted with permission from ref 721. Copyright 2016 WILEY-VCH Verlag GmbH & Co. KGaA, Weinheim.

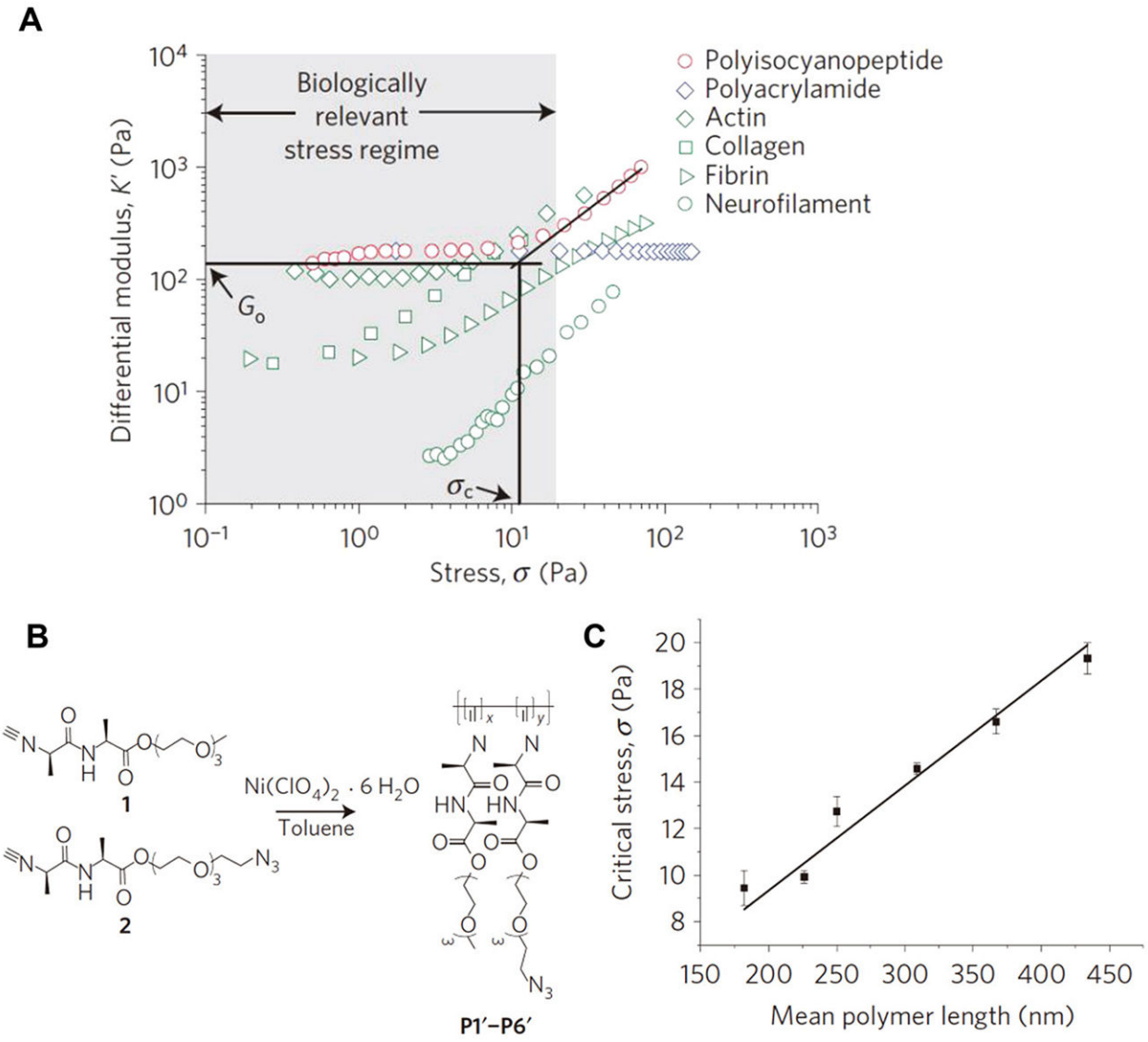

Figure 16.

Nonlinear elasticity of hydrogels. (A) Differential modulus-stress plot showing the stress-stiffening behavior of some biopolymers. (B) Synthesis of polyisocyanopeptides with varying polymer chain lengths (mean polymer length) by adjusting the molar ratio of catalyst to monomer, which results in (C) different mean critical stress levels. Reprinted with permission from ref 36. Copyright 2015 Nature Publishing Group.

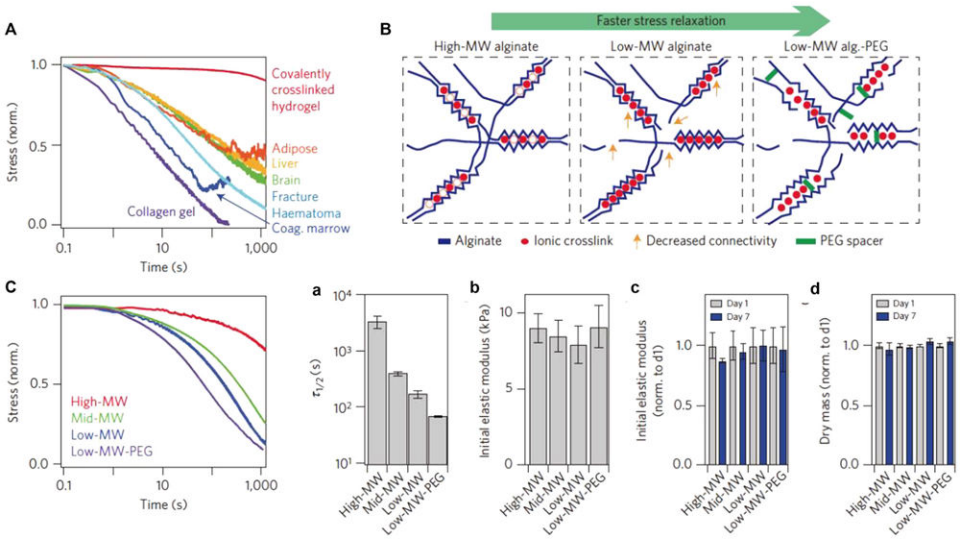

Figure 17.

Engineering the viscoelasticity of hydrogels to mimic that of living tissues. (A) Viscoelastic behaviors of some living tissues and hydrogels. (B) Schematic of designing alginate hydrogels with varying stress-relaxation rates by the combinatorial use of different molecular weight alginate macromers, ionic cross-linking densities, and short PEG spacers covalently linked to the alginate backbone. (C) Stress-relaxation behaviors of alginate hydrogels. (D) The stress-relaxation time scale (a), initial elastic modulus (b), and initial elastic modulus after 1-day and 7-day cultures (c), and the dry mass (d) of alginate hydrogels. Reprinted with permission from ref 37. Copyright 2016 Nature Publishing Group.

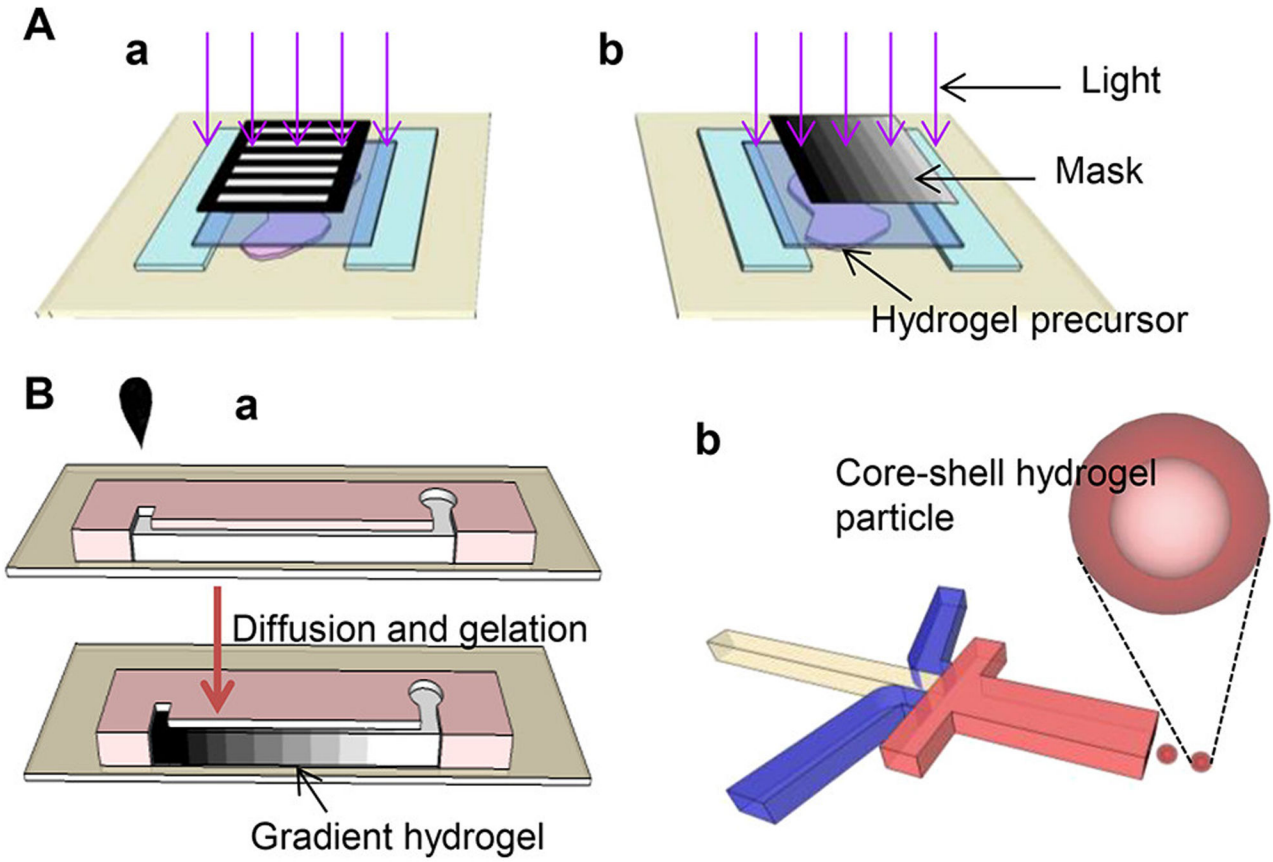

Figure 18.

Spatial modulation of hydrogel mechanical properties. (A) Schematic of photopatterning hydrogels with bar-coded (a) and gradient (b) stiffness. (B) Schematic of the microfluidic fabrication of hydrogels with a mechanical gradient (a) and core–shell (softer-stiffer) hydrogel particles (b).

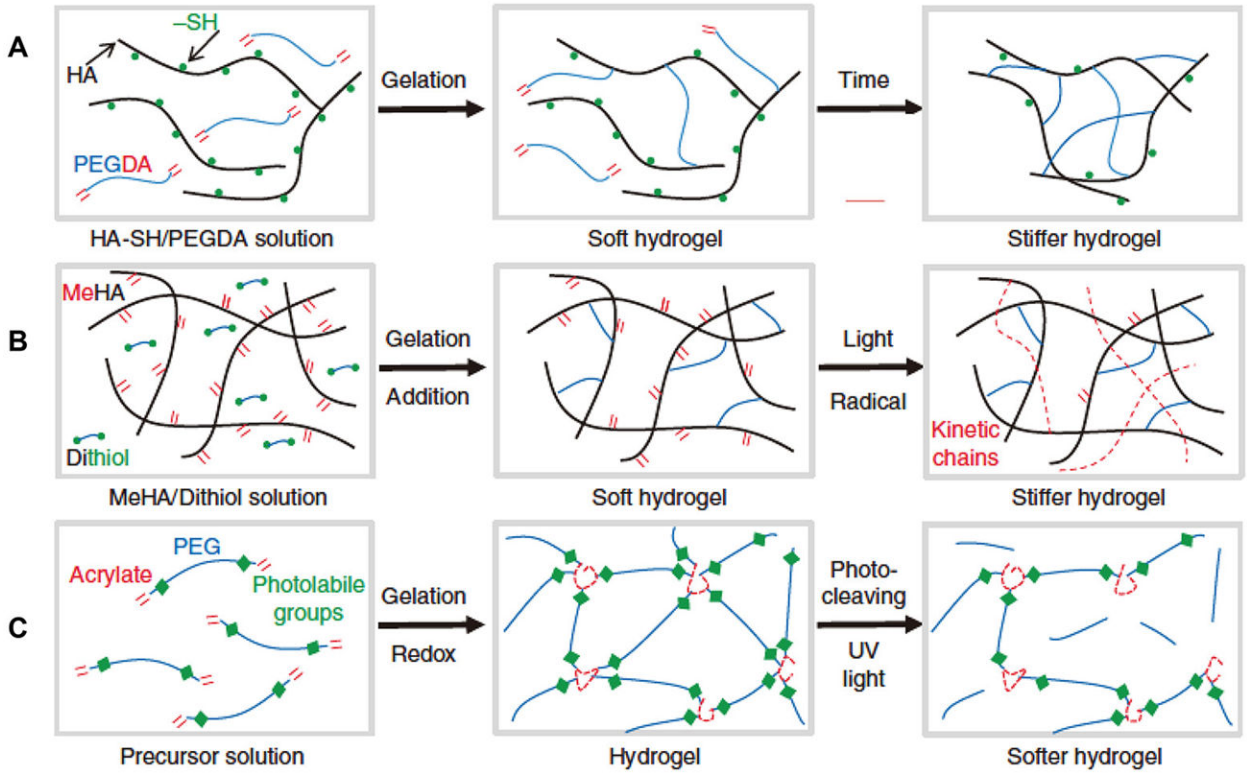

Figure 19.

Temporal modulation of hydrogel mechanical properties. (A) A slow Michael-type addition reaction to cross-link thiolated HA with PEGDA. The reaction dynamics, and thus the stiffening process, can be controlled by changing the PEGDA molecular weight. (B) Stiffening of HA hydrogels through a sequential cross-linking strategy. HA macromers are modified with methacrylate and partially cross-linked with DTT via Michael-type addition reactions. The initial hydrogels are then UV-cross-linked to induce stiffening. (C) Light-mediated softening of a photodegradable PEG-based hydrogel. Photolabile groups are incorporated into di(meth)acrylated PEG macromers, which are then cross-linked to form photodegradable hydrogels. Upon exposure to UV light, the cross-linkages are cleaved, resulting in hydrogel softening. Reprinted with permission from ref 47. Copyright 2012 Nature Publishing Group.

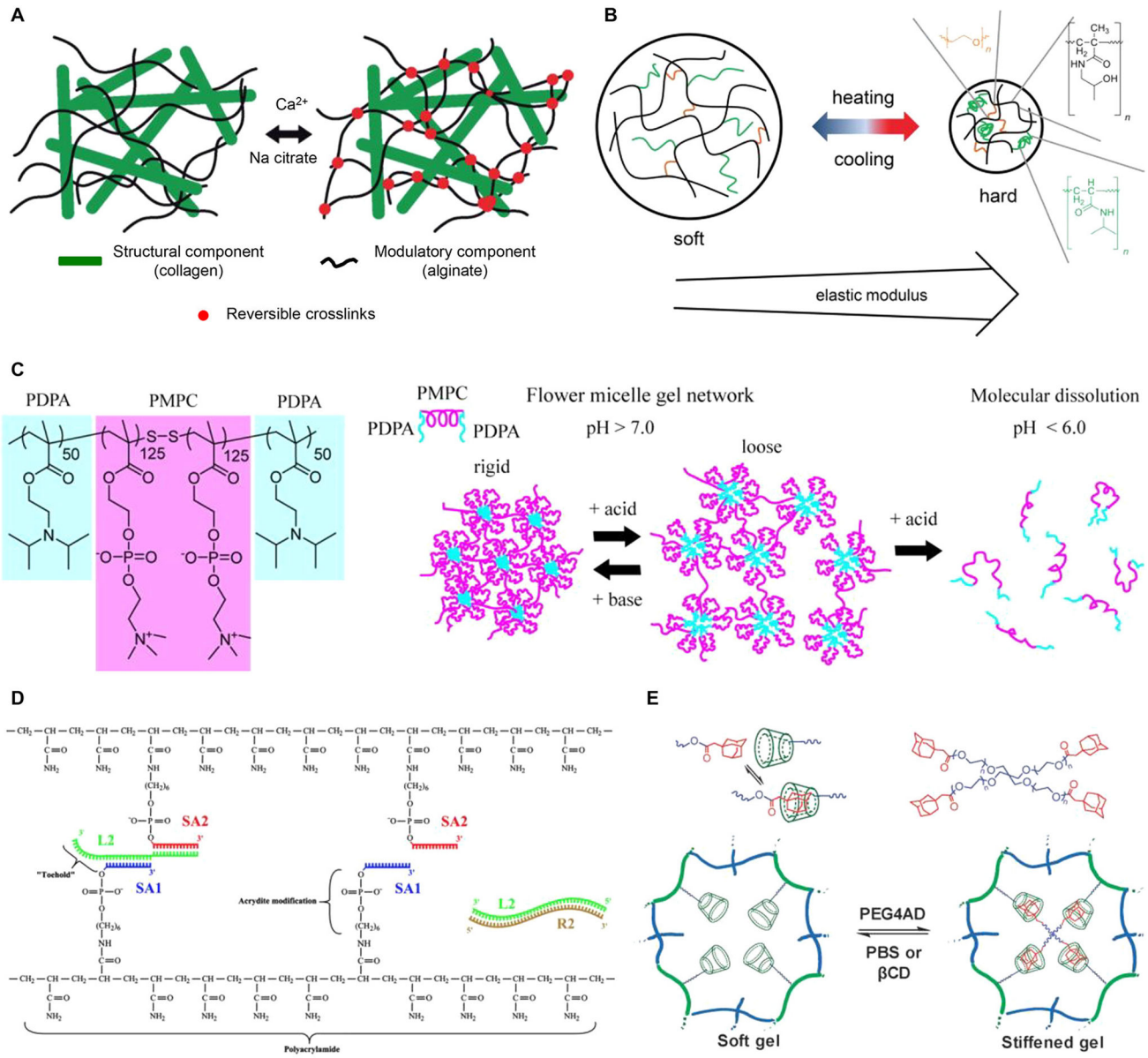

Figure 20.

Schematic of hydrogels with reversibly modulated mechanical properties. (A) Ca2+-cross-linked alginate-based hydrogel. Reprinted with permission from ref 803. Copyright 2010 WILEY-VCH Verlag GmbH & Co. KGaA, Weinheim. (B) Thermal-responsive PNIPAAm-based hybrid hydrogel. Reprinted with permission from ref 804. Copyright 2015 WILEY-VCH Verlag GmbH & Co. KGaA, Weinheim. (C) pH-sensitive triblock hydrogel. Reprinted with permission from ref 805. Copyright 2011 American Chemical Society. (D) DNA-cross-linked PA hydrogel. Reprinted with permission from ref 808. Copyright 2012 Biomedical Engineering Society. (E) Supramolecular hydrogel with host–guest interactions. Reprinted with permission from ref 809. Copyright 2016 Royal Society of Chemistry.

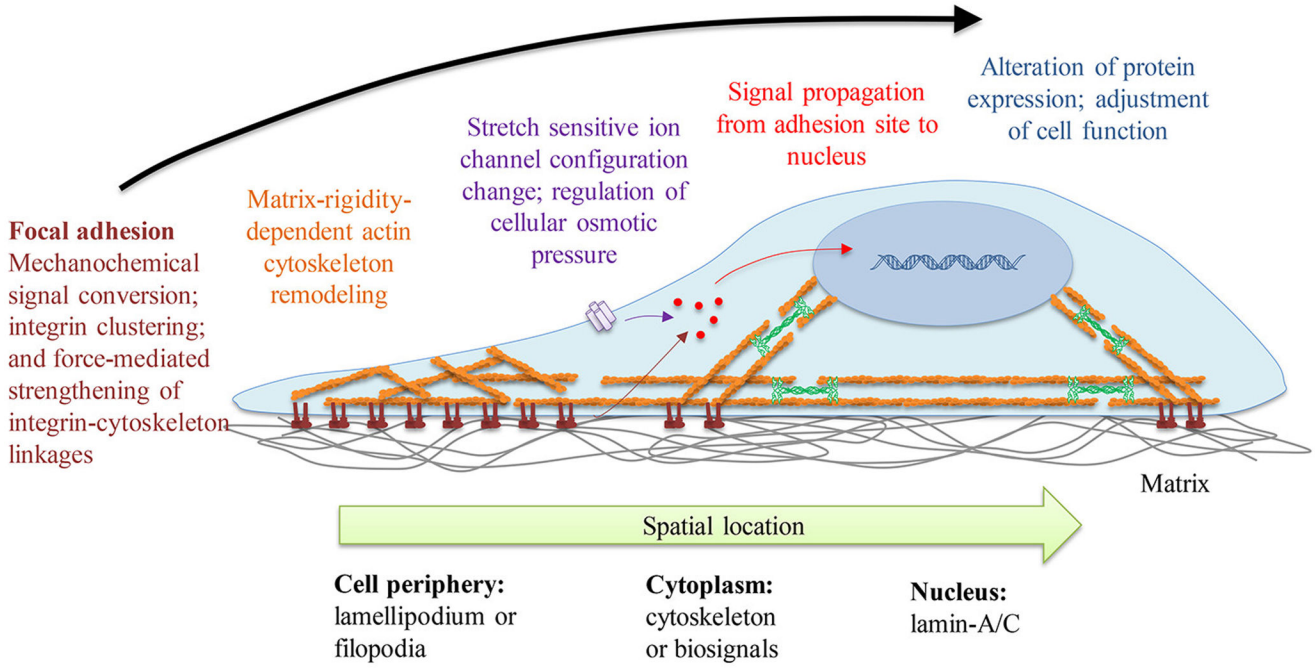

Figure 21.

Cellular mechanosensitive system. The cell-adhesions, myosin-filaments system, tension-sensitive ion channel, and nuclear lamina both can act as the cellular mechanosensors which are distributed from cell–ECM interfaces to cell nuclear.

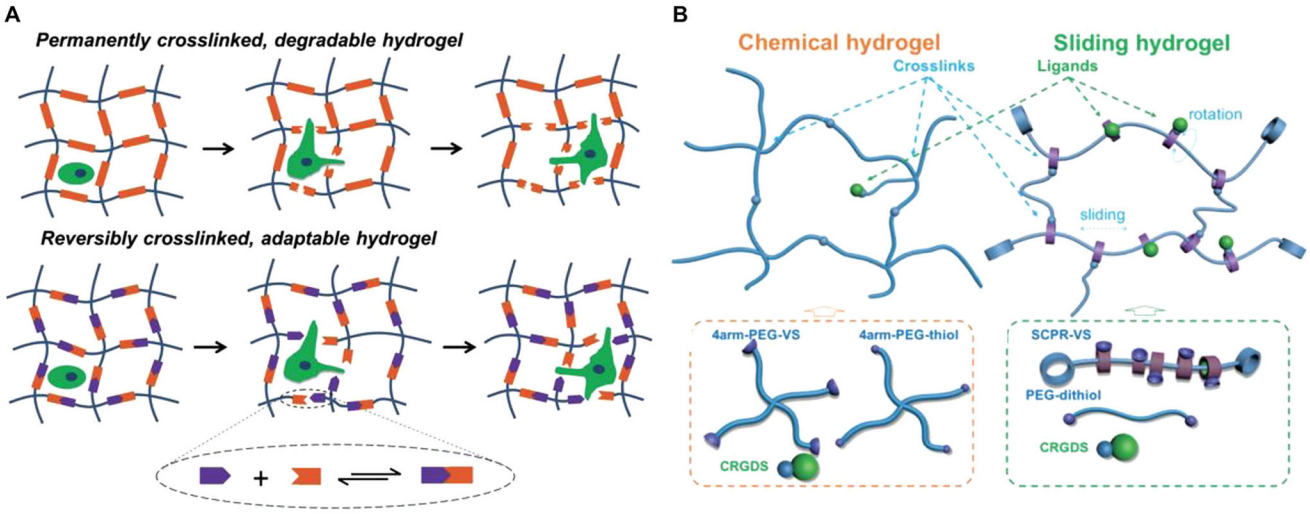

Figure 22.

Adaptable hydrogels. (A) Comparison of a reversibly cross-linked, adaptable hydrogel with a permanently cross-linked, degradable hydrogel. Reprinted with permission from ref 827. Copyright 2015 WILEY-VCH Verlag GmbH & Co. KGaA, Weinheim. (B) Comparison of an adaptable hydrogel based on sliding cross-linkages with a covalently cross-linked hydrogel. Reprinted with permission from ref 828. Copyright 2015 WILEY-VCH Verlag GmbH & Co. KGaA, Weinheim.

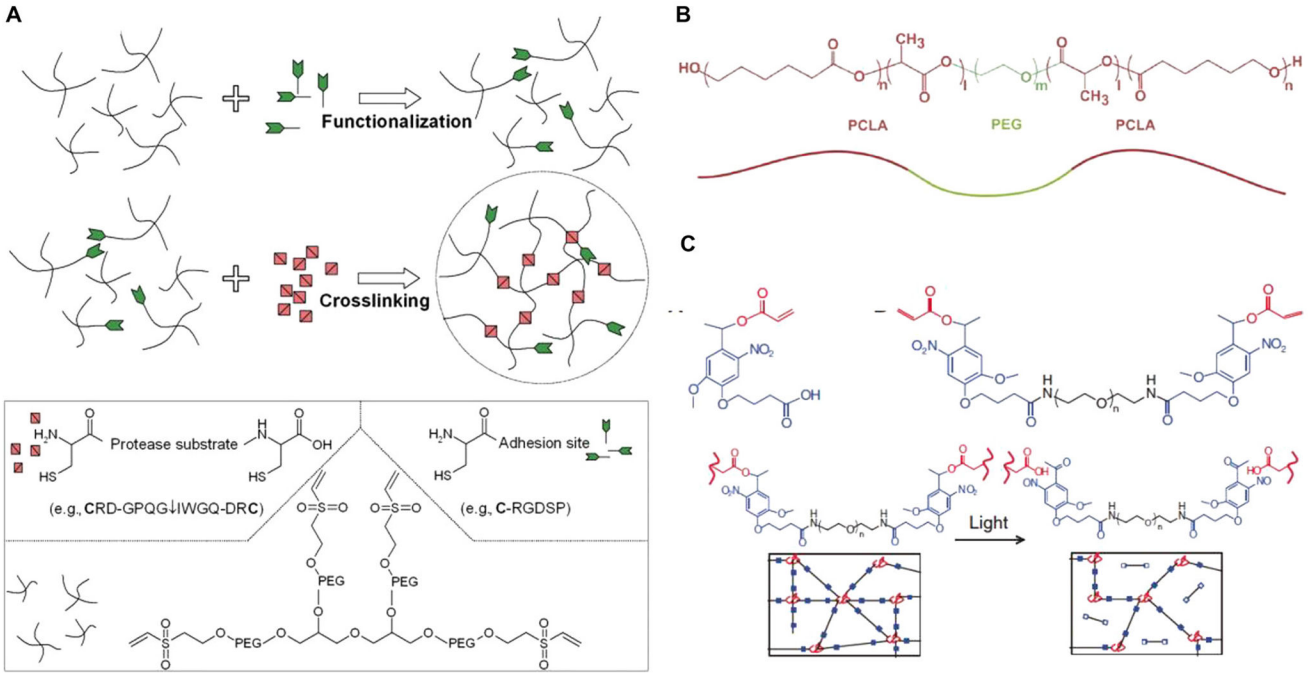

Figure 23.

Hydrogels with different degradation mechanisms. (A) An enzymatically degradable PEG-based hydrogel. Vinyl sulfone-modified multiarm PEG macromers are functionalized with cell adhesion peptides and then cross-linked with bis-cysteine MMP-sensitive peptides to form enzyme-degradable hydrogels. Reprinted with permission from ref 838. Copyright 2003 Nature Publishing Group. (B) Molecular structure of a hydrolytically degradable triblock copolymer, i.e., PCLA-PEG-PCLA. Reprinted with permission from ref 839. Copyright 2011 Elsevier, Ltd. All rights reserved. (C) A photodegradable PEG-based hydrogel. Such a photodegradable hydrogel system has been used for engineering softening hydrogels. Reprinted with permission from ref 459. Copyright 2009 American Association for the Advancement of Science.

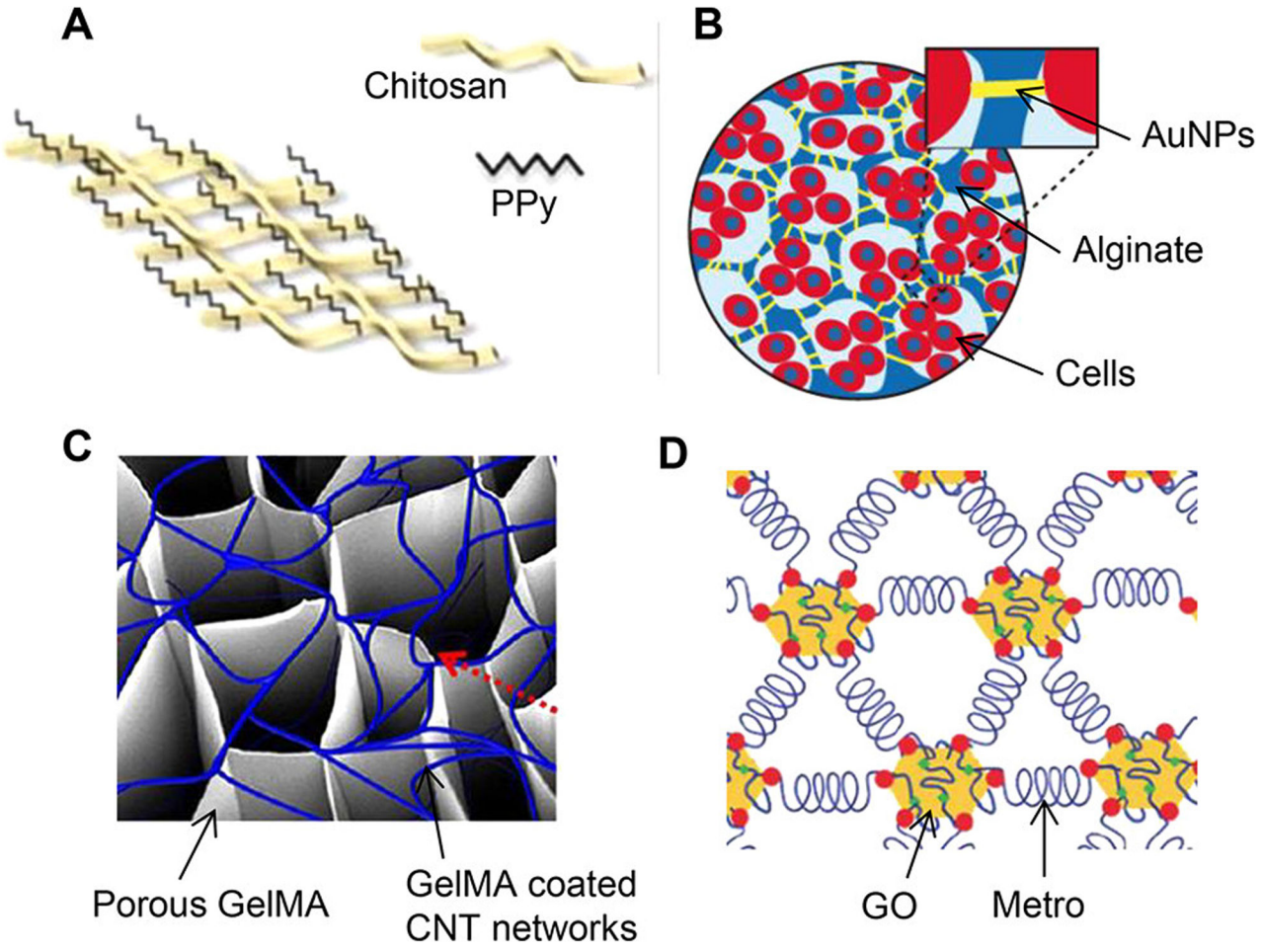

Figure 24.

Electrically conductive hydrogels. (A) PPy-chitosan hydrogel. Reprinted with permission from ref 898. Copyright 2015 American Heart Association, Inc. (B) AuNP-alginate hydrogel. Reprinted with permission from ref 695. Copyright 2011 Nature Publishing Group. (C) CNT-GelMA hydrogel. Reprinted with permission from ref 899. Copyright 2013 American Chemical Society. (D) GO-MeTro hydrogel. Reprinted with permission from ref 900. Copyright 2016 WILEY-VCH Verlag GmbH & Co. KGaA, Weinheim.

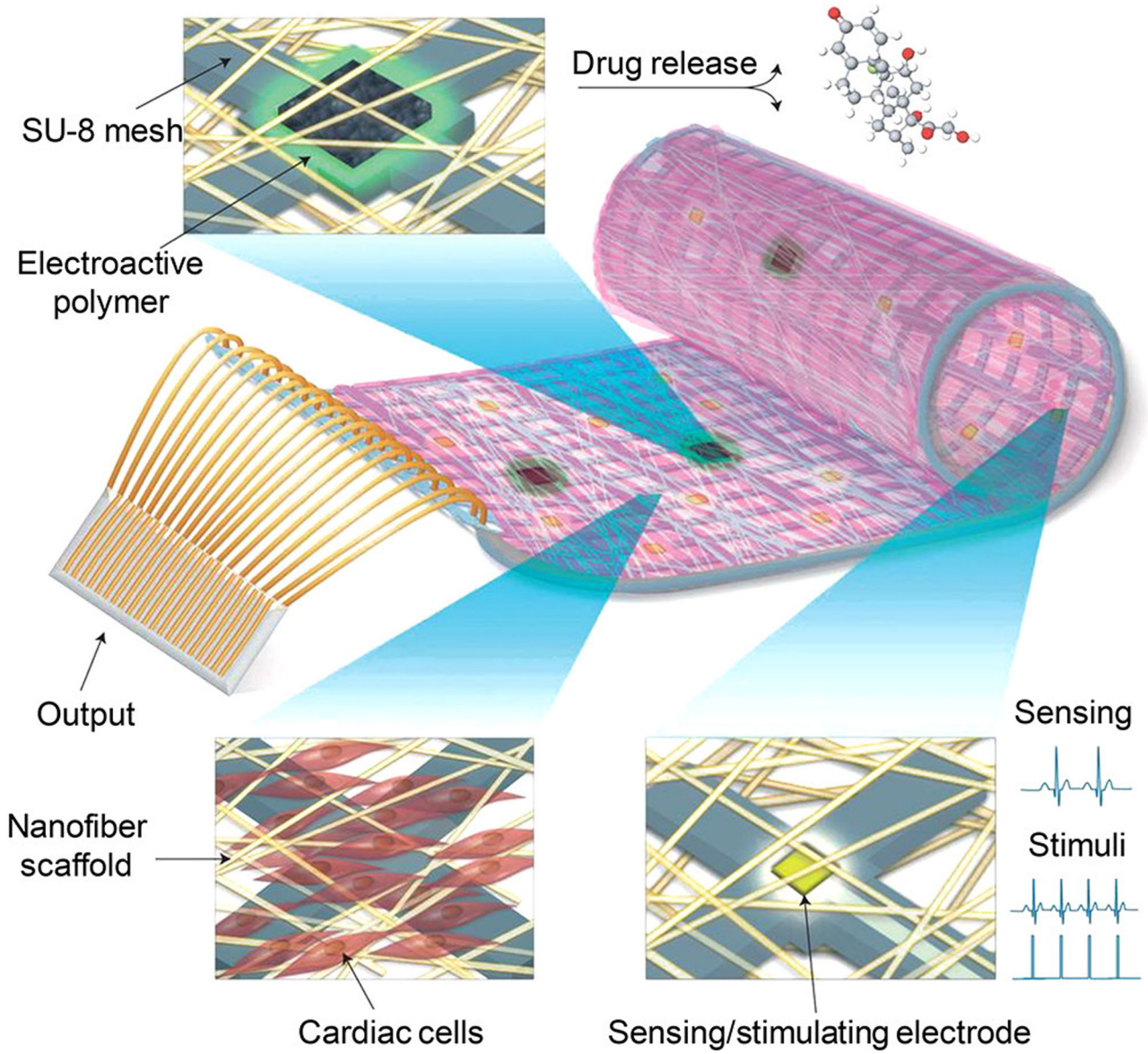

Figure 25.

Schematic of a microelectronic cardiac patch. Such electronic scaffolds enable the electrically controlled release of biomolecules, the electrical stimulation of cells and engineered tissues, and the electrical sensing of cell responses and engineered tissue performances. Reprinted with permission from ref 941. Copyright 2016 Nature Publishing Group.

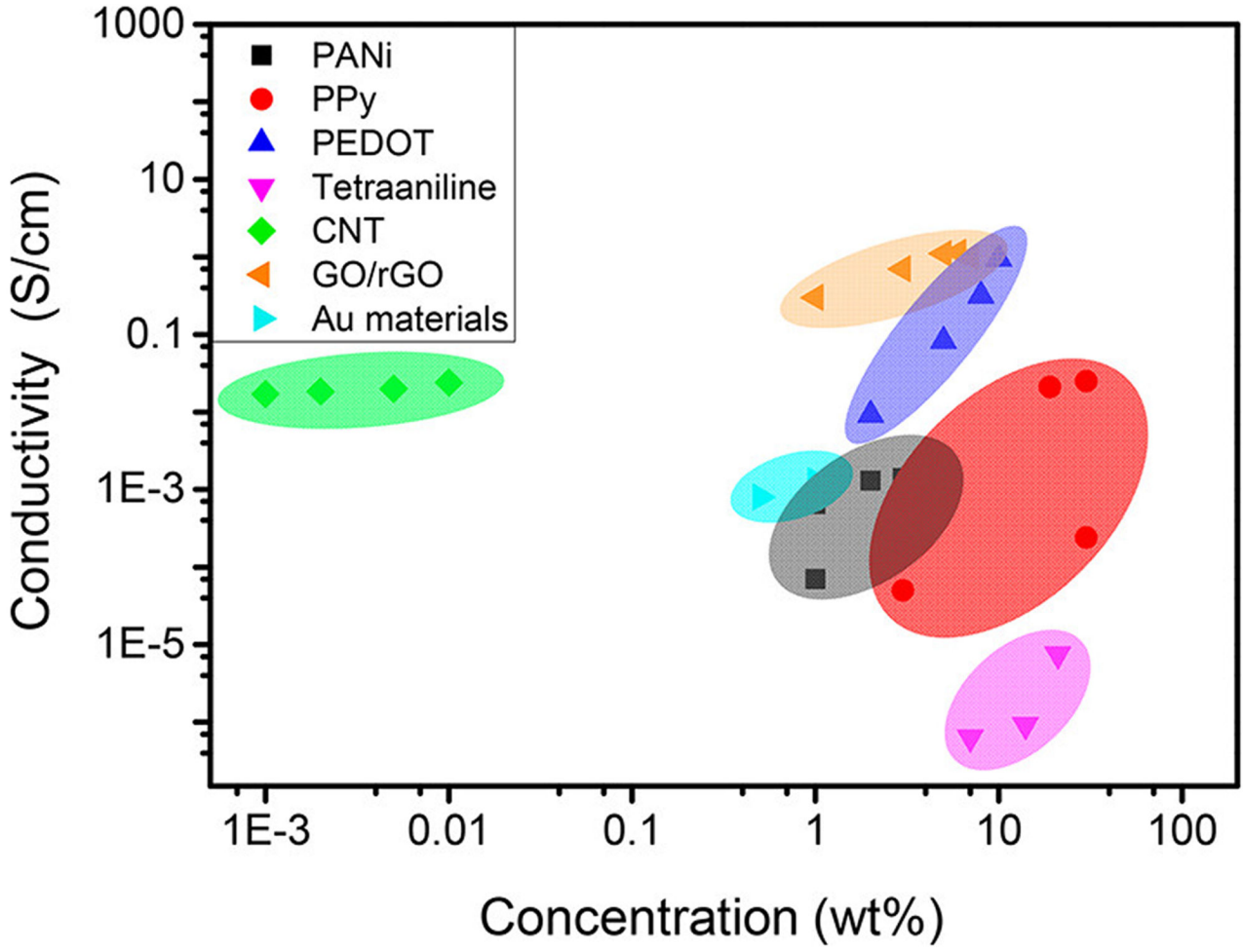

Figure 26.
Conductivities of conductive biomimetic materials as a function of concentrations.

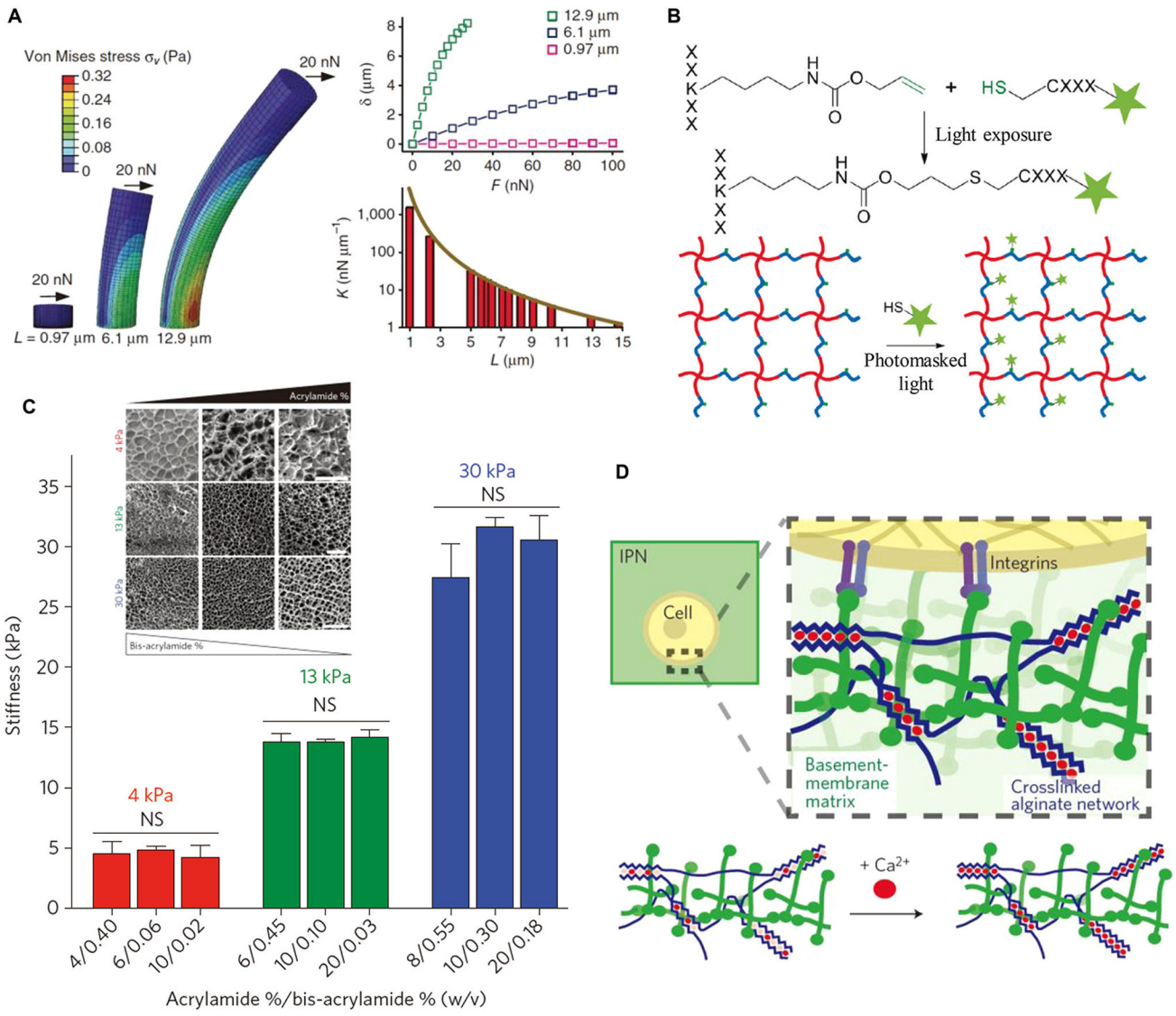

Figure 27.

Independent control over biomimetic material properties. (A) Microfabrication. By varying the height of PDMS microposts but keeping the diameter the same, the effective stiffness (or spring constant) of the microposts is tuned independent of adhesion-ligand density and surface chemical properties. Reprinted with permission from ref 978. Copyright 2010 Nature Publishing Group. (B) Chemical modification. Cysteine-containing peptides are incorporated into PEG-based hydrogels via a thiol–ene click reaction with independent control over the stiffness and adhesion-ligand density. Reprinted with permission from ref 458. Copyright 2010 American Chemical Society. (C) Composition change. PA hydrogels are fabricated with independently controlled stiffness and pore size (or porosity) by adjusting the acrylamide/bis-acrylamide ratio. Scale bars: 50 μm. Reprinted with permission from ref 30. Copyright 2014 Nature Publishing Group. (D) Cross-linking regulation. The stiffness of IPN hydrogels made from a reconstituted basement membrane matrix and alginate is tuned by simply increasing the Ca2+ concentration used for cross-linking alginate

independent of the pore structure and adhesion-ligand density. Reprinted with permission from ref 378. Copyright 2014 Nature Publishing Group.

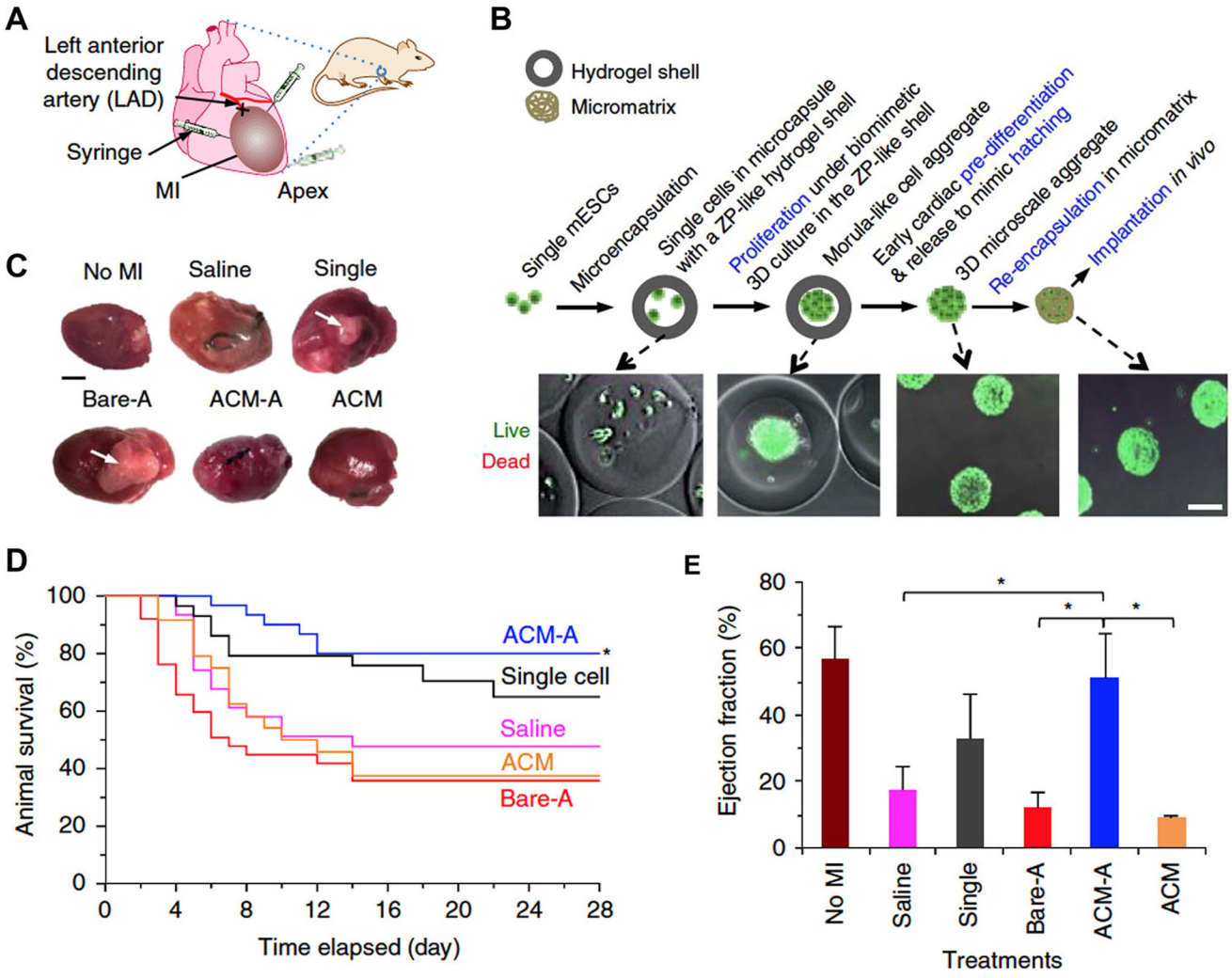

Figure 28.

Cardiac regeneration using cell aggregate-laden hydrogel vehicles. (A) Schematic of hydrogel injection at different locations for repairing myocardial infarction (MI) in a mouse disease model. (B) Overview of the bioinspired process for fabricating murine ESC aggregate-laden alginate-chitosan micromatrix (ACM) vehicles together with live/dead staining images. Scale bar: 100 μm. (C) Gross images of a normal heart and MI hearts administered five different treatments (ACM-A, cell aggregates with ACM encapsulation; Bare-A, bare predifferentiated aggregate). Arrows indicate granulomas generated in single-cell (Single)- and Bare-A-treated mice. Scale bar: 3 mm. (D) Survival of the mouse disease model at 4 weeks; the ACM-A group exhibited significantly higher survival than all the other groups. (E) Ejection fraction results; the ACM-A treatment significantly enhanced heart function after MI. Reprinted with permission from ref 1032. Copyright 2016 Nature Publishing Group.

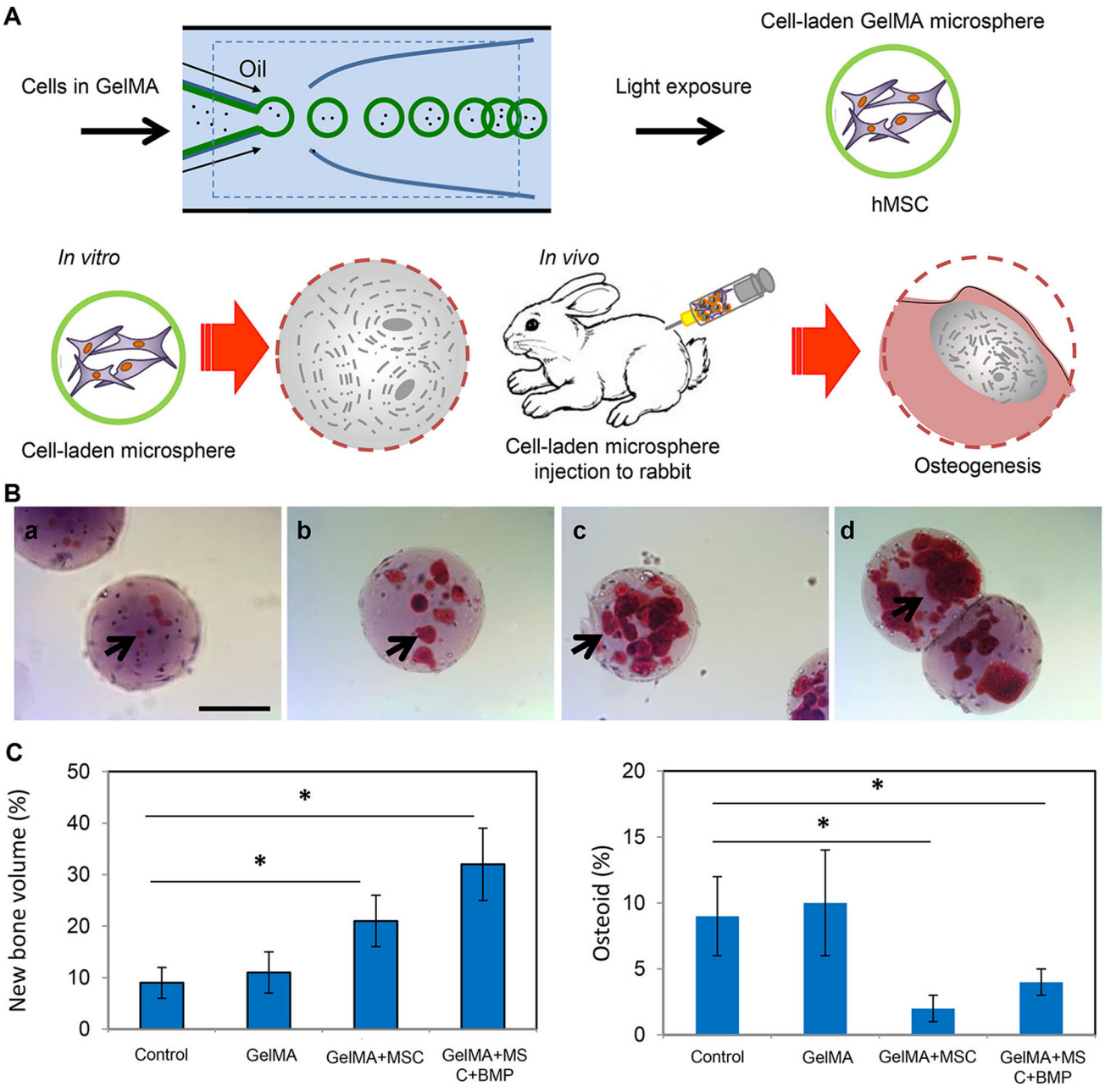

Figure 29.

Bone regeneration using cell-laden GelMA microspheres. (A) Schematic illustration for the fabrication of cell-laden GelMA microspheres using a photo-cross-linking-microfluidic method, and in vitro and in vivo applications for osteogenesis and bone regeneration in a rabbit model. (B) Alizarin red staining results of cell-laden GelMA microspheres after (a) 1, (b) 2, (c) 3, and (d) 4 weeks of culture for in vitro osteogenesis. Scale bar: 100 μm. (C) Histomorphometric results (%) of new bone (left) and osteoid (right) formation. Reprinted with permission from ref 1083. Copyright 2016 WILEY-VCH Verlag GmbH & Co. KGaA, Weinheim.

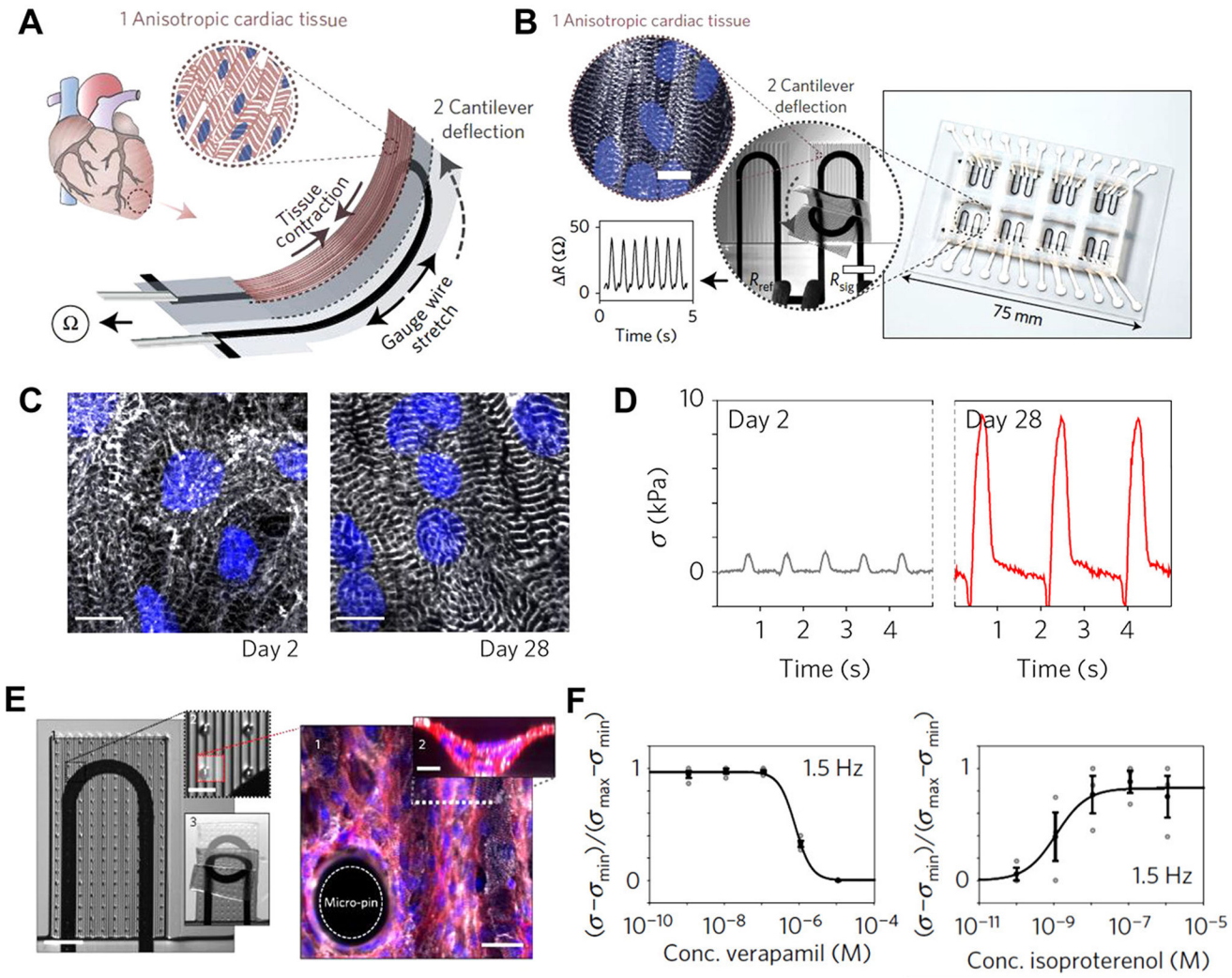

Figure 30.

Heart-on-a-chip. (A) Schematic illustration of a heart-on-a-chip fabricated by a multimaterial 3D printing technique. (B) Overview of a printed chip, and a confocal microscopy image of immunostained cardiac tissue. Blue, DAPI nuclear stain. White, α-actinin. Scale bars: 10 μm. (C) Images of immunostained laminar cardiac tissues on chip cantilevers on day 2 (left) and day 28 (right), respectively. Blue, DAPI nuclear stain. White, α-actinin. Scale bars: 10 μm. (D) Contractile twitch stress generated by laminar cardiac tissues on day 2 (left) and day 28 (right), respectively. (E) A modified chip cantilever with supporting thicker laminar cardiac tissue (left), and immunostained thicker laminar cardiac tissue (right). Blue, DAPI nuclear stain. White, α-actinin. Red, actin. Scale bars: 30 μm for (1), and 10 μm for (2). (F) Dose–response curve for verapamil (left) and isoproterenol (right). Reprinted with permission from ref 944. Copyright 2016 Nature Publishing Group.

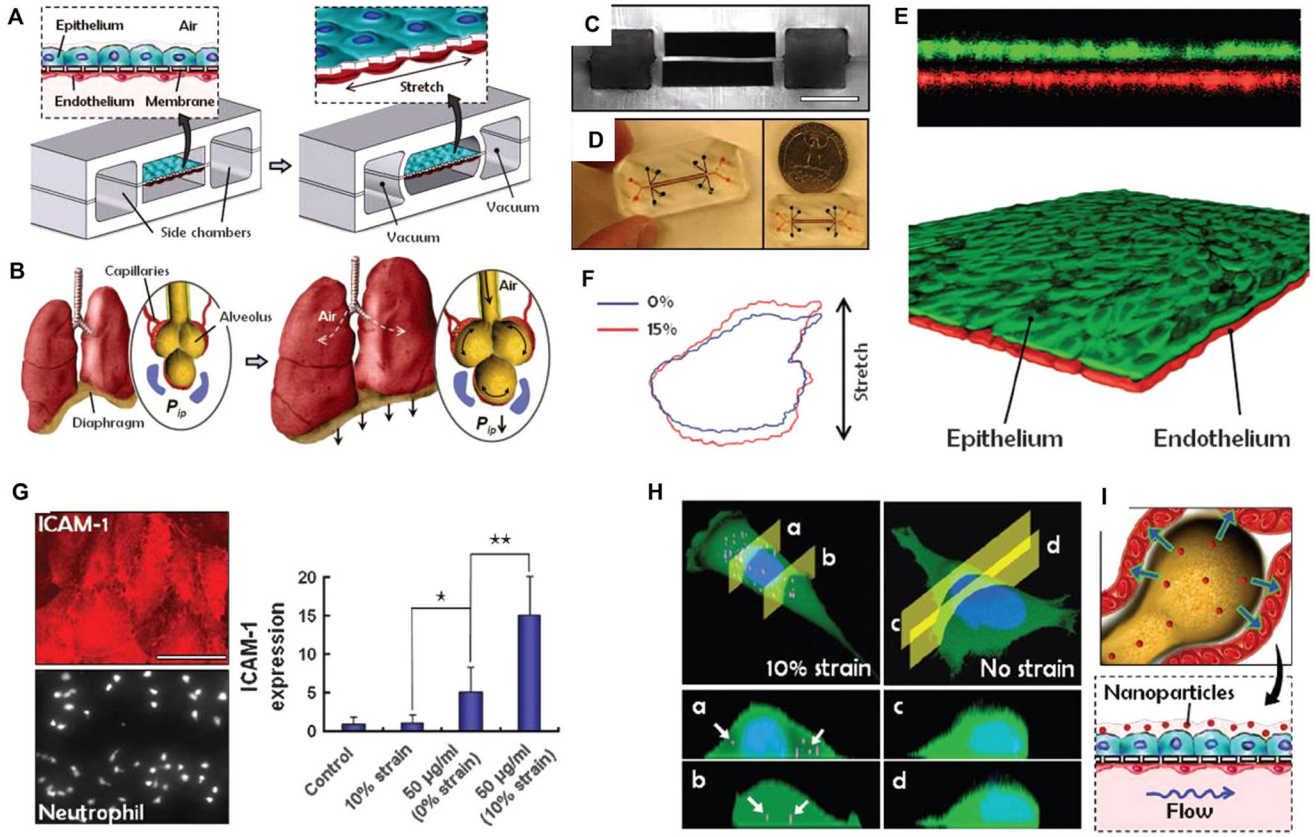

Figure 31.

Breathing lung-on-a-chip. (A) Schematic illustration of the design of the breathing lung-on-a-chip. (B) Sketch diagram of the physical stretching process of the alveolar–capillary interface in the lungs during inhalation. (C) Cross-sectional view of microfluidic chip. Scale bar: 200 μm. (D) Overview images of a chip device. (E) 3D confocal reconstruction of the epithelial–endothelial tissue interface generated on the chip. (F) Functional tissue membrane generated 15% strain in cells. (G) Toxicological study of silica nanoparticles based on the lung chip. Left, endothelial expression of intercellular adhesion molecule 1 (ICAM-1) and neutrophil adhesion in the lower channel. Right, mechanical strain and silica nanoparticles synergistically increased the expression of ICAM-1. Scale bar: 50 μm. (H) Mechanical strain (10%) promoted the cellular uptake of polystyrene nanoparticles (100 nm). Internalized nanoparticles are indicated with arrows. (I) Schematic illustration of mimicking nanoparticle transportation across the alveolar–capillary interface with the lung chip. Reprinted with permission from ref 1163. Copyright 2010 American Association for the Advancement of Science.

Table 1.

Some important aspects of different degradation mechanisms.

	Enzymatic degradation	Hydrolytic degradation	Photolytic degradation
Sensitive moieties	MMP-, plasmin-, and elastase-sensitive peptides	Ester, hydrazine, and acetal linkages	Azobenzene, o-nitrobenzyl, and coumarin
Degradation times	Hours to days	Days to weeks	Seconds to minutes
Influence factors	Sequences of enzyme-sensitive peptides, concentration and activity of enzymes	Molecular weight of monomer, hydrogel concentration and water content, solution pH, ratio of hydrolysable linkages in network backbone	Light wavelength, intensity, irradiation time, and the site of photosensitive moieties in network, the ratio of host-guest inclusion complex
Advantages	Predictable cell-mediated degradation	Mild reaction conditions without involving any trigger molecules, biocompatible byproducts	High controllability on spatiotemporal degradation, deep tissue regulation of hydrogel degradation
Disadvantages	Limited controllability on spatiotemporal degradation	Difficult to predict degradation kinetics, limited controllability on spatiotemporal degradation	Light-induced harmful effects to cells, potential toxic byproducts

Table 2.

Conductive additives used for fabricating conductive biomimetic materials and their biomedical applications and performance.

Type of additive	Conductive additive	Hydrogel	Concentration	Method	Advanced property	Application	Performance	Ref.
Conductive polymers	PANi	PEGDA	1 and 3 wt%	In situ precipitation of PANi in PEGDA solution	Improved conductivity of 1.1 × 10^{-3} mS/cm, enhanced water retention and proton conductivity	Neural tissue engineering	Promote cell attachment and neural differentiation of PC12 and hMSC cells with improved extension of neuritis and expression of membrane neurite marker growth associated proteins	944
		Cellulose	/	Oxidizing aniline inside of cellulose hydrogel using Ammonium persulfate	Improved conductivity to 0.68 S/cm, reduced strength, elongation at break and moisture content	Neural tissue engineering	Excellent biocompatibility, promote cell adhesion of RSC96 cells, and guide extension of neurons in neural repairing in adult SD rats	945
		Quaternized chitosan	1–4 wt%	Adding aniline and reacting	Improved conductivity of 4.3–15.7 × 10^{-4} S/cm, electrostatic adherence ability	Tissue engineering and antibiosis	Good antibacterial activity for both Gram-negative and Gram-positive bacteria *in vitro* and *vivo*, improved biocompatibility, promote the proliferation of C2C12 myoblast cells	946-947
		Polyaniline/myo-inositol hexakisphosphate	/	Gelating PANi using myo-inositol hexakisphosphate	Conductive and biocompatible	Tissue engineering	Promote cell adhesion and proliferation of rat endothelial progenitor cells, and induce milder inflammatory responses after implantation	948
		GelMA	0.16 M aniline monomers	In situ polymerization of aniline monomers within GelMA matrix	Improved conductivity with low resistance and impedance	Tissue engineering	Biocompatible, promote cell adhesion and	913

Type of additive	Conductive additive	Hydrogel	Concentration	Method	Advanced property	Application	Performance	Ref.
							spreading of C3H/10T1/2 murine mesenchymal progenitor cells, and can be fabricated to microarchitecture with defined pattern to guide cell growth	
	PPy	Chitosan	3 and 30%	Grafting pyrrole to chitosan using chemical oxidative polymerization	Improved conductivity of 2.4×10^{-4} S/cm, semiconductive properties	Cardiac tissue engineering	No influence on cell attachment, metabolism or proliferation *in vitro*, enhanced Ca^{2+} signal conduction and improved electric coupling *in vitro*, decreased QRS interval and increased transverse activation velocity and improved heart function when injected *in vivo*	897
		Oligo(polyethylene glycol) fumarate	0.4 M pyrrole solution	Immersing oligo(polyethylene glycol) fumarate network in pyrrole solution	Improved conductivity and reinforced mechanical properties	Neural tissue engineering	Biocompatible, promote cell attachment and neural differentiation, increase neurite lengths	949
		Alginate	0.001-0.02 M pyrrole solution	Chemically polymerizing pyrrole within alginate hydrogels using $FeCl_3$	Improved conductivity of 1.1×10^{-4} S/cm, increased stiffness	Neural tissue engineering	Promote cell adhesion, growth and expression of neural differentiation markers of hBMSCs, and induce mild inflammatory reactions after implantation	950
		HA	0.01-0.1 M pyrrole solution	Mixing pyrrole and PyHA solution and chemically polymerizing pyrrole using ammonium persulfate	Improved conductivity of 7.27 mS/cm, increased stiffness	Tissue engineering	Promote attachment and growth of fibroblasts	951

Type of additive	Conductive additive	Hydrogel	Concentration	Method	Advanced property	Application	Performance	Ref.
		Collagen/alginate	19-30 wt% of Alg-graft-PPy	Incorporating Alg-graft-PPy with collagen/alginate solution	Improved conductivity of ~25 mS/cm	Injectable hydrogel for tissue engineering	Rheological capacity and syringeability, support cell viability of hBMSCs	952
		Poly(hydoxyethyl methacrylate)	/	Potentiostatic electropolymerization of pyrrole	Charge storage capacity of 10 mC/cm^2	Enzyme-based biosensor	Increased apparent Michaelis constant and biotransducer sensitivity, improved stabilization	953
		Poly(acrylic acid)	/	Dispersing of PPy powder in poly(acrylic acid) solution	Improved conductivity, electro-induced gel swelling capacity	Controlled drug delivery	Controlled drug diffusion from conductive hydrogels under electric field	954
	PEDOT	PVA	1-3 wt%	Electropolymerization	Charge storage capacity of 52-72 mC/cm^2, low electrical impedance	Neural tissue engineering	Improved proliferation of olfactory ensheathing cells, significant increasd proportion of flatter cells with extended cytoplasm	955
		Agarose	0.01 M EDOT solution	Electrodepositing of EDOT inside of hydrogel	Improved conductivity	Neural tissue engineering	Promote directional and controlled axonal regeneration in nerve gap in rats	914
		Poly(3,4 ethylenedioxythiophene)/para-toluenesulfonate	0.1 M EDOT solution	Electrodepositing of EDOT	Improved conductivity with low impedance	Neural electrodes for cochlear	Improve electrical properties without affecting the mechanical properties of the electrode array, remain conductive under 2 billion electrical pulses	639,956
		Methacrylated PVA	/	Electrodepositing of EDOT	Improved conductivity	Neural electrodes and neural tissue engineering	Promote proliferation of olfactory ensheathing cell and neural differentiation of OECs co-cultured with PC12 cells	957

Type of additive	Conductive additive	Hydrogel	Concentration	Method	Advanced property	Application	Performance	Ref.
							under electrical stimulation	
		PVA	0.1 M EDOT solution	Galvanostatic electrodeposition of ethylenedioxythiophene	Enhanced conductivity of 1.1±0.2 S/cm, increased charge storage capacity and stiffness	Medical electrodes with drug delivery capability	Promote cell proliferation of PC12 cells and neurite extension, and improve attachment and differentiation of neural like cells with the delivery of nerve growth factor	958-959
		Bacterial cellulose	/	Immersing BC microfiber in EDOT solution	Core/shell BC/PEDOT hydrogel microfiber, improved conductivity	Controlled rug delivery and tissue engineering	Controlled delivery of diclofenac sodium under electrical stimulation, excellent biocompatibility and electroactivity of the hybrid microfibers for PC12 cell culture	960
	Tetraaniline	PEG	3 wt% of chitosan-graft-aniline tetramer	Grafting tetraaniline on chitosan and then blending with PEGDA solution	Improved conductivity of ~10^{-3} S/cm, reinforced mechanical properties	Cardiac tissue engineering	Adhesiveness to host tissue and antibacterial property, support cell viability of C2C12 cells before and after injection, tunable release C2C12 myoblasts and H9c2 cardiac cells after cell delivery	961
		Oxidized alginate	7.1-21.3 wt%	Incorporating tetraaniline-graft-OA with oxidized alginate	Improved conductivity of 7.52 × 10^{-6} S/cm and reinforced mechanical properties	Injectable hydrogel for tissue engineering	Support cell growth of MSCs, induce mild inflammation response when implanted into chick chorioallantoic membrane for 1 week	962
Carbon-based materials	CNT	Collagen	0.5-2.0 mg/mL	Dispersing in chitosan solution and mixing with collagen solution	Improved conductivity and reinforced mechanical properties	Cardiac tissue engineering	Promote cell viability, adhesion and beating	963

Type of additive	Conductive additive	Hydrogel	Concentration	Method	Advanced property	Application	Performance	Ref.
							function of HL-1 cardiomyocytes	
		GelMA	1-5 mg/ml	Blending and sonicating	Low impedance, increased compression modulus	Cardiac tissue engineering	Improved cardiac cell adhesion, organization and cell-cell coupling, and the tissues resist damage by a model cardiac inhibitor	898
		Gelatin	0.5-2.5 mg/mL	Mixing SWCNTs in gelatin solution	Improved conductivity of ~4× 10^{-5} S/cm, reinforced mechanical properties	Cardiac tissue engineering	Promote cardiac contraction and the expression of electrochemical associated proteins *in vitro*, and the conductivity hydrogels structurally integrate with the host myocardium and improve the heart function after implantation *in vivo*.	964
		Collagen I/Matrigel	20-100 μg/mL	Mixing carbon nanotube dispersion with hydrogel solution	Improved conductivity of 2.4 S/m	Neural tissue engineering	Promote neurite outgrowth in isolated dorsal root ganglia, and further promote the neurite outgrowth and neurite length under electrical stimulation	965
		Collagen	10-50 μg/mL	Mixing carbon nanotube dispersion with collagen solution	Improved conductivity	Neural tissue engineering	Support cell viability but inhibit cell proliferation of Schwann cells in 2D culture, while in 3D culture the cell proliferation, viability, or morphology are not influenced	966
		PHEMA	1-6 wt% to HEMA	Mixing	Improved conductivity of 8.0 × 10^{-2} S/cm, reinforced mechanical properties	Neural tissue engineering	Improved biocompatibility, protect SHSY5Y neuroblastoma	967

Type of additive	Conductive additive	Hydrogel	Concentration	Method	Advanced property	Application	Performance	Ref.
							cells from electrical potential application with no loss of cell activity	
		Chitosan	0.5 mg/mL	Blending, sonicating and electrodepositing	Excellent electrochemical activity and conductivity, high content of oxygen functional groups	Microbial electrocatalysis	Increased current generation and the maximum power density	968
	Carbon nanobrush	Poloxamer	0.1-5 vol%	Blending	Improved conductivity	Tissue engineering	Cardiac fibroblasts and myocytes are survived and proliferated in hydrogel containing 0-1vol % carbon nanobrush	647
	GO	Methacryloyl-substituted tropoelastin	1 and 2 mg/mL	Mixing and sonicating	Improved conductivity and resilience	Cardiac tissue engineering	Biocompatible, support growth and function, and enhance activity and maturation of cardiomyocytes, induce mild inflammatory response after implantation *in vivo*	899
		PEGDA700-Melamine/HA	0.5 mg/mL	Mixing	Improved conductivity of 2.84 × 10^{-4} S/cm, soft and anti-fatigue mechanical property	Cardiac tissue engineering	Promote the expression of cardiac specific proteins of adipose tissue-derived stromal cells after injection of cell-laden hydrogel into MI area of rats, and improve the transmission of mechanical and electrical signals and heart functions	969
	rGO	PA	0.3 wt%	Blending GO with PA and then reducing	Improved conductivity of 1.3× 10^{-4} S/cm, reinforced mechanical properties	Muscle tissue engineering	Enhance proliferation and myogenic differentiation of C2C12 cells, and combining electrical stimulation further	937,970

Type of additive	Conductive additive	Hydrogel	Concentration	Method	Advanced property	Application	Performance	Ref.
							enhanced the myogenic gene expression	
		Acrylamide	2-4 wt% to acrylamide	Reducing GO by polydopamine and then polymerizing acrylamide	Improved conductivity of 0.18 S/cm, high stretchability and toughness, self-healable	Medical electronics	Self-adhesiveness to skin, self-healability resembling to natural tissue both mechanically and electrically, excellent biocompatibility without causing any inflammation after implantation *in vivo*	971
	Carbon nanofiber/rosette nanotube	PHEMA	5-10 mg/mL CNF, 0.01-0.05 mg/mL RNT	Mixing	Improved conductivity and hydrophilicity, increased surface roughness	Cardiac tissue engineering	Promote cell viability and adhesion of a transformed human cardiomyocyte cell line, injectable	972
	rGO/CNT	Oligo(poly(ethylene glycol) fumarate)	~5% rGO, ~0.5% CNT	Covalently embedding by chemical cross-linking and followed by reducing	Improved conductivity of 5.75 × 10^{-3} S/m, reinforced mechanical properties	Neural tissue engineering	Biocompatible, promote cell proliferation and spreading of PC12 cells, and improve the neural differentiation and robust neurite formation under the application of nerve growth factor	973
Gold based materials	AuNP	Chitosan	0.5-1.5 wt%	Blending	Improved conductivity of 0.13 S/m,	Cardiac tissue engineering	Support viability, metabolism, migration and proliferation of MSCs, enhanced cardiomyogenic differentiation under electrical stimulation	974
		Thiol-2-hydroxyethyl methacrylate/hydroxyethyl methacrylate	/	Reducing colloidal Au and Au^{3+} ions inside of hydrogel in sodium borohydride solution	Improved conductivity of 15.3 S/m, reduced stiffness	Cardiac tissue engineering	Tunable conductivity and elasticity suitable for engineering cardiac tissues, excellent	920

Type of additive	Conductive additive	Hydrogel	Concentration	Method	Advanced property	Application	Performance	Ref.
							biocompatibility, support cell adhesion of neonatal rat cardiomyocytes, promote Cx-43 expression and cardiac function under electrical stimulation	
	AuNR	GelMa	0.5-1.5 mg/mL	Mixing AuNR with GelMA solution	Improved conductivity with low impedance, and reinforced mechanical properties	Cardiac tissue engineering	Promote cell retention, viability, metabolic activity, tissue formation, cardiac specific protein expression and synchronous beating function of isolated cardiomyocytes	[975]

Table 3.

Representative FDA-approved biomimetic material-based products for human tests since 2012. Data were obtained from http://www.fda.gov/ and https://clinicaltrials.gov/. For earlier examples, please refer to an existing review.[1109]

Material	Product name	Company	FDA clearance date	Product description	Clinical trial
Collagen	VASCADE Vascular Closure System (VCS)	Cardiva Medical, Inc.	01/13/2013	A collagen patch derived from bovine tissue Potential tissues: vascular, cardiac tissue	263/275 success
Collagen	MACI® /Autologous Cultured Chondrocytes on a Porcine Collagen Membrane	Vericel Corporation	12/13/2016	An autologous cellularized scaffold Potential tissues: cartilage, bone	49/65 success
HA	MONOVISC™	Anika Therapeutics, Inc.	02/25/2014	A single injection gel Potential tissues: knee	121/181 success
HA	GEL-SYN™	Institut Biochimique S.A. (IBSA)	20/12/2013	An artificial gel composed of sodium hyaluronate Potential tissues: knee, connective tissue	181/192 success
HA	Medtronic CoreValve System	Medtronic CoreValve LLC	30/3/2015	An artificial membrane sheet Potential tissues: vascular, cardiac tissue	34 /147 success
HA	Healon® EndoCoat Ophthalmic Viscosurgical Device	Abbott Medical Optics Inc.	07/02/2012	A clear, thick liquid Potential tissues: eyes	21/199
Bovine tissue	Edwards SAPIEN XT Transcatheter Heart Valve - P130009/S034	Edwards Lifesciences LLC	08/09/2015	A transcatheter aortic valve Potential tissues: cardiac tissue	77/96 success
Collagen and silicone	Omnigraft Dermal Regeneration Matrix	Integra LifeSciences Corporation	01/0 7/2016	Double-layered membrane. The top layer is silicone and the layer next to the wound is collagen Potential tissues: foot wounds	79/154 success
Sodium carboxymethylcellulose	Radiesse Injectable Implant	Merz North America Inc.	06/04/2015	A white, sterile, injectable gel Potential tissues: hands	64/85 success
PEG	ReSure® Sealant	Ocular Therapeutix, Inc.	01/08/2014	A synthetic glycol hydrogel contains a blue visualization aid Potential tissues: eyes	302/305 success
PEG	Adherus AutoSpray Dural Sealant	HyperBranch Medical Technology, Inc.	03/30/2015	A membrane consists of synthetic, absorbable sealant materials	113/124 success
PLLA	Absorb GT1™ Bioresorbable Vascular Scaffold (BVS) System	Abbott Vascular,Inc.	07/05/2016	A bioresorbable vascular scaffold Potential tissues: cardiac tissue	/
Nitinol	Valiant Thoracic Stent Graft with Captivia Delivery System	Medtronic Vascular	01/22/2014	An injectable soft scaffold Potential tissues: vascular, cardiac tissue	/
PMMA	Bellafill PMMA Collagen Dermal Filler	Suneva Medical, Inc.	12/23/2014	An injectable synthetic gel Potential tissues: skin	56/87 success
Cyanoacrylate	VenaSeal Closure System	Covidien LLC	02/20/2015	A kind of viscous liquid Potential tissues: vascular	107/108 success

Material	Product name	Company	FDA clearance date	Product description	Clinical trial
PET	Edwards SAPIEN3 Transcatheter Heart Valve	Edwards Lifesciences LLC	08/18/2016	A catheter-based artificial aortic heart valve Potential tissues: cardiac tissue	/
Combined hydrogel	Raindrop® Near Vision Inlay	ReVision Optics, Inc.	06/29/2016	A gel that can be implanted in the cornea Potential tissues: eyes	336/344 success
Polylactide-co-glycolide acid co-polymer and polydiaxanone	Closer Vascular Sealing System (VSS)	Rex Medical, LP	02/12/2016	An insertion sheath, dilator and an implant contained in a delivery system Potential tissues: vascular	216/220 success

Table 4.

Representive works on 3D scaffold-, hydrogel- and nanogel-based immunomodulation.

Biomaterial system	Delivered agent	Delivered cell	Performance	Ref.
In-situ crosslinking dextran-based hydrogels	MIP3α, plasmid DNA antigen, IL-10-silencing siRNA	\	Recruited immature DCs; triggered a strong shift towards antigen-specific Th1 response *in vivo*	1253
		\	Recruited immature DCs; effective IL-10 gene knockdown in migrated primary DCs *in vitro*	1235
	IL-10-silencing siRNA, CpG oligonucleotides, TLR9 agonist (poly(I:C))	\	Dual-delivery of IL-10-silencing siRNA along with CpG ODN to the same DCs significantly enhanced their Th1/Th2 cytokine ratio; simultaneous immunotherapy with CpG ODN and IL-10 siRNA enhanced immune protection of an idiotype DNA vaccine in a prophylactic murine model of B cell lymphoma	1254
In situ crosslinking alginate-based hydrogels	CCL21, CCL19	DCs	Recruited activated antigen-specific T cells	1230
	IL-2, CpG oligonucleotides	\	Promoted cellular infiltration	1245
	IL-15 superagonist, CpG oligonucleotides	DCs	Promoted immune cell accumulation and matrix infiltration; concentrated the cytokine in the tumor site and suppressed tumor growth	1255
	Celecoxib, PD-1 monoclonal antibody	\	Increased effector T cell infiltration; improved overall survival in mice bearing B16-F10 tumors or 4T1 breast cancer tumor	1256
In situ crosslinking PEO-based hydrogels	Plasmid DNA encoding human pSEAP	\	High serum levels of the protein for a significantly longer period of time relative to that achieved with unformulated DNA injections	1257
Macroporous alginate scaffolds	IP-10, IL-15 superagonist, anti-CD3, anti-CD28 and anti-CD137 antibodies	\	In a mouse breast tumor resection model, the implants effectively supported tumor-targeting T cells throughout resection beds and associated lymph nodes, and reduce tumor relapse; in a multifocal ovarian cancer model, the polymer-delivered T cells triggered regression	1258
Collagen sponge scaffolds	LT-β receptor	Stromal cell line (TEL-2)	Formed an organized secondary lymphoid-like with compartmentalized zones of B-cell and T-cell clusters, high endothelial venule-like vessels, germinal centers and networks of follicular DC; induced antigen-specific, IgG-isotype antibody formation	1231
PEG-based hydrogels	Coumermycin	\	Released the vaccine by the oral administration of the stimulus molecule novobiocin resulting in successful immunization of the mice	1259
Macroporous PEG-based hydrogel scaffolds infused with collagen	CCL21	T cells, DCs	Promoted intra-scaffold migration of encapsulated T-cells and DCs, with T-cell migration dependent on the connecting pore size	1260
Macroporous PLGA scaffolds	GM-CSF, CpG oligonucleotide, tumor lysate	\	Recruited DCs and programmed them to induce robust prophylactic immunity against murine B16-F10 melanoma tumor	1233
		\	Coordinated regulation of a DC network dramatically enhanced host immunity in mice	1234
PLGA microparticles	Plasmid DNA antigens, IL-10-silencing siRNA	\	Enhanced immune response and modulated DCs and mice toward a strong antigen-specific Th1 responses; effective IL-10 gene knockdown; enhanced upregulation of maturation markers in primary DCs *in vitro*	1261
Macroporous PLG scaffolds	GM-CSF, Flt3L, CCL20	\	Induced specific anti-tumor T cell responses and long-term survival in a therapeutic B16-F10 melanoma model	1240

Biomaterial system	Delivered agent	Delivered cell	Performance	Ref.
Decellularized bone	Interferon-gamma, IL-4	\	Promoted sequential M1 and M2 polarization of primary human macrophages; increased vascularization in subcutaneous implantation murine model	1262
PMASH hydrogel capsules	Model OVA, multiple OVA peptides	\	Resulted in presentation of OVA epitopes and subsequent activation of OVA-specific CD4 and CD8 T cells in vitro; OVA-specific CD4 and CD8 T cells are also activated to proliferate in vivo following intravenous vaccination of mice with OVA protein- and OVA peptide-loaded PMASH hydrogel capsules	1263
Chitosan-based thermogels	None	T cells	Proliferation and gradual release, and the encapsulated T cell phenotypes were influenced by surrounding conditions and by tumor cells, while maintaining their capacity to kill tumor cells	1264
pHEMA-pyridine nanogels	BSA, fibronectin	\	Enhanced intra-articular retention and delivery of proteins; efficient priming of OVA-specific CD8+ T cells	1247
		\	Size dependent retention of protein-nanoparticle in rat knee joint	1246
Liposomal polymeric nanogels	TGF-β inhibitor SB505, IL-2	\	Delayed tumour growth; increased survival of tumour-bearing mice; increased the activity of natural killer cells and of intratumoral-activated CD8+ T-cell infiltration	1265

pHEMA = poly(hydroxyethyl methacrylate); PMASH = disulfide poly(methacrylic acid); PEO = polyethylene oxide; Th1 = T helper 1; MIP = macrophage inflammatory protein; IL = interleukin; CCL = CC-chemokine ligand; CpG = cytosine-phosphate-guanosine; GM-CSF = granulocyte-macrophage colony-stimulating factor; PD-1 = programmed death 1; LT = lymphotoxin; CTL = cytotoxic T-lymphocyte; pSEAP = secreted embryonic alkaline phosphatase OVA = ovalbumin; Flt3L = Fms-related tyrosine kinase 3 ligand; BSA = bovine serum albumin